The Dissertation Committee for Mason David Gemar
certifies that this is the approved version of the following dissertation:

Subnetwork Analysis for Dynamic Traffic Assignment:

Methodology and Application

Committee:

Randy Machemehl, Supervisor

Zhanmin Zhang

Stephen Boyles

William O'Brien

Talia McCray

Subnetwork Analysis for Dynamic Traffic Assignment: Methodology and Application

by

Mason David Gemar, B.S., M.S.

Dissertation

Presented to the Faculty of the Graduate School of

The University of Texas at Austin

in Partial Fulfillment

of the Requirements

for the Degree of

Doctor of Philosophy

The University of Texas at Austin

December 2013

ACKNOWLEDGEMENTS

I would like to first thank the University of Texas, specifically the Cockrell School of Engineering and the Civil, Architectural and Environmental Engineering Department, whose exceptional faculty and staff have made this possible. In particular, the guidance of those on my dissertation advisory committee, Dr. Machemehl, Dr. Zhang, Dr. Boyles, Dr. O'Brien, and Dr. McCray, has been greatly appreciated. A special thank you to my advisor, Dr. Machemehl, for his support throughout my time here at the University of Texas and for providing me the opportunity to complete my dissertation and earn my doctorate in civil engineering. I also owe my gratitude to Mr. and Mrs. Gerry and Mildred Franklin for providing a Thrust Fellowship awarded to me throughout my time at the university.

Additionally, I would like to acknowledge the efforts of several individuals who assisted throughout the research process. I would like to thank Matt Pool, Travis Owens, Michael Levin, and Mubassira Khan, fellow University of Texas graduate students, as well as David Kan and Anisah Cross, interns from the USIT program, who helped with various tasks important to the completion of this research. I owe a special thank you to Jack Bringardner who spent a great deal of time and effort as a collaborator on this research. I am very grateful for having the support of so many individuals in the transportation engineering program at the university. I would also like to thank the Network Modeling Center team at the Center for Transportation Research, notably Natalia Ruiz Juri, Jennifer Duthie, and Dennis Bell, who provided invaluable input, guidance, and support for this research effort. Additionally, I would like to acknowledge the Southwest Region University Transportation Center and the Texas Department of Transportation for sponsoring the research that formed the basis of this dissertation.

I would like to thank my parents, Gary and Jan, and my sister Michelle for their love and support. I would like to extend my gratitude to my friends, classmates, and coworkers. They have all been there for me as I completed this dissertation, especially Rebecca, who with her love and patience saw me through to the end.

Subnetwork Analysis for Dynamic Traffic Assignment: Methodology and Application

Mason David Gemar, Ph.D.

The University of Texas at Austin, 2013

Supervisor: Randy Machemehl

Dynamic traffic assignment (DTA) can be used to model impacts of network modification scenarios, including traffic control plans (TCPs), on traffic flow. However, using DTA for modeling construction project impacts is limited by the computational time required to simulate entire roadway networks. DTA modeling of a portion of the larger network surrounding these work zones can decrease the overall run time. However, impacts are likely to extend beyond typical boundaries, and determining the proper extents to be analyzed is necessary. Therefore, a methodology for selecting an adequate portion to analyze using DTA, along with provision for properly analyzing the resultant subnetwork, is necessary to determine the magnitude of construction impacts.

The primary objectives of this research center on evaluating subnetwork sizes to determine the appropriate extents required to analyze network modifications and developing a strategy to account for impacts extending beyond the subnetwork boundary. The first objective is accomplished through an in-depth review of subnetwork sizes relative to multiple impact scenarios. Three statistical measures are implemented to evaluate the adequacy of a chosen subnetwork relative to the derived impact scenarios based on an assessment of boundary demand. Ultimately, the root mean squared error is used successfully to provide a series of recommended subnetwork sizes associated with an array of possible impact scenarios. These recommendations are validated, and

application of the proposed methodology demonstrated, using five scenarios selected from real-world network modifications observed in the field.

When a subnetwork is not large enough and impacts to inbound trips pass beyond the boundary, there is a change in flow at this location that can be represented by a change in the demand assigned to the subnetwork at each entry point. As such, two strategies for adjusting the demand at subnetwork boundaries are implemented and evaluated. This includes use of results from static traffic assignment (STA) models to identify where flow changes occur, and implementation of a logit formulation to estimate demand adjustments based on differences in internal travel times between base and impact scenario models. Based on preliminary results, the logit method was selected for large-scale implementation and testing. In the end, an inconsistent performance of the logit method for full implementation highlights the limitations of the methodology as applied for this study. However, the results suggest that a refined strategy that builds on the foundation established could work more effectively and produce valuable subnetwork demand estimates in the future.

This research is used to provide recommendations for selecting and analyzing subnetworks using DTA for an array of common impact scenarios involving network modifications. The tradeoffs between improved efficiency and reduced accuracy associated with using subnetworks are thoroughly demonstrated. It is shown that a considerable amount of computational time and space, as well as effort on the part of an analyst, can be saved. A number of limitations associated with subnetworks are also identified and discussed. The proposed methodology is implemented and evaluated using several software programs and as a result, a number of useful tools and software scripts are developed as part of the research. Ultimately, the valuable experience gained from performing an extensive review of subnetwork analysis using DTA can be used as a basis from which to develop future research initiatives.

TABLE OF CONTENTS

LIST OF TABLES

LIST OF FIGURES

1. INTRODUCTION

Traffic control plans (TCPs) are used to coordinate the phasing of roadway construction projects in order to provide a detailed strategy for maintaining traffic operations in the construction activity area, including adjustments to roadway alignments, capacities, and detours. These plans are necessary to minimize the construction project impacts on traffic safety and mobility. Often, the requirements of TCPs are written in proposal documents and specify conditions such as maintaining the number of available roadway lanes, on and off ramps, and lighting and traffic signal accommodations during construction of each phase, as well as communication with drivers through use of variable message signs (VMS). These plans frequently include detailed drawings showing signing and pavement markings, temporary pavement sections and roadway realignments, barriers and barricades, and temporary lighting and traffic signals. In addition, detailed microsimulation analyses may be necessary to determine impacts of planned construction phasing on traffic flow along an impacted corridor and adjacent roadways. Outputs of these models, along with visualization tools, can be used to evaluate the ability of the TCP to maintain appropriate traffic operations and adequate roadway capacity during construction activity. Nonetheless, these models are often based on existing levels of demand and are limited in scope.

Microsimulation models do not typically take into account changes in driver behavior and network flow patterns throughout the greater area from the propagation of disruptions caused by roadway construction. Furthermore, the extents of the models are based on requirements established by the sponsoring transportation agency and stipulated in proposal documents, often a product of prior experience, general guidelines, and engineering judgment. However, every project is unique, and unforeseen impacts can cause congestion on roadways beyond the identified area, placing a greater strain on the network than anticipated or mitigated using TCPs. As such, it would be very valuable to efficiently analyze a larger portion of the network to accurately determine these impacts

and conceivably provide a tool that can more adequately identify the area to be analyzed in more detail as part of a microsimulation model.

It has been demonstrated through prior research that dynamic traffic assignment (DTA) models can provide a mesoscopic-level forecast of changes in driver behavior and traffic flow caused by modifications to roadway capacities due to construction projects (Pesti et al., 2010). These models can be used to effectively determine network impacts resulting from short- and long-term duration construction projects on area traffic patterns by properly identifying the locations where congestion is prevalent. However, DTA models often require copious amounts of computational time and computer memory to run on large urban networks. It can take hours, days, or even weeks to complete a single DTA model run, and properly evaluating TCPs may require the creation of many model variations to represent all of the alternatives and phases for a single construction project.

It has been speculated that the majority of impacts due to construction activity occur over a localized area around the project. As a result, the short-range boundaries of microsimulation models may appear justified. Furthermore, selection of only a small portion of a large network serves to simplify the evaluation process and reduce the resources necessary to complete analyses, including DTA models (Zhou et al., 2006; Xie et al., 2010; Boyles, 2012a). However, impacts are likely to extend beyond typical boundaries, and determining the proper extents to be analyzed is necessary. Therefore, a methodology for selecting an adequate subnetwork to analyze using DTA, along with provision for properly analyzing the resultant subnetwork, is necessary to determine the magnitude of construction impacts and the area where more detailed analysis using microsimulation models is required for evaluating TCPs. Ultimately, selection of a subnetwork is intended to reduce the resources necessary for evaluating a multitude of scenarios contained in a TCP, and a proper subnetwork selection methodology can be used to maintain the accuracy of DTA model results relative to analysis of the full network.

It is acknowledged that a level of uncertainty may exist relative to implementing a subnetwork analysis using DTA to evaluate a TCP or other impact to a network. An engineer may ask any number of questions, including the following: Why use DTA to analyze these types of impacts? What are some of the benefits in terms of computational time and space that can be achieved using a subnetwork analysis for a particular network? For a particular impact scenario, or series of scenarios, what subnetwork size is best? Or, given a specific size of subnetwork, generally, what level of accuracy can one expect from the model relative to analyzing the entire region? Lastly, if one chooses a subnetwork size, are there any adjustments that can be made to the model, efficiently and effectively, to improve its accuracy?

The main goal of this research is to provide answers to these questions, and ultimately, demonstrate how a process of subnetwork selection and analysis can be implemented with DTA to assess network modifications. It is intended that the proposed strategy reduce the amount of time necessary to model impacts to large, regional transportation systems in an accurate manner relative to the full network. The process involves investigating different subnetwork sizes, as well as developing procedures to account for the external portion of the network. This is accomplished through an in-depth evaluation of the developed methods for subnetwork selection and analysis using multiple test scenarios on several real-world networks. These scenarios are intended to vary in location, size, and scope in order to test the robustness of the process.

The purpose of this research is to develop a method for implementing DTA to evaluate the impacts of TCPs or other network modifications on area traffic patterns and provide a more accurate representation of subsequent congestion for construction management personnel and traffic engineers who evaluate these plans. The methodology has been divided into two parts. The first step involves identifying the relevant extent of the network area around the modification, or subnetwork, necessary to evaluate in detail for a

given scenario. Secondly, the research aims to identify a method for adjusting the subnetwork model to account for impacts occurring outside the selected area.

The process relies heavily on the use of Geographic Information System (GIS) software to visually inspect different types of TCP scenarios, to aid in the implementation of the methodology, and to review measurable changes in traffic characteristics throughout the network. Other database processing tools and scripts are also necessary to scan through and extract pertinent information from the substantial amount of data associated with DTA models. The intent is to provide a user-friendly interface between software programs and tools that enables one to initiate the subnetwork analysis and assess impact scenarios with relative ease, demonstrating the versatility of the programs for creating evaluation tools and visual elements. This requires identification of appropriate strategies for assessing different subnetwork sizes relative to impact scenarios, reviewing model inputs and outputs, and modifying the model to account for impacts beyond the subnetwork as necessary to improve the accuracy of the model relative to full-scale analysis.

This report outlines the project background, including problem description and project objectives, followed by a literature review undertaken to investigate the viability of using DTA and subnetwork analysis to evaluate network modifications, including TCPs. This review is followed by a detailed overview of the methodology used to select, analyze, and visualize subnetworks within the larger Austin and Dallas-Fort Worth (DFW) area DTA models. Methods for utilizing different software programs and data processing tools required to evaluate multiple strategies and scenario results are also presented. A chapter demonstrating the processes utilized for selecting subnetworks, completing analyses, extracting and visualizing results, as well as evaluating different subnetworks for a sample set of scenarios using the downtown Austin network follows.

This preliminary assessment is followed by a detailed investigation of different subnetwork sizes for multiple impact scenarios, as well as a proposed strategy implemented to account for changes occurring outside of the subnetwork based on changes to travel times within it. An evaluation is performed using the DFW mega-region, one of the largest transportation systems in the country, in order to fully demonstrate the intrinsic value of subnetwork analysis. In addition to a detailed discussion of the subsequent results, guidance relative to selection of a subnetwork given a particular impact scenario is provided, along with identification of the trade-offs associated with implementing subnetwork analysis. Lastly, conclusions and recommendations for future research are presented. The following chapter provides an overview of the problem description and project objectives.

2. PROJECT BACKGROUND

As highway infrastructure, particularly in urban areas, is repaired and rebuilt, construction must be completed while traffic demands continue to be accommodated. TCPs must be developed to identify a strategy for maintaining traffic during construction activity in such a way that maximizes user safety and minimizes user cost. Essentially, all modifications to transportation infrastructure require TCPs. These plans must be evaluated prior to implementation to assure construction management personnel and transportation engineers that impacts to traffic along affected roadways will not include excessive delay. Agencies around the country have noted the importance of developing appropriate TCPs for construction activity and monitoring the effectiveness of these plans with respect to mobility and safety (Kim et al., 2008; Ullman et al., 2009; Pesti et al., 2010).

To aid in this evaluation process, a GIS tool was developed to provide Texas Department of Transportation (TxDOT) employees with the ability to quickly check traffic counts and compare them to the updated capacities of TxDOT roadways in work zones. The tool enables a user to select links in the GIS tool, adjust geometric attributes of the roadway as identified in a TCP, and complete updated capacity calculations based on procedures outlined in the Highway Capacity Manual 2010 (HCM 2010). However, the tool is limited to evaluating existing pre-construction volume versus capacity changes due to construction along only those roadways operated by TxDOT.

Travelers often alter their travel paths in response to construction activity and as traffic congestion information becomes more widely available, travelers can be expected to more actively choose alternate paths to minimize their travel time. When a roadway is impacted by construction, these changes in travel behavior are likely to affect the surrounding network. DTA analysis techniques provide a resource for predicting how travelers react to the kinds of network changes imposed by TCPs beyond a local area.

Unlike conventional static network analysis techniques that rely on estimates of instantaneous travel times, DTA utilizes experienced travel times to determine route choice behavior. The advantage is that travel times actually experienced along a route provide a more accurate representation of reality, often different than those expected when a traveler leaves their point of origin. Since these experienced travel times are anticipated to influence traveler decision-making along network routes, using a measure of these travel times provides the means for a more accurate and realistic simulation of travel behavior. This is especially relevant when modeling user reactions to capacity disruptions, such as those experienced within work zones.

To implement DTA models, a software program called Visual Interactive System for Transportation Algorithms (VISTA) has been created. The program enables a user to construct network elements, such as links and nodes, and input detailed information about those elements, including roadway capacity and intersection control. The user also inputs time-dependent demand information and the software applies embedded processes and algorithms to complete a DTA analysis. Currently, the Center for Transportation Research (CTR) at the University of Texas at Austin utilizes the VISTA software to analyze DTA models on networks in the Austin and Dallas-Fort Worth (DFW) metropolitan areas. As such, this software will be used to complete DTA analyses for this project. While the software also contains a basic GIS tool for visualizing and editing network elements, it has significant limitations. Therefore, the supplemental use of advanced GIS software is desired.

Visualization capabilities are critical tools for the evaluation of TCP-related network impacts. Visuals can be created to enable simple and efficient identification of problem areas. As noted, an ArcGIS software tool was recently created for the Dallas District of TxDOT to assist construction management personnel with TCP reviews. As such, ArcGIS has been identified as a crucial element for use in visualization of DTA analysis results. Not only does the software have data storage and mapping capabilities for

evaluating results, but automated processes can be developed within the software to streamline necessary selection and extraction routines. Beyond GIS interfacing, other important uses of DTA results have been identified.

In addition to construction management personnel, traffic engineers have considerable interest in the impact of TCPs on area networks. Typically, traffic engineers are responsible for evaluating network impacts resulting from TCPs for major roadway improvement projects, or other types of network modifications, such as the addition of transit services or adjustments to traffic control. To accomplish these reviews, they often rely on microsimulation tools to complete necessary analyses. However, these models require the user to supply traffic volumes as well as many other detailed inputs representing a vast amount of collected information. For a large network, these analysis tools may require substantial computational time and effort, in addition to the model preparation process. DTA models can supply the traffic volume input data required for microsimulations and they can be administered more efficiently for analyzing large areas.

While a number of useful tools have been identified for processing and evaluating outputs from DTA software in a user-friendly format for traffic engineers and construction management personnel, these tools are inherently dependent on the quality of the analysis results. A special process is needed to properly analyze the area impacted by a TCP and provide adequate results in an efficient manner. The goal is to maximize accuracy while minimizing the computational time to complete an analysis. The following sections detail the problem description and subsequent objectives identified for this research project.

Problem Description

The ArcGIS tool created for the TxDOT Dallas District enables the user to evaluate the pre-construction traffic volume versus the adjusted capacity of a roadway due to

construction impacts along TxDOT operated roadways. However, this capability provides a limited understanding of the impacts to traffic in the area, extending beyond the TxDOT roadways, particularly when capacities calculated by the software reach levels at or below the currently observed volume. Issues stem from the fact that volume-to-capacity (V/C) ratios do not provide a thorough measure of congestion, such as density, travel time, or queue length, and they cannot account for upstream impacts caused by capacity restrictions or bottlenecking. Therefore, the tool makes no adjustment to account for problematic V/C ratios and how they may cause changes to travel paths and resultant traffic volumes compared to pre-construction conditions. It also lacks the ability to calculate anticipated changes in travel time or speed along the impacted roadway caused by congestion.

Furthermore, the tool does not have the capability of assessing impacts to the surrounding network, including upstream links, due to changes in travel behavior exhibited by roadway users. DTA provides a means of simulating traffic and determining travel behavior along network roadways, as well as how that behavior changes with time. Additionally, it has been demonstrated as an effective means of evaluating the impact of construction projects on area traffic, specifically those impacts occurring beyond the immediate vicinity of construction activity (Pesti et al., 2010). Monitoring mobility impacts in and around work zones, including congestion, has been noted as important in the successful development, implementation, and evaluation of TCPs (Kim et al., 2008; Ullman et al., 2009). Therefore, the ability to accurately predict the scope and magnitude of these impacts using DTA models can be an extremely valuable tool for use in the construction planning process.

Unlike static traffic assignment (STA) models, which allow V/C ratios to defy real-world limitations and exceed one, DTA models prevent volumes from surpassing available capacity by propagating congestion upstream of bottleneck locations. Therefore, instead of simply identifying the link causing the problem, where V/C ratios approach or exceed

one, DTA models represent the impact of a bottleneck on upstream links, along with the adjacent network, by simulating queuing and the rerouting of traffic as users migrate to alternate paths. This provides a more accurate representation of the real impacts of network modifications on the surrounding network, such as those initiated from a TCP.

The downside is that running a network model using DTA takes much longer than an STA model. It has been stated that DTA models take, on average, ten times longer to run than an STA model for the same network (Daganzo, 1995). This is due to the fact that DTA models require extensive time-dependent inputs and iterative solution algorithms. While STA analyses take less time to complete and provide valuable information for long-range planning, they rely on the assumption that the rate traffic leaves each origin is a constant function over a given time horizon (Merchant and Nemhauser, 1978). This assumption has been shown to be impractical for real-world scenarios, particularly with respect to short-duration analysis time periods. Due to the temporary nature of construction phases and roadway configurations during related activities, short-duration analyses are imperative for the proper evaluation of TCPs. Therefore, the use of DTA analyses as a tool in this process, though more computationally intensive, appears justified.

Currently, there exist base DTA models created by CTR for the DFW region, the Austin region, and the Austin downtown network. As an example, setting up and completing a DTA model analysis for the evaluation of a TCP using the entire DFW network would require weeks of computational time even though, theoretically, a much smaller portion of the network would be significantly affected by a work zone. A technique that will intelligently choose only the critical portion of an urban network surrounding a designated work zone, enabling completion of a DTA analysis in much less time, is needed. This technique has been identified as subnetwork analysis.

While performing a DTA analysis on a full network can take days or even weeks to complete, reducing the size of the analysis to a subnetwork could drastically reduce the necessary computational time required to provide sufficient results for the impacted area. The trade-off when using a subnetwork analysis is the accuracy of results. If one truncates the network, impacts to driver behavior occurring beyond the boundary are likely lost. However, steps can be taken to ensure that the network components included in the subnetwork are those that absorb the majority of the impacts of the TCP, or at least the primary impacts. Furthermore, techniques can be implemented to estimate the effect of changes in travel behavior occurring outside the subnetwork in order to include a simplified, and much less computationally burdensome, account of these impacts in the analysis results.

There currently exists a process for completing a DTA analysis on a subnetwork that was initiated by researchers at CTR. This strategy involves setting the boundary for the subnetwork based on engineering judgment, where the boundaries are existing nodes, or intersections, in the larger network. These nodes are then modified to become new origin-destination (O-D) centroids in the subnetwork. The destinations of all inbound and outbound vehicles passing through the new centroids are extracted and the information is used to generate a modified O-D matrix. Available traffic counts at these locations may be used to update demand proportions at each centroid; however, the network elements surrounding the subnetwork are subsequently ignored.

While this process greatly simplifies the analysis, it fails to capture changes in route-choice behavior that may occur outside the subnetwork that impact trip entry and exit points along the boundary as this detailed information is not available from traffic counts. The simplified process may be adequate if network impacts are caused by a random incident with a short-range area of influence; however, for a TCP, it is likely that at least a portion of users would be aware of the construction activity prior to leaving their point of origin. In other words, commuters could choose a different route to work before

leaving their home based on knowledge of construction within the network impacting their typical route. This decision would not be captured using the above method. Therefore, to more accurately analyze the subnetwork, a more intricate process of treating the surrounding network and subsequent user decisions is needed. A process for taking into account trips traversing the subnetwork that originate outside of the subnetwork will have to be derived to properly model changes in user behavior that occur on the surrounding network.

Ultimately, subnetwork analysis capability is intended to allow an analyst to run a traffic simulation model on a specific portion of a larger network. A properly implemented subnetwork process would enable one to complete a detailed DTA model of only the surrounding roadways impacted by a TCP, while simultaneously taking into account external impacts in an efficient and accurate manner. This would greatly reduce the computational resources required to run a simulation, providing practical results for the software user in a timely fashion. While a subnetwork analysis strategy has been developed for static network analyses, the capability within a DTA framework has not been fully established for this type of application. As such, instituting a process for performing DTA with subnetwork analysis capability would provide numerous benefits for assessing area traffic impacts relative to network modifications, proving especially useful for the evaluation of TCPs. Furthermore, the results and visual tools provided can be developed to include useful assessments of network performance measures.

Research Objectives

The primary objective of this study is to provide and evaluate a methodology for performing a DTA analysis on a portion, or subnetwork, of a larger network that produces accurate results while requiring only a fraction of the computational time of reanalyzing the entire network. With respect to this objective, there are two main questions that this research proposes to answer. First, is there a size of subnetwork one

can select such that the impacts to travel behavior are largely contained within the chosen extents? Second, for a given subnetwork size, if we know that changes in travel behavior are likely to occur externally, is there an efficient strategy for adjusting the demand at the subnetwork boundary to reflect these changes and more accurately account for subsequent impacts within? Therefore, there are two primary components of the strategy for implementing a subnetwork analysis for use with DTA.

The first involves developing a process for selecting an adequate portion of the complete network. The subnetwork must be large enough to include the roadway links most significantly impacted by a network modification, while being small enough to minimize the computational requirement. The accuracy of the results relative to a full network analysis depends on ensuring that all, or the majority, of impacted links are included in the subnetwork. One of the challenges is discerning the proper subnetwork size for different impact scenarios. Outlining a strategy for choosing an appropriate subnetwork size relative to an impact scenario, as well as identifying proper procedures for selecting network elements and analyzing a subnetwork using a DTA is important for completing this objective.

The proposed approach for accomplishing this task involves an in-depth assessment of DTA models, including subnetwork analyses, for different impact scenarios. An attempt is made to answer the first question posed above by assessing the demand at the boundary of the subnetwork for different sizes. This is based on the process developed by CTR that establishes the boundary demand based on vehicle flows extracted from the full model's results. As such, if the demand between the base and impact scenario is consistent across the boundary, then one may conclude that only marginal impacts extend beyond. Conversely, if impacts occur throughout the external portion of the network, then the demand at the boundary of the subnetwork is likely to be significantly different.

The second part of the strategy involves accounting for the portion of the greater network not included in the subnetwork. It is believed that answering the second question can be accomplished by evaluating techniques for making necessary demand adjustments at the subnetwork boundary. Route choice behavior in traffic assignment models is commonly based solely on travel time or, more specifically, reducing individual user travel times throughout the network. Therefore, changes to traffic flow, and subsequent estimates of demand at the subnetwork boundary, attributable to user behavior are anticipated to be influenced by changes in travel times within the subnetwork. If a network modification causes travel times to increase in the surrounding vicinity, users are anticipated to change their route in an attempt to minimize their travel time. Therefore, focusing on the assessment of travel time changes occurring within the subnetwork due to a network modification appears essential to the task of determining what, if any, adjustments to the boundary demand are necessary.

In all, the boundary demands extracted from the full models for both the base and impact scenarios, as well as those modified to account for impacts beyond the subnetwork, can be evaluated across multiple model runs using statistical analysis processes. The accuracy of the subnetwork model results relative to a full network analysis across different subnetwork sizes can also be evaluated by investigating aggregate measures of internal travel times. It is intended that this evaluation be used to provide recommendations or guidelines to aid in the selection and analysis of subnetworks for different impact scenarios.

The steps involved with achieving the primary objectives will include developing the methodology using a prototype network, testing and evaluating that methodology, and establishing a process for implementation. Assessing the validity of the results for the subnetwork analyses will require running the full network under different TCP scenarios to test and cross-check the results. Therefore, the Austin downtown network has been chosen as the prototype for this study. The Austin downtown network has been created

and updated to include nearly all roadways within the boundaries. Furthermore, the network has been calibrated thoroughly using existing traffic counts and signal timing information from the City of Austin. Despite this level of detail, it is a smaller network and does not require many hours or days to complete a DTA analysis on its entirety. Demonstrating application of the methods developed using a larger, regional network is important. This implementation can fully exhibit the value of subnetwork analysis in terms of computation time and space savings required for analyzing an impact scenario.

Additional secondary objectives for the study revolve around generating, visualizing, and reporting results from the analyses conducted. There are a number of manual and automated processes and procedures to be implemented to complete the project objectives. Several of these processes have been initiated by CTR, but a number of new tools, scripts, and processes are required. This necessitates the use of multiple software programs, including ArcGIS, for selecting subnetwork elements, compiling data, and displaying results in a standardized and consistent manner. Direct measures of network performance can also be extracted from full-network and subnetwork DTA analyses. Reviewing different models and scenarios requires the capability of properly evaluating network conditions, both before and after network modification, through the provision of traffic performance measures.

The above objectives, ranging from selection and evaluation of a subnetworks using DTA to compilation and visualization of model results, demonstrate the versatility and substance of the proposed research. DTA models have been shown to provide valuable insight into the spatial and temporal impact of modifications to a transportation network, capturing changes in user behavior and subsequent traffic congestion. This is of great interest to traffic engineers and construction management personnel who are in charge of designing and evaluating TCPs and other network modifications. Furthermore, evaluating DTA model results with the aid of visualization tools span both planning and engineering applications.

3. LITERATURE REVIEW

A literature review was undertaken to obtain the information necessary to support development of solutions to the research problem and completion of the proposed objectives. A large amount of research has been completed detailing development and use of DTA models to more accurately describe the nature of user behavior and subsequent impacts on network traffic flows and congestion. In large part, the use of DTA has been initiated to better capture the impact of congestion on a network, a valuable tool when determining the impact of incidents or changes to network components. To do this, DTA models must adequately describe the propagation of traffic flow across links and nodes. As such, DTA models have evolved accordingly and a number of techniques, including advanced traffic flow models, have been established.

In addition, the use of subnetworks for analyzing the localized impacts of incidents or network modifications has been introduced for a number of real-world and theoretical applications. These initiatives have dealt with the process of selecting the subnetwork elements and subsequent verification of the accuracy and adequacy of the results with respect to full network analyses or actual traffic counts. Since use of subnetwork analysis involves potential adjustments to demand for these models, strategies to account for changes in travel behavior beyond the subnetwork boundary have been initiated. Other applicable tools have also been demonstrated. Uses of subnetwork analyses have ranged from STA theory and network adaption to DTA analysis, covering an assortment of applications.

Additionally, the use of DTA analysis results for creating visuals and interfacing with other types of software packages has some precedent. While many of these applications are in early stages of implementation, they demonstrate the vast potential for DTA analysis and its wide-range of functionality. Furthermore, the use of network analysis results for planning and engineering purposes, including applicable performance

measures, has been in practice for some time. The use of GIS tools for compiling and displaying these results has precedence.

The discussion of these important aspects related to the proposed research is found in the following literature review sections. The review begins with an overview of fundamental concepts relative to the proposed research, followed by a discussion of the theory and applications of DTA analysis, including a description of the cell-transmission model utilized by the VISTA DTA software. Subsequent sections detail the theory behind the development and use of subnetwork analysis and a discussion of the use of network analysis results for planning and engineering purposes, including GIS applications.

Fundamental Concepts

Traffic assignment represents the fourth step of the traditional four-step transportation planning model or Urban Transportation Model System (UTMS) [1) trip generation; 2) trip distribution; 3) mode choice; 4) traffic assignment] (Hanson and Giuliano, 2004). This planning model became standardized by the Bureau of Public Roads (BPR) in the 1960's. While each step is inherently valuable for transportation planning, the traffic assignment step is a critical component for determining where traffic congestion occurs on a network, a fundamental attribute of immense value to traffic engineers, whose accurate prediction and adequate treatment is too often elusive. Newer planning models with additional stages have been developed as part of state-of-the practice procedures for metropolitan planning organizations; however, the traffic assignment step remains the last component, thus driving the output for all planning applications (Hanson and Giuliano, 2004). To set the stage for network modeling, one must begin with the fundamental composition of a transportation network as derived from the basic foundation of roadways and intersections.

A typical transportation network can be fundamentally divided into a series of nodes, representing intersections, and links or arcs, commonly representing roadways connecting these intersections. The combination of these two elements provides the basis for the physical network, often called a graph. Certain nodes, called centroids, act as specific origins and/or destinations for users traversing the network and are paired to characterize specific trips. Typically, centroids represent the centers of mass of geographic areas having approximately homogenous trip-related activity. These geographic areas or zones could be census tracts or traffic analysis zones. Special links, called connectors, join centroids to the basic nodes and links that represent actual streets or highways. The number of trips between each origin and destination pair, for each accessible mode of transportation, is derived from the first three steps of the transportation planning model and is usually represented in an origin-destination (O-D), or demand, matrix. This leaves the last step of routing traffic through the network between the origin and destination pairs, or traffic assignment.

To establish a means of assigning traffic to a network, a level of service or level of impedance must first be defined for each link. This impedance is represented by travel time, cost, safety, or some other measure attributable to the relative impediment associated with using a link. For use in transportation networks, link impedance must be designated using mathematical functions dependent specifically on the amount of flow assigned to a particular link. While impedance can be described using a number of values, it is typically represented in terms of travel time, as travel time has been determined to be the primary deterrent to traffic flow and is highly correlated with most other cost measures (Sheffi, 1985).

As such, link performance functions are used to describe travel time on a given link as a function of its traffic volume. These performance functions depend on the basic assumption that travel time increases as flow increases and have been adapted to a specific format by the BPR (Sheffi, 1985). The resultant form of these equations defines

travel time on a link as a function of its free-flow travel time, traffic flow, and capacity. These functions are commonly used in transportation flow theory and, along with demand functions, which describe the number of trips between each (O-D) pair, are essential to the development and stabilization of traffic assignment models. These models are dependent, not only on the functions discussed above, but on the underlying theory of network equilibrium.

Traffic assignment models rely on several fundamental concepts used to describe network user behavior. The primary theory is the principle of user equilibrium, which states that the travel times on all *used* paths between a specific O-D pair are equal and minimal (Sheffi, 1985). In other words, any route chosen by users between an origin and destination is one with the least amount of travel time. All available paths that result in a longer travel time will not be utilized. This principle is based on several assumptions, the first being that users have perfect knowledge of the network and the travel times required to traverse each path. Second, it assumes that users will make the correct decision regarding route navigation that effectively minimizes their travel time, and that all users exhibit identical behavior (Sheffi, 1985).

The next related postulation is the shortest path assumption, which states that users will always choose the route or path between O-D pair that minimizes their travel time. This is a key element used to describe route choice behavior and the input parameters for mathematical functions used in quantitative analyses. While each of these assumptions can be argued on their validity or merit, the underlying idea that users seek to minimize their travel time is relatively sound when considering the travel most commonly forecasted, and a primary component of peak period demand, the home-based work trip or commute.

Another strategy developed for minimizing travel times or user costs is the system-optimization program. This condition results from users making individual route choices

with the goal of minimizing the total system travel time, or the total travel time for all users on the network (Sheffi, 1985). While this strategy results in optimal network conditions, it is not considered to be stable as it does not adequately represent actual behavior or equilibrium unless congestion is ignored. It often yields a flow pattern with lower travel times, but its value is limited to providing a benchmark solution for comparison with user equilibrium results.

For many traffic assignment models, establishing network-wide user equilibrium requires updated values of travel time generated by link performance functions. Specifically, modeling route choice behavior based on the goal of minimizing overall user travel times requires the definition of individual link travel times, changing as a function of the assigned flow. The equilibrium of user travel times can be achieved iteratively as users are loaded onto a network and travel times are updated via the performance functions. However, the use of link performance functions contains a fundamental flaw; they remain consistent regardless of changes to the network over time, a characteristic rarely observed in the real world. This constant relationship provides the basis for static traffic assignment (STA) models.

For travel forecasting models, cost and time of travel are critical components in their influence of travel choices (Chiu et al., 2011). STA models are often used to determine these measures for a network; however, the variables utilized in this process do not vary with time. Although STA is good for estimating long-term traffic forecasts at a macroscopic level, it has a number of limitations beyond the failure to account for time variability, most notably those identified below (Chiu et al., 2011).

1) **For a given link, inflow is always equal to outflow.** Travel time increases indeterminately as the volume on a link increases, even to a point beyond which volume exceeds capacity (V/C > 1). When this occurs, STA models identify congestion occurring on that link alone.

2) **A volume-to-capacity ratio (V/C) greater than one may occur.** However, use of V/C ratios does not directly correlate to congestion. A V/C greater than one only implies congestion will be present, but does not necessarily mean that the true congestion will be on that particular link. In fact, it is more likely to be present upstream of the bottleneck. Furthermore, capacities generally do not correspond to maximum link flows; therefore, the identified link volumes are commonly associated with the demand, not the actual accommodated flow.
3) **Queue spillback is not represented.** Since capacities can be exceeded, queues do not form on links and thus, the spillback of congestion onto upstream links cannot be readily identified.

As a result of the stated deficiencies, STA procedures are inadequate to properly evaluate transportation networks and impacts due to changes within (Chiu et al., 2011). DTA is seen as a means to provide a more detailed analysis of traveler choices and traffic flows, as well as cost and time measures, and how they vary over a specified time period. The following sections detail the history, underlying theory, and basic framework of DTA models and how their use can be valuable for forecasting travel behavior and traffic flow, particularly with respect to the impact of TCPs.

Dynamic Traffic Assignment Theory

Since the 1970's, researchers have been developing and improving methods for modeling time-variable travel behavior in order to more adequately forecast how network flows change throughout a peak period or over the course of an entire day. These efforts have been made in response to the limitations of STA models, which are unable to provide disaggregate, hour-to-hour flows and related travel times. DTA provides the ability to investigate hourly changes in traffic flow with the flexibility to analyze regional or corridor level travel behavior (Chiu et al., 2011). DTA models have recently become a practical option for modeling traffic as a supplement for existing static models and

microsimulation tools. The continued development of DTA theory and subsequent simulation models for real-world applications has provided the necessary means of time-dependent traffic flow modeling.

An Overview of Dynamic Traffic Assignment

The concept of implementing time-variable traffic assignment theory goes back to 1978, when Merchant and Nemhauser introduced an algorithm for DTA using mathematical programming (Merchant and Nemhauser, 1978). Merchant and Nemhauser point out that STA relies on the assumption that the rate at which vehicles leave an origin traveling to a specific destination remains constant over time. However, in reality, this assumption is fundamentally flawed even when investigating travel behavior over a short amount of time, such as a peak period. To provide a more practical representation of traffic, one must take into account time-variant demand, essential for modeling the impact of congestion on the network.

More recently, researchers have defined DTA as a type of problem that incorporates decision variables, behavioral and system based assumptions, and data representing a traffic system, including time-varying flows (Peeta and Ziliaskopoulos, 2001). DTA models are unique in that they represent traffic dynamics and human behavior and as such, are characterized by more random and complex inputs. As a result, DTA models do not generally provide explicit solutions; instead, methodologies are used to derive more heuristic outcomes. This represents a departure from the more deterministic realm of STA. Solution methodologies vary between analytical and simulation-based approaches. Although mathematically complex and devoid of exact solutions, DTA models can be used to provide real-world representations of traffic flow and congestion.

Fundamental to DTA applications, traffic flow dynamics allow for a direct connection between travel time and congestion (Chiu et al., 2011). If link outflow is less than link

inflow, congestion occurs and subsequent link travel times increase as a result. This often occurs at a bottleneck in the system, or where a capacity reduction occurs. DTA models simulate flow such that congestion causes queuing to form on the impacted link, beginning at the end of the link. This continues until the queue reaches the link entrance, at which time the inflow equals the outflow and the link enters a steady-state condition. When this condition is reached, queue spillback occurs. While not characterized by STA models, this phenomenon can be propagated throughout a network using DTA modeling techniques.

DTA expands on the idea that users will choose a route with the purpose of minimizing their individual travel time or some other measure of associated cost or disutility (Chiu et al., 2011). The interactions between users are modeled using traffic assignment algorithms and iterative procedures designed to satisfy the user equilibrium condition. For DTA, modifications to the traditional user equilibrium approach are required. Users are assumed to modify their paths en-route based on prior experience, and the ability to anticipate future conditions in order to minimize their experienced travel time (Chiu et al., 2011). This concept initiated development of the time-dependent shortest path algorithm, which takes the place of the original version that uses a snapshot of travel times.

Formulation of a time-dependent shortest path algorithm began with modifications of the static approach (Ziliaskopoulos and Mahmassani, 1993). This involved determining shortest paths between origin and destination centroids based on the departure time for each vehicle. This methodology was then refined for more universal application with real-world networks accommodating all specified time intervals.

In a series of technical papers, time dependent or dynamic shortest path algorithms were investigated. The underlying concept is that the dynamic shortest path algorithm must determine link costs or travel times dependent on the link entry time (Chabini and Dean,

2000). In other words, all link costs are associated with a specific departure time and, as such, are indicative of variability with respect to time. The resultant algorithm structure is imperative for accurate, real-time DTA models.

Research completed at the Massachusetts Institute of Technology investigated shortest path solutions for discrete time networks, and algorithms were formulated for implementing in transportation analysis applications. The developed algorithms offer efficient means of providing shortest path solutions while analyzing the wait time at nodes (or intersections) by use of deterministic discrete time intervals (Chabini and Dean, 2000). It was determined that using discrete time measurements enabled the storage of necessary network data using minimal computer memory.

Subsequently, a number of algorithm structures were derived based on specific objective functions, constraints, source/destination classifications, and network data structures (Chabini and Dean, 2000). The objective most commonly utilized in transportation analyses is the minimum travel time function, thereby implying that users will choose routes that minimize their individual travel times. Additionally, DTA is often easier to solve in networks consistent with the FIFO condition. Therefore, the shortest path problem is set up imposing a cost constraint on waiting at a node with an upper and lower bound consistent with the FIFO condition. The optimal algorithm is then designed by determining either the shortest paths from a single origin to all potential destinations, or from all potential origins to a single destination, and looped for each discrete departure time over a preset horizon, then repeated for each source or destination throughout the network. This time dependent shortest path (TDSP) algorithm structure was rigorously tested for computational efficiency and proven optimal for use in DTA problems for transportation networks.

Furthermore, the DTA problem requires that the user equilibrium principle be expanded to cover each departure time individually instead of the entire analysis period, resulting in

what is known as dynamic user equilibrium (DUE) (Chiu et al., 2011). As such, time dependent route choices for users leaving an origin are dependent on congestion levels caused by users who have an earlier, same, or later departure time. This requires an iterative process that, for most large networks, cannot be solved exactly and thus, leads to a heuristic solution.

Important characteristics of DTA models:

1) Vehicles departing at different times are assigned different routes depending on conditions of the network (Chiu et al., 2011).
2) Vehicles departing at the same time between the same O-D pair, but taking different routes, should have the same experienced travel time.
3) Experienced travel time is only realized at the end of the trip (not at departure).
4) Time-varying traffic flow conditions occur on the network (Peeta and Ziliaskopoulos, 2001).
5) Randomness associated with traffic flow dynamics and human behavior is incorporated.
6) A universal or necessarily unique solution is not provided.
7) Models are not characterized by standard mathematical properties.
8) The process fosters both analytical and simulation-based approaches to solution methodology.
9) Models are used to represent real-world characteristics of traffic flow.

DTA models are designed to provide route travel times, determine updated shortest paths at different time intervals, and assign vehicles to routes to approximate DUE (Carey and Subrahmanian, 2000; Chiu et al., 2011). Essentially, these three components comprise the necessary features for any software package to be capable of performing DTA. DTA models typically determine travel times resulting from route choices and load vehicles on the network with assigned paths based on the lowest possible travel times for each O-D pair (Chiu et al., 2011). After each time period, the shortest path set is updated and

vehicles with the current departure time are loaded and those already on the network are rerouted, accordingly. As vehicles are routed and rerouted through the network to the new shortest paths, the system moves closer to equilibrium. It should be noted that this process is done carefully to ensure that traffic isn't shifted in a manner that would overcorrect for the travel times. Only a portion of vehicles are moved, and are moved to a number of the shortest paths. Once vehicles have been assigned, the process repeats until a specific end criterion or convergence is reached.

DTA models can be evaluated for solution sensitivity and stability (Chiu et al., 2011). The extent a solution varies as a function of parameters can be measured such that the impact of changes to the network, such as those prescribed in TCPs, can be evaluated. The gap criterion for convergence can also influence the stability of the solution reached when the algorithm terminates. If modifications to a network are to be properly evaluated, such as a change in capacity, the individual equilibrium solutions for each alternative must be determined at a greater precision than the difference in the solutions found. Otherwise, the disparities could be attributed to imprecision in the results obtained and any real differences could be obscured.

It is important to note that research of DTA models has shown that minor modifications to the network should not result in significant impacts to flows or conditions far from the location of the change, such as a capacity reduction typical of a TCP (Chiu et al., 2011). If these impacts are observed, it may be evidence of a problem with the DTA solution and should be scrutinized accordingly. One way to do this is to analyze the DTA model using more strict convergence criteria. It should, however, be noted that when a network exhibits considerable congestion and queuing, small perturbations may result in substantial impacts. This demonstrates the need to thoroughly evaluate the results obtained when examining alternative scenarios.

For DTA models, the spatio-temporal vehicle trajectories can be characterized and subsequent travel times and congestion measures can be extracted. This allows for compiling more realistic and useful results when compared to STA models. DTA outputs can be used to find time-varying speed, travel time, queue lengths, routes, average densities and flows, and volume profiles. DTA models typically allow for mesoscopic simulation, which is more computationally efficient than microscopic simulations for larger networks, though the results are more aggregate. Furthermore, it provides a more detailed review of traffic operations than macroscopic analyses that are unable to generate the level of resolution needed for extracting speed, density, and flow rates (Florian et al., 2008; Kamga et al., 2011; Pool et al., 2012a). Mesoscopic models can simulate intersection and link-specific properties, useful for evaluating traffic flow. Providing a level of detail beyond STA models and a computational savings over microsimulations, DTA models demonstrate their versatility for use with transportation networks of varying size, including city-wide or corridor-level analyses.

A number of tools and models are available for analyzing different aspects of existing and planned transportation systems, including macroscopic analytical methods and microscopic simulation models. Many microsimulation models use distinct route choice behavior to determine how simulated vehicles select and update their route (Chiu et al., 2011). Typically, these choices and updates are based on instantaneous travel times measured at the time the vehicle departs, without consideration of subsequent congestion generated in later time periods. While instantaneous travel time information may indeed be available to a user, researchers have determined that actual route choice behavior is often dependent on experienced travel times.

Experienced travel times are based on user knowledge of the conditions of a network based on previous experience and the anticipation of congestion along particular route options (Peeta and Ziliaskopoulos, 2001). Accounting for this experience in a traffic model requires an iterative process designed to incorporate the learned behavior of users

such that they will adjust their route choices until a shorter experienced travel time cannot be achieved. DTA models utilize the iteration process to adjust user route choice behavior to be consistent with the minimum experienced travel time. These experienced travel times must be used for determining route choices, not instantaneous travel times even if route updating is applied; otherwise, they are not true DTA models (Chiu et al., 2011).

This concept signifies an attempt to model real behavior, based on user experience, not instantaneous decisions made en-route based on short-term information. Instantaneous travel time is typically used for STA models and microsimulations. Experienced travel times are often different, and resultant route choices may differ since link travel times typically vary depending on the arrival time at the upstream node. This is not captured when using instantaneous travel times, since the travel time is assumed to be the same on downstream links as when the vehicle originally departs the origin, or whenever the instantaneous travel times are observed.

A comprehensive review of prevailing research revealed DTA models can be formulated using mathematical programming, optimal control, variational inequality, and simulation-based approaches (Peeta and Ziliaskopoulos, 2001). Specifically, the research presented herein utilizes a simulation-based DTA model. Therefore, this methodology is discussed in more detail in the following subsection.

Simulation-Based Dynamic Traffic Assignment Models

DTA models are often designed to incorporate some simulation logic while being more computationally efficient in order to encompass corridor specific traffic flows and en-route changes across a regional network (Peeta and Ziliaskopoulos, 2001). Specifically, simulation-based DTA models use a traffic simulator to generate traffic flows and represent real-world traffic dynamics (Carey and Subrahmanian, 2000; Peeta and Ziliaskopoulos, 2001). Instead of utilizing analytical evaluation to solve the DTA

problem, this methodology addresses flow propagation and spatio-temporal relationships using simulation. This is done since mathematical formulations for these complex interactions are not readily available (Peeta and Ziliaskopoulos, 2001). The idea is to provide a solution that, although not derived analytically, is more meaningful from a practical standpoint. Since the simulator is used to determine the optimal solution, it should be noted that the network's level of detail has implications in terms of computational requirements.

Several simulation-based mechanisms have been created and implemented, including iterative algorithms used to obtain both user equilibrium and system optimal solutions (Peeta and Ziliaskopoulos, 2001). Information about O-D demands over the entire planning horizon, along with a combination of both microscopic and macroscopic user characteristics have been used to find computationally feasible solutions. The traffic simulator is used in place of complicated analytical formulations for use with general networks. Modeling different user types with varying levels of available information and behavioral responses can be more computationally inefficient when modeling real-world network conditions. In addition, the use of a simulator in conjunction with an iterative process can result in a substantial computational burden, and the DTA simulation may not be feasible for large-scale networks without careful consideration of the model construct.

Recent developments have implemented effective computational procedures requiring fewer inputs to generate realistic solutions (Peeta and Ziliaskopoulos, 2001). Several DTA models have also incorporated forecasted traffic conditions to supplement existing information to predict O-D demands. This strategy, combined with the use of mesoscopic traffic simulators has been successful at modeling traffic flow. Simulation models address many of the limitations of analytical formulations, with few drawbacks.

Improvements in modeling techniques, along with their inherent capabilities, enable DTA to be used for a wide-array of applications (Peeta and Ziliaskopoulos, 2001). The need to implement DTA for modeling large-scale networks using both robust and computationally efficient solution methodologies has encouraged advancement. Research has been completed with the goals of improving algorithm formulation, consistency verification, robustness and stochastic system inputs, stability, and demand estimation and prediction. However, there are a number of factors that can hinder DTA simulation models, including incorrect estimations of time dependent O-D demand and invalid assumptions about driver behavior patterns, user information levels, and system related parameters.

Many of the aforementioned shortcomings can be mitigated using real-time data as inputs; however, this information is rarely available to incorporate in an efficient manner. In addition, random inputs that influence the performance of DTA models include demand, supply (incidents), and user classes. Those models that incorporate uncertainties in order to enhance system performance are considered to be robust, and those that demonstrate the ability to provide reliable results regardless of conditions, are deemed stable. Furthermore, the capability of the DTA model to predict time-dependent demand, and subsequently load the network, is essential for accurately modeling traffic flow. It is perhaps the most challenging step in DTA applications.

This use of time-dependent demand in DTA models allows for a relaxation of steady-state user equilibrium assumptions (Peeta and Ziliaskopoulos, 2001). In other words, constantly changing demand and traffic conditions, along with the stochasticity of network parameters, challenges the notion that true user equilibrium is ever really achieved. Flow propagation and modeling traffic flow along links and throughout the network are other fundamental issues involved with DTA modeling. Strategies have included link performance functions, dominant in STA modeling, and exit functions in the past; however, the use of hydraulic flow theory coupled with fundamental traffic

engineering concepts has yielded more effective strategies. The following section provides an overview of the progression from early dynamic flow models to more modern techniques used in DTA software packages today.

Development of a Traffic Flow Model

The traffic flow model is one of the most critical underlying elements for establishing a realistic DTA model (Bar-Gera, 2005). Flow models are used for determining how traffic moves along a link, resulting in an estimate of link travel time, and are typically simplified in order to save computational time (Carey and Subrahmanian, 2000). The first traffic flow model, developed by Merchant and Nemhauser, involved a time-variable flow rate loaded on a network with a single destination and discrete time intervals (Merchant and Nemhauser, 1978).

While the early model addressed many shortcomings of STA, it failed to account for queue spillback or the ability to adequately model where true congestion lies on the network, and relied on the assumption that all vehicles traversing a link have the same delay. The use of exit functions as part of the Merchant-Nemhauser model was limited by the lack of accounting for the impact of downstream congestion. It was also designed for a simple network representation and was not efficient for solving complex networks with multiple O-D pairs. As a result, other methods were introduced to account for these deficiencies, including the point queue model.

The point queue model implements fundamental traffic engineering measures, capacity and free-flow time, to solve DTA in continuous time. This model involves dividing links into a physical section, representing the length of the link over which vehicles traverse at free-flow speed, and a point queue at the end of the link, representing a conceptual space where vehicles are held until they can be released to downstream links. While the point queue model can represent link congestion and resolves the limitations of exit functions,

it allows for queues to form without taking up physical space. This unrealistic assumption fails to account for queue spillback from one link to the upstream link(s). To adequately describe how queues form and interruptions can impact flow upstream and downstream of their occurrence, flow theory was developed to apply fundamental relationships between speed, density, and flow as established in the Lighthill-Whitham-Richards (LWR) model.

This model was used to represent flow as a function of speed and density, and facilitated the identification of changes in flow rate or density along a section of roadway or link at a particular time, called shockwaves, using kinematic wave theory (Lighthill and Whitham, 1955). This theory was originally formulated for describing fluid motion, but was effective in later application to traffic flow dynamics in the LWR model. As such, the graphical representation of shockwaves and mathematical derivation of shockwave speeds enable the subsequent detection of queue spillback. Essentially, queue spillback occurs when the backward propagation of queue dissipation (shockwave 1) does not overtake the upstream propagation of queue formation (shockwave 2) prior to when it reaches the begin-point of a link. The derivation of shockwave speeds and flow-density relationships involves a complicated series of differential equations. Therefore, research was invested in developing a simplified method for solving the LWR model.

A simplification of the LWR model was proposed in the early 1990's by evaluating cumulative flows, or number of vehicles passing a location by a specified time, solely at initial conditions and boundary points (Newell, 1993a). The graphical representation of cumulative counts at these boundary conditions can be used to establish estimates of the queues at a specific point in time on a link and observed link travel times. This enables one to investigate the properties of shockwaves at boundary points alone using graphical or numerical techniques, a process that greatly simplifies their assessment.

The resultant process became known as Newell's Method and was derived using a triangular shaped representation of the flow-density relationship through linear wave speeds, one for free-flow travel (positive slope) and the other for propagation of traffic congestion (negative slope) (Newell, 1993b). This simplification allowed for the classification of traffic conditions for any measure of flow rate, at a specific location and time, as either free-flow or congested. This methodology was verified as an adequate strategy for evaluating congestion and subsequent queuing caused by bottlenecks, such as freeway merge points, and was later developed into a dynamic flow model incorporating multiple departure times and O-D pairs (Newell, 1993c). Newell's Method represented a major breakthrough in flow theory and paved the way for other approximations of the complicated LWR model through utilization of simplified representations of the flow-density relationship.

Two additional, related methodologies for modeling traffic flow using kinematic wave theory were later developed, the cell-transmission model (CTM) and the link transmission model (LTM). In general, the CTM represents flow along a link as a function of free-flow speed, maximum flow (or capacity), the backward propagation of speed, and the jam density (Peeta and Ziliaskopoulos, 2001). The CTM demonstrates the implementation of hydrodynamic theory to model traffic flow (Daganzo, 1994). The method represents the change in density along a link that would be observed at shockwaves. It models this behavior, which can be used to simulate real-world traffic flow, without the requirement of complicated calculations.

For the CTM, the links themselves are divided into homogeneous cells, equal to the distance traveled at free-flow speed during one time interval (Daganzo, 1994; Peeta and Ziliaskopoulos, 2001). Vehicles are propagated through the cells based on linear constraints and the model updates conditions of the link at each time interval. Flows between cells, and subsequent links, are determined based on link and cell capacities, along with an additional term to account for queue spillback. Congestion occurs when

cells cannot accommodate upstream flows and queues propagate upstream from one cell to the next as they reach capacity. The ability of the model to duplicate real-world flow conditions has been verified using a number of simulations and analyses.

Since calculations are required for each cell at every time interval, the computational time for complex networks can far exceed that of simpler methods (Daganzo, 1995). It was found from full-network adaptation that the computational time for evaluating a network using the CTM for DTA is approximately ten times that of STA modeling. Despite the longer computational time, the CTM has been shown to be an advanced method for improving route choice predictions, adding a real-world element to the traffic assignment process and providing more practical results. Ultimately, the purpose of the CTM is to counter the deficiencies discovered using earlier methodology, such as the LWR model and Newell's method, particularly for application with larger, more complex networks.

The advantages of cell transmission include simplicity, versatility, and linearity (Peeta and Ziliaskopoulos, 2001). However, it has been shown that adherence to FIFO conditions is restrictive, and use of the CTM can cause considerable discrepancies when compared to path travel times obtained from microsimulation results (Astarita et al., 2001). Therefore, recognizing the limitations of the CTM is important and the methodology applied for the treatment of flow movement at nodes is crucial.

While the CTM divides up links into individual components, the LTM focuses only on the endpoints of the links. Essentially, the LTM isolates flows between links, as derived based on the evaluation of connected link capacities and cumulative counts at the link endpoints (Yperman, 2007). This is a simplification of the methodology developed for the CTM and is based on a computationally efficient algorithm. It results in an accurate depiction of transition flows between links, congestion, and queuing at all types of link intersection configurations while requiring less computational time and effort. It achieves this by establishing a time interval based on the time to traverse the shortest link in the

network and isolates conditions at each node such that every intersection can be evaluated independently.

While the LTM offers a strategy that can be more efficient than the CTM, it requires more computer memory (Yperman, 2007). Furthermore, current software used by CTR, VISTA, implements the CTM to depict traffic flow in its DTA analyses. Since VISTA is being used for the DTA analyses completed as part of this project, it has been described in detail herein. Overall, the CTM demonstrates a step in the progression of DTA methodology toward implementation with models for large and complex networks. The evolution of this methodology has resulted in the proper representation of time-variable travel behavior, accurate propagation of traffic flow across and between links, and analytical simplification through simulation modeling. While significant in its own right, establishing a traffic flow model represents only one of the primary components required in a DTA process.

Route Assignment

Link travel times are estimated as traffic flow model outputs at each time step in the DTA model. As these travel times are updated, new shortest paths are determined. The key at that stage is determining how many vehicles to move from the previous shortest path, to the newly derived shortest path. When a DTA model is initiated and vehicles are loaded for the first time interval, all vehicles are assigned to the shortest path derived from the assumption that vehicles are initially moving at free-flow speed. As more and more vehicles are loaded by way of the dynamic trip tables, the experienced link travel times will gradually change, particularly as congestion forms on the network.

New link travel times result in an updated list of shortest paths found using a TDSP algorithm. From this point, several methods have been developed for determining how many vehicles to move from the current route assignment to the new set of shortest paths.

The most basic strategy is the method of successive averages (MSA). This method was initially developed for use with STA; however, it has been shown to work well for use in DTA models (Mahut et al., 2004).

MSA is based on moving a predetermined number of vehicles to the set of shortest paths at each step that shortest paths are derived (Sheffi, 1985). Essentially, at each model iteration, path travel times are derived using a traffic flow model. If all vehicles are not already on the identified shortest paths, a new shortest path solution will be obtained. The assignment of vehicles to shortest paths is based on the all-or-nothing approach, whereby the entire O-D demands are assigned to the new shortest paths. However, a multiplier is used to limit the amount actually moved so that the new paths don't become overloaded and resultant travel times don't actually increase.

The multiplier used for MSA is equal to one divided by the iteration number. Therefore, a progressively smaller portion of vehicles is assigned to the newly derived shortest paths with each iteration. To determine when to stop the iteration process, a convergence criterion is set. Typically, this criterion is related to the total travel time of all vehicles on their current path, versus the total travel time they would experience if they were on the derived shortest paths for that iteration. The smaller the difference between the two, the closer the model is to reaching convergence at equilibrium.

While convergence will eventually be achieved using MSA, the progressively decreasing step size taken at each iteration means it could take a very long time. Also, setting an arbitrary factor, such as one divided by the iteration number, as the step size does not represent the most comprehensive solution method. A better process would take advantage of information obtained at each iteration, specifically, how close the current solution is to reaching equilibrium, and use it to help choose where to send vehicles (direction) and how many to send (step size). Two methods have been utilized to more intelligently determine direction and step size based on this philosophy.

One strategy developed is called simplicial decomposition. Simplicial decomposition is based on the equilibrium principle, that users will only change routes if they can minimize travel costs, and that an equilibrium solution can be obtained when all users are on shortest paths (Smith, 1979; Smith, 1983). In effect, there are many possible solutions or path sets for large networks, meaning that deriving an equilibrium solution could be a time-intensive process. To reduce the computational time required to reach equilibrium, the associated algorithm utilizes a restricted set of possible shortest paths compiled from intermediate iterations (Smith, 1983). At each iteration, a set of shortest paths for each departure time is obtained and associated travel times are derived using a traffic flow model. An all-or-nothing solution path set is derived based on these travel times and added to the restricted set (if not already included).

The identified path sets that represent lower travel times than the current solution are combined using a weighted average to determine the amount to move in each improvement direction (Smith, 1983). The weights for each direction are based on the degree of improvement, or decrease in travel time obtained, if all of the vehicles were placed on that particular path set. The new path flows are then determined accordingly. The solution conditions guarantee that the equilibrium exists and that a unique solution can be obtained efficiently; however, this is only definitive for STA and while nearly always true for DTA, is not absolutely assured. Nevertheless, the methodology has been proven for use with DTA models with the ability to achieve DUE (Smith, 1993).

Another methodology for establishing an equilibrium solution for path assignment, also developed initially for STA, is called the gradient projection method. This method is again based on the user equilibrium principle and uses a system of equations for establishing path travel times as a function of path flows. These path flows are set at each time interval based on combinations of gradients, or derivatives, calculated for estimated travel time functions for each path. The gradients are projected using Newton's Method to find an appropriate solution set for the path flows for a specific time interval. Again,

the method involves derivations that limit updates to the solution set as a combination of only those paths that would result in a travel time savings if vehicles were moved to those paths. This effectively establishes a DUE solution.

The proper development of a DTA model involves combining a traffic flow model with the ability to compute time-dependent shortest paths and establish dynamic user equilibrium. Using continuous flow trajectories based on kinematic wave theory for traffic flows and physical queues, an exact DTA formulation was created by Bar-Gera (Bar-Gera, 2005). This formulation offers a solution methodology consistent with conservation of flow, FIFO, and user equilibrium that can be applied to roadway networks. A discrete trajectory model was also created to provide an approximate solution to the continuous model, resulting in a more efficient analytical approach.

Implementation of this method allows for a user-defined aggregation level to be set to appropriately balance desired accuracy and computational time. This method was verified for application with real-world networks and demonstrated an important integration of all necessary components needed for defining a DTA model. As a result of the aforementioned contributions to DTA theory, methodology, and model formulation, the strategies developed for implementing DTA models have been demonstrated for a number of real-world applications.

Dynamic Traffic Assignment Applications

A number of DTA models and software applications have been adapted for real-world applications. Many of these models have been developed for evaluating Advanced Traveler Information Systems (ATIS) and Advanced Traffic Management Systems (ATMS). A number of other simulation-based models, included in software programs, have also been created for city networks. These models have been developed to

supplement STA models and provide real-time analysis tools for city planners and traffic engineers.

One example was the development of a route guidance component for a DTA system used to generate real-time, predication-based guidance information for travelers (Ben-Akiva et al., 1997a). The idea was to use current and predicted states of the system to make recommendations about optimal route selections, and then check for consistency between current travel times and those that result from anticipated user-route choices for each time interval. Another similar tool was designed to measure the effectiveness of ATMS applications by simulating dynamic traffic flow and the impact of real-time information on vehicular movements and route choice behavior (Ben-Akiva et al., 1997b). The developed simulator was used to monitor dynamic traffic flow and evaluate the effectiveness of an Intelligent Transportation System (ITS) for regulating control devices and providing route guidance information to users in real time. Ultimately, evaluations of network improvements and congestion levels based on predicted O-D demands for different ATMS strategies were completed using measures of traffic flows, densities, speeds, and travel times.

Other researchers have developed models to evaluate the effectiveness of ATIS tools using DTA, notably comparing the performance of systems designed to provide route guidance information based on achieving system optimal status versus user equilibrium conditions on a test network (Mahmassani and Peeta, 1993). Another, simulation-based model was created with a focus on the development of path-dynamics for analysis in support of advanced traffic management and information systems (ATMIS) for large networks (Jayakrishnan et al., 2001). The model focused on the difference between macroscopic modeling, where only nodes of significance to route decisions are represented, versus microscopic modeling, where links are divided to account for any change in geometric attributes. A hybrid approach was also presented and the model was

successfully demonstrated to handle calibration and path-related dynamics for large networks using case studies.

A simulation-based DTA model was also created to analyze a section of the roadway network in the city of Calgary, Canada (Mahut et al., 2004). A dynamic O-D matrix was created using trip generation and distribution results from a regional planning model and calibrated using turning movement counts. A comparison of the model results versus an independent set of turning movement counts yielded an R-squared value greater than 0.90 for three 15-minute time intervals evaluated during the morning peak hour. The outcome was used to show that a DTA model can provide a superior means of duplicating real-world traffic flow over STA, along with the value of model calibration.

A second DTA model implemented by the same research team was created to monitor and manage real-time ITS applications, including route guidance and ATMS (Florian et al., 2008). The purpose was to develop a method for evaluating ITS measures off-line, with the potential for embedding a DTA model on-line, within an ITS application, to provide a means of adaptive traffic management. The DTA model was created using a software code and involved dynamic route assignment with an event-based traffic simulation component. It was tested on a medium-sized roadway network for Stockholm, Sweden, and was found to provide an acceptable level of equilibrium convergence within a reasonable computational time.

DTA modeling has also been implemented for examining incident management. As part of testing methodologies for rerouting traffic around incidents on two city networks, Chicago, IL and Birmingham, AL, it was determined that DTA models could be a valuable tool for transportation agencies (Sisiopiku et al., 2007). The capabilities of DTA models for incident management was demonstrated effectively using case studies comparing network travel times when route guidance information was provided to users versus when it wasn't.

In 2011, a series of DTA models were created to evaluate the impact of incidents on a portion of the Chicago network (Kamga et al., 2011). The scenarios were evaluated by comparing measures of the total network travel time, travel time variability, and vehicle miles traveled with incidents (with and without provision of information to travelers) versus the measures obtained from a base scenario. It was determined that the evaluation provided a realistic representation of the scope and magnitude of impacts caused by incidents on a network in terms of congestion and route choice behavior.

Another DTA model was used to assess the impact of incidents on network performance to evaluate the impedance of emergency response times due to resultant congestion (Sisiopiku and Cavusoglu, 2012). It was determined that utilization of a DTA model resulted in more realistic estimates of duration and intensity of traffic disruptions. Subsequent travel times output from the DTA model were used to estimate response times for emergency services departing stations around the city, allowing for improved dispatching decisions and response operations.

Other examples of DTA applications for corridor and city-wide networks exist. In 2005, the New Jersey DOT developed a DTA model for a section of Interstate 80 to evaluate a number of deployment scenarios for ITS technologies (Chien et al., 2005). Calibrated using available traffic counts, the DTA model proved useful for demonstrating potential uses of traffic management and control devices by providing spatio-temporal vehicle trajectories, as well as establishing a tool for future transportation modeling and planning applications.

A DTA model was also created as part of a tool for assessing road construction impacts for the El Paso region (Pesti et al., 2010). The purpose was to determine the impact area and severity of construction projects in the region using realistic estimates of travel time and subsequent level-of-service (LOS) for network elements. The use of a DTA model enabled the assessment of impacts, not only close to the construction activity, but in other

parts of the network. As a result, recommendations could be made about construction timing and phasing. Lastly, a DTA application was used for the Dallas-Fort Worth region to compare the results of STA and DTA models (Boyles et al., 2008). The results indicated that STA models could substantially underestimate congestion, and accounting for time-variable demand and traffic flow dynamics using DTA models can provide more realistic route assignments.

Many of the simulation-based traffic assignment and city-wide network applications discussed above involved utilization, and in some cases development, of DTA modeling software. These software packages, including the software program used for this research, are introduced in the following section.

Dynamic Traffic Assignment Software

Evaluation of traffic impacts caused by network modifications is facilitated by the development and implementation of software capable of handling the simulation of DTA components. Again, these components are represented by including a traffic flow model, such as the CTM, the TDSP algorithm, and a method of establishing route choice equilibrium for time-variable demands or DUE. Early DTA models involved theoretical applications or case studies using simple prototype networks that could be performed using limited computational resources. Later implementation for complex, real-world networks involved developing software packages capable of handling the components of DTA simulation models.

While several software packages exist for microsimulation analysis, including CORSIM and VISSIM, they require complete and detailed network elements and inputs to properly simulate traffic flow, resulting in a substantial data collection effort and computational burden for large networks. The purpose of DTA modeling software is to predict realistic assigned link volumes through a more mesoscopic approach to traffic simulation (Florian

et al., 2008). The process sacrifices a level of precision for a reduction in the computational time necessary to perform dynamic traffic flow modeling in an efficient manner for large networks.

One of the earliest software programs used for modeling traffic dynamics is called CONTRAM (Florian et al., 2008). This software was developed in Europe and models continuous traffic flow with an iterative approach to solving DUE. Another one of the first software programs, called DYNASMART, was developed for evaluating traffic management and traveler information systems using DTA (Mahmassani and Peeta, 1993). DYNASMART had the capability of not only simulating vehicles traversing a network, but also route choice decisions made at each node along a network. Essentially, the software was used to assign demand from dynamic O-D matrices to available paths and simulate the resultant traffic flow. This early software was used to fulfill a specific role in the overall DTA process.

Another, more comprehensive, software program was later developed for evaluating ATMS applications, a simulator called Dynamic Network Assignment for the Management of Information to Travelers (DynaMIT). The purpose of the DynaMIT software was to generate guidance information for predicted departure times, pre-trip path selections, mode choice decisions, and route choice behavior (Ben-Akiva, 1997b). The software uses both historical traffic conditions and real-time information to estimate dynamic O-D matrices. Overall, the software balances accuracy and computational time in an effort to predict traffic conditions, including queuing and congestion, based on aggregate and disaggregate traffic data, for better application of ATMS strategies.

A more recent adaptation of the DYNASMART software was used for the evaluation of construction impacts in the El Paso region (Pesti et al., 2010). The software application, called DynusT, utilizes geometric attributes for roadway network elements, which can be reviewed in a GIS interface, along with dynamic O-D matrices. For the specific

application identified, construction projects were coded into the software and travel time outputs were used for establishing LOS ratings necessary to evaluate area impacts.

A specialized software package called VISTA was also created for DTA modeling applications. As mentioned previously, VISTA is the software package chosen to complete DTA analyses for this research and is therefore discussed in more detail herein. The software incorporates a JAVA-based Graphical User Interface (GUI) accessible over the internet, providing versatility, interactivity, and accessibility for users (Ziliaskopoulos and Waller, 2000). It provides access to a database structure complete with input and output data, a GIS interface for mapping and editing network elements, and files for reporting analysis results. Attributes for network elements can be modified, including link lengths, number of lanes, capacities, and free-flow speeds, along with signal timing plans at nodes. VISTA also has the capability to connect to servers for handling the substantial computational effort required of DTA models associated with large networks.

The VISTA software's functionality is controlled by its model structure, including a series of modules accessible through the user interface (Ziliaskopoulos and Waller, 2000). These modules control functions, such as traffic simulators, DTA processes, network routing algorithms, and signal optimization functions. The DTA model structure uses the CTM for traffic flow modeling, incorporates a version of DYNASMART for modeling different user classes, utilizes TDSP and routing algorithms, including MSA and simplicial decomposition, and implements a departure-based and fixed arrival time approach for simulating DUE.

Precedents for using VISTA, demonstrative of its DTA capability, include models created by the New Jersey DOT for evaluating ITS and route guidance applications, the Regional Planning Commission of Greater Birmingham for investigating the impacts of incidents on network performance, and researchers in New York for simulating DTA models for incidents with and without provision of traveler information (Chien et al.,

2005; Kamga et al., 2011; Sisiopiku et al., 2012). Perhaps more applicably, researchers at CTR regularly analyze DTA models developed for the City of Austin, along with the Dallas-Fort Worth (DFW) region. For example, VISTA was used to evaluate DTA versus STA modeling results for the DFW region (Boyles et al., 2008).

One of the key setbacks of using DTA analyses is that they can take a substantial time to build, properly calibrate, and complete. While DTA models offer more realistic results, they take a much longer computational time than STA models. The VISTA DTA model for the DFW region takes weeks to reach an acceptable level of convergence. As mentioned, a strategy to reduce the computational time has been proposed, which involves completing a detailed analysis of only a select portion, or subnetwork, of a large network, while removing or at least simplifying the surrounding network and its impact on the selected portion. The development of this strategy has some precedent in STA and the following section offers a review of relevant literature available on subnetwork analyses.

Subnetwork Analysis

The concept behind DTA analyses is to adequately and accurately represent traffic flow on a real network, while maintaining computational efficiency and mathematical feasibility (Peeta and Ziliaskopoulos, 2001). As noted, maintaining computational efficiency can be difficult, particularly when attempting to preserve the accuracy of model results. Typically, when alternate network scenarios are evaluated, DTA models are run multiple times using the entire network, though this process can be computationally inefficient. It has been suggested that if the computational time is too burdensome for large networks, the network can be divided into subnetworks (Peeta and Ziliaskopoulos, 2001).

The use of subnetworks in traffic assignment problems has definite potential, as they have been implemented for a number of STA and DTA applications. Particularly, the theory behind subnetwork analysis has been advanced within STA. This development is encouraging for proper implementation with DTA, and with the fact that DTA models take much longer to run, the possible benefits appear substantial. However, the caveat is that the established methodology is specific to STA, and any extension for use with DTA will require significant modifications. Nonetheless, the approach for developing a proper subnetwork analysis with STA is presented here to provide introductory and background material.

Subnetwork Analysis: Theory

Two primary issues arise with the use of subnetwork analyses for traffic assignment problems. The first is determination of the proper size of the selected subnetwork. The second is the treatment of the outer network, or portion not included in the subnetwork. While subnetwork selection is critical, proper treatment and estimation of route choice behavior beyond the boundary of the subnetwork can ease the burden associated with defining the limits. It could be suggested that a proper boundary be set to contain all route choice behavior influenced by a network modification. However, the involved selection strategy could vary significantly depending on the scenario, and the limits needed to contain all applicable route choices could involve selection of nearly the entire base network, thereby greatly diminishing the benefit of using a subnetwork. The development and use of subnetwork analyses as a means of achieving efficiency dates back to the 1970's; however, recent developments in strategy for use with STA offer a more practical track toward implementation with DTA.

The most recent approach proposed for completing subnetwork analyses for use with STA, involves a bush-based sensitivity analysis. A bush-based representation of a network involves the creation of a restricted subnetwork for each origin node that

encapsulates only the links that users from that origin might plausibly use on the paths to their destinations (Boyles and Waller, 2011). Bush-based solutions are extremely efficient as they keep track of a set flow over a limited number of links. The purpose of using a sensitivity analysis is to adequately estimate route diversions that occur outside of the subnetwork (Boyles, 2012a). Route choices and subsequent subnetwork entry points are sensitive to shortest path solutions determined inside the subnetwork.

The proposed process requires creating artificial arcs to represent all possible paths connecting each origin and each subnetwork boundary node, and relies on the proper development of cost functions for the artificial arcs. Determining proper equilibrium shortest paths relies on the principle of user equilibrium, or the fact that all used paths have equal and minimal travel costs regardless of route. It is proposed that an equilibrium cost over all possible paths can be determined and assigned to the artificial arcs and a solution obtained efficiently from implementation of the bush-based sensitivity analysis. Subsequently, artificial arcs are also created to connect boundary nodes, thus, accommodating route changes that impact the entry/exit point of trips using the subnetwork.

Two methods were initially proposed for the equilibrium estimation. The first method implements network transformations and the second iteratively solves a system of linear equations (Boyles, 2012a). While the first method proved to be more efficient, it was not found to work for networks involving a large number of destination nodes or complex geometries, limiting its application for real-world networks. The second method proved to be more universally applicable, but not as efficient. Nonetheless, the methods examined were demonstrated for test networks, with the linearization approach applied to city of Austin network.

It was found that the proposed methodology applied to a subnetwork of the downtown area achieved a solution much closer to the true equilibrium than simply implementing a

fixed trip table. It was also stated that creating the contracted network, maintaining the intact subnetwork and replacing the outer network with artificial links, along with computing new equilibrium travel times took 90 minutes to complete. However, obtaining an equilibrium solution for a specific scenario using the subnetwork reduced the computational time from twenty minutes to three minutes when compared to analysis of the entire network.

It should be noted that subnetwork analysis requires an initial equilibrium solution for the entire network. Its main function is the efficient evaluation of alternate scenarios, whereby the network is modified in some way, and only the subnetwork is required to be reanalyzed in detail. So although setting up a subnetwork can take additional time, the computational benefit can be achieved over the course of multiple scenario analyses. Furthermore, the strategy of using a fixed trip table implies all trips will continue along the optimal path determined from the base analysis, only allowing for trip change behavior to occur within the subnetwork (Boyles, 2012a). In other words, user routes are fixed outside of the subnetwork and any reaction to network modifications within the subnetwork are restricted to that region, resulting in substantial congestion.

Conversely, the proposed methodology accounts for route decisions made beyond the subnetwork allowing for a better representation of real-world behavior, particularly when guidance information is available to users or network modification effects, such as construction impacts, are known from prior experience (Boyles, 2012a). Conclusions were deduced by comparing results obtained using the proposed strategies versus reanalysis of the entire network. It is particularly noteworthy that the proposed methodology was much more accurate than use of fixed trip tables for scenarios involving capacity reductions, as would be anticipated for TCP impacts.

A modification to the original bush-based sensitivity analysis strategy was used to establish a third, more efficient method for finding travel cost sensitivities. The proposed

method achieves simplicity by formulating the system of linear equations, proposed as the second method above, as a solution to a convex optimization program (Boyles, 2012b). As such, the computational time required to determine the cost functions for the artificial arcs is reduced, and an equilibrium solution can be achieved more efficiently. This method reduces the time required to form the contracted network by approximately an order of magnitude. Therefore, for the Austin network, the set-up computational time was reduced from ninety minutes to approximately nine minutes. Thus, with the subsequent speed of obtaining equilibrium solutions for alternative scenarios already achieved, the overall computation time for applying the subnetwork analysis process was greatly reduced.

It should be reiterated that the aforementioned subnetwork analyses depend on cost functions for the artificial arcs, essentially establishing link performance functions both inside and outside of the subnetwork. These link performance functions and their subsequent derivatives identify costs that are dependent on link flows, allowing one to determine estimates of path costs and subsequent equilibrium solutions. However, these link performance functions are specific to STA analyses and are not applicable for use with DTA. Therefore, a modified procedure, perhaps incorporating a similar strategy of sensitivity analysis to capture changes in subnetwork demand relative to changes in internal travel times, would be required.

Subnetwork Demand Estimation

It has been identified that the performance of a subnetwork model may depend on the ability to account for the impacts of a network modification that extend beyond the boundary of the contracted model (Zhou et al., 2006 and Boyles, 2012a). Accounting for these impacts can be accomplished by estimating changes to flow patterns and related demand along the boundary of the subnetwork. A number of strategies have been evaluated for estimating subnetwork demand, including accounting for impacts to the

external portion of the network through adjustments to the subnetwork O-D matrix. Furthermore, methods have been implemented for evaluating the performance of subnetwork models, as well as testing for differences between demand matrices. These techniques can be used to assess the validity of a subnetwork analysis and the adequacy of any changes to demand used to reflect impacts beyond the subnetwork relative to full network analyses.

The strategies identified for estimating subnetwork demand, including necessary adjustments, primarily revolve around maximum utility or maximum entropy principles as they relate to route selection. The idea is to account for the external portion of the subnetwork by identifying the likely influence of a network modification on the attractiveness of available route choices. For the subnetwork analysis for STA described above, the method utilized estimated changes to demand based on the simplification of the external portion of the network and the corresponding route choices (Boyles, 2012a). Travel times associated with these route choices were tied to the artificial arcs that connected internal centroids and representative external centroids that remained in the contracted network. The method was shown to provide more accurate results than using fixed trip tables, or demand extracted directly from the full baseline model and left intact. Another estimation technique was developed to produce subnetwork demand matrices without relying on trip destinations extracted from the full model, only link flows, using the maximum entropy concept.

The study examined the derivation of subnetwork demand matrices based on link flow rates generated from full-network traffic assignment models or traffic counts (Xie et al., 2010). Derivation of the demand table is the first step required to run a subnetwork model. The researchers recommended using the link-flow pattern from the full network or traffic counts as inputs to a maximum entropy based formulation for estimating the subnetwork O O-D D table. This theory is applied on the basis that the least cost path is also the one that maximizes entropy; therefore, flow patterns can be estimated and

demand formulated in a manner consistent with the principle of user equilibrium. This means the subnetwork demand can be derived using readily available input information.

A notable limitation of the study was the assumption that the O-D flow rates remain unchanged for any impact scenario and impacts extending to the external network are ignored. However, it is recognized that a modification within the subnetwork may impact link flows across the boundary and any subsequently derived O-D table; thus, the larger the external portion of the network, the more problematic application of the methodology becomes. Essentially, the purpose was to derive an O-D table based on link flows alone, such as those from a traffic count, irrespective of original O-D patterns obtained from a full network analysis. It was intended that resulting flow patterns for the subnetwork model match those obtained from the full network model to counteract instances where a subnetwork model provides independent results with respect to the full network analysis from which it was extracted (for that portion of the network), i.e. where the subnetwork user equilibrium solution is independent and therefore different than what may be achieved from the full network analysis.

A different approach to deriving subnetwork demand can be implemented on the basis of maximizing utility through discrete choice formulation. Discrete choice models are based on an individual's preference for an alternative based on its perceived utility and the assumption that users will choose a route that provides the highest utility (Sheffi, 1985; Koppelman and Bhat, 2006). Ultimately, this utility represents the value of the alternative to a user and can be derived mathematically. One type of discrete choice model, the multinomial logit model, determines the probability that users will select a particular route alternative from a set of more than two alternatives, and if the population is known, the corresponding number of users choosing each can readily be quantified.

For the multinomial logit model, the probability distribution function of the route travel times must be known in order to determine the probability of a particular path being

chosen (Sheffi, 1985). The model requires the assumption that the utilities and error components of all alternatives are independently and identically distributed (Sheffi, 1985; Koppelman and Bhat, 2006). The utility can then be defined based on the travel time for the given paths and a random error term. This random error term is assumed to be equal for all paths, so it may be excluded from the formulation (Sheffi, 1985). A calibration or sensitivity parameter is then multiplied by the travel time on a given path. The sensitivity parameter accounts for the impact of route travel time on the number of users that choose a particular path. In other words, a calibrated parameter of zero indicates that the available paths will be used equally regardless of travel time differences, while a value approaching infinity implies all users select a path based solely on travel time.

A precedent for utilizing a logit formulation for estimating modifications to demand estimation for subnetwork models using DTA exists (Zhou et al., 2006). The study focused on providing an updated dynamic O-D matrix for a subnetwork using a two-stage process. The first stage requires extracting path-based traffic assignment results from the full network analysis, and the second stage involves updating the O-D demand based on archived traffic measurements extracted from the subnetwork. The purpose was to investigate external trips that involve the choice of traversing or bypassing the subnetwork. As a result, adjustments can be made to the O-D table based on operational changes in the subnetwork induced by a network modification.

The fundamental idea is that the subnetwork model is able to capture changes that would occur within the full network due to a network modification. To do this, the developed methodology evaluates changes to the subnetwork's performance due to a network modification, and estimates how external-to-external trips may be affected. It assumes that if the performance degrades, that the demand for the subnetwork is likely to diminish resulting in trips bypassing the subnetwork that would otherwise have traversed it. The performance of the subnetwork is based on the estimated average travel times for traversing verses bypassing trips. The demand is adjusted in a manner consistent with

maximizing utility using a foundational logit formulation, and the DTA-based subnetwork demand estimation procedure was effectively demonstrated using a sample network.

Implementing a strategy similar to that used for maximizing entropy or maximum utility based route selection appears promising for use with DTA models since travel time is a primary model output obtained from vehicle trajectory data. This type of formulation can be used to account for demand changes based on measured differences in travel times between scenarios. In the case of subnetwork analyses, particularly those used for evaluating network modifications that are expected to impact travel times and subsequent route choice behavior, this methodology could be implemented to adjust demands at the subnetwork boundary as a function of the experienced travel times within. If adjustments are made to the subnetwork demand, or even if they are not, evaluation of the quality of the results must be undertaken. In addition, the adequacy of the demand formulation itself can be examined using a number of techniques.

To evaluate subnetwork performance and, ultimately, the associated demand formulation, a number of studies have utilized measures of root mean squared error (RMSE) (Zhou et al., 2006; Xie et al., 2010; Boyles, 2012a). These statistics have been implemented to validate link flows across all links within a subnetwork, and in the case of DTA, all time periods as well. Although RMSE has been used in a number of research studies to assess the validity of model performance associated with demand estimation procedures, several additional strategies have been introduced to accomplish this task.

One such study identified several variations of the mean absolute percentage error (MAPE) to specifically assess the quality of O-D matrix estimation (Cools et al., 2010). MAPE is based on the absolute percentage error (APE) and uses the mean to normalize individual error values. While bounded on the low side by an error of 100 percent, there is no upper bound on the MAPE. To appropriately set a bound for the statistic, the

modified MAPE can be used; however, this formulation was found to treat large positive and negative errors differently in application. Therefore, a new statistic was introduced, the mean censored absolute percentage error (MCAPE). The MCAPE overcomes the prior shortcoming by limiting positive values of the statistic to a maximum of 100. In all, it was found that using the proposed MCAPE was particularly advantageous for evaluating O-D matrices as demonstrated from a number of case studies. Furthermore, when used alongside traditional measures, the MCAPE value could be used to effectively investigate differences between O-D matrices.

Both the RMSE and the MCAPE are based on the assumption that simulation results are independent and identically distributed (IID). However, this is not often the case since output data is often autocorrelated. To overcome violations of the IID assumption, the structural similarity (SSIM) index has been tested for application with O-D matrix evaluation (Djukic et al., 2013). The SSIM index was originally introduced to assess differences between images based on structural information, taking into account local spatial correlation (Wang et al., 2004). Individual pixels are compared between images within user-defined windows that capture similarities across a localized area. The index value for a particular pixel is based on weighted estimates of local statistics, with a weight inversely proportional to the distance away from the select pixel. The overall image quality can be evaluated using the mean index value across all local windows. The index is calculated on a scale of -1 to 1, with a value of one representing an exact copy of an image and negative one being the opposite.

The similarity in structural composition between images, divided into pixels, and matrices, divided into cells, makes the SSIM potentially useful for comparing O-D matrices. Under the assumption that similarities exist between nearby origins and destinations, and that O-D pairs may be spatially or temporally correlated, cells of an O-D matrix composed of individual demand values can be evaluated for structural similarities. Prior research has explored whether using the APE, mean squared error

(MSE), or RMSE value alone is adequate criteria for assessing the quality of estimated O-D matrices (Djukic et al., 2013).

The research introduces use of the SSIM index for comparing dynamic O-D matrices, specifically identifying the limitations associated with measurements of MSE. The MSE measures the absolute differences between individual O-D values without encompassing any spatial or temporal correlation that may exist across O-D pairs or origin-destination-time interval (ODT) combinations. It was implied that a statistical measure that ignores this potential correlation is not as effective or accurate as one that does, such as the SSIM index.

The research showed that calculated values of MSE may be inconsistent with measurements of the SSIM index, limited by an inability to uncover differences in structural composition. It was revealed that MSE values alone may over- or under-estimate differences between O-D matrices, leading to potentially incorrect conclusions about the validity of estimated demands. It was thoroughly demonstrated that the SSIM index can be used to quantify the similarities between two O-D matrices on the basis of structural correlations, such as space and time, holding an advantage over traditional criteria. Ultimately, when used in conjunction with other measures, the SSIM index can be an effective means of assessing the quality of demand estimations when compared to target O-D matrices. While these statistical measures can be applied to assess demand changes, they can also be used to evaluate subnetwork selection.

Subnetwork Selection

Although accounting for changes to route choice behavior in the outer region of the network caused by impacts inside the subnetwork is important, there is an advantage to ensuring that many user choices are captured within the subnetwork detail. Therefore, setting a proper boundary is also critical. Choosing a subnetwork area that is too small

will make it more difficult to identify localized route choice behavior caused by network impacts and may place an unnecessary burden on the assessment of the outer region that could impact the quality of the results obtained. On the other hand, choosing an area that is too large will diminish the advantage achieved in terms of computational time and effort from using a subnetwork analysis. Furthermore, it has been suggested that modifications to networks should result in localized impacts to traffic flows, and conditions far from the location of change should be largely unaffected (Chiu et al., 2011; Chen et al., 2011).

Determining the area of impact to traffic flows caused by network modifications has been studied with respect to network vulnerability, reliability, and accessibility (Jenelius et al., 2006; Taylor et al., 2006; Taylor and D'Este, 2007; Knoop et al., 2007; Chen et al. 2010; Chen et al., 2011). The evaluation of network connectivity and travel time, as well as sensitivity or severity of resultant consequences caused by network degradation, have led researchers to look at several strategies involving the evaluation of network modifications and subnetwork identification. One methodology involves pre-selecting links by their potential for vulnerable impacts to the network and evaluating this subnetwork of links versus the list determined from full-scale simulation (Knoop et al., 2007).

The purpose of this strategy is to determine if a less-intensive method of identifying vulnerable links could be established as an alternative to time-intensive computation methods involving simulation of the entire network. The evaluation of indicators intended to measure the potential vulnerability for links within three different test networks was unable to properly identify the most vulnerable links determined from full-network DTA analysis and had little correlation with the list found from simulation. Therefore, it was determined that preselecting candidate critical links using the indicators did not provide a good assessment of actual critical links.

An alternate strategy for identifying critical links is to systematically evaluate all links in the network and rank them in terms of a vulnerability assessment (Jenelius et al., 2006; Taylor et al., 2006; Taylor and D'Este, 2007; Chen et al. 2010; Chen et al., 2011). Those links with the highest ranking can be grouped into a subnetwork for more detailed evaluation of critical scenarios. If the impacts are far-reaching, or more localized but substantial, then the network receives a higher vulnerability ranking. Nonetheless, the impact area is determined to be, effectively, a subnetwork that requires attention relative to the specific scenario. In one study, not only determining the subnetwork of most critical links, but also establishing a methodology for identifying the portion of the network impacted by network modifications was developed.

Development of a systematic approach for identifying the area impacted by network modifications, such as those initiated as part of TCPs, is of particular interest. In the study, a vulnerability assessment in terms of the impact of removing a link on a congested roadway network was presented (Chen et al., 2011). This was completed by measure of a calculated vulnerability index for the entire network or a subnetwork under normal conditions and after removal of a link. It was determined that with the creation and use of a subnetwork, the impact in terms of vulnerability could be measured for successive scenarios involving the systematic removal of one link at a time from the network. The vulnerability index could be ranked for each of these removal scenarios and those links with the largest index values determined to be the most critical. Evaluation of the network demand and selection of the subnetwork were discussed in detail, as presented below.

The paper notes that conventional research has used the "full network scan" approach to identify critical links by iteratively removing links from the network and measuring the impact on the entire network in terms of reduced performance (Chen et al., 2011). While this may be a sound methodology for networks with minimal trips, it may not be appropriate for those with larger demands (and more congestion), and thus, using traffic

assignment models would be better. It was reiterated that DTA models for large networks or those with large demands can be computationally intensive; furthermore, using a full scan approach for a city-wide system may take weeks or longer to process.

Therefore, identifying links that are potentially vulnerable to significant impacts to the network and running an analysis solely on these links (i.e. subnetwork) has intrinsic value in terms of minimizing computational time (Chen et al., 2011). Furthermore, modeling travelers' behavior with respect to link closures and network modifications is identified as a key issue with respect to identifying critical links in the network. Travel time uncertainty has been identified as a major factor influencing route choice, resulting in demand uncertainty. The paper identifies that route choice is dependent not only on shortest paths, or overall travel time savings, but on reducing travel time variability or improving reliability.

The associated risk-taking behavior of individual users and the impact on network reliability analyses has been documented, though the authors point out that these assessments have not yet taken into account changes to demand and risk-taking behavior due to link closures for determining critical links in the network (Chen et al., 2011). Thus, the study proposes a way of identifying the most critical links using an impact-area vulnerability analysis on a congested network by investigating a localized impact area instead of the entire network. This determination was based on experimental results which indicated that the impact of a link closure will be mostly limited to a local area, rather than the entire network. Furthermore, by limiting the more detailed analysis to a smaller area, the computational time to perform the analysis could be greatly reduced, once again emphasizing the primary purpose of subnetwork analysis.

The basis for identifying a smaller impact area, versus evaluation of the entire network for each link closure, is founded on the assumption that a link closure will have significant impacts to the adjacent, or more localized portion of the network, and those

impacts are not likely to propagate through the entire network. It is speculated that a link closure will cause congestion in the impact area, primarily (Danczyk and Liu, 2009). It should be noted these findings were based on major, unexpected incidents, not necessarily planned construction. For pre-planned construction events, with information provided to the public, changes in travel patterns were proportional to the availability of viable alternative routes in the area. Furthermore, prolonged link closures result in users establishing new routes and a reluctance to revert back to the original after reopening.

The identification of the local impact area, or subnetwork, and its associated links and nodes can be based on the determination of a size parameter (Chen et al., 2011). The size parameter is an integer value that identifies the depth order of neighboring links to include in the subnetwork. In other words, a size parameter value of one would designate inclusion of only those links directly adjacent to the closed link, i.e. those connected to its end nodes would be included in the subnetwork. Subsequently, a vulnerability index value can be established for the subnetwork for each link closure within its boundaries (as controlled by the size parameter). The rank of each vulnerability index value can then be established for the individual scenarios, and the order of critical links within each designated subnetwork can be established. In addition, the global link vulnerability index can be established for the entire network (denoted as the "true" vulnerability index), as well.

It is therefore expected that the vulnerability index for the subnetwork should be strongly correlated to the index value for the entire network based on the assumption that impacts due to link closures will be largely localized (Chen et al., 2011). Measuring the correlation between the ranks achieved using the subnetwork versus the entire network can be completed using a Spearman Rank Correlation. If, as speculated, a strong correlation between the subnetwork ranks and the global network ranks can be achieved, then the subnetwork analysis can be justified and computational time savings realized.

The paper uses two case studies to illustrate implementation of the algorithms and impact area vulnerability analysis on real-world roadway networks (Chen et al., 2011). The first was completed for Sioux Falls, SD where a number of assumptions for the BPR function and user types (including proportions) were implemented. For different levels of congestion, the network efficiencies were evaluated based on different link closures. The Sioux Falls network was evaluated for correlation between the top 10 most critical link rankings using the impact area network (with a size parameter of 3) versus the global network. It was found that a strong correlation existed between the two, with a Spearman's rank correlation coefficient of 0.97. Therefore, it was determined that using the subnetwork analysis would be appropriate for accurately determining the critical links. It was further determined that as the travel demand variability increases, this correlation decreases. However, all of the scenarios showed a high correlation between the subnetwork and global network results.

Another case study was completed on the Hong Kong, China roadway network. To evaluate the subnetwork analysis methodology, a full network scan approach was first utilized to identify critical links (Chen et al., 2011). It was found from analyzing the entire network, that the more urban (dense) section of the network was more resilient to link closures than the more sparsely connected suburban sections. It was again determined that increasing the demand variability (and associated risk-taking behavior of users) resulted in much different rankings of vulnerability for certain critical links, again establishing the importance of demand uncertainty on the network evaluation.

For the vulnerability analysis per impact area, network attributes were recorded for varying size parameters and, as expected, the size of the impact area increased (along with the correlation with the global network) with increases in the size parameter (Chen et al., 2011). However, an increasing correlation coefficient value appeared to exhibit diminishing returns. A size parameter of 5 had nearly the same resultant correlation

coefficient as a value of 9. Ultimately, the research indicated that selecting a size parameter that is too small would result in the misidentification of critical links.

As expected, increasing the size parameter resulted in more computational time to perform the analysis (Chen et al., 2011). The computational time was found to increase nearly exponentially with an increase in size parameter. Using a size parameter of 5 across 500 candidate links in the network (which was found to identify 100 percent of the most critical links in the global network), the computational time was determined to be approximately 14 percent of that using the full-scan network approach (about 7 times faster). An in-depth evaluation of different size parameter values, in terms of accuracy versus computational time, resulted in the following recommendation: the size parameter should not be less than 3 or greater than 10 (too large a value results in too much computation time).

Overall, the case studies underscored the impact of demand uncertainty (and user route-choice behavior) on the user equilibrium function, along with the computational time versus accuracy trade-offs of using a subnetwork for evaluating a vulnerability index (Chen et al., 2011). It was determined through the case studies that a strong correlation exists between the subnetwork and global network analyses, using the aforementioned methodology, dependent on entering an appropriate size parameter. It was recommended that an investigation of scenarios involving multiple link closures or other network impacts, along with additional evaluations of appropriate size parameters, be part of future research.

Ultimately, the implementation of subnetwork analyses has been proven valuable for accurately evaluating network modifications while reducing the necessary computational time required to assess multiple scenarios, as would be expected with TCPs. While some research supports the supposition that traffic flow and route choice impacts are confined to the area surrounding the impact location, the foundation has been established for both

the adequate selection of a subnetwork and treatment of the surrounding area using sensitivity analysis. Additional applications suggest selection and implementation of subnetwork analyses can be very valuable for traffic assignment models.

Subnetwork Analysis: Additional Applications

As mentioned above, establishing a subnetwork or a subset of select links within a large network for additional evaluation has been completed for evaluating network vulnerability or network modifications. Additional theoretical and practical applications include creating traffic assignment models for portions of large, regional networks. One such example was the extraction of a portion of the Chicago network for further evaluation of incident impacts using DTA models; however, no explanation was given for how the subnetwork was selected or calibrated (Kamga, 2011). Other subnetwork models have been implemented to represent a specific portion of a larger network, such as a downtown area, constrained by natural boundaries and individually calibrated.

An early practical application involved the development of dynamic O-D matrices for portions of a large network (Chang and Tao, 1999). The method involved delineating subnetworks at cordon lines for an urban network. In theory, dynamic O-D matrices could be estimated for the subnetworks based on traffic sensors at the cordon lines, and subsequent O-D flows for the larger network could be obtained using these subsets of cordon line flows. In other words, combinations of inbound and outbound flows from each of the subnetworks could be used to find relationships between subsets of cordon line flows and ultimately determine the network-wide O-D flows. The purpose of the methodology was to establish an accurate estimation of the network-wide dynamic O-D flows based on aggregation of subnetwork models created using area traffic sensors.

A more practical application of DTA subnetwork analysis was established using a portion of the Calgary, Canada road network to evaluate the effectiveness and accuracy of a DTA

model (Mahut et al., 2004). The development of the DTA model first involved setting the subnetwork boundary. The subnetwork was established for the southern portion of the city due to its separation from the remainder of the community by a river with limited crossings. As a result, a trip table for the subnetwork could be created by manipulating the O-D information for an existing STA model available for the full-network. The new trip table and subsequent simulated turning movements were calibrated using a series of traffic counts obtained at 72 intersections within the subnetwork. The DTA model for the subnetwork was used to simulate traffic flows for the evaluation of model development and calibration techniques by comparing model results with additional traffic counts. As noted earlier, it was found that the DTA model performed very well, emphasizing the importance of model calibration and verification.

Models have also been created for traffic assignments involving subnetworks for the city of Austin. A subnetwork STA model was created for the evaluation of the bush-based sensitivity analysis on the downtown Austin area (Boyles, 2012a; 2012b). This model was created using boundaries established by major roadways on the east and west edges of downtown Austin, with the northern boundary being the University of Texas campus, and the southern boundary being Lady Bird Lake. The defined boundaries represent a natural separation from the rest of the Austin regional network.

In addition to the use for STA model runs, the same subnetwork has been calibrated and verified for use with DTA applications using 24-hour traffic counts, along with updated time-variable demand matrices. Additional information about intersection control, including traffic signal timing plans, was also input into the VISTA software for use with DTA. Link attributes, including number of lanes and capacity, were also verified. The downtown Austin network, like the Calgary subnetwork, was specially configured for individual use, designated to function independently from the surrounding network.

Currently, the use of subnetworks for DTA models involves a significant simplification of the analysis process and a large amount of calibration and verification using traffic counts and field review. Essentially, these subnetwork applications are designed to be self-sufficient. Significant potential lies in using subnetworks if a strategy for proper selection and analysis can be established that will result in ample reduction of computational time while maintaining accurate and reliable results. The extensive calibration and verification efforts needed for the subnetwork to function independently could negate the benefit of reduced analysis effort. Nevertheless, the use of subnetwork analysis for determining impacts to network vulnerability, reliability, and accessibility caused by modifications to network elements, along with all of the notable applications highlight the value of obtaining DTA analysis outputs and results for further evaluation.

Uses for DTA Model Outputs and Results

Application of DTA models has been shown to yield valuable results for analyzing ATMS and traveler information systems, TCPs and construction impacts, as well as traffic flow and user behavior across large scale and complex networks or subnetworks. These results have been shown to be more accurate than those provided from STA models, even though DTA requires more computational effort. The results of DTA models have been used to derive the following performance measures: density, queuing, VMT, VHT, travel time, speed, LOS, emissions, and number of lane changes.

Furthermore, DTA results have been used to develop network vulnerability, reliability, and accessibility measures. The dynamic and spatial nature of DTA network results allow for their use with GIS software, as well as adaptation as input for microsimulation models. The following sections identify typical uses of DTA model results for analyzing networks and specific alternatives or scenarios, along with the ability to interface DTA model outputs with other software programs.

Relevant Outputs and Network Measures

Typical results obtained from DTA analyses include link and path travel times and volumes generated from raw model outputs of vehicle trajectories. These values can be aggregated over specific corridors, O-D pairs, or entire networks. Combining travel time with geometric or geographic information can be used to provide a multitude of traffic engineering and planning based metrics. A number of applications of these results are described in more detail below.

As noted earlier, a number of studies have used DTA models for analyzing traveler information and management systems. Several studies have used network travel time measures to assess scenarios across multiple deployment strategies (Mahmassani and Peeta, 1993; Ben-Akiva et al., 1997a; Sisiopiku et al., 2007) In a similar manner, performance measures, including travel time, speed, and density, were defined in such a way as to capture the spatial and temporal effectiveness of a management system to control traffic flow (Ben-Akiva et al., 1997b). For spatial evaluation, measurements were taken over roadway sections, entire paths, O-D pairs, and entire networks, and for temporal evaluation, measurements were taken at different intervals, or summed over specified time periods. Spatio-temporal vehicle trajectories were used for evaluating ITS technologies deployed by the New Jersey DOT (Chien et al., 2005). These uses demonstrate the versatility of DTA results for providing a thorough evaluation of network modifications.

Other research projects intended to assess incident management and response times have used DTA models to provide measures of congestion, in addition to travel times (Kamga et al., 2011; Sisiopiku and Cavusoglu, 2012). These studies used outputs of link traffic flow and queuing, as well as travel time variability and VMT in their evaluations. Another important example is found in the assessment impacts of construction projects using measures of LOS obtained from DTA model results (Pesti et al., 2010). These

projects represent examples of how DTA models can be used to provide direct measures of network performance; however, additional techniques to analyze and utilize DTA models have been developed.

Notably, a number of studies have utilized DTA model results to investigate network vulnerability, reliability, and accessibility due to the social, economic, and environmental consequences of disruptions to a transportation network. These performance measures, particularly vulnerability, have been implemented to determine elements of roadway networks that are at risk by determining the sensitivity to incidents and the probability of an incident occurring, as well as estimating the scope and magnitude of consequences from the incident or link closure associated with the rest of the network (Jenelius et al., 2006; Taylor et al., 2006; Taylor and D'Este, 2007; Chen et al., 2010; Chen et al., 2011). Typically, the derived performance measures are used to compare the network before incident and during a link failure. The overall goal of these assessments is to identify elements of the network that are highly averse to failure and those not as critical.

In one study examining network vulnerability, the consequences of a failing link or set of links was estimated by measuring the increase in generalized travel costs (Jenelius et al., 2006). The calculated increase in travel cost for the entire network can be aggregated over individual nodes and links. Overall, the measures assumed inelastic demand, that the event duration is long enough that a new user equilibrium will be established, but short enough that the demand will not significantly change, and only route choice is affected.

Another study was used to develop a method for assessing vulnerability in roadway networks based on the social and economic impacts of link degradation represented by changes in accessibility (Taylor et al., 2006; Taylor and D'Este, 2007). The study considered multiple indices of accessibility, including generalized travel cost, and applied them through a series of case studies. In the case of generalized cost, these indices can be quantified by looking at the disutility of travel, such as distance, time, and money due to

link failure measured from a comparison of before and after DTA results (Taylor et al., 2006). The overall intention is to determine which links are most vulnerable or critical in the network, and to measure and assess the risk associated with these critical portions of the network.

Other research has been undertaken to investigate accessibility measures for assessing the performance of urban networks (Chen et al., 2010). One study looked at the vulnerability of transportation networks operating at a degraded level based on the travel time or general cost increase caused by one or more link failures while cognizant of behavioral-based user responses. This was accomplished using demand modeling to estimate long-term equilibrium with the network deficiencies. The study used a utility-based measure (user's perceived utility for different travel choices) to quantify accessibility.

As shown before, the results indicated that degrading certain links (greatly reducing their capacity) in a network causes trips from certain origins or zones to be cancelled or postponed, causing the number of trips generated and distributed to subsequent destinations to be reduced (Chen et al., 2010). With the new equilibrium solution obtained for the normal and degraded networks, the accessibility measures were calculated and the finding was that all of the accessibility measures decreased for the degraded network. It was determined that O-D pairs with higher reductions in accessibility are more vulnerable. It was also determined that if users have more route choices and more traveler information, their O-D pairs, and subsequently the network as a whole, will be less vulnerable to degradation in performance.

In a subnetwork study assessing network vulnerability, a reliability-based user equilibrium (RUE) model was utilized to examine the variable behavior of different network users, along with demand variations caused by incidents, such as those involving link closures (Chen et al., 2011). A key to the methodology was the modeling of user risk-taking behavior under travel time uncertainty, which involves the use of a travel time

budget, denoted as the sum of the expected travel time and a safety margin. The solution to the RUE is based on the supposition that all travelers, under travel time uncertainty, try to choose a reliable shortest path to achieve the minimum travel time budget.

To identify critical links in a congested roadway network, a vulnerability index based on network efficiency was formulated (Chen et al., 2011). The network efficiency for a congested roadway network was defined as a function of the mean travel demand, the proportion of trips of each type, and the minimum travel time budget between each O-D pair, summed over all O-D pairs. With the efficiency defined, the vulnerability index of the network due to closure of a link was calculated as the difference of the efficiency under normal or base conditions less the efficiency with the link closure, divided by the efficiency under normal conditions. With the calculation of the vulnerability for each link closure, the critical links, or those that yield the largest vulnerability index values, could be identified.

Demonstrating the connection between the two, many of the above studies included assessments of reliability, in addition to vulnerability. Measures of reliability that can be established for a link include the probability that it is operational (versus failed) and travel time variability (Taylor et al., 2006; Taylor and D'Este, 2007). It can also be seen as the user's perspective of the quality of the system or certainty in estimating their own travel time, dependent on available information, and defined as deficient if one's expectations are not regularly fulfilled (Jenelius et al., 2006). A number of other studies have focused on network reliability assessments.

In one study, a measurement of travel time reliability was established using travel time data collected along a highway in California (Lam and Small, 2001). The reliability was determined by calculating the difference between the 90^{th} percentile travel time value and the median. The results were used to estimate a value of time and a value of reliability

and their relationship to congestion pricing, noting that the value of reliability has received little attention in prior research.

Another study investigating the importance of travel time reliability in user's travel route choices again looked at the concept of a travel time budget (Lo et al., 2006). Noting the importance of travel time reliability in route choice decisions, the study was used to develop an approach that related travel time variability, due to capacity variations, to risk aversion in route choice behavior, focusing on how a degraded system could influence these decisions. The strategy was based on the idea that travelers will factor in travel time reliability, based on past experiences, into their decision making process regarding route choices.

A couple of additional studies used evaluations of travel time budgets, a combination of the average travel time and a safety margin, to investigate variable demands. These studies assessed travel time reliability based on variability in travel times, as well as the resultant influence on route choice behavior (Shao et al., 2006; Siu and Lo, 2008). Since stochastic variations may exist in both demand and capacity, or supply, travel times can become uncertain, as well (Siu and Lo, 2008). One paper noted that integrating user departure times and route choices with travel time variability requires DTA models. Ignoring stochastic effects causes models to underestimate the real travel time budgets that users would have when given prior knowledge of the network (commuters). The model results were used to determine which links would result in the largest improvement (minimization) to overall travel time budget, if improved. This emphasizes that ignoring stochastic effects could lead to misidentifying the links that should be improved.

The research notes that travel utility is inversely proportional to travel time, so to maximize the utility one must minimize their travel time or travel time budget. The above studies demonstrate how DTA results can be used to assess traveler information systems,

incidents, and other network impacts, as well as provide measures of network vulnerability, reliability, and accessibility through evaluation of travel times, travel time variability, travel time budgets, and overall route choice behavior. Outside of traffic assignment applications, measures of accessibility, including those that go beyond simply looking at travel time, have been demonstrated in a related manner.

Behavioral travel patterns have been shown dependent on one's perception of their spatial and temporal environment (McCray et al., 2003). GIS software allows for observations of space-time accessibility considering mobility constraints on a disaggregate level. This can allow one to examine trips beyond the time element and to investigate spatial patterns. Looking at these travel patterns and area demographics using GIS software can enable one to examine accessibility to jobs, schools, healthcare facilities, etc. relative to different demographic groups. The use of GIS software to establish changes in travel patterns over space and time is a viable approach for investigating accessibility based on disaggregate data.

It has been noted as important to utilize disaggregate level data and socioeconomic characteristics to properly model accessibility (Handy and Niemeier, 1997). GIS software enables one to combine DTA results, including many network performance measures, with demographic information using both mapping and database elements. Furthermore, the value of GIS software as a planning tool has been demonstrated through a number of applications ranging from the municipal to state-wide level. The effectiveness of GIS tools has been exhibited by its ability to store, analyze, and display geographical information based on the "locational, descriptive attribute, and temporal character of phenomena" (Hanson and Giuliano, 2004). These qualities are critical for the conveyance of transportation information, and are applicable to DTA results.

Space-time models offer a good option for the development of an accessibility framework that can be used to analyze transportation equity issues, yet they depend on

comprehensive information about individual trips. Fortunately, this detail can be provided as output from DTA models and mapped using GIS software. The perceived value of integrating DTA model results with GIS software has been established, and several applications of this connection have been employed. In addition, other uses of DTA model results with respect to interfacing with additional software programs have been demonstrated.

Interfacing DTA Model Results with Other Software Programs

Several strategies for interfacing DTA model outputs with other software programs exist, and a number of practical applications have been established. Many of the aforementioned applications of DTA models using software programs involve an element of GIS capability. This is due to a need for the software to provide for the graphical creation and manipulation of network elements. Users must be able to visualize these elements to properly connect links and nodes to form a network; therefore, geographical coordinate information and subsequent element attributes must be established and maintained.

A good demonstration of this process is provided using the GIS tool conveniently interfaced with the VISTA software and made readily accessible from the program's menu options. Creating, editing, and visualizing network elements in VISTA can be achieved using the JAVA-based GIS "Editor" tool. The associated database stores spatio-temporal data using geographic coordinates and time stamp information (Ziliaskopoulos and Waller, 2000). Thus, in addition to visualizing network elements, the GIS tool can be used to create simulations and animate vehicles traversing the network, as well as to generate visual representations of output data using color-coded links for convenient illustration of volume and travel time information.

One of the aforementioned studies assessing the reliability and vulnerability of network links specifically utilized GIS software to visualize traffic assignment results (Jenelius et al., 2006). Initially, geographic data, including node coordinates, were imported into GIS software and combined with other geospatial information to provide additional information about the relative surroundings of nodes, links, and impact areas. The resultant link volumes and travel times for different failure scenarios were also visualized and compared using the GIS software. Additionally, a study investigating the proper calibration of DTA models used GIS software to map network elements and input area land use information (Mahut et al., 2004). The GIS software was also used to create visuals showing vehicle paths in order to identify the potential cause of discrepancies between DTA model results and traffic counts.

In addition to producing helpful visuals using GIS software, outputs from VISTA and other DTA models have been used to create microsimulation models. This is related to use of GIS software to visualize DTA model results that can be used to determine the extent of impact areas that might require more in-depth microsimulation analysis. The use of DTA results to interface with microsimulation software has been documented through prior research (Chiu et al., 2011; Kamga et al., 2011). Specifically, VISTA has been identified for its ability to interface with traffic simulators, such as CORSIM, VISSIM, and signal optimization software like SYNCHRO (Kamga et al., 2011). VISTA has also been demonstrated to utilize inputs from transportation planning software, such as TRANSCAD, in order to create networks (Kamga et al., 2011; Pool et al., 2012a). These software exchanges have proven valuable for a number of transportation planning and engineering applications.

Recently, researchers at CTR developed a detailed strategy for extracting model results from VISTA and importing them into the microsimulation software, VISSIM (Pool et al., 2012a). Three possible approaches have been developed for this process: 1) exporting the entering vehicle flows at the periphery of the microsimulation network and turning

movement volumes at included intersections; 2) exporting O-D matrices for the modeled area; 3) exporting vehicle paths for import directly into VISSIM. Essentially, outputs generated from vehicle trajectories created by the DTA models can be used as inputs for creating corresponding VISSIM models. While these microsimulations require additional formatting, including appropriate parameter inputs and model calibration, along with separate creation of network elements and attributes, they can be used to provide a more in-depth simulation of area traffic operations and generate detailed results.

The versatility of DTA models and their outputs, defined as more realistic in their representation of traffic flow, route choice behavior, and congestion, has been demonstrated through a number of studies and research initiatives. This review has shown how DTA models can be used extensively for evaluating TCPs and construction project impacts. Specifically, the interfacing capabilities of VISTA have been thoroughly exhibited, representing how important a goal it was in its development. This unique flexibility and widespread applicability have been important factors in its choice of use for this research.

4. ANALYSIS FRAMEWORK

As previously stated, the purpose of this study is to develop a method for selecting and analyzing a portion of a large network, or subnetwork, using a DTA model for the evaluation of network impacts, including those imposed by TCPs. The literature review provided an extensive background for the development of the analysis framework and methodology for this project. This included an overview of transportation planning, traffic network analysis, STA and DTA theory, subnetwork analysis, and software interfacing, as well as relevant applications of all components.

Again, accomplishing the primary objectives associated with this research involves an in-depth evaluation of subnetwork sizes relative to multiple network modification scenarios, as well as developing an efficient and effective method for adjusting boundary demands to account for impacts extending beyond the subnetwork. It is intended to establish criteria to help planners and engineers select a proper subnetwork to use for reviewing a specific impact scenario. This is done by reviewing the extent of impacts resulting from a network modification relative to different subnetwork sizes. This process can help determine whether impacts are expected to be contained within a subnetwork of given size or estimate how much of the impact is likely to remain unaccounted for using the specific selection extents. Furthermore, if the size is inadequate to contain the majority of the impacts, a method is proposed for adjusting the subnetwork boundary demand to account for external impacts. This procedure will be used to evaluate trips entering the subnetwork.

As such, the project framework has been established based on proposed methods for subnetwork selection, analysis, and evaluation; results extraction and compilation; and statistical testing procedures. This includes extensive utilization of software scripts and models, including those compiled in ArcGIS and Matlab, to provide the necessary tools for completing the process. The following sections detail the analysis framework,

including Network Notation and Definitions, DTA Analysis Methodology, Subnetwork Selection, Subnetwork Analysis and Evaluation, Subnetwork Demand Estimation, and Presentation of Results.

Network Notation and Definitions

In order to adequately present the DTA and subnetwork analysis methodology, it is necessary to introduce the notation and terms used in the report. The following network definitions are presented to maintain consistency between the methodology, analysis, and results. As noted earlier, the term network is used to describe the physical construct of a series of streets, represented by links, and intersections, represented by nodes. Let $G = (N, A)$ represent a directed network with a set of N nodes and A arcs or links. G is said to be directed, meaning each link is associated with a direction of flow (Sheffi, 1985). Further, the network is connected, and as such, every node in the network is accessible from every other node using a path (or route) of intermediary links. Therefore, a path is a sequence of directed links (Sheffi, 1985). Each link is established by its beginning (i) and end node (j) as link (i, j) with length ℓ. The travel time on link (i, j) is given by t_{ij} and traffic flow on each link as x_{ij}. Additionally, each link is assigned a capacity, or maximum flow, given by C_{ij}.

For STA models, a link performance function establishing travel time as a function of flow, $t_{ij}(x_{ij})$, is used. These functions represent the impedance to flow or delay and, consequently, are strictly positive, strictly increasing, and analytic (Boyles, 2012a). This means that the travel time to traverse a link will not be zero or approach zero as flow increases, and the resulting function is infinitely differentiable. While link performance functions are not used directly with more modern DTA models, the association between flow and travel time is important for this type of study. Additionally, as noted in the literature review, the current methodology for establishing equilibrium within DTA was based on methods derived for use with STA models. The development of subnetwork

analysis strategies including route choices made beyond the subnetwork boundary has also been largely confined to STA applications. Therefore, this relationship is referenced here.

For a transportation network, users travel between specific origin nodes (r) and destination nodes (s). As such, each path connects an origin-destination or O-D pair (r, s) and is further denoted as π_{rs}. Each O-D pair has an associated demand given by d^{rs}, with individual path flows given by h^{π} and path travel times denoted by c^{π}. A demand equality is then established as $\sum_{\pi \epsilon \pi^{rs}} h^{\pi} = d^{rs}$. O-D matrices pertain to the demand matrix (r, s) with rows representing origins and columns representing destinations. Furthermore, a relationship between path flows and travel times is established from the sum of individual link performance measures across those that make up each respective path. These relationships are determined based on the path-link incidence relationship defined as: $\delta_{ij}^{\pi}\ where\ \delta_{ij}^{\pi} = \begin{cases} 1\ if\ path\ \pi\ uses\ link\ (i,j) \\ else\ 0 \end{cases}$. This relationship is used to establish the following equations:

$x_{ij} = \sum_{\forall \pi} h_{\pi}\, \delta_{ij}^{\pi}$ where the link flow (x_{ij}) is the sum of the path flows (h_{π}) that use link (i, j), distinguished by an indicator variable (δ_{ij}^{π}) taking the value 1 (if link used) and 0 (if not used) and

$c^{\pi} = \sum_{i,j} t_{ij}\, \delta_{ij}^{\pi}$ where the path travel time (c^{π}) is the sum of the individual link travel times (t_{ij}) for the links that compose path π.

The network G is determined to be dynamic if the travel times associated with traversing each link vary depending on the time of day, τ, at which the travel is initiated (Chabini and Dean, 2000). In other words, τ is defined as the departure time. Therefore, O-D demands, as well as link flows, travel times, etc. are all further denoted by the departure

time τ for a DTA analysis. It is also assumed that the time-dependent network is a series of discrete time intervals (t) over a finite horizon of T denoted by $t \in \{0, 1, 2 \dots T\}$

A subnetwork is defined as a subset of elements within network G, denoted as $G_S = (N_S, A_S)$. Network elements composing G can be identified as either internal, part of G_S, or external, not part of G_S. This establishes the fundamental terminology for a transportation network and subnetwork with either static or dynamic attributes.

There are several additional network-related terms requiring definition before presentation of the analysis methodology:

- *Set of all Paths* (Π) – defined as the list of all individual paths (π) in the network, typically disaggregated by O-D pair (Π^{rs}).
- *Set of All O-D Pairs* (RS) – defined as the list of all O-D pairs in the network.
- *Path-Flow Matrix* (H) – defined as the matrix of volumes established for each departure time-path $(\tau - \pi)$ pair (row-column).
- *Weight Parameter*(λ) – defined as the step size or portion of the vehicles moved toward the optimal set of shortest paths, e.g. as part of MSA defined as $1/iteration\ number$.
- *Size Parameter* (ς) – defined as the number or order of connected links to be included in a link selection set.
- *Sensitivity Parameter* (θ) – defined as a constant that scales perceived (or experienced) travel time (Sheffi, 1985).
- *Relative Gap* – defined as the ratio of the total network travel time divided by the travel time if all users were on their shortest path minus one. Relative gap is a method of determining convergence, or a way of determining how close the model is to reaching true equilibrium. The closer the relative gap is to zero, the closer the model is to user equilibrium.

- *Cost Gap* (g_n) – defined as the difference between the cost, or travel time, on a path (π) used by vehicle (n) and the cost on the cheapest path, or shortest path, available to n, or as $g_n = c^{\pi n} - c^{*n}$. This quantity can be summed over the entire network to provide a total cost gap, $G = \sum_{\forall n} g_n$. The total cost gap can then be calculated as a percent of the total cost of paths used by all vehicles, $G\% = \frac{G}{\sum_{\forall n} c^{\pi n}}$.

The following quantities describe traffic conditions on network components and performance measures used in the analysis and evaluation of results:

- *Average Link Travel Time* ($\bar{t}_{ij}$) – defined as the total time for each vehicle to traverse a link (t_{ij}) divided by the number of traversing vehicles (n) during a specified time interval, or as $\bar{t}_{ij} = \frac{\sum_{\forall n} t_{ij}^n}{n}$ measured in units of seconds or converted to minutes.
- *Average Link Travel Speed* ($\bar{u}_{ij}$) – defined as a traffic stream measure based on the travel time observed on a known length of roadway (link) (HCM, 2010). As such, this measure is established as the link length ℓ in feet divided by the average travel time ($\bar{t}_{ij}$) for all vehicles to traverse the link for a specified time interval, or as $\bar{u}_{ij} = \frac{\ell}{\bar{t}_{ij}}$ measured in units of feet per second or converted to miles per hour.
- *Average Path Travel Time* ($\bar{c}_{rs}^{\pi}$) – defined as the sum of all path travel times (c^{π}) for all paths (π) connecting a specified O-D pair (r, s) for all vehicles (n) traversing those paths divided by the total number of traversing vehicles over some specified time interval, or as $\bar{c}_{rs}^{\pi} = \frac{\sum_{\forall \pi} \sum_{\forall n} c_{rs}^{\pi,n}}{n}$ measured in units of seconds or converted to minutes.
- *Utility of Path Choice* (U_{π}^{rs}) – defined as the total satisfaction that a path choice (π) connecting a specified O-D pair (r, s) provides a user.

- *Link Volume* (V_{ij}) – defined as the number of vehicles that pass a given point on a roadway (link) during a given time interval (HCM, 2010) measured in units of vehicles.
- *Volume-to-Capacity* (V/C) *Ratio*– defined as the ratio of flow rate to capacity for a roadway segment or link (HCM, 2010).
- *Link Density* (κ_{ij}) – defined as the number of vehicles occupying a roadway segment (link) at a particular instant (HCM, 2010) measured in units of vehicles per feet or vehicles per mile.
- *Link Flow Rate* (q_{ij}) or (x_{ij}) – defined as the equivalent hourly rate at which vehicles pass a given point on a roadway (link) over a time interval of less than one hour (HCM, 2010) typically measured in units of vehicles per hour or converted to vehicles per minute. Additionally, flow rate is a function of space mean *speed* multiplied by *density* and as such, can be found using the equation $q = u\kappa$.
- *Free-flow Speed* (u_f) – defined as the theoretical speed when the density and flow rate on a roadway segment (link) are both near zero (when flow of traffic is unaffected by upstream or downstream conditions) (HCM, 2010).
- *Level of Service* (LOS) – defined as a stratified performance measure that represents the quality of service as measured on an A-F scale, with LOS A representing the best operating conditions and LOS F the worst (HCM, 2010). This measure is determined using thresholds identified in the Highway Capacity Manual (HCM) 2010, and can be specified for links representing urban streets by the ratio of *average link travel speed* versus *free-flow speed* $\left(\frac{\bar{t}_{ij}}{t_f}\right)$ and for freeway links by the *density* (κ_{ij}).
- *Root Mean Squared Error* $(RMSE)$ – defined as the square root of the sum of the squared errors across values predicted by a model or estimator versus observed data. It is used to estimate the general dispersion of data by quantifying their relative error.

- *Absolute Percentage Error* (APE) – defined as the absolute value of the difference between the mean of values $(\bar{x}_{rs})$ and an individual sample value (x_{rs}), normalized by the mean of the values, for a specific O-D pair (r, s), expressed as a percent, or as $APE = \left|\frac{\bar{x}_{rs} - x_{rs}}{\bar{x}_{rs}}\right| * 100$.
- *Mean Absolute Percentage Error* $(MAPE)$ – defined as the average of the absolute percentage errors across all O-D pairs (RS).
- *Mean Censored Absolute Percentage Error* $(MCAPE)$ – defined as a modification of the MAPE such that large positive error values are limited to a maximum value of 100 (Cools et al., 2010).
- *Structural Similarity* $(SSIM)$ *Index* – defined as an index derived to assess the quality of an image, or the difference between two images, based on the degradation of structural information. Applied to traffic assignment modeling, the index can capture the structural similarity between estimated and referenced O-D matrices through the comparison of O-D pairs; used to evaluate the quality of demand estimates (Djukic et al., 2013).

Additional information on some of the above performance measures can be found in the HCM 2010. In addition, speed-density, speed-flow, and flow-density relationships have been derived and subsequently utilized as part of the methodology for establishing flow models for DTA, as noted in the literature review. The above notation and definitions establish a foundation for the analysis methodology and strategies for evaluating subnetwork selection sizes and demand adjustments.

DTA Analysis Methodology

As part of the project framework, the next objective is to present the proposed analysis methodology. The analysis process that includes modeling networks and subnetworks for scenarios, including base conditions and construction or TCP alternatives, is based on the DTA model framework. As mentioned earlier, the DTA methodology was chosen due to

its ability to more realistically model traffic conditions, including congestion and queuing effects, and user behavior across a network in a time-variable setting. Therefore, it is important to detail the implementation of the components of the DTA model structure.

In any DTA application, there are three primary components: 1) the traffic flow model, 2) the time-dependent shortest path algorithm, and 3) the equilibrium solution method. For this study, the implementation of the three components and the supporting methodology is controlled by the DTA modeling software utilized. In this case, the VISTA software program has been chosen for creating the DTA models. VISTA applies the CTM for modeling traffic flow, a TDSP algorithm for generating shortest paths, and either a modified version of MSA or simplicial decomposition to perform the path assignment for achieving an equilibrium solution. The flow chart in Figure 4.1 illustrates the progression of the DTA modeling process in VISTA.

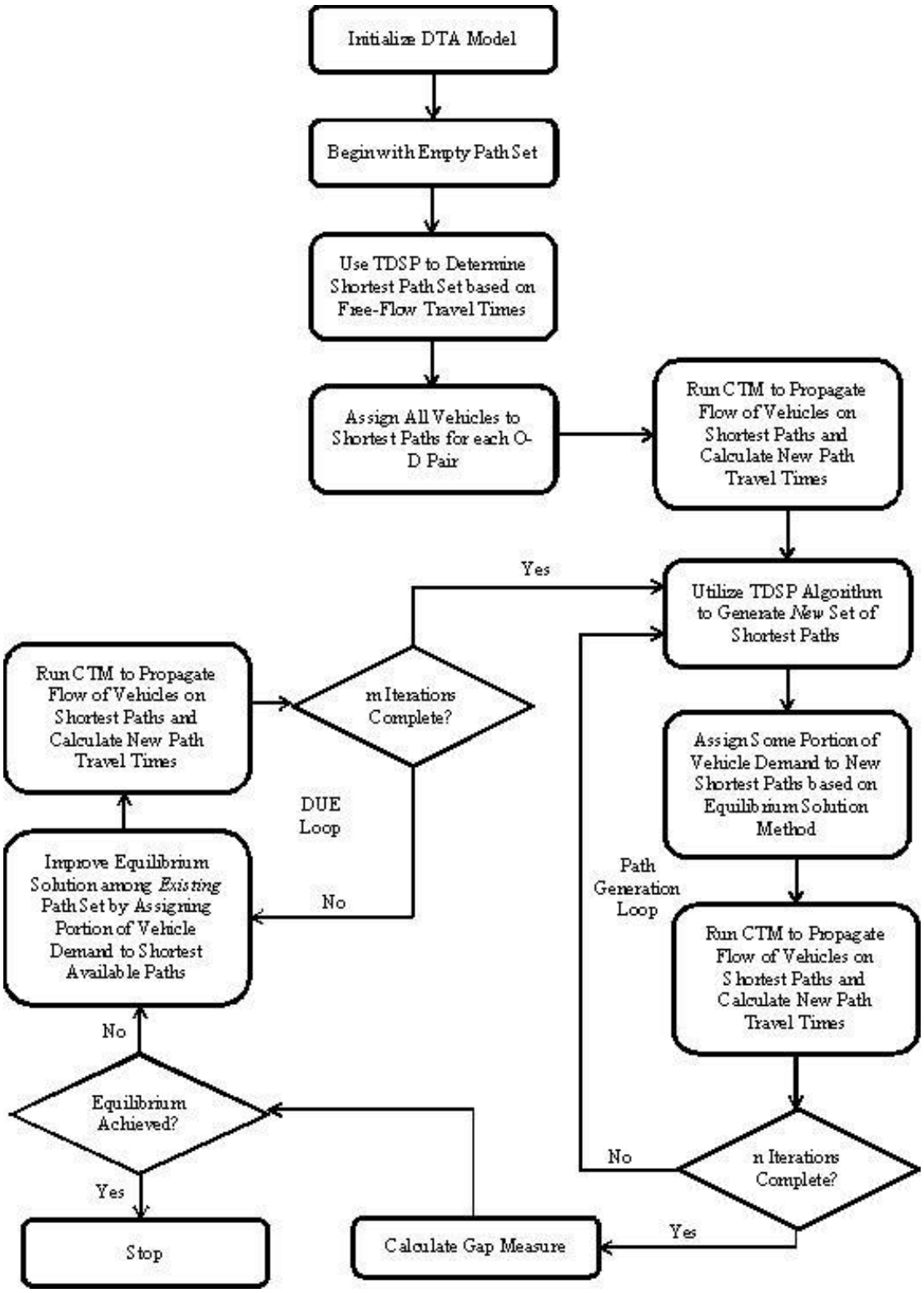

Figure 4.1 Flow Chart of DTA Analysis Process in VISTA

As shown in the flow chart, VISTA initializes the model and creates shortest paths based on the free-flow travel time for all paths in the network. This becomes the initial shortest path solution set. Vehicles are assigned to these paths and propagated through the network using the CTM. Next, two loop processes are utilized by VISTA. The first involves generating shortest path sets using TDSP and assigning vehicles to these paths based on the equilibrium solution method. Once a user-specified number of iterations (n) are completed, the relative gap is calculated and evaluated. If equilibrium has been achieved and the model is close enough to convergence, or a pre-specified maximum number of iterations have been completed, the model is stopped. If these conditions are not met, the model proceeds to the DUE loop. Here, the model attempts to improve the equilibrium solution among the existing set of paths; this is also known as restricted equilibrium. After a user-specified number of iterations (m) are completed, the model proceeds back to path generation using TDSP, and the process continues until equilibrium conditions are achieved or a maximum number of iterations for the model are completed.

To provide a more in-depth review of the components of the DTA, the processes are described herein. This begins by looking at the chosen flow model, the CTM, in more detail. As described in the literature review, the CTM involves dividing each link into a finite number of cells (Daganzo, 1994). The length of each of these cells is equal to the distance a vehicle travels at free-flow speed on the link for one time step. In VISTA, this time step is specified by the user during preparations to run the DTA model (typically 3 to 10 seconds). Next, the cells across a link are numbered consecutively beginning at the upstream end (from $i = 1\ to\ I$). The general equation governing the number of vehicles in each cell is as follows (Daganzo, 1994):

$$n_i(t+1) = n_i(t) + y_i(t) - y_{i+1}(t)$$

Where: $n_i(t)$ is the number of vehicles in cell i at time t

With this established, the flow between cells is defined as follows:

$y_i\,(t)$ is the number of vehicles entering cell i at time t

$y_{i+1}(t)$ is the number of vehicles exiting to cell $i+1$ at time t

And $y_i\,(t) = \min\{n_{i-1}(t), Q_i(t), \left(\frac{w}{v}\right)[N_i(t) - n_i(t)]\}$

Where: $n_{i-1}(t)$ is the number of vehicles in cell $i-1$ at time t

$Q_i\,(t)$ is the capacity flow into cell i at time t

$N_i(t) - n_i(t)$ is the amount of empty space in cell i at time t

w is the backward wave speed

v is the free-flow speed

The cell occupancies and transition flows between cells are updated at every time step (Daganzo, 1994). This configuration allows VISTA to model the propagation of time-dependent flow along a link. With this flow model implemented, the link travel times and subsequent path travel times can be calculated. These path travel times can then be used to determine the shortest path between each O-D pair using the TDSP algorithm. This algorithm is a modified version of Dyjkstra's algorithm implemented for STA. As such, the dynamic modification of the algorithm for use with DTA is presented below, along with supporting assumptions and theory.

The TDSP algorithm depends on the following assumptions:

1) First-in, First-out (FIFO) – the first vehicle to arrive on a link is the first vehicle to depart the link.
2) Waiting is not allowed at nodes.
3) The network is strongly connected, meaning, for any departure time (τ) there is at least one path (π) for every O-D pair (r, s).

Furthermore, TDSP relies on Bellman's Principle, which allows one to use information about intermediate shortest paths between O-D pairs to define shortest paths for other O-

D pairs. This enables the extension of shortest paths by utilizing the already identified shortest path to the previous node, instead of examining the full path set leading back to the origin. This can be defined by the following: if $\pi^* = [r, i_1, i_2, \dots, i_n, s]$ is a shortest path between r and s with departure time τ, then $[r, i_1, i_2, \dots, i_k]$ is a shortest path between r and i_k, also with departure time τ.

The modified version of Dyjkstra's Algorithm is presented as follows:
For each node i: the following is stored,

- A label C_i representing the arrival time for the shortest known path from r to i (or ∞ if unknown)
- A predecessor P_i identifying the second-to-last node on the shortest known path from r to i (or $\emptyset$ if unknown)

There also is established a list called "UnSetNodes" comprised of nodes that haven't yet been assigned a shortest path.

Given: Origin node r, departure time τ
Find: Shortest paths to all nodes $i \neq r$
Initialization:

Set C_r to τ and $C_i = \infty$ for all $i \neq r$,

Set $P_i = \emptyset$ for all i,

Put all nodes into UnSetNodes,

Iteration:

Step 1) Let i be the node in UnSetNodes with the lowest C_i label

Step 2) Remove i from UnSetNodes

Step 3) For each link (i, j), incident to node i, do the following:

If $C_i + t_{ij}(C_i) < C_j$ then $C_j = C_i + t_{ij}(C_i)$ and $P_j = i$

Step 4) If UnSetNodes is empty, then STOP; else, return to Step 1

The above algorithm will determine the shortest path for each node i for each departure time τ. Due to Bellman's Principle, this gives us the shortest path for each O-D pair in the network. With the shortest paths identified for each O-D pair in the network and each departure time using the above algorithm it can now be determined how many vehicles from the overall demand should be allocated to the shortest paths at each iteration step.

The process begins with assigning all vehicles to the shortest path set determined using free-flow travel times, and then recalculating path travel times using output from the CTM. Using these times, a new set of shortest paths for each O-D pair is established based on the departure time and impact of the vehicles already on the network. It is not optimal to assign all vehicle flow, after the first iteration, to the newly defined shortest path set since this will likely overload the paths and unduly increase the travel time for the routes. This process would likely cause the model to overcompensate at each iteration and never reach equilibrium. Therefore, a portion of the vehicles are assigned to the new shortest paths found after each subsequent iteration in an attempt to gradually move toward an equilibrium solution.

As identified in the literature review, several equilibrium solution methods, initially derived for use with STA, have been implemented with DTA models. These methods have also been incorporated into VISTA. One of the more simple strategies is the Method of Successive Averages (MSA); a process that requires minimal computational effort, but may take a long time to converge. While simplicial decomposition and gradient projection methods have been developed as improvements over MSA, they are computationally intensive and do not guarantee a more efficient convergence, particularly with small networks or subnetworks. Furthermore, modifications to the MSA methodology have improved its performance with respect to achieving an equilibrium solution (Pool et al., 2012b). These variations fall into the category of MSA-based heuristics.

To reiterate, MSA assigns the portion of vehicles to move between paths based on a progressively smaller weight (λ), or step size, defined as the quantity of one divided by the iteration number. Essentially, the assigned path-flow matrix (H) is updated for each iteration as follows:

$$H \leftarrow \lambda H^* + (1 - \lambda)H$$

Where: $\lambda \in [0,1]$

H^* is the optimal path-flow matrix based on the newly identified shortest paths

H is the existing path-flow matrix

Two of the methods for improving MSA utilized by VISTA include partial demand loading and origin-destination-time interval (ODT) based vehicle-path-cost sorting (or ODT path sorting) (Pool et al., 2012b). These methods are presented since they have been found, in combination, to provide an optimal convergence for the downtown Austin DTA network model, a model chosen as the prototype for establishing the subnetwork analysis methodology. The partial demand loading strategy is an MSA procedure that uses an incremental demand assignment for a fixed number of iterations (D) (Pool et al., 2012b). Over the first D iterations (user defined), the procedure assigns a fraction equal to one divided by D $(1/D)$ times the total ODT demand to the corresponding shortest path. The shortest path is recalculated at each iteration and the demand is reassigned accordingly. The goal of this modification is to spread out the assignment of demand to more paths earlier in the process to avoid oversaturating portions of the network when the step size remains large during the first few iterations.

The second methodology, ODT path sorting, is used after the initial several iterations to further improve the equilibrium solution process. This process assigns the same portion of vehicles (λ) to the new shortest paths for every ODT pair. For each O-D pair, the total number of vehicles moved to the shortest path designation for the current iteration is determined by sorting all paths (π) based on the cost gap of vehicles on the path ($\sum_{\forall n} g_n^\pi$) and moving vehicles with the highest cost gap (g_n^π) until a desired quota is

met. The purpose of this strategy is to achieve a faster convergence by prioritizing the movement of vehicles on the higher-cost paths relative to their shortest available path. With the methodology now established for all three components, the process of running a DTA model in VISTA can be examined.

To use the VISTA software to process a DTA model, the network must first be created. This can be done by importing network elements from another software program, such as TRANSCAD or ArcGIS, or building the network using the VISTA Editor tool. This includes creating links and nodes and entering element attribute information, such as link capacity, number of lanes per link, and traffic control at each node. Once the network has been created, dynamic demand tables with time-dependent O-D matrices must be created and imported. This is often done by taking a static O-D matrix for the same network and dividing and calibrating it for specific time periods, generally 15-minute intervals, using available traffic counts. Typically, dynamic O-D tables are created and calibrated for a peak period, as these are the most desirable times to model for evaluating traffic congestion.

For the specific models generated in this study, the primary network utilized is the Austin downtown network. The Austin downtown network is a subnetwork itself and the boundaries were carefully selected based on border characteristics, including major roadways and natural boundaries. This includes establishing Lamar Boulevard as the western border, I-35 as the eastern border, Ladybird Lake as the southern border, and the north edge of the University of Texas campus as the northern border. The DTA model in VISTA for the Austin downtown network contains 1,578 links, including 329 connectors, and 717 nodes, including 171 centroids (origin and destination).

This network can be utilized as a stand-alone prototype due to the fact that it has been set up and calibrated for use by CTR and CAMPO using available traffic count and signal timing information. Furthermore, CTR has performed an extensive review of the

geometric elements of the subnetwork, including general connectivity and directional movements, speed limits, number of lanes, and available intersection movements. Figure 4.2 illustrates the comparison between the downtown network components in ArcGIS (extracted from VISTA) and the Google map of the same area. The map shows the roadway and natural boundaries established for the subnetwork.

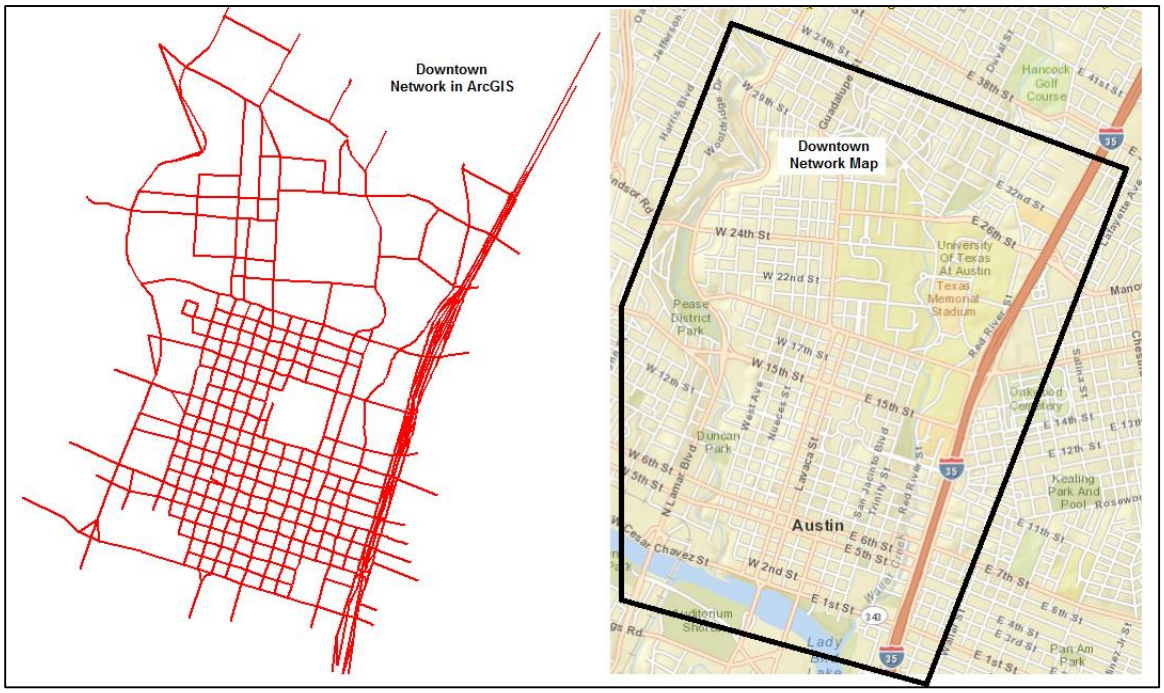

Figure 4.2 Comparison of the Austin Downtown Network Between ArcGIS Layout and World Street Map (Map Source: Esri, DeLorme, NAVTEQ, USGS, Intermap, iPC, NRCAN, METI, TomTom, 2013)

Once the geometric elements and dynamic demand matrices are incorporated and all components verified, the network is ready to run. The process of running a DTA model in VISTA can be completed by manually initiating a series of modules or using a JavaScript code developed by CTR. The modules are used to complete individual tasks such as preparing the network and demand, running path generation and DUE, or validating data. While the DTA model can be run using the modules manually for any network size, the JavaScript code can only be run on smaller networks. For the Austin downtown network, the JavaScript code is used to run a series of VISTA modules automatically. This code implements MSA with optional modifications, like those described above, to achieve

convergence, and operates utilizing a sequence of prompts that require user inputs, including those shown below:

- Network Name: name of the network to be analyzed using DTA
- Maximum Iterations: maximum number of iterations to run the path generation and DUE processes
- Minimum Gap (%): cost gap convergence threshold ($G\%$) for stopping the model (e.g. 0)
- Minimum Number of New Paths (% of Total Paths): minimum number of new paths to generate at an iteration as a proportion of the total number of paths already created
- Compute True Gap: determines whether or not to have the model generate a new set of shortest paths at the end of the last iteration to find the absolute least cost path for each ODT combination and calculate the resultant gap for the model
- Prevent Gap Increase: allows the user to set the model to revert back to the previous iteration if the gap increases as a result of moving vehicles to new paths in the current iteration
- Seed Random Number Generator (RNG): allows the user to seed the random number generator such that random decision processes in the model will be same across multiple runs, controlling for random differences in model results
- Type of Assignment: methodology utilized for assigning vehicles to shortest paths as part of the equilibrium solution process (e.g. ODT Path Sorting)
- Type of Initial Assignment: special methodology utilized for assigning vehicles to shortest paths during the first few iterations to avoid oversaturating the network (e.g. Partial Demand)
- Number of Initial Iterations: number of iterations over which the initial assignment is implemented

- Type of Lambda: type of weight parameter or step size (λ) to utilize in the assignment of vehicles to the shortest path set (H^*) (e.g. $1/iteration\ number$ for MSA)

With these values entered, the methodology for performing the DTA analysis is implemented by VISTA for the number of iterations specified. Following the model run, the results can be imported into the VISTA GUI for review. These results can also be output for additional evaluation.

This outlines the process for performing a DTA analysis on a network using the VISTA software. The computational time for completing the model process varies depending on the number of iterations specified and the size of the network. To achieve a reasonable gap size ($G\%$), typically less than 5 percent, many iterations need to be completed, and this can be magnified depending on the size and complexity of the network. The smaller the gap size, the closer the model is to equilibrium and the more accurate the results are likely to be. Consequently, the purpose of the study is to perform DTA using a subnetwork in order to save on the computational time to complete the specified iterations required to achieve a minimal gap. As stated earlier, this process requires two steps; 1) identifying the subnetwork area and 2) accounting for the area outside of the subnetwork in the analysis to the extent practical. These steps are discusses in more detail in the subsequent sections.

Subnetwork Selection

Subnetwork selection is the first component in the methodology for analyzing a subnetwork. Choosing the appropriate subnetwork is critical for encompassing the impacts from a construction project, TCP, or other type of network modification. Establishing a procedure for selecting an adequately-sized subnetwork requires a selection strategy, as well as a process for evaluating different sizes for multiple impact

scenarios. Some of the procedures identified in the literature review concerning subnetwork selection have been assessed and implemented for preliminary investigation. Several additional strategies have been considered based on assumptions about the impact range of capacity restrictions on link elements.

It is expected that the TCP components will define impacts to roadways that can be reflected by modifying specific links in the network, typically involving capacity reductions or complete element closures. Therefore, selection of the subnetwork specifically revolves around identifying the link(s) to be modified as part of the TCP and systematically selecting all surrounding network elements (links, nodes, connectors, and centroids) based on the particular method chosen. The strategies identified for review with respect to subnetwork selection include the following:

- Selecting all elements within a predefined (default) radius around the modified link(s) (e.g. one-half mile)
- Selecting elements based on identification of paths that use the modified link(s), including all elements within a specified radius anticipated to encompass most of the potential path-choice behavior made by those users
- Selecting elements based on a radius that encompasses changes in volume or travel time beyond a specified threshold identified from running an STA model on the full network for both base and impact scenario conditions
- Selecting elements based on a user-specified size parameter (ς) that identifies the connected order extending out from the modified link(s) to include in the subnetwork (e.g. a size parameter of one selects only the links directly connected to the modified link while a size parameter of two also includes the links connected to the first order selections)

Figure 4.3 illustrates the selected order process based on a chosen size parameter of one versus two.

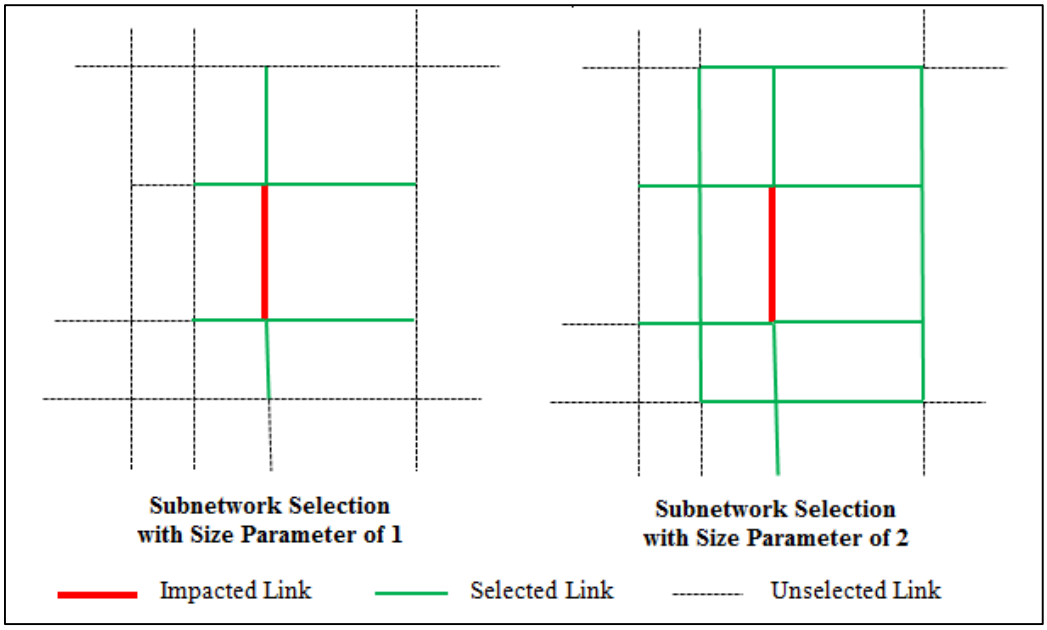

Figure 4.3 Demonstration of Connected Order Selection with Different Size Parameters

The above strategies were examined using ArcGIS within which the network elements could be easily mapped, visualized, selected, and extracted. Furthermore, the subnetwork selection process could be automated using modeler tools in the software program based on select user inputs. Implementation of the above strategies for testing and evaluation purposes is discussed herein.

It should be reiterated that the subnetwork analyses completed for this study are based on use of the Austin downtown network as a prototype. This is due to the fact that the network has been calibrated thoroughly and covers a small enough area that the full network can be run using DTA in a relatively short time. Furthermore, a full base-network run is always required for comparison with all subnetwork scenarios, regardless of the implemented strategy, whether they are utilized for testing purposes or practical application. This is important for evaluating the proposed strategies for subnetwork selection, and more importantly, appropriately accounting for the area outside the subnetwork in the scenario analyses.

It should also be noted that all of the aforementioned strategies for subnetwork selection must include the nodes attached to any links selected in the process. This is due to the fact that new centroids are created at the boundary points and the software must use an existing node to perform this modification. The first couple of strategies implemented involve setting a radius to mark the boundary of the subnetwork with the impacted link(s) as the center. To set a radius in ArcGIS for selecting all contained network elements for subnetwork designation, a model within the software was created to perform the process automatically, requiring that the user specify the radius value (in feet). For the first strategy, the user only needs to select and input a radius, such as one-half mile, and the appropriate selection tool can be run.

The model created in ArcGIS for selecting all elements within a radius is illustrated in Appendix A, Figure A.1. The dialogue box for user inputs is shown in Figure 4.4, below. The automated process begins by selecting all links in the link shapefile within the specified radius, then selecting all nodes connected to these links in the node shapefile. Then, all connector elements connected to any selected nodes are also selected from the connector shapefile and lastly, all centroids connected to those connectors are subsequently selected from the centroid shapefile. The selected elements are then copied into a new shapefile for each element type, respectively (selected links, nodes, connectors, and centroids).

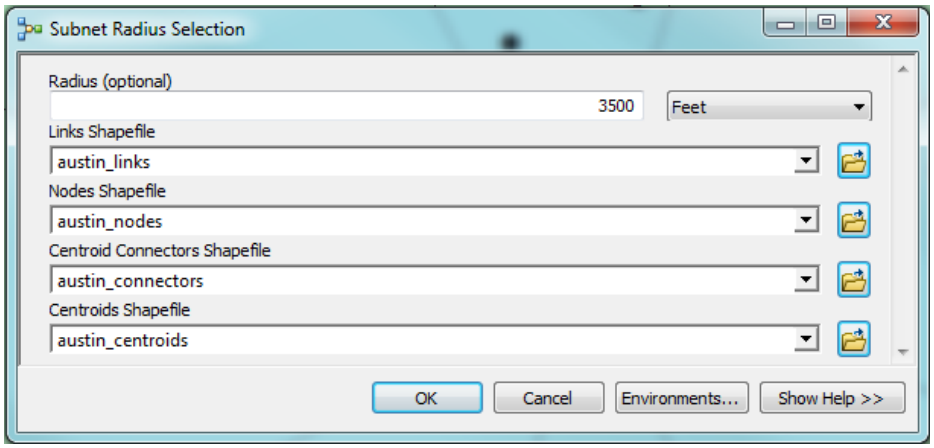

Figure 4.4 User Input Prompt for the ArcGIS Radius Selection Model

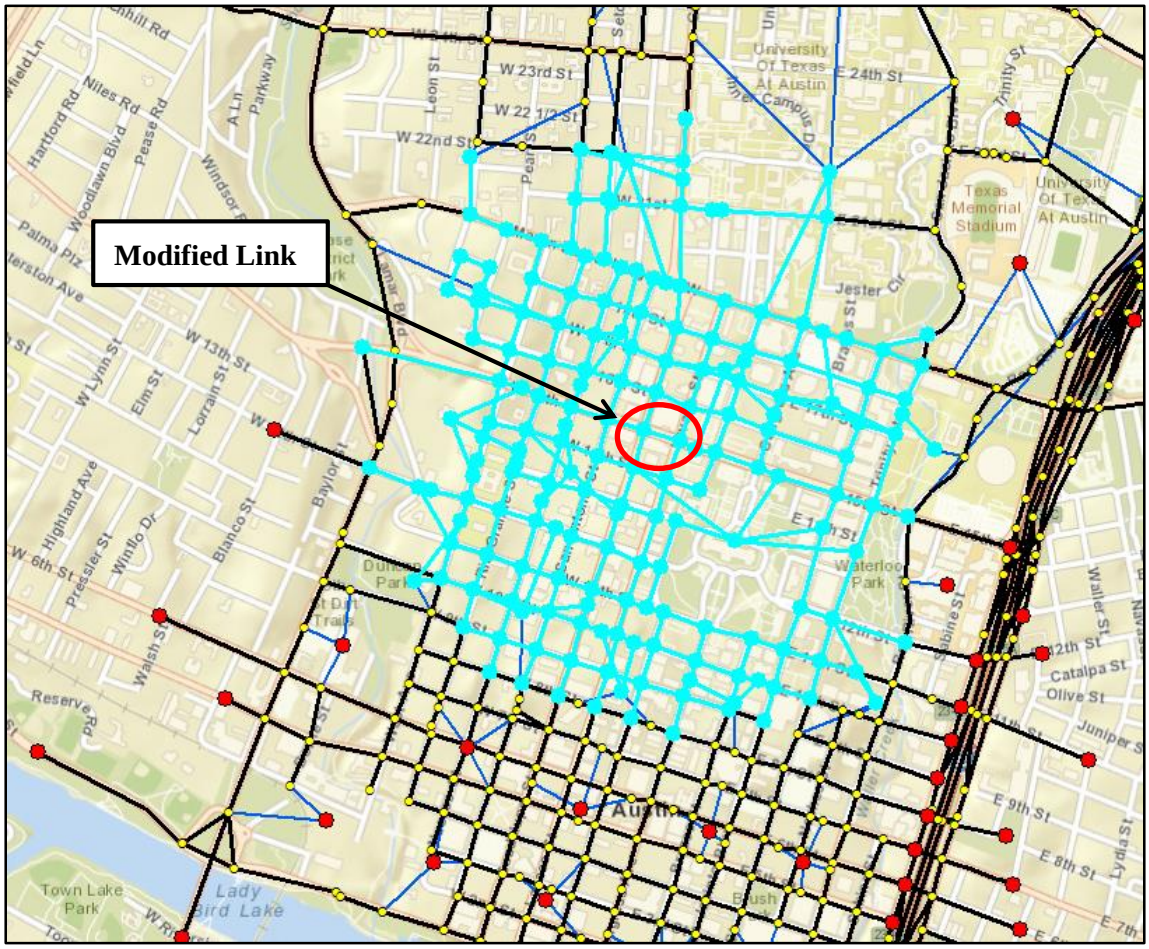

Figure 4.5 Sample Half-Mile Radius Selection in ArcGIS (Basemap Source: Esri, DeLorme, NAVTEQ, USGS, Intermap, iPC, NRCAN, METI, TomTom, 2013)

Figure 4.5 shows the selected elements of the network for a radius of a half-mile around a modified link along 15th Street between Guadalupe Street and Lavaca Street. For the other radius selection strategies, involving DTA path evaluation and STA results, a more detailed process is required prior to determining the radius. The strategy for identifying the paths that use a particular link in the DTA base model requires using a series of VISTA queries and several visualization tools in ArcGIS.

The following details the process for finding vehicle IDs associated with paths that use a particular link, and with these IDs, determining what paths the vehicles use after impacts to the select link have been imposed. This methodology can be used to find where vehicles divert their routes if they can no longer use a particular network link or the travel time associated with using the link is increased to a point where an alternative route is selected, enabling one to determine the spatial impact area of a link modification. Finding these vehicles in the alternate or modified network scenario can be used to identify their new paths. This can be done by isolating and subsequently visualizing these new paths in ArcGIS to get what is essentially, the first order impact area. These impacts are identified as first order since they involve only the vehicles that want to use the impacted link. They do not take into account the change in path selection among other vehicles that may occur as a result of these vehicles taking new paths and any subsequent congestion effects these decisions may cause.

The identified process is presented using an example TCP scenario where the eastbound direction of 2nd Street in downtown Austin has been closed between Colorado Street and Congress Avenue (a real-world TCP scenario obtained from a local consulting firm). The first step in the procedure is to identify the paths associated with using a particular link of interest in the network. This can be done by running the following Structured Query Language (SQL) query in the VISTA GUI while the base network is open:

Command:

select a.id,count(*) as volume,avg(sim_exittime-sim_departure)/60 as average_tt_minutes,a.origin,a.dest,links from vehicle_path a, vehicle_path_time b where b.sim_path=a.id and sim_departure>=*begintimeinterval* and sim_departure<*endtimeinterval* and *linkofinterest*=any(links) group by a.id,links,origin,dest

The above command will create a table in VISTA that contains the path IDs, path volumes, average path travel times, origins, destinations, and incident path links for any used path that includes the specified link (e.g. 118434, above). This table can then be downloaded, viewed, and manipulated in Excel. To reduce clutter, it is helpful to sort the paths by volume to isolate the most commonly used paths for visualization in case the link has a large number of associated paths. Once this file has been modified accordingly, it can be imported into ArcGIS and used to create a series of path shapefiles by means of another created model.

The model created in ArcGIS for creating a path shapefile based on links extracted from the links shapefile is shown in Appendix A, Figure A.2. This process begins with the user specifying the maximum number of paths to include in the final, merged shapefile. In other words, the user can determine how many paths to visualize that include a particular link in order to limit the number to be evaluated. If the paths are ordered with highest volume first, the paths will be selected by the model in descending order of utilization.

Once the user has input the number of paths to include, the software selects all links in the link shapefile associated with a particular path ID in the Excel table created using the above instructions. It then groups these links into an individual path shapefile and repeats this process until all the paths have been created or the maximum, user-specified number of paths has been reached. The model then merges all of these files into a single path shapefile. The associated symbology can then be adjusted to aid in visualizing the

direction of the paths, similar to the map shown in Figure 4.6. This process can be used to identify the extents of the path set for users of a particular link, a valuable tool regarding subnetwork selection and evaluation. It can provide a general idea of where route deviations may occur due to a network modification, helping identify the extents of possible impacts.

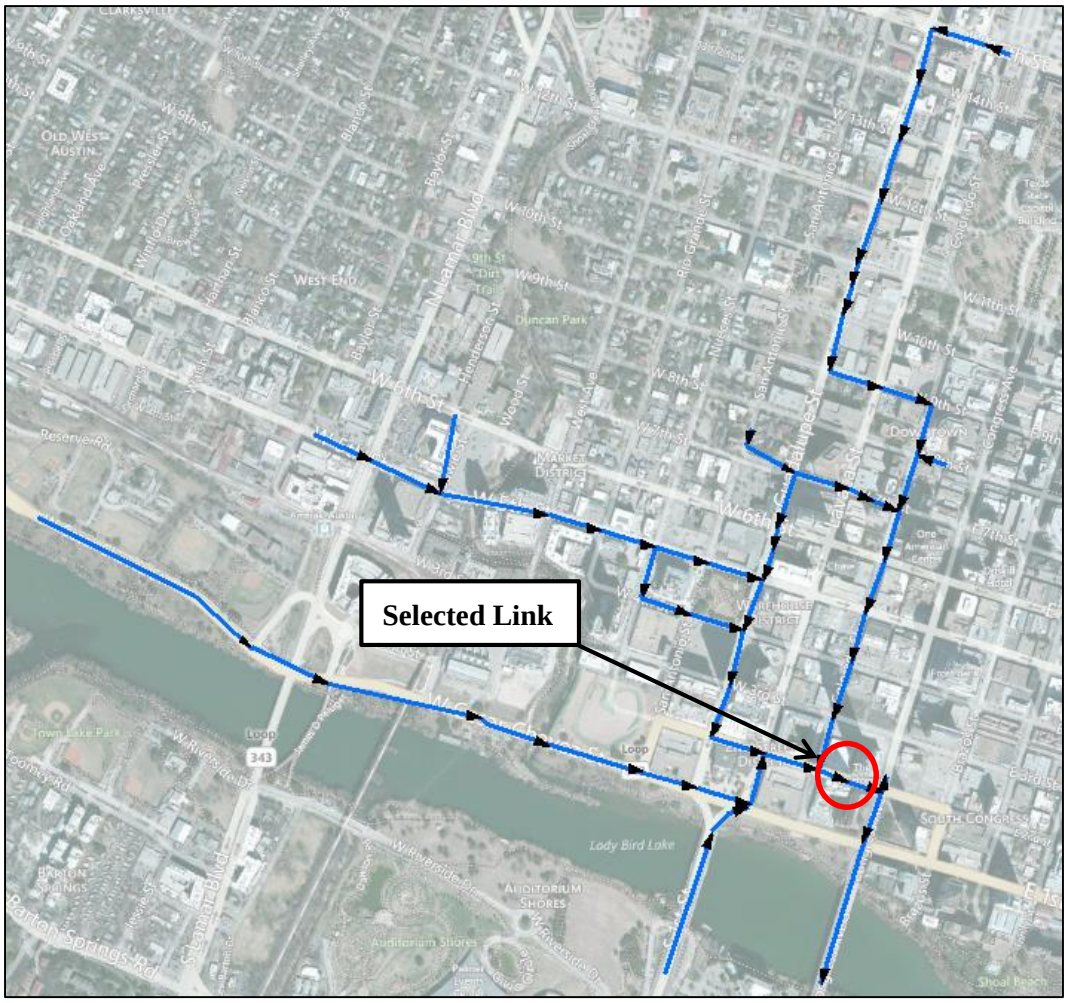

Figure 4.6 Visualization of Paths Using a Selected Link (Basemap Source: BING © 2010 Microsoft and its Data Suppliers)

A similar process can be completed to extract the vehicles that use the identified paths and locate these vehicles in an impact scenario network to determine their new paths with the 2nd Street link disabled. This process must be completed using the full alternative

network, since the demand table and subsequent vehicle IDs will match appropriately; however, the IDs will be different for a subnetwork where the total demand is reduced and vehicle IDs are arbitrarily assigned. As such, this process is for evaluation purposes only since using the full DTA model in the impact scenario is not the goal of the study. Nevertheless, this does provide a valuable tool for evaluating path changes with respect to vehicles that would use the modified link(s), and subsequently, the subnetwork selection itself.

This process begins with creation of a table in VISTA, within the base network, of the path IDs that use the modified link, as extracted using the aforementioned methodology. This table of these path IDs can be used along with the VISTA vehicle ID output table that includes the respective paths that they have been assigned, in order to isolate the vehicles using paths that include the link of interest. These vehicle IDs can then be extracted and used to create a VISTA table in the network database for the impact scenario. With this table properly input, these vehicle IDs can be matched to their new paths in the impacted network. The first step of isolating the vehicle IDs using the paths identified in the base scenario network within a specified time interval is completed using the following query:

select * from vehicle_path_time where dta_path in (select *columname* from *vistatablename*) and sim_departure>=*begintimeinterval* and sim_departure<*endtimeinterval*

The results of the above query can then be downloaded to an Excel file and the associated vehicle IDs can be extracted for creating the appropriate table in the impact scenario network in VISTA. Once this table has been added to VISTA, the new paths that these vehicles utilize can be isolated for visualization. The following query can be used to isolate the new path IDs that the identified vehicles are assigned, along with providing volume and travel time summaries:

select a.id,count(*) as volume,avg(sim_exittime-sim_departure)/60 as average_tt_minutes,a.origin,a.dest,links from vehicle_path a, vehicle_path_time b,vehicle_ids_*linknumber* c where b.sim_path=a.id and c.veh_id=b.id and sim_departure>=*begintimeinterval* and sim_departure<*endtimeinterval* group by a.id,links,origin,dest

The above command will create a table in VISTA that can be exported to Excel and manipulated for importing into ArcGIS. With this file for the impact scenario created, a similar process of preparation can be implemented, including sorting the paths by volume and running the associated model in ArcGIS to create a merged shapefile of the identified paths (see Figure 4.6). Figure 4.7, shows the visualization of the base scenario paths (overlaid in blue) and the impact scenario paths (in red).

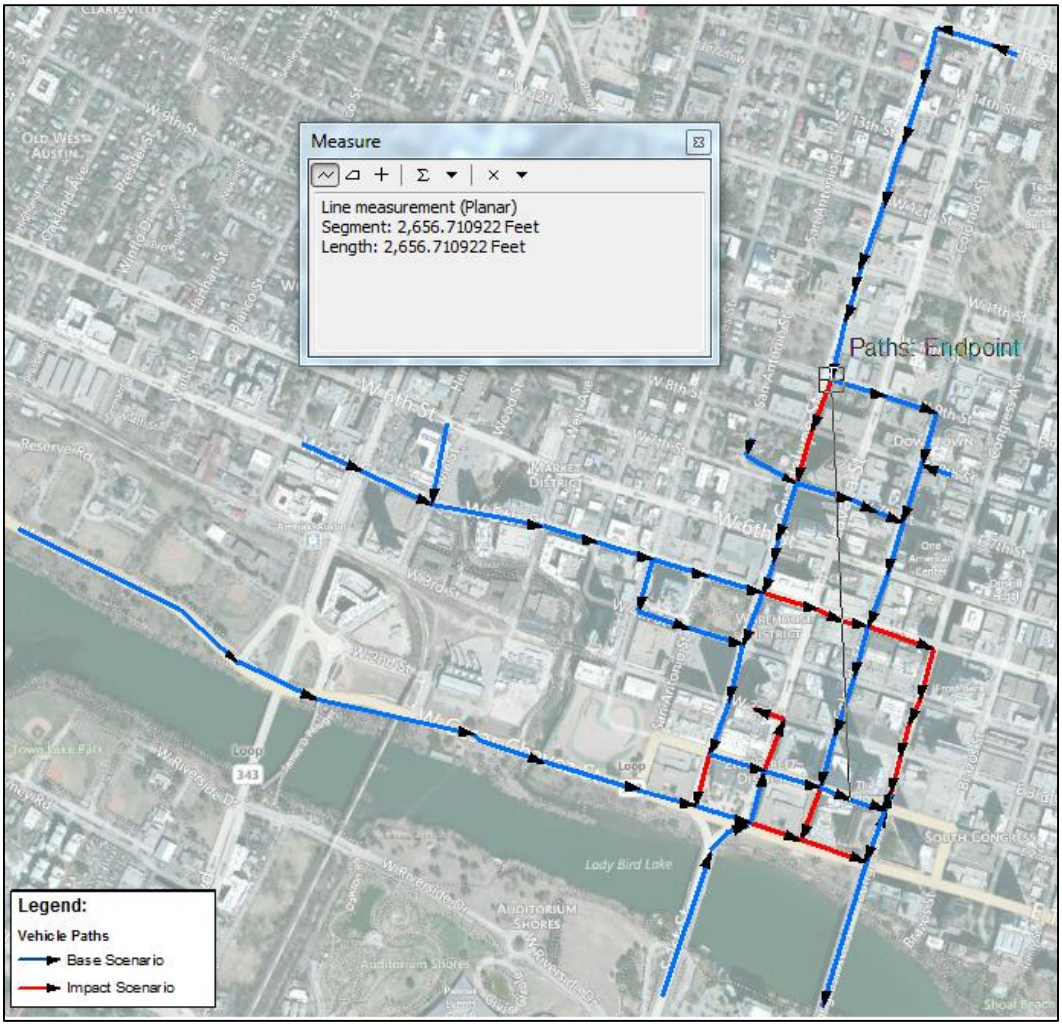

Figure 4.7 Visualization of Paths Rerouting Vehicles Around the Modified Link (Basemap Source: BING © 2010 Microsoft and its Data Suppliers)

This map allows one to identify path changes that reroute travelers around the closed link. This illustration can also be used to determine a radius that would encompass all these first order routing impacts, as shown in the figure. This radius could then be input into the radius-based subnetwork selection model to select the elements to include in a subnetwork. Again, this process involves using the full alternate scenario network; nonetheless, it can be utilized to evaluate possible default radius selection options for different impact scenarios.

Another option, that does not require a DTA analysis of the full alternate network, is to use STA results to identify changes to the network caused by the TCP. Once these changes have been identified, a radius can be selected to encompass the extent of these changes, similarly to the above strategy. Therefore, instead of running a DTA model of the full network for the base and alternate conditions, an STA model is used. The purpose of using an STA model is to estimate potential impacts without the computational burden of utilizing a full DTA model. As noted, STA models can generally be run for a large network in an order of magnitude less time than a DTA model. Using warm-start techniques, where the alternate scenario builds off the results of the base scenario, these models can be run even faster.

This process begins with exporting information from the DTA base network, including link and node attributes and the dynamic demand table, into an Excel spreadsheet created specifically for implementation with an STA analysis software code. This code uses a special algorithm process to quickly and accurately apply STA to reach convergence with a relative gap of nearly zero. A special Excel spreadsheet has been set up to transfer the DTA information into STA format, including reassessing link IDs, establishing a static demand matrix, and creating link performance functions. Once the Excel spreadsheet has been updated for the identified network, select entries can be exported for use with the STA code.

The code is used to run STA on both the base and alternate networks to compare the change in volume and travel time experienced on links throughout the network. This information can then be imported into ArcGIS by joining the STA output tables with the link shapefile attribute table in ArcGIS. With this complete, visualization of the results can be completed using the appropriate shapefile symbology, as shown in Figure 4.8.

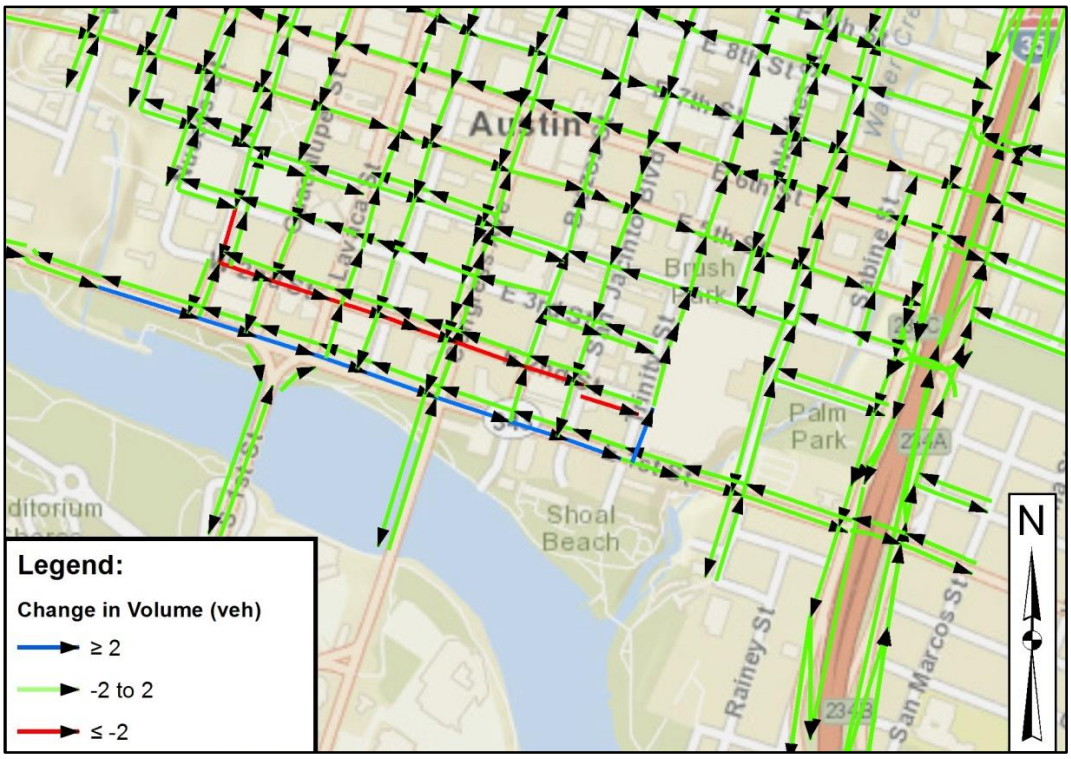

Figure 4.8 Visualization of Volume Changes Using STA (Basemap Source: Esri, DeLorme, NAVTEQ, USGS, Intermap, iPC, NRCAN, METI, TomTom, 2013)

The map in the above figure illustrates where volume changes were recorded by the STA model for the 2nd Street closure scenario. Those links in blue represent increases in volume (2 or more vehicles), and those in red represent volume decreases (including the 2nd Street link closed in the TCP scenario). In a similar process to the one previously discussed, this map can be used to establish a radius that encompasses the impacted area in terms of either volume changes (as shown) or travel time changes output from the STA model. This radius can then be input into the radius selection model in ArcGIS and the resultant, selected network elements extracted for subnetwork analysis.

The last identified strategy for subnetwork selection involves identifying a size parameter that selects links, along with other network elements, connected to the modified link(s) by specifying a limit of connecting order (as illustrated in Figure 4.3 on page 93). This process is based on the strategy identified in the literature review for subnetwork

selection with respect to network vulnerability assessments (Chen et al., 2011). In the cited report, the optimal size parameter was identified to be in the range of 3 to 9, based on case study analyses. As such, a model was created in ArcGIS to enable a user to specify a size parameter and review the selected elements for extraction. This model is shown in Appendix A, Figure A.3, along with the associated user input prompt in Figure 4.9.

The selected order model process begins by automatically selecting links in the link shapefile connected to the modified link(s), along with selecting the endpoint nodes for these links. Any subsequent connectors and centroids connected to these elements are also selected. This process extends outwardly from the modified link(s) until the connected order is satisfied based on input size parameter. The selected elements are then copied into a new shapefile for each element type, respectively (selected links, nodes, connectors, and centroids). It should be noted that this selection strategy is completely based on the user input of the size parameter and, as such, is dependent on the engineering judgment of the user for defining the extents of the subnetwork. A default size parameter may be established once evaluation of the strategy is completed. An example subnetwork selection (2^{nd} street TCP scenario) for a size parameter value of 5 using this methodology is provided in Figure 4.10.

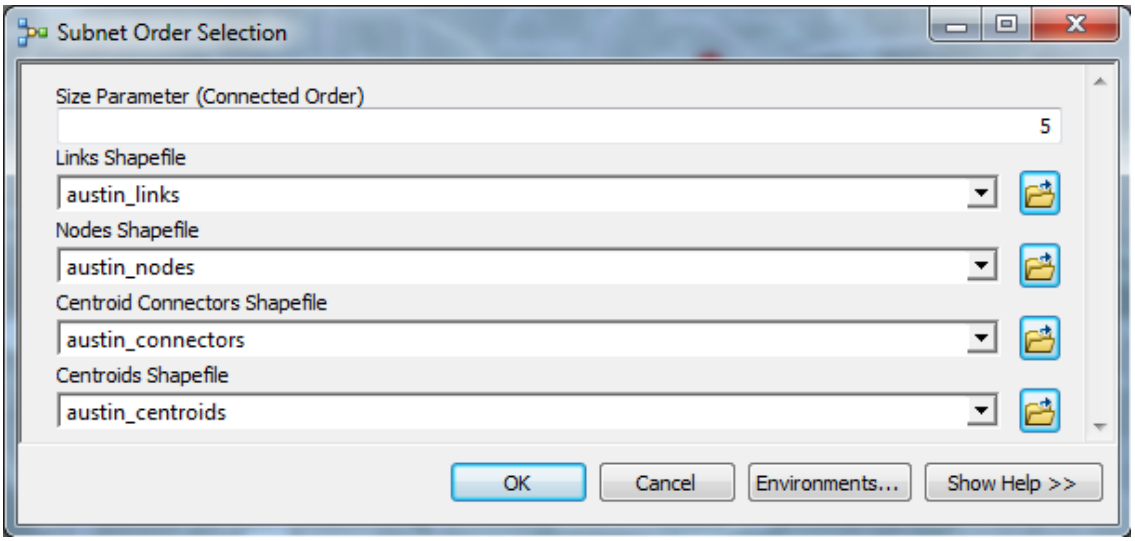

Figure 4.9 User Input Prompt for the ArcGIS Connected Order Selection Model

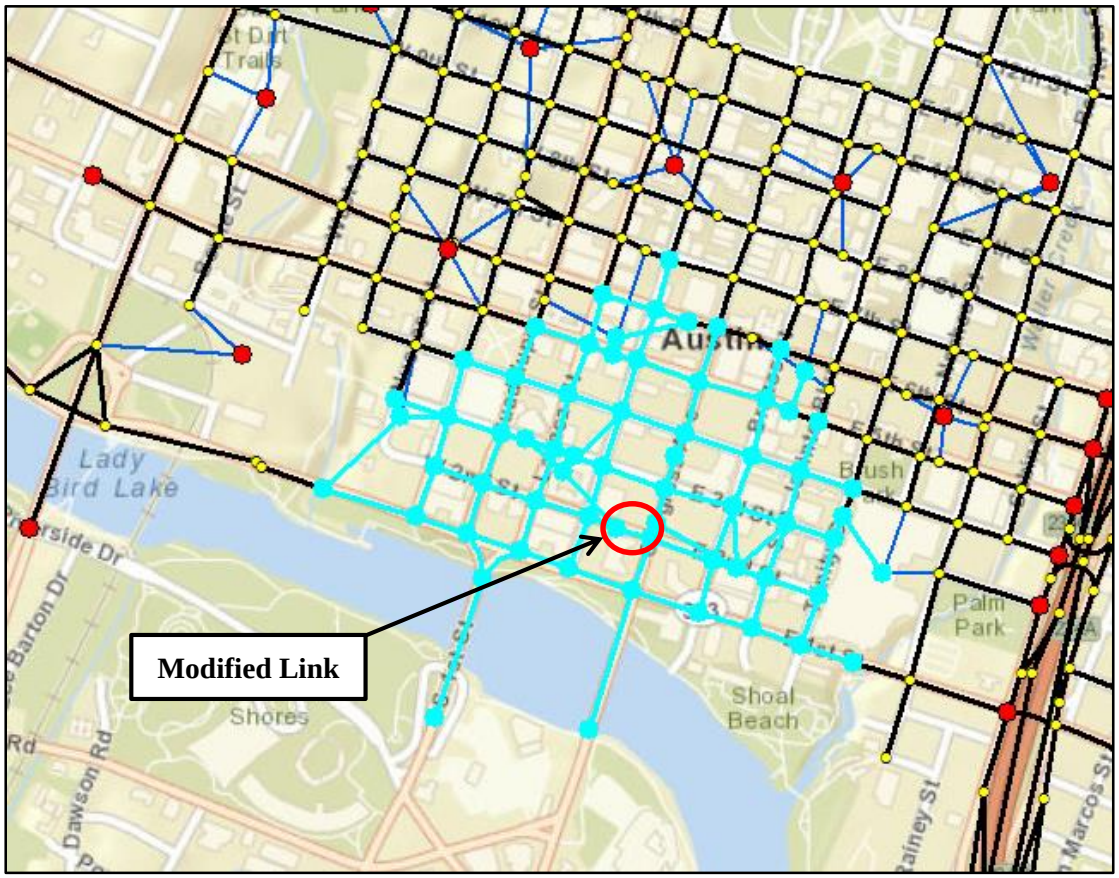

Figure 4.10 Sample Connected Order Selection with Size Parameter of 5 in ArcGIS (Basemap Source: Esri, DeLorme, NAVTEQ, USGS, Intermap, iPC, NRCAN, METI, TomTom, 2013)

This completes the demonstration of the proposed methods implemented and evaluated for subnetwork selection. Once a method is chosen for subnetwork element selection, it is necessary to select a subnetwork size for evaluation. The next section describes the process for assessing subnetworks of different sizes for multiple scenarios.

Evaluation of Subnetwork Sizes

The purpose of evaluating subnetworks of variable sizes for different scenarios is to test the adequacy of a proposed selection strategy for accommodating a potential scenario of interest. The process is intended to provide guidance to those implementing subnetwork analyses relative to choosing a size sufficient to capture the primary traffic impacts caused by a network modification. While some impacts are anticipated to extend beyond the boundary of a subnetwork, prior research suggests most, if not all, will be limited to a localized area (Chen et al., 2011). Though likely dependent on the scenario's scale, it is intended that the estimated area of influence be identified and included in the subnetwork.

To evaluate different subnetwork sizes for multiple scenarios, the selected order process was chosen. As described earlier, implementation of this method involves selecting network elements based on a user-specified size parameter that designates the connected order extending out from a modified link to include in the subnetwork. This method was chosen due to the documented precedence of implementation to evaluate the impact of disabling a link on the adjacent network. The accompanying research recommends a size parameter (connected order) between 3 and 9 (Chen et al., 2011). A size parameter of 3 is relatively small for this type of analysis and review process since it provides such a limited level of connectivity around the modified link. Therefore, only parameters of 5 or greater are considered for purposes of this research.

To evaluate subnetworks consistent with different size parameters, a number of impact scenarios must be tested. Once these scenarios have been selected, they can be implemented and the impact of a network modification assessed. Consequently, the size of subnetwork selected may also be evaluated to determine if enough of the impacts are contained. The primary method of evaluation involves reviewing extracted boundary demands for each subnetwork size. This is due to the method in which the boundary demands are obtained.

Using the process established at CTR, boundary demands are extracted from the vehicle trajectory information obtained from the full network analysis. Vehicles passing through the subnetwork boundary maintain their trip end and associated centroid ID within the subnetwork, and their entry point assigned as the other trip origin, as previously described. Therefore, impacts extending beyond the boundary will be reflected by changes to the demand at the boundary. Comparing boundary demands between base and impact scenarios can then be used to determine if the subnetwork size is adequate. It is assumed that if boundary demands are similar enough, that is, they are not statistically different, it can be concluded that no significant impacts extend beyond the boundary.

To test for potential differences, a number of statistics will be calculated and compared between scenarios. This will involve running both the full network for both the base and impact scenarios, extracting boundary demands across all subnetwork sizes, and computing the statistical measures. The statistics to be evaluated include the root mean squared error (RMSE), the mean censored absolute percentage error (MCAPE), and the structural similarity (SSIM) index. The primary assessment of the scenarios will be completed based on statistical hypothesis tests comparing means of these measures across multiple runs of the base scenario, as well as a number of impact scenarios.

Since the DTA model produces slightly different results each time it is run using VISTA, ten runs of the full network for each preliminary test scenario will be used to compute

these statistics. Ten runs have been chosen since this number appears adequate to provide a sample distribution for each scenario, as well as a paired t-test, without requiring an inordinate amount of time and effort, as well as computer space. It is intended that these statistics be used as aggregate measures of the variation in boundary demand resulting from each model run. Use of these measures is assumed to be valid as long as they, and the disaggregate data they represent (ODT demand), consistently follow a normal distribution.

In addition, prediction intervals will be calculated and evaluated for these measures. It is speculated that the results of the hypothesis tests will support the use of prediction intervals through the provision of consistent conclusions. In other words, where the demand measure for an impact scenario falls outside of the prediction interval for the base scenario, the hypothesis test should verify that the impact scenario is indeed statistically different. Therefore, the prediction interval can be used without the full hypothesis test for reviewing additional scenarios. This is due to the basic function of the prediction interval and is important for several reasons.

The prediction interval is used to determine the range of values within the distribution of a population, a range within which a subsequent data point should fall. Therefore, a calculated prediction interval for a set of base scenario demand measures can be used to assess whether a single impact scenario measure falls within the same distribution. If it does, the impact scenario does not demonstrate a statistically significant difference, i.e. significant impacts of the modification do not extend beyond the boundary of a chosen subnetwork. Use of the prediction interval is intended to save substantial time and effort necessary for evaluating remaining impact scenarios, as performing the hypothesis test will require running each impact scenario multiple times and use of the prediction interval for the base scenario only requires running the impact scenario once.

As previously noted, the outward impacts resonating from a network modification that impact inbound trips are anticipated to be reflected by the entering boundary demand. Primary impacts to internal-to-internal or internal-to-external trips are expected to be captured within the subnetwork model. As a result, the inbound boundary demand is presumed to be the primary representation of impacts extending beyond the subnetwork that are of principal concern. This includes trips with destinations inside the subnetwork, or external-to-internal trips, as well as those that traverse the subnetwork, or external-to-external trips. Therefore, the boundary demand that will be evaluated includes only the inbound trips.

The hypothesis tests for the scenarios will involve calculating the RMSE, MCAPE, and SSIM index using the average of the demand extracted from the base scenarios as the benchmark, or target value. The mean of the base scenario runs is used in the absence of a true or real-world estimate of the demand and acts as a representation of the aggregation of the model results. The following formulas are used to calculate each of the statistical measures. First, the RMSE is calculated across all O-D pairs (RS) and time periods (T) as follows:

$$RMSE = \sqrt{\left(\frac{1}{n}\right)\sum_{rs,t}(\bar{d}_t^{rs} - d_t^{rs})^2} \quad \forall rs \in RS \quad \forall t \in T$$

where $\bar{d}_t^{rs}$ is the average demand for each O-D pair (r, s) and time period (t), d_t^{rs} is the demand for a particular run for that same ODT combination, and n is the total number of ODT combinations for which demand exists. Likewise, the MCAPE is calculated across all O-D pairs (RS) and time periods (T) using the same notation as the RMSE and with the following expression:

$$MCAPE = \left(\frac{1}{n}\right)\sum_{rs,t} min\left\{100, \left|\frac{\bar{d}_t^{rs} - d_t^{rs}}{\bar{d}_t^{rs}}\right| * 100\right\} \quad \forall rs \in RS \quad \forall t \in T$$

The SSIM index is calculated using a special modification for comparing demand matrices for a specified time interval (t), where the rows represent origins $(r,\ \forall r \in R)$ and the columns represent destinations $(s,\ \forall s \in S)$. Its application requires use of a local window or square-section of O-D pairs that moves cell-by-cell across the entire matrix. This subsection is used to account for local spatial correlation. This requires the origin and destination IDs to be listed in the matrix in an order consistent with their location such that neighboring centroid IDs in the matrix represent centroids located in close proximity to each other spatially. An SSIM index value is determined for each local window based on a weighted distribution across the cells (O-D pairs) contained within the window. As such, the included cells are given a weight that changes as a function of the chosen distribution, typically with a decreasing value moving further away from the center of the window.

The local window is typically an $N \times N$ matrix with cell weights established based on a circular symmetric Gaussian weighting function with diminishing weights extending out from the center cell (Wang et al., 2004; Djukic et al., 2013). Several additional weighting strategies have been evaluated with respect to the Austin downtown network to determine the optimal distribution to use based on the network topology (Bringardner et al., 2013). Four combinations were tested within a 3x3 square window such that only adjacent centroids to the center cell are contained, as shown in Figure 4.11. It was determined that the window with a cross-shaped weight distribution was appropriate for analysis (highlighted in Figure 4.11). The basis for this strategy is that only adjacent cells with the same origin *or* same destination receive weights and are contributory to the local SSIM index.

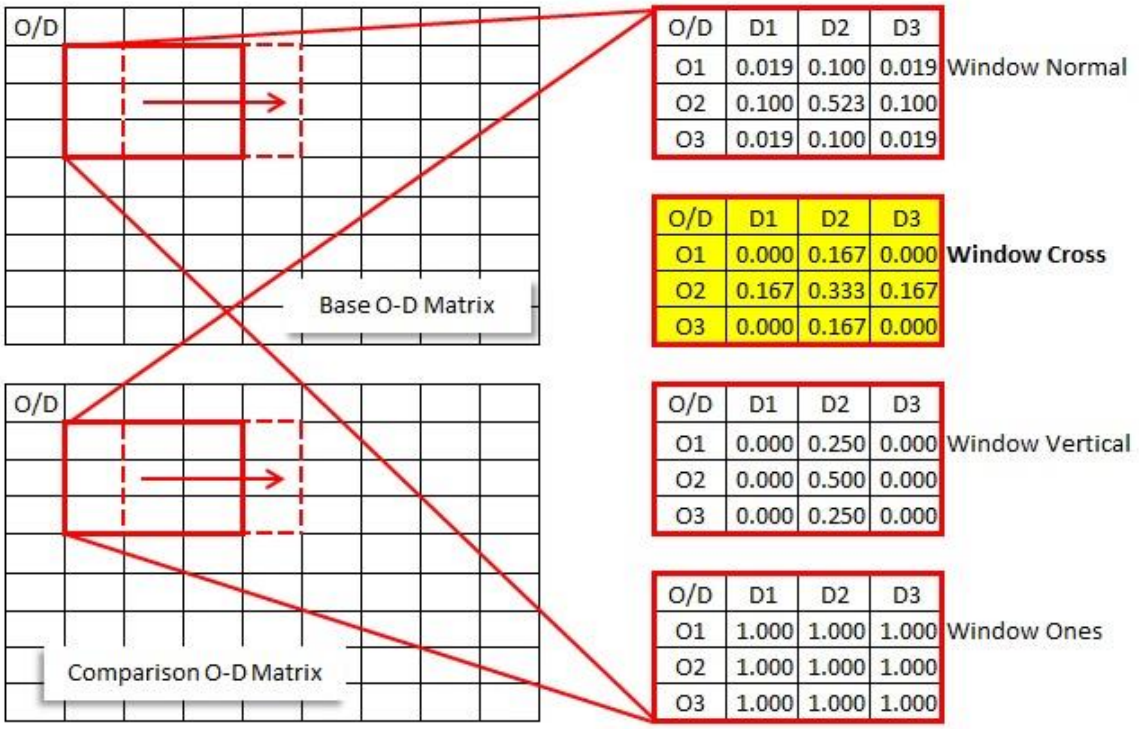

Figure 4.11 Multiple Strategies for Applying Local Window Within Base and Comparison Matrices

Once a window size and weighting strategy have been chosen, effectively establishing a spatial weights (sub)matrix, the SSIM index for each window, as well as the entire matrix can be determined. The index is based on a combination of three components that compare the mean, variance, and covariance between the two demand matrices (Djukic et al., 2013). The resulting equation for calculating the SSIM index for the local window extracted from each demand matrix is shown below:

$$SSIM(\bar{d}, d) = \frac{(2\mu_{\bar{d}}\mu_d + C_1)(2\sigma_{\bar{d}d} + C_2)}{(\mu_{\bar{d}}^2 + \mu_d^2 + C_1)(\sigma_{\bar{d}}^2 + \sigma_d^2 + C_2)}$$

where $\mu_{\bar{d}}$ is the mean and $\sigma_{\bar{d}}$ is the standard deviation of the spatial weights matrix for the base (average) demand $(\bar{d})$, μ_d and σ_d are the mean and standard deviation for the spatial weights matrix for the comparison demand (d), $\sigma_{\bar{d}d}$ is the covariance term used to

quantify the structural similarity between the two demand matrices, and C_1 and C_2 are constants used to stabilize the index when the means and variances are close to zero (Dkujic et al., 2013). The constants are calculated as $C_1 = (K_1 L)^2$ and $C_2 = (K_2 L)^2$ where L is the dynamic range (equal to the maximum cell demand [$\max(\bar{d}_t^{rs}, d_t^{rs})$]) and K_1 and K_2 have default values of 0.01 and 0.03, respectively (Wang et al., 2004). The local index value is calculated for each step as the window is moved across the demand matrices. The overall SSIM index can then be computed as the mean of the local SSIM indexes:

$$MSSIM(\bar{D}, D) = \left(\frac{1}{M}\right) \sum_{m=1}^{m} SSIM(\bar{d}_m, d_m)$$

where $\bar{D}$ is the base (mean) demand matrix, D is the comparison demand matrix, m is the index of the local window with M total windows across the entire O-D matrix. The SSIM is symmetric, so regardless of order, the comparison of the two matrices produces the same index value. The index is bounded by -1 and 1, such that the SSIM is one if and only if the matrices are the same. When the SSIM is zero, there is no spatial correlation between the base and comparison matrix and the demands are overtly dissimilar. Since the SSIM index was originally established to compare two images, a value of -1 suggests an inverse relationship exists, similar to the comparison of an original image and its negative.

The above formulas have been coded into Matlab so that the necessary calculations can be completed automatically once the demand matrices have been input accordingly. Again, for the subnetwork size assessment, the average boundary demand across 10 base runs is used to establish the base matrix, with individual base and impact runs used to provide comparison matrices. Therefore, an SSIM index value can be computed for each model run.

Once the RMSE, MCAPE, and SSIM index have been calculated for each individual model run, statistical tests can be performed. These tests can be completed based on the assumptions that the runs are independent and the values are identically (normally) distributed with equal variances between samples. The assumption of independence between the runs is based on the fact that the individual model runs will be completed from scratch. So although the network and the inputs are the same, the path sets, route assignments, and results will be cleared between each run. The assumption of normal distribution can be verified using a Lilliefor or Anderson-Darling test. The Lilliefor test is commonly implemented for small sample sizes ($n < 30$). The assumption of equal variances with the base and comparison sample sets can be verified using a standard F-test.

Once the assumptions have been verified, the next step is to determine whether the means of the statistical measures across ten runs are statistically different between the base and impact scenarios. This requires not only 10 runs of the base scenario, but 10 runs of the impact scenario. A preliminary sample size of 10 has been chosen since each of the models for the full network takes a considerable amount of time and computational effort and memory. As a result, an independent sample t-test will be used to test the hypothesis. The subsequent hypothesis is expressed as follows:

$$H_o\colon\ \mu_1 = \mu_2\ , \qquad The\ means\ are\ equal$$
$$H_a\colon \mu_1 \neq \mu_2\ , \qquad The\ means\ are\ not\ equal$$

The number of degrees of freedom for the test is given by: $df = n_1 + n_2 - 2\ =\ 10 + 10 - 2 = 18$. For a significance level (α) of 0.05, the threshold t-statistic for a two-tailed test is $t_{0.025,18} = 2.101$. If the t-value produced from the hypothesis test is greater than or equal to 2.101, the null hypothesis is rejected and it can be concluded that the two means are not equal. Therefore, it can be inferred that the base and impact scenario demands are not statistically similar at the 0.05 level of significance. This difference in the demands is

based on the differences in traffic flows that result from the network modification, further implying that the impacts extend beyond the subnetwork boundary. Essentially, if the null hypothesis is not rejected, it is concluded that significant impacts do not extend beyond the boundary and the chosen subnetwork size is adequate.

Another way to investigate the measures produced from the two samples and determine if they are statistically similar is to produce confidence or prediction intervals. The confidence interval is useful in that it establishes a bound on the mean that is being tested. A 95-percent confidence interval indicates one can be 95-percent confident that the population mean falls within the range calculated. The prediction interval, on the other hand, establishes a range within which one would expect a future or new data point to fall. For a 95-percent prediction interval, one can be 95-percent confident that a future point falls within this range. This is the appropriate interval for determining whether an impact run falls within the expected range about the mean of the base runs to the level of confidence specified.

Essentially, the base runs are used to establish a range of boundary demands that would be expected based on random differences in the model results. If the demand extracted at a subnetwork boundary from an impact scenario does not fall within the range, one can reasonably assume that this demand is outside what would be expected of random effects, at the significance level specified. The equation for the prediction interval is shown below:

$$PI = \bar{x} \pm t_{\alpha/2,n-1} s \sqrt{1 + \left(\frac{1}{n}\right)}$$

where $\bar{x}$ is the mean, $t_{\alpha/2,n-1}$ is the t-statistic for α level of significance and a sample size of n, and s is the standard deviation for the sample. For a significance level (α) of 0.05, the t-statistic for a sample size of 10 is $t_{0.025,9} = 2.262$. This interval is used in conjunction with the hypothesis test to determine if the prediction interval is robust for

evaluating whether the impact scenario demand measure falls within the expected range of the base scenarios. It is intended that the prediction interval be used to evaluate scenarios and respective subnetwork sizes in place of full hypothesis testing for additional scenarios. As previously noted, the prediction interval is intended to be used to evaluate a single run of the impact scenario model instead of the 10 runs specified for the hypothesis test. Therefore, scenarios and subnetwork sizes can be evaluated more efficiently.

The above process has been established to evaluate changes to subnetwork boundary demand across different subnetwork sizes for multiple impact scenarios. The ultimate goal is to provide guidance relative to selecting an appropriate size of subnetwork necessary to model the primary impacts of a network modification throughout a localized area. With this in place, the second part essential for implementing a proper subnetwork analysis can be explored. The process involves adequately accounting for changes in travel behavior and route choices occurring outside of the selected subnetwork. The following section describes the development of a strategy for estimating adjustments to the subnetwork boundary demand in an attempt to account for these impacts.

Subnetwork Demand: Accounting for the Outer Network

Currently, there is a method for creating a subnetwork from a larger network that was developed at CTR. This methodology does not consider the treatment of areas beyond the subnetwork; rather, it creates new origin and destination centroids at the boundary of the subnetwork and generates O-D demands at these centroids based on the inbound and outbound trips produced as part of prior analysis of the base (full) network. Again, it is likely that some impacts due to modification of elements within the subnetwork, such as link capacity changes imposed as part of TCPs, extend beyond a localized area and the subsequent boundary for a chosen subnetwork.

Therefore, two alternate strategies were developed and evaluated in an attempt to account for impacts to the outer network for proper subnetwork analysis. One of these strategies involves adjusting the demand at the subnetwork boundary based on preliminary results from full network STA models. While these models represent the entire network, a process for analyzing a subnetwork was established and implemented for STA, as identified in the literature review (Boyles, 2012a and 2012b).

The process identified for use with STA models involved the creation of artificial arcs to represent a constricted version of the network outside the subnetwork, relying on performance functions defined for these artificial elements. Since link performance functions are not utilized in DTA, this methodology cannot be implemented for purposes of this study. Nonetheless, the defined STA procedures fundamentally involve implementing a sensitivity analysis such that the subnetwork demand is responsive to changes in travel time resulting from a network modification. This results in production of a modified demand table for the subnetwork that accounts for estimated impacts extending beyond the subnetwork. So although the process used cannot be applied for DTA directly, it provides a foundational strategy for estimating demand for a contracted network that can be implemented.

In an attempt to implement a strategy similar to the sensitivity analysis used in the STA subnetwork application, an alternative to the STA-based adjustment was established. The second strategy involves implementation of a discrete choice formulation was examined for determining adjustments to the DTA subnetwork boundary demand. For both strategies developed as part of this study, setting up the subnetwork base demand in VISTA is required.

Generating the initial boundary demand is completed as part of the process used by CTR for setting up a subnetwork by way of a JavaScript code. The code first establishes new centroids at the boundary nodes of the subnetwork based on information extracted from

the selection of the subnetwork in ArcGIS. Subsequently, a new O-D table is created consisting of the boundary centroids, along with the original centroids that were included as part of the subnetwork selection. The base demand at the boundary is representative of the flow of vehicles passing through the boundary nodes extracted from the full network at 15-minute intervals. These vehicles maintain their internal origin/destination designation. Therefore, vehicles traveling into the subnetwork retain their destination centroid and their origin becomes the boundary centroid through which they pass in the full network model. Likewise, vehicles exiting the subnetwork retain their origin centroid and the boundary centroid through which they exit along their assigned path becomes their new subnetwork destination. As such, creation of subnetwork demand requires vehicle trajectory output from a model run of the full network under base conditions, essentially resulting in a fixed trip table.

Prior analysis has shown that adjustments to subnetwork demand matrices to account for impacts beyond the subnetwork can yield a better performance of subnetwork models when compared to these fixed trip tables (Boyles, 2012a). Therefore, implementing a method for adjusting the boundary demand is likely to provide more accurate results. At CTR, improving subnetwork models is often accomplished by adjusting the subnetwork demand to match proportions of traffic flowing out of boundary centroids for each time interval using cordon traffic counts. To use this data, however, the exact cut-off point for the subnetwork boundary is determined based on locations where these existing traffic counts are available. For the subnetwork selection for a TCP evaluation, this count information is not anticipated to be available or necessary for determining the boundary or required modifications to the O-D demand. Furthermore, while these counts are useful for determining the proportion of traffic or volume using adjacent links, they cannot be used to identify where these vehicles are going or from where they are coming, which is imperative for demand estimation.

Instead, for purposes of this study, the adjustments to traffic demand at the boundary nodes will be based solely on anticipated impacts to traveler behavior caused by the TCP that occur beyond the subnetwork. This process can help account for limitations related to using traffic counts to adjust demand by implementing a more comprehensive strategy. It is therefore crucial that these adjustments are made based on sound estimating procedures. The following sections detail the two strategies developed for adjusting demand at boundary centroids to reflect changes in route decision behavior occurring beyond the boundary of the subnetwork.

Demand Estimation Strategy I

The first proposed strategy for making adjustments to the subnetwork demand at boundary centroids involves identification of TCP impacts across the full network found using a comparison of STA model results from base and TCP scenarios. The purpose of using STA models for comparison is to estimate potential network-wide impacts without the computational burden of utilizing a full DTA model. As noted, STA models can generally be run for a large network in much less time than a DTA model. While the results from STA and DTA models are anticipated to differ, it was speculated that the STA models may provide useful insight about where traffic may be diverting due to TCP scenarios, both within and beyond the subnetwork boundaries. From this information, boundary centroids anticipated to have demand changes could be identified and adjustments made relative to volume changes found from the STA comparison.

The base and impact scenarios can be analyzed using a special modification of Bar-Gera's STA code developed to compare two network scenarios. The process to create inputs for the code begins with exporting information from the DTA base network, including link and node attributes and the dynamic demand table, into an Excel spreadsheet created specifically for implementation with the STA analysis. The Excel spreadsheet has been set up to transfer the DTA information to STA format, including

reassigning link IDs, establishing a static demand matrix, and inputting data for link performance functions. Once the Excel spreadsheet has been updated for the identified network, select entries can be exported for use with the STA software C code. Inputs for the code include three created text files from the Excel spreadsheet containing the following information: 1) network demand, 2) base network link attributes, and 3) alternate (impact) network link attributes.

The STA code outputs information identifying the change in volume and travel time experienced on links throughout the network from a comparison of the two scenarios. This information can then be imported into ArcGIS by joining the STA output tables with the link attribute table. The GIS software is used to facilitate the identification of where volumes change between scenarios at the boundary of the subnetwork. It is intended that the proportional shifts from the STA model results be implemented in the DTA subnetwork demand matrix, accordingly. For example, if volumes are found to decrease (or increase) along paths that pass through the subnetwork, as identified from the STA results, this proportional change can be applied to the subsequent O-D pairs in the demand matrix for the subnetwork DTA model. These volume changes across the subnetwork boundary are illustrated for a sample scenario in Figure 4.12.

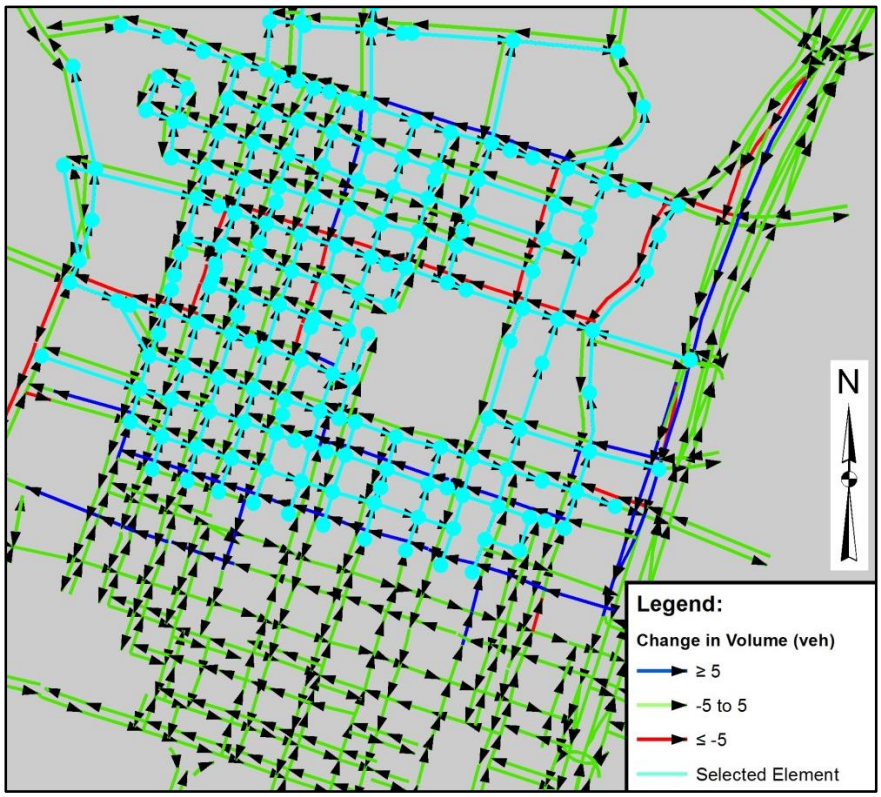

Figure 4.12 Sample Subnetwork with Volume Changes from STA Results

The above figure illustrates where volume increases and decreases along with the selected subnetwork boundary. As shown, this can be used in an attempt to determine which boundary nodes, and their associated O-D demands, are likely to have volume changes in the subnetwork DTA model for the impact scenario. Again, since the STA model is closely associated with the DTA model in its formulation and the resultant comparison accounts for base and impact scenario conditions, this process is seen as a viable methodology for O-D demand updates in DTA.

Demand Estimation Strategy II

The second proposed strategy is based on using a logit formulation to determine adjustments to the proportions of travelers entering at each boundary centroid, or accessing the subnetwork at all, based on changes to travel times within the subnetwork.

This aims to make adjustments to boundary demands that would theoretically occur due to the perceived change in utility of certain path choices that cross the subnetwork boundary. The motivation behind using this type of model is to adjust the demand along the subnetwork boundary to more accurately produce the results that would be acquired from running the full model.

Use of a logit model formulation has been chosen for assessment due to its ability to determine the proportion of users choosing a particular alternative based on the perceived utility, often quantified using travel time. Since DTA models evaluate travel times for different routes and assign vehicles based on the objective of minimizing user travel times, the number of vehicles assigned a particular path between an origin and destination can be estimated accordingly. The following equations demonstrate the logit formulation beginning with the utility function for each alternative:

$$U_i^{rs} = -\theta c_i^{rs} + \varepsilon_i^{rs} \quad \forall\, i, r, s$$

where *U* is the total utility of alternative i for O-D pair (r, s), θ is the sensitivity parameter, *c* is the observed utility (path travel time [typ.]), and ε is the unobserved utility (random variable). The next equation is for the choice probability for each path:

$$P_i^{rs} = \frac{e^{-\theta c_i^{rs}}}{\sum_{j=1}^{J} e^{-\theta c_j^{rs}}} \quad \forall\, i, r, s$$

where P_i^{rs} is the proportion of users choosing alternative i $(i = 1,2, \dots, J)$ from a set of alternatives J for O-D pair (r, s). If the total demand (D^{rs}) for O-D pair (*r*, *s*) is known, the specific number of users (d_i^{rs}) choosing alternative i can also be determined:

$$d_i^{rs} = P_i^{rs} D^{rs} \quad \forall\, i, r, s$$

Application of a logit model for use with DTA subnetwork analyses involves acquiring a set of data to calibrate the sensitivity parameter (θ). In order to do so, the proportion of vehicles assigned each of the alternate paths must be known, as well as the perceived (or experienced for use with DTA) travel times on those paths. Once parameter values have been calculated across different O-D pairs, they can be used, along with updated travel times, to predict the corresponding proportion of users that will be assigned each path. This formulation works well within the capabilities of DTA subnetwork analysis to predict path changes that might occur due to a type TCP impact scenario.

As alluded to previously, adjusting the boundary demand can be completed using a multiplication factor for the origin and destination centroids based on known proportions of entering vehicles obtained from traffic counts. Previously, this paper proposed the use of STA results as a proxy for known traffic counts. This particular method, on the other hand, focuses on the use of data produced by running DTA subnetworks for both the base and impact scenario conditions.

The first scenario modeled is the base scenario and it is used to calibrate the logit model. This calibration determines the sensitivity parameters for O-D pairs using the existing proportions of users that pass through a boundary centroid en route to a particular destination within the subnetwork. Next, a TCP (or other modification) scenario is imposed on the subnetwork resulting in new traffic flows and travel times. The updated internal travel times are then used to determine the new proportion of vehicles entering the subnetwork boundary at each centroid, as well as estimate those that may avoid the subnetwork altogether. This methodology is intended to account for updates to external-to-external and external-to-internal trips.

For these external-to-external trips, users have the option of entering the subnetwork as part of their route or avoiding it altogether. For a bypassing trip, only an external travel time is utilized. This travel time is assumed to remain fixed between scenarios. For

traversing trips, three travel time components must be considered: 1) an external entering travel time, 2) an internal travel time, and 3) an external exiting travel time, as illustrated on the left side of Figure 4.13.

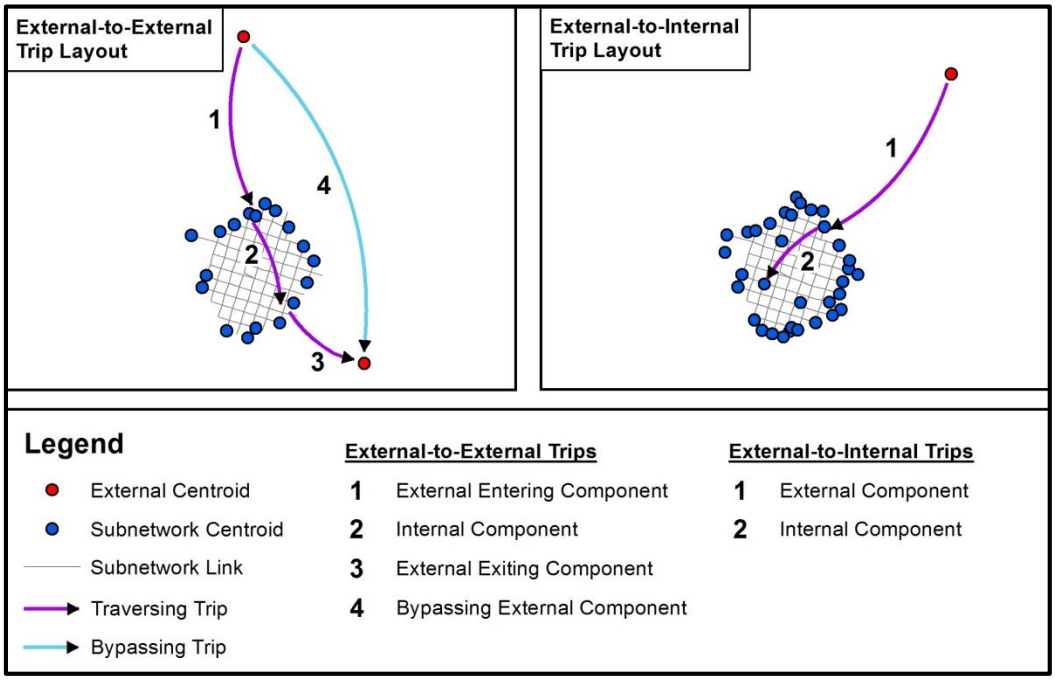

Figure 4.13 Centroid Layout Establishing Trip Components

These external components are also assumed to remain fixed and all are extracted from the full base scenario model. The internal travel times are extracted from base and impact subnetwork models, respectively, accounting for differences between scenarios. The internal travel time is estimated for the portion of the trip between the boundary origin centroid (entry point) and the boundary destination centroid (exit point). The sum of these travel times is then compared to a representative bypassing travel time between the external origin and destination centroids.

The existing demand is used along with the travel time components to calibrate the sensitivity parameter for a specific external O-D pair and time period using a logit model. Specifically, the bypassing and traversing demand, along with the respective travel times,

for the base scenario are used to determine the proportion of users that choose to enter the subnetwork. For the impact scenario, the calibrated sensitivity parameter and the updated internal travel times are used to compute a new proportion and subsequent boundary demand. This effectively estimates the change in number of users choosing to traverse versus bypass the network based on a change in the internal travel time attributed to a network modification.

Since the choice between traversing and bypassing the subnetwork is inherently dual, a binary logit model can be used to compare the representative traversing and bypassing travel times between external centroids. The resulting equation is shown below.

$$P_i^{rs,\tau} = \frac{e^{\theta[-(TT_{External}^{\tau} + TT_{Internal}^{\tau} + TT_{External}^{\tau})]}}{e^{\theta[-(TT_{External}^{\tau} + TT_{Internal}^{\tau} + TT_{External}^{\tau})]} + e^{\theta[-(TT_{External}^{\tau})]}} \quad \forall\, i, r, s, \tau$$

where $P_i^{rs,\tau}$ is the proportion of users choosing alternative i (represented above as traversing the subnetwork) for O-D pair (r, s) at a given departure time interval (τ) as a function of the sum of the traversing and bypassing travel times (TT), respectively. With the total demand ($D^{rs,\tau}$) for O-D pair (r, s) at a given departure time interval (τ) known, the specific number of users ($d_i^{rs,\tau}$) choosing alternative i can be determined:

$$d_i^{rs,\tau} = P_i^{rs,\tau} D^{rs,\tau} \quad \forall\, i, r, s, \tau$$

As identified in the literature review, a precedent exists for using a logit formulation, similar to the one identified above, to adjust demand for a subnetwork (Zhou et al., 2006). However, the implemented method was used to assess demand relative to external-to-external trips only. It is anticipated that changes to internal travel times will not only influence the user's decision of whether to enter the subnetwork, but where to enter it as well. Therefore, this research implements the logit formulation to also account for changes to external-to-internal trips, and the subsequent influence on subnetwork boundary demand in a similar manner.

For these trips, there are two components of the experienced travel times used to represent the choice utility, as illustrated on the right side of Figure 4.13 on page 123. The first is the external travel time (1), or the travel time between an external centroid and a boundary centroid. The next component of the experienced travel time is the internal travel time (2), which varies depending on the scenario imposed on the subnetwork. The internal travel time extracted from the base scenario subnetwork model (no network modification) is again needed to calibrate the model.

The extracted demand at each boundary node within a choice set is used to determine the proportion of users that cross each boundary origin (entry point) as part of their route selection. Using this information, along with the base scenario travel times, the sensitivity parameter can be calibrated for a specific O-D pair and time period. For the impact scenario, the calibrated sensitivity parameter and the new internal travel time extracted from the impact scenario subnetwork model are used to compute a new proportion and subsequent demand for each boundary origin.

In this formulation, the utility is simplified to be the experienced (shortest path) travel time since these travel times are readily available from DTA model outputs. The formula is also separated by departure time interval to take into account the time-variable nature of the models, as demonstrated in the equation below:

$$P_i^{rs,\tau} = \frac{e^{\theta[-(TT_{Internal}^{\tau} + TT_{External}^{\tau})]}}{\sum_{\forall j} e^{\theta[-(TT_{Internal}^{\tau} + TT_{External}^{\tau})]}} \; \forall \; i, r, s, \tau$$

where the proportion of trips ($P_i^{rs,\tau}$) for O-D pair (*r*, *s*) using boundary centroid *i* from a set of J alternatives at a given departure time interval (τ) is presented as a function of the sum of the internal and external travel times (TT). As demonstrated for the external-to-external trips, the total demand ($D^{rs,\tau}$) for external O-D pair (*r*, *s*) at a given departure time interval (τ) can be used to determine the specific number of users ($d_i^{rs,\tau}$) choosing alternative i:

$$d_i^{rs,\tau} = P_i^{rs,\tau} D^{rs,\tau} \quad \forall\, i, r, s, \tau$$

Originally, it was intended that the formulation be representative of a multinomial logit model such that the set of J alternatives could be greater than two. However, this would require more detailed information be known about each possible entry point (alternative i), such as the estimated travel time along unused paths between O-D pairs and disaggregate travel times for each individual vehicle. While this information could be used to provide a more precise formula, it would require numerous complex calculations along with several time consuming algorithms and software scripts to extract the necessary data from the DTA models. Since the goal is to provide a method for adjusting the boundary demand that accounts for impacts to the external network without a full network model, a complicated and time-consuming process to provide this estimation is not desired. Instead, the formula can be simplified as a binary logit model for implementation, such that only two boundary nodes (entry-point alternatives) are considered at a time.

In order to simplify the inputs required for the logit formulas, the network can be divided into regions that contain major roadway corridors or represent a demand cluster. Rather than using each individual external centroid in the logit formulation, the number of calculations can be greatly reduced by grouping them together into a "megacentroid", as demonstrated in Figure 4.14. Once the external centroids have been grouped into representative megacentroids, each one can act as a pseudo external origin/destination within each region.

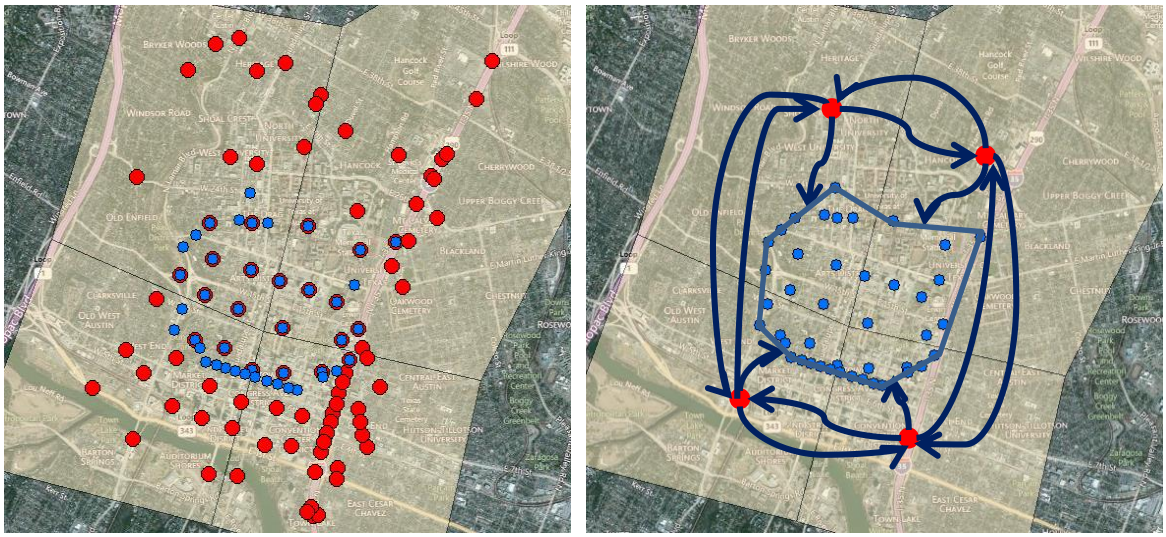

Figure 4.14 Transformation of External Centroids into Megacentroids (Basemap Source: BING © 2010 Microsoft and its Data Suppliers)

Producing the above logit formulation is relatively straightforward; however, the implementation for a subnetwork involves a number of challenges. Primarily, division of the network into sections is somewhat arbitrary, though this can be completed based on user inputs. Furthermore, while the implementation of megacentroids substantially reduces the number of calculations required, there may still be many destinations inside the subnetwork (including along the boundary) that must be considered. The logit model is intended to be applied for each internal destination centroid from every boundary centroid over all time intervals where nonzero demand exists in the base model. Therefore, the formula accounts for each trip, within a given time period, from the megacentroid to each internal centroid by estimating the shortest paths relative to the available entry points (boundary centroids).

In addition to the computational effort required to analyze each O-D pair for each time interval, the logit formulation method ultimately involves three runs of the subnetwork. The first run is the base run used to produce internal travel times for the given proportional splits along the subnetwork boundary extracted from the full network base model. The second is for the alternate scenario, providing new internal travel times for the impacted subnetwork. These new travel times are then used to adjust demand along

the subnetwork boundary using the logit formulas presented above. After the boundary demands have been adjusted, the subnetwork is then run again in an attempt to provide a more accurate representation of the impacts of the TCP scenario by accounting for the external portion of the network.

This concludes the discussion of the proposed methodology and preliminary steps for applying subnetwork selection and analysis. Full implementation of the above strategies involves a significant effort and relies heavily on development of software processes beyond those previously discussed. An in-depth investigation of applicable procedures and implementation of software tools have been undertaken to develop important guidance for choosing a subnetwork size and an efficient process for adjusting demand to account for impacts outside of the subnetwork.

5. PRELIMINARY RESULTS AND ADDITIONAL SOFTWARE IMPLEMENTATION

The implementation and preliminary assessment of strategies proposed for completing an efficient and accurate subnetwork analysis were undertaken to test the chosen methodology prior to large scale application. This investigation was largely focused on development of a process for choosing an appropriately sized subnetwork and accounting for impacts that extend beyond the subnetwork for an impact scenario. It involved a significant feasibility analysis revolving around a review of applicable procedures and development of automated scripts to efficiently interface between software programs.

The subnetwork selection strategy has been described in detail, including implementation with ArcGIS. As noted, the connected order strategy was chosen for further evaluation, though both radius selection and connected order selection methods have been developed for application with the software. Nevertheless, this represents only a preliminary step in the process of examining subnetwork analysis procedures. The core of the methodology proposed involves evaluation of subnetwork sizes relative to different impact scenarios and application of a strategy designed to account for impacts extending beyond the subnetwork boundary. This section describes implementation of the proposed methods to perform these tasks. It also presents a preliminary assessment and selection of a candidate strategy for adjusting boundary demands to account for impacts outside of the subnetwork. Lastly, procedures and software codes developed for compiling and presenting pertinent analysis results are described.

Preliminary Implementation and Evaluation of Subnetwork Sizes

In order to properly evaluate the methodology associated with subnetwork size evaluation, a number of preliminary test scenarios were chosen for review. The process constituent to this research is inclusive of subnetworks representing size parameter inputs

(i.e. connected order) of 5, 7, and 9 for each test scenario. Several variations of typical network modifications associated with TCPs were chosen to comprise these scenarios.

Each chosen impact scenario is defined by three primary characteristics, roadway location, link capacity reduction, and number of modified links. The downtown Austin network, chosen for preliminary analysis, is partly composed of a number of one-way principal arterials. To test the subnetwork size selection, three site locations were chosen within the downtown network, including modifications along two one-way arterials and one two-way arterial. The first roadway chosen for analysis was Guadalupe Street, a southbound one-way arterial with four lanes at the site location. The second roadway chosen was 7th Street, an eastbound one-way arterial with four lanes. The third roadway was 15th Street, an east-west two-way arterial with six lanes (three in each direction). These locations, identified in the map provided in Figure 5.1, were chosen due to their importance relative to afternoon peak-period mobility.

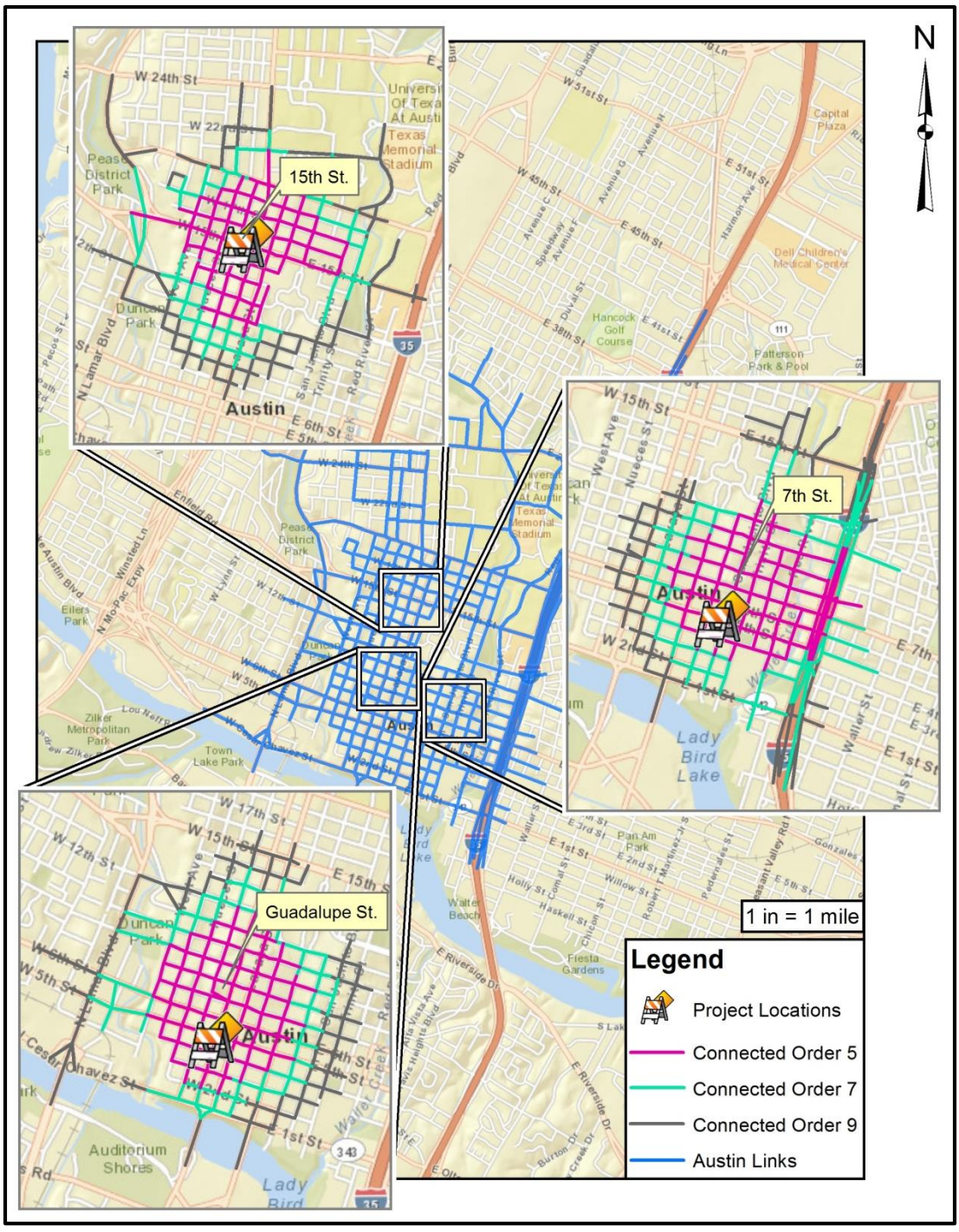

Figure 5.1 Test Scenario Location Map (Basemap Source: Esri, DeLorme, NAVTEQ, USGS, Intermap, iPC, NRCAN, METI, TomTom, 2013)

To define the impact scenarios, capacity reductions of 25 percent, 50 percent, and 100 percent were chosen in combinations involving one link, two links, or three links along each selected roadway. Therefore, network modifications tested range in magnitude from a 25-percent capacity reduction of one link, to a 100-percent capacity reduction of three consecutive links. This range of scenarios was selected consistent with typical construction project characteristics observed during a field review of the downtown Austin network. Since up to three network links will be modified, the locations along each roadway chosen can be identified.

The limits of the associated network modifications include Guadalupe Street, between 6th Street and 9th Street; 7th Street, between Brazos Street and Neches Street; and 15th Street, between Nueces Street and Lavaca Street. For 7th Street, the beginning location is mid-block between Brazos Street and San Jacinto Boulevard due to the link being separated by a network tie-in with a centroid connector. For 15th Street, the scenarios involve modifying the roadway in the westbound direction only. This was chosen since the network link elements are directional and modifications to both directions would involve modifying twice the number of links intended for review.

For preliminary investigation of the methodology, six specific scenarios were selected for in-depth evaluation. An effort was made to select these scenarios representative of a comprehensive range of possible network modifications. Therefore, the trial scenarios included a 25-percent capacity reduction to one link, a 50-percent reduction to two consecutive links, and a 100-percent capacity reduction across three consecutive links along a corridor. To assess some of the variation expected between scenarios and locations within the network, application of the modifications was dispensed accordingly. To control for location, all three scenarios were tested along Guadalupe Street. To control for project scope, the mid-range scenario characteristic of a 50-percent capacity reduction to two links was tested at all three locations. A second, 100-percent capacity reduction was also tested at 7th Street to further investigate the most substantial impact scenario.

The procedure for this experiment was to develop software code for data manipulation and calculation of the statistics identified in Chapter 4. For this preliminary analysis, 10 DTA model runs of the network under base scenario conditions were completed using VISTA, along with 10 runs of the network for each impact scenario. The following steps were then initiated to extract the necessary data and assess the DTA results accordingly:

1) Subnetwork elements selected as part of the connected order selection process were exported from ArcGIS into text documents, one for both nodes and centroids and another for both links and connectors
2) A representative subnetwork was created in VISTA using the exported lists of network elements
3) A JavaScript code provided by CTR was used to extract the subnetwork demand for each DTA model run for the base and impact scenarios
4) The extracted dynamic O-D tables for each subnetwork were exported from VISTA and imported into Excel
5) A developed Matlab code was used to import and join the table of ODT combinations based on a unique identifier (a unique ID composed of the concatenated origin, destination, and time period IDs for each demand entry)
6) The joined demand table was converted from the ODT format used by VISTA into a separate O-D matrix for each time period, as required to run the code for the SSIM evaluation using Matlab
7) Statistical measures for the RMSE, MCAPE, and SSIM index were calculated in Matlab and stored for comparing the individual base and impact runs to the average of the base runs (as discussed in Chapter 4)
8) In Matlab, prediction intervals were calculated across the 10 base runs and 10 impact runs along with a record of the number of impact runs that fell within the base interval and the number base runs that fell within the impact interval
9) Hypothesis tests were conducted using code written in Matlab, including those for assessing normal distribution (Lilliefor and Anderson Darling tests), equal

variance between samples (F-test between base and impact runs), and equal sample means (t-test between base and impact runs)

With this information compiled, the data could be exported into Excel for additional review. Outputs for the individual hypothesis tests, including identification of accepting or rejecting the null hypothesis, along with calculated values of the RMSE, MCAPE, SSIM index, prediction interval, and the number of runs falling within the interval were provided from the Matlab code. The developed code for each of the applicable processes identified above, including that required to output the appropriate results, is available in Appendix B.

The Matlab code created for joining the matrices, converting the demand format, calculating the statistical error measures, and running applicable hypothesis tests was intended to help automate the procedure for the purposes of efficiency and ease of replication. Joining is a common database procedure that matches two tables based on a unique identifier (Bringardner et al., 2013). For this process, the numerical concatenation of the origin, destination, and time period ID values serves as a unique identifier. This process guarantees that the corresponding demand from each of the different runs of the base network and the impact scenario can be matched appropriately to complete the necessary error calculations.

However, it is not uncommon that a demand value for a specific identifier does not exist for one or more runs. In other words, all of the runs do not produce a subnetwork demand value for the exact same combination of ODTs. The code accommodates this by storing the unique identifier regardless of the number of times it appears across the runs, and assigns a demand value of zero when it is missing from a particular demand table. This important characteristic demonstrates why the code is robust for keeping track of the corresponding model demands and performing subsequent computations. After running this Matlab code, the data is in a format suitable for reviewing the RMSE and MCAPE.

For the preliminary review, statistical measures were calculated using the fully joined ODT table composed of all 20 base and impact runs necessary to evaluate a specific scenario. As mentioned in Chapter 4, the statistics are calculated by comparing each base and impact scenario demand table to the average demand across all 10 base runs. The 20 resultant values for the base and impact scenario runs were then assessed to verify parametric statistical assumptions. A 95-percent prediction interval was also determined for the statistics for base and impact runs separately, and then each impact scenario's mean value (across the 10 runs) was compared against the mean of the base runs using a two sample t-test to determine if the difference was statistically significant. Essentially, the same procedure was carried out for the RMSE, MCAPE, and SSIM index measures; though, evaluating the SSIM index required some additional data manipulation.

The VISTA software stores dynamic O-D tables with a row for each ODT demand entry. However, the published Matlab code written to assess the SSIM index requires the standard O-D matrix format with rows representing origins and columns representing destinations (Wang et al., 2004). To ensure compatibility, the fully joined ODT table consisting of the multiple model runs was then separated into unique O-D combinations for each time period and converted to an appropriate matrix for analysis (Bringardner et al., 2013). Once the matrices are stored, several input parameters for the SSIM code are needed for initialization.

One minor parameter for the SSIM index is the dynamic range. As mentioned, the SSIM index was originally created to assess differences between images. For an image, the dynamic range is represented by the maximum value that can be stored in an individual pixel, which varies from 0 to 255. To apply this concept for use with an O-D matrix, the dynamic range should be set as the maximum ODT demand value identified in the table.

Spatial weights matrices are one of the most important factors for determining the SSIM index (Bringardner et al., 2013). This matrix, also known as the convolution kernel or

local window, represents how correlated a single ODT cell is to the surrounding ODT demand values. The purpose of using this local window is to account for spatial correlation among O-D pairs, as discussed in Chapter 4. The central pairing (middle of the local window) is usually assigned the highest weight. Essentially, the RMSE and MCAPE can be thought of as having a window with a value of one for the central feature and zero everywhere else.

As identified previously, a number of strategies for assigning a local window were assessed. A 3x3 window was chosen for application, including only the immediately adjacent centroids because the demand from two origins away is less likely to be associated with the central feature demand and in some cases, involves a rather large distance between. Assigning the same weight to features irrespective of distance from the central feature was seen as an unnecessary constraint to impose beyond the adjacent centroid. A window with a cross-shaped distribution was also used, implying that only demand *from* the same origin and *to* the same destination should be included in the analysis of local windows. Figure 5.2 demonstrates how the local window is applied to an O-D pair in the network layout. For identification purposes, the center (featured) O-D pair is circled in a bold outline in the figure.

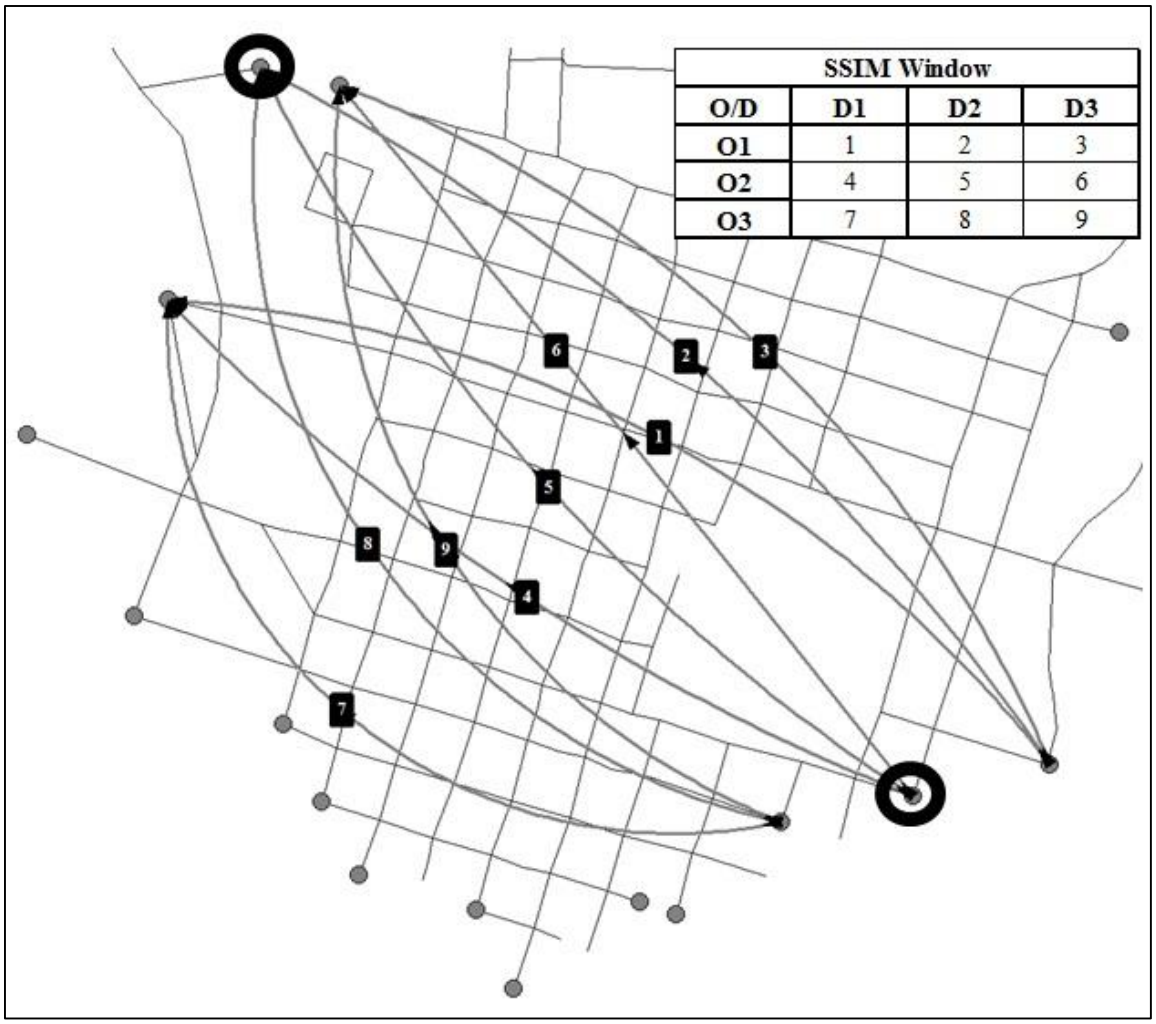

Figure 5.2 Sample Diagram of Applying the Spatial Weights Window to an Origin-Destination Table (Bringardner et al., 2013)

In the above figure, the spatial relationship between the featured O-D pair and the adjacent O-D pairs is illustrated. Additionally, the association between the geographic locations of the centroids and the layout of the local window, represented by the matrix in the upper-right corner, is demonstrated using the numbering scheme. The numbers in the matrix are consistent with the O-D pair connections shown spatially. Figure 5.2 also reveals the importance of the layout of the O-D matrix and the necessity for it to correspond to the geographic location of the centroids. Note that the figure excludes internal centroids for added clarity.

In order for the window to be applied, a scheme was developed to catalog origins and destinations in the O-D matrix consistent with their location such that adjacent centroids are also neighbors in the matrix (Bringardner et al., 2013). Boundary centroids were considered first since the assessment of subnetwork sizes focuses on the demand originating at the boundary. This is because differences between boundary centroid demands represent impacts due to a network modification that are not contained within the selected subnetwork.

As such, boundary origin centroid IDs were identified based on their clockwise order beginning at due north and entered into the O-D matrix in accordance with that order. Boundary destination centroid IDs were then listed in the same manner to form a matrix consistent with the geographic relationship between centroids. The portion of the O-D matrix connecting boundary origins to boundary destinations is visually represented by the local SSIM window shown in the upper-right corner of Figure 5.2.

The remaining internal origin and destination centroids were also investigated to determine if their assigned IDs corresponded to their geographic location. In general, sequentially numbered internal destination centroids corresponded to their geographic nearest neighbors for the downtown network. Using this method, the spatial relationship between internal centroids is not as consistently correlated with their ordering in the O-D matrix as the boundary centroids, but the pattern was reliable enough for determining the SSIM index since the boundary centroids comprise the only demand variation.

Within the Matlab code used for calculating the SSIM index for each demand matrix extracted from the model runs, a similar procedure was incorporated for comparing the calculated SSIM indices between scenarios as that applied for the RMSE and MCAPE. The local windows extracted from the demand matrix for each individual impact run were compared against a representative base matrix. By compiling local SSIM indices computed using these windows, the mean SSIM index across the entire O-D matrix was

calculated for each time period of interest for all impact runs for each scenario. A prediction interval was also established for the base runs and compared to the impact scenario SSIM index for each run.

Once all of the statistical measures were compiled for a particular scenario and exported to an Excel file, the results could be organized for review. The statistical measures were computed and hypothesis tests verified for 1-hour and 2-hour periods of the simulation for each of the six scenarios. The 1-hour period was intended to represent the PM peak-hour conditions and was extracted from a half-hour after the beginning to one hour and a half into the simulation. The 2-hour period was taken from a half-hour after the beginning to two and a half hours into the simulation to represent the PM peak period. These portions of the simulation results were selected because the early and later time periods capture effects of the network algorithm during uncongested states associated with loading and unloading the network.

It was found that a majority of the equal variance and normality tests passed for the RMSE, MCAPE, and SSIM index. Furthermore, four out of the six scenarios that failed either the Lilliefor or Anderson-Darling normality test passed the equal variance test. Even though a few of these parametric statistical assumptions were violated according to the test results, enough passed to indicate that the statistics used for the prediction interval and the hypothesis test for equal sample means are still valid. One possible reason for unequal variance, generally represented by greater variability for the impact scenarios, is that modifications to the network are likely to induce greater instability in the results. For example, discontinuity resulting from a link closure along a single corridor used by multiple routes could substantially alter the path sets for multiple O-D pairs.

Unfortunately, the prediction interval range did not appear to be consistent between scenarios, implying that a standard interval cannot be applied to an estimated mean

demand. This may be due to using a relatively small sample size (10), or it may be due to the variation associated with incorporating the results across multiple DTA runs. It is expected that through randomness incorporated in the VISTA models, a considerable amount of variation may be incurred from running the same model more than once. Using additional model runs of each scenario might improve the ability to establish a more consistent prediction interval range.

It was discovered from the test scenarios that the RMSE gave the most promising results for identifying true differences associated with the impact scenario based on the incremental growth of a subnetwork. The RMSE results for all six scenarios across the 1-hour and 2-hour time periods are shown in Tables 5.1 and 5.2, respectively. The results for both the base and impact scenarios are compiled across each of three subnetwork sizes, including connected orders of 5, 7, and 9.

Table 5.1 Preliminary Test Results for 1-Hour Analysis Period Using RMSE

Scenario	Location	Subnetwork Size (Order)	Impact Size	Capacity Reduction	Hypothesis Testing				Prediction Interval			
					Equal Variance*	Normality Lillifor**	Normality A-D**	Equal Mean***	Lower	Upper	Range	Alternate Runs Within
Base	Guadalupe St	5	1	25		Y	Y		1.73	4.81	3.08	10
Impact	Guadalupe St	5	1	25	Y	Y	Y	Y	2.42	4.27	1.85	9
Base	Guadalupe St	7	1	25		Y	Y		1.57	4.37	2.80	10
Impact	Guadalupe St	7	1	25	Y	Y	Y	Y	2.33	3.90	1.57	9
Base	Guadalupe St	9	1	25		Y	Y		1.64	3.40	1.76	10
Impact	Guadalupe St	9	1	25	Y	Y	Y	Y	1.84	3.33	1.49	10
Base	15th St	5	2	50		Y	Y		1.89	3.60	1.72	10
Impact	15th St	5	2	50	Y	Y	Y	N	2.19	4.05	1.86	10
Base	15th St	7	2	50		N	N		0.33	5.30	4.97	10
Impact	15th St	7	2	50	N	Y	Y	Y	2.45	3.75	1.30	5
Base	15th St	9	2	50		Y	Y		1.24	3.15	1.91	9
Impact	15th St	9	2	50	Y	Y	Y	Y	1.71	3.27	1.56	10
Base	7th St	5	2	50		Y	N		1.93	2.97	1.04	5
Impact	7th St	5	2	50	Y	Y	Y	N	2.31	3.52	1.21	8
Base	7th St	7	2	50		Y	Y		1.36	2.32	0.96	6
Impact	7th St	7	2	50	Y	Y	Y	N	1.58	2.74	1.16	9
Base	7th St	9	2	50		Y	Y		0.85	2.16	1.31	10
Impact	7th St	9	2	50	N	Y	Y	Y	1.15	1.77	0.62	6
Base	Guadalupe St	5	2	50		Y	N		1.53	4.69	3.16	10
Impact	Guadalupe St	5	2	50	N	Y	Y	Y	2.40	3.90	1.50	8
Base	Guadalupe St	7	2	50		Y	Y		1.53	4.51	2.98	10
Impact	Guadalupe St	7	2	50	Y	Y	Y	Y	2.23	4.16	1.94	9
Base	Guadalupe St	9	2	50		N	Y		1.57	3.90	2.34	10
Impact	Guadalupe St	9	2	50	N	Y	Y	Y	2.20	3.25	1.05	6
Base	7th St	5	3	100		N	N		1.92	2.93	1.01	0
Impact	7th St	5	3	100	Y	Y	Y	N	8.98	10.68	1.70	0
Base	7th St	7	3	100		N	Y		1.23	2.81	1.58	6
Impact	7th St	7	3	100	Y	Y	Y	N	2.12	3.36	1.24	4
Base	7th St	9	3	100		Y	Y		0.84	2.18	1.34	10
Impact	7th St	9	3	100	Y	Y	Y	N	1.36	2.17	0.81	6
Base	Guadalupe St	5	3	100		Y	Y		1.55	4.50	2.95	0
Impact	Guadalupe St	5	3	100	Y	Y	Y	N	6.01	7.56	1.56	0
Base	Guadalupe St	7	3	100		Y	Y		2.23	4.78	2.56	7
Impact	Guadalupe St	7	3	100	Y	Y	Y	N	3.43	5.64	2.21	5
Base	Guadalupe St	9	3	100		Y	Y		1.25	4.00	2.75	10
Impact	Guadalupe St	9	3	100	Y	Y	Y	Y	2.16	3.70	1.54	7

* Y = Accept H_o: $\sigma_1^2 = \sigma_2^2$; N = Reject H_o, conclude H_a: $\sigma_1^2 \neq \sigma_2^2$ (at the 95-percent confidence level)

** Y = Accept H_o: Distribution is normal; N = Reject H_o, conclude H_a: Distribution is not normal (at the 95-percent confidence level)

*** Y = Accept H_o: $\mu_1 = \mu_2$; N = Reject H_o conclude H_a: $\mu_1 \neq \mu_2$ (at the 95-percent confidence level)

Table 5.2 Preliminary Test Results for 2-Hour Analysis Period Using RMSE

Scenario	Location	Subnetwork Size (Order)	Impact Size	Capacity Reduction	Hypothesis Testing				Prediction Interval			
					Equal Variance*	Normality Lillifor**	Normality A-D**	Equal Mean***	Lower	Upper	Range	Alternate Runs Within
Base	Guadalupe St	5	1	25		Y	Y		1.58	4.41	2.83	10
Impact	Guadalupe St	5	1	25	N	Y	Y	Y	2.41	3.74	1.33	9
Base	Guadalupe St	7	1	25		Y	Y		1.80	4.01	2.21	10
Impact	Guadalupe St	7	1	25	N	Y	Y	Y	2.53	3.57	1.04	6
Base	Guadalupe St	9	1	25		Y	Y		1.75	3.16	1.41	10
Impact	Guadalupe St	9	1	25	Y	Y	Y	Y	1.84	3.24	1.40	10
Base	15th St	5	2	50		Y	Y		2.11	3.36	1.26	1
Impact	15th St	5	2	50	N	Y	Y	N	-6.52	13.49	20.01	10
Base	15th St	7	2	50		N	N		0.46	5.38	4.92	2
Impact	15th St	7	2	50	Y	Y	Y	Y	-7.98	14.52	22.50	10
Base	15th St	9	2	50		N	N		1.28	3.17	1.89	2
Impact	15th St	9	2	50	Y	Y	Y	Y	1.94	2.57	0.63	6
Base	7th St	5	2	50		Y	Y		1.71	2.47	0.76	4
Impact	7th St	5	2	50	Y	Y	Y	N	2.00	2.98	0.97	8
Base	7th St	7	2	50		Y	Y		1.26	2.07	0.81	6
Impact	7th St	7	2	50	Y	Y	Y	N	1.67	2.34	0.67	4
Base	7th St	9	2	50		Y	Y		1.00	2.05	1.05	10
Impact	7th St	9	2	50	Y	Y	Y	Y	1.14	1.85	0.70	9
Base	Guadalupe St	5	2	50		Y	Y		1.45	4.33	2.88	10
Impact	Guadalupe St	5	2	50	N	Y	Y	Y	2.34	3.45	1.11	8
Base	Guadalupe St	7	2	50		Y	Y		1.76	4.14	2.38	10
Impact	Guadalupe St	7	2	50	Y	Y	Y	Y	2.26	4.04	1.78	10
Base	Guadalupe St	9	2	50		Y	Y		1.77	3.54	1.76	10
Impact	Guadalupe St	9	2	50	Y	Y	Y	Y	2.20	3.15	0.95	8
Base	7th St	5	3	100		Y	Y		1.71	2.37	0.67	0
Impact	7th St	5	3	100	Y	Y	Y	N	8.69	9.93	1.24	0
Base	7th St	7	3	100		N	N		1.19	2.57	1.38	0
Impact	7th St	7	3	100	Y	Y	Y	N	2.54	3.52	0.97	0
Base	7th St	9	3	100		Y	Y		1.00	2.05	1.04	9
Impact	7th St	9	3	100	Y	Y	Y	N	1.44	2.20	0.75	6
Base	Guadalupe St	5	3	100		Y	Y		1.56	4.12	2.57	0
Impact	Guadalupe St	5	3	100	Y	Y	Y	N	4.95	6.43	1.48	0
Base	Guadalupe St	7	3	100		Y	Y		2.42	4.47	2.06	6
Impact	Guadalupe St	7	3	100	Y	Y	Y	N	3.37	5.37	1.99	6
Base	Guadalupe St	9	3	100		Y	Y		1.64	3.51	1.86	10
Impact	Guadalupe St	9	3	100	Y	Y	Y	N	2.23	3.67	1.44	8

* Y = Accept H_o: $\sigma_1^2 = \sigma_2^2$; N = Reject H_o, conclude H_a: $\sigma_1^2 \neq \sigma_2^2$ (at the 95-percent confidence level)
** Y = Accept H_o: Distribution is normal; N = Reject H_o, conclude H_a: Distribution is not normal (at the 95-percent confidence level)
*** Y = Accept H_o: $\mu_1 = \mu_2$; N = Reject H_o conclude H_a: $\mu_1 \neq \mu_2$ (at the 95-percent confidence level)

The tables reveal that the results from the 1-hour time period were the same as the 2-hour time period except for one of the Guadalupe Street scenarios (3 links, 100-percent capacity reduction). The resultant demand tables for the smallest impact scenario in terms of scope (1 link, 25-percent capacity reduction) were not found to be statistically different

from the base scenario results for each subnetwork size, while the largest impact scenario (3 links, 100-percent capacity reduction) was determined to be statistically different for nearly all subnetwork sizes evaluated. In other words, the scope of the impact scenario appeared to influence whether the hypothesis test revealed statistically significant differences in boundary demand, as expected. Evidence was also found to support the conclusion that the location of the scenario (roadway) also mattered.

In order for a statistical measure to provide insight into what size of subnetwork is required for analysis of a given scenario, it must reveal statistically significant differences using the hypothesis test for equal sample means at a specified confidence level. In other words, for subnetworks that are too small to contain a majority of the traffic impacts, it should indicate that sample means are statistically different between the base and impact scenario (reject the null hypothesis). Thus, a failure to reject the null hypothesis reveals that the resultant measures of the demand error are not statistically different and that the subnetwork is indeed adequate. The threshold where the transition from statistically similar to statistically different occurs provides valuable support for a recommended subnetwork size given a particular scenario. The preliminary RMSE results, as shown in the tables, demonstrate the ability to identify this threshold.

The preliminary analysis of the MCAPE and SSIM index appeared to provide a less meaningful outcome. The results using 1-hour and 2-hour periods are provided in Appendix C, Tables C.1 through C.4. Evaluation of the statistical measures across multiple runs revealed that the resultant demand tables for the impact scenarios are statistically different from their respective base scenario outputs, regardless of location, scenario or subnetwork size. This was demonstrated by a rejection of the null hypothesis for equal sample means in every instance but one (see Appendix C). However, for the smaller-sized subnetworks, fewer impact scenarios were found to fall inside the 95-percent prediction interval for both statistics, even though the hypothesis test found that nearly every scenario was statistically different. Since the prediction interval for the base

scenario captured more of the impact scenario measures as the subnetwork size increased, it is speculated that even larger subnetworks are required to achieve statistical equivalence between scenarios using these measures.

The inability of the SSIM index and MCAPE to detect a sample size large enough to contain discernible differences might be related to the calculation of the statistics (Bringardner et al., 2013). Since the MCAPE establishes a relative percentage, it has a tendency to inflate differences. For example, a large portion of the impact scenario's error could be the result of several matched ODT combinations where one impact run has zero demand and the mean base demand (from the baseline comparison matrix) is a minimal, but non-zero value. Much like the issue associated with using volumes produced during loading and unloading of the network, with minimal and largely fluctuating demand, comparing a zero in the impact case against a value of one in the baseline would result in a 100 percent error. However, the real difference for this ODT combination might be caused by a single vehicle switching back and forth between two shortest paths at each subsequent iteration. The SSIM index could have a similar limitation by accounting for the large error associated with random demand fluctuation between nearby centroids. The SSIM methodology should be able to account for some of this through the spatial weights matrix, but a more intricate weighting strategy than the one originally developed may be able to mitigate this issue.

Nonetheless, the preliminary investigation revealed that a recommendation for subnetwork size could be provided using an assessment of the RMSE. It was determined that additional scenarios and subnetwork sizes could be evaluated in a similar manner, as discussed in the following chapter. A preliminary examination of the strategies developed for purposes of accounting for impacts extending beyond the subnetwork boundary was also undertaken.

Preliminary Evaluation of Strategies for Subnetwork Demand Estimation

In an attempt to assess the viability of performing a subnetwork analysis for DTA that adequately takes into account the outer portion of the network, the two methods introduced in Chapter 4 for adjusting the demand at the subnetwork boundary were tested. This included the adjustment based on STA results comparing the base and impact scenarios, as well as the adjustment using a logit formulation to account for changes in internal travel times between scenarios. The purpose of testing both strategies was to select the method producing the most promising results for large-scale implementation and evaluation.

Two different TCP scenarios within the downtown Austin network were used to examine these methods. The first was characterized by a two-thirds capacity reduction in the westbound direction along five links of 15th Street intended to simulate the closure of two of the three westbound lanes between San Antonio Street and Congress Avenue. A second, smaller impact scenario involved closing the only eastbound lane for two links along 2nd Street between Colorado Street and Congress Avenue. These capacity adjustments were imposed on the networks used to run the STA and DTA analyses for the two proposed strategies.

The 15th Street scenario involved using an arbitrary subnetwork radius of one-half mile or 2,640 feet around the impacted links. To select the subnetwork, the radius selection tool (model) created using ArcGIS was utilized, and the selected network elements were exported for use with VISTA and the STA code for further analysis. The radius selection tool was used here to test the developed model's viability for future use.

For the 2nd Street scenario, the connected order selection tool was utilized. A size parameter (ς) of five was used as a means of capturing the limited anticipated impact of the scenario, thus resulting in a smaller subnetwork. This also served to test the validity

of DTA results using a smaller subnetwork relative to the full network. Two different selection methods were used for the scenarios to determine whether taking into account the outer network could eliminate the need for a comprehensive and detailed selection strategy, including choice of subnetwork size adequate to contain all significant impacts. The following sections detail the preliminary implementation of the subnetwork analysis strategies and evaluation of the results relative to re-analysis of the full network for each impact scenario.

Demand Estimation Strategy I

To implement the first strategy, the Austin downtown DTA model was converted into an STA format to produce base and impact scenario results quickly and consistently with the data used for counterpart DTA model runs. A sample of the results obtained from running the STA C-code is displayed using ArcGIS in Figure 5.3.

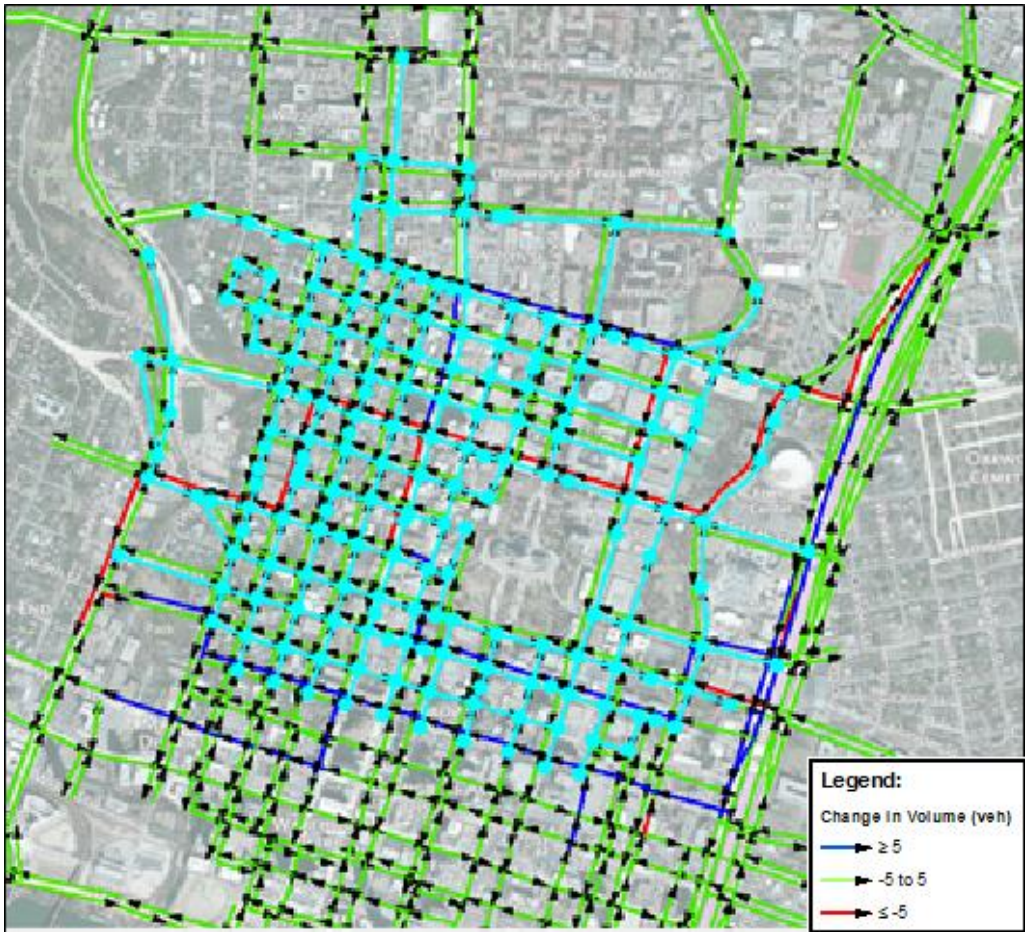

Figure 5.3 Sample STA Results for 15th Street Traffic Control Plan Scenario (Basemap Source: BING © 2010 Microsoft and its Data Suppliers)

These results are illustrated using color-coded links. Links exhibiting a volume decrease of greater than or equal to five vehicles are shown in red and an increase of greater than or equal to five vehicles are shown in blue. If there was a change of less than five vehicles, then the link are represented in green. These thresholds were chosen based on identifying the links perceived to exhibit significant impacts from the TCP scenario. The subnetwork selection is shown in cyan.

As noted in the discussion of this strategy in Chapter 4, identification of entry points to the subnetwork that exhibit noticeable volume fluctuations are required for determining the location of subsequent boundary demand adjustments for the DTA model. As such,

the nodes along the border of the subnetwork were examined to determine the corresponding changes in flow between the base- and impact-scenario STA models. Tables 5.3 and 5.4 summarize the volume changes found and subsequent demand changes implemented at the associated boundary centroids for the DTA models based on these results. The tables display the relevant results for both the 15th Street and 2nd Street scenarios, respectively. The demand change column contains the values to be multiplied by the base demand for the corresponding origin or destination centroid to establish an adjusted demand. After the updates were made to the dynamic O-D table in VISTA, the subnetwork was rerun to produce the proceeding results.

Table 5.3 STA Demand Adjustments for 15th Street

Border Nodes									
	STA Network							DTA Network	
Node Type	Node ID	Link Type	Location	# Links	Volume Before	Volume After	% Change	Node ID	Demand Change
Origin	5197	Inbound	MLK and Red River	1	1335	1273	-4.65	155197	0.9535
Origin	5772	Inbound	12th and I-35 SBFR	1	146	151	3.81	155772	1.0381
Origin	12098	Inbound	11th and Sabine	1	511	505	-1.09	162098	0.9891
Origin	5732	Inbound	10th and Red River	1	428	438	2.33	155732	1.0233
Dest	5135	Outbound	12th and Lamar	1	1483	1421	-4.18	255135	0.9582

Table 5.4 STA Demand Adjustments for 2nd Street

Border Nodes									
	STA Network							DTA Network	
Node Type	Node ID	Link Type	Location	# Links	Volume Before	Volume After	% Change	Node ID	Demand Change
Origin	5751	Inbound	Cesar Chavez at Convention Ctr	1	2009	2027	0.89	155751	1.0089
Dest	5751	Outbound	Cesar Chavez at Convention Ctr	1	2187	2059	-5.85	255751	0.9415
Dest	5752	Outbound	6th and Brazos	1	164	292	78.05	255752	1.7805

The results taken from the first two hours of simulation generated by the different DTA model runs have been summarized in the graphs shown in Figures 5.4 and 5.5. As a

measure for comparing the different scenarios on an aggregate level, the sum of the average travel time across all links appeared to provide the most consistent comparison measure. In order to guarantee that results were not misrepresenting the total travel time, links exiting the subnetwork were excluded. These links were found to be at free-flow speed regardless of flow due to the artificial sink represented by the centroids created at the subnetwork boundary. In the full network case, these links were no longer at the boundary and their travel times were much greater than free flow, so they were removed from the comparison.

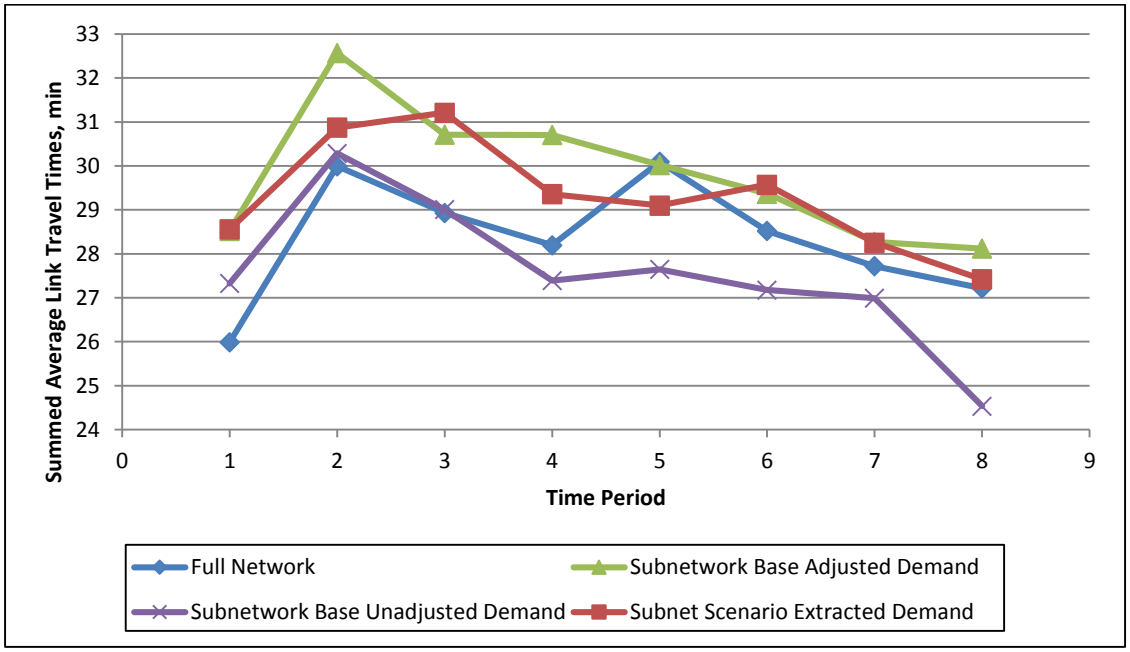

Figure 5.4 STA Adjusted Demand Results for 2nd Street (First Two Hours of Simulation)

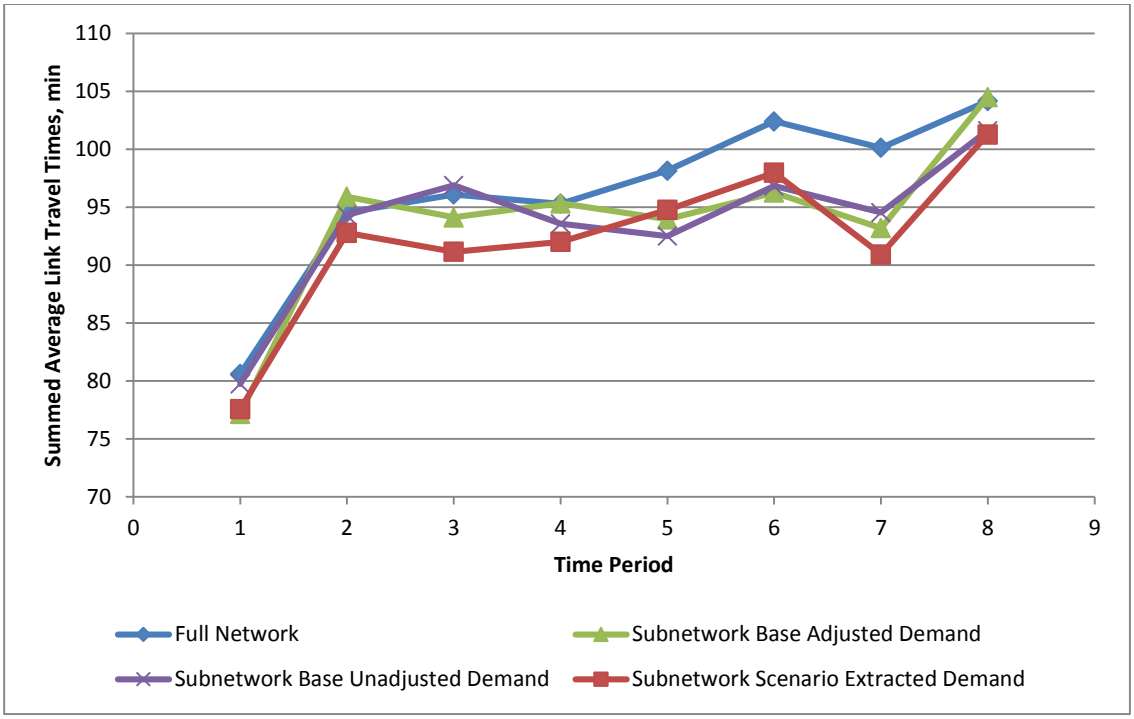

Figure 5.5 STA Adjusted Demand Results for 15th Street (First Two Hours of Simulation)

The travel time measures extracted from the full network with the TCP scenario represent the target values, and the extracted subnetwork demand from this network represents the most accurate demand estimation that could be approximated using subnetwork analysis. These runs represent certain benchmarks for evaluation, though neither of these would be available in a real-world scenario where only the subnetworks from the base network would be created in order to achieve the goal of saving computational time.

For the 2nd Street scenario, implementing the adjusted demand appears to result in a model that overestimates travel times during the first hour of simulation; then, it appears to follow the extracted demand results for the second hour. The second hour has more reliable demand estimations and it behaves more accurately since earlier demands have already been loaded on the network. The 15th Street model appears to fluctuate more randomly with respect to the target values and where the adjusted demand indicates an improvement over the unadjusted demand model. Overall, the results from the STA-

based demand adjustments indicate no consistent or substantial improvement over the unadjusted demand models. This may suggest that the subnetworks were large enough such that no major fluctuations in demand reached the boundary centroids.

The differences in the results obtained from the full network with the TCP scenario versus the subnetwork run with the extracted demand from this model suggest that variations in the results may be explained by random error or the nature of the assignment methodology used by the software. The DTA models were run with 50 iterations of the DUE process, including 20 with path generation/DUE and 30 with DUE only, and a cost gap (g_n) of 1.3 percent or less (gap criterion used in VISTA; see Chapter 4) was achieved for all of the subnetworks. However, differences due to the nature of the computational processes would be expected and may explain some of the seemingly random trends identified in the results. This could signify that running the models to a smaller gap may be necessary to identify changes attributable to the demand adjustments. It also suggests that if a gap of approximately 1.5 percent is acceptable, small changes in demand should not be expected to generate considerable differences in model results.

Demand Estimation Strategy II

The logit model was implemented for the 15th Street scenario in order to demonstrate the proficiency of this strategy for estimating changes to demand along the boundary of a subnetwork. Only one scenario was selected due to the inordinate amount of time required to adequately test the strategy and complete the calculations manually. Manual manipulation of the data was required to properly evaluate the step-by-step implementation of the procedure.

To simplify the logit calculations, the network was divided into quadrants. Specifically, two of the quadrants were analyzed for demand adjustments relative to changes to entry points along the boundary, as well as external trips between regions. For the sample

analysis, the northeast and southeast quadrants were chosen based on the impact scenario. Since 15th Street was modified with reduced capacity in the westbound direction only and the focus here is on external-to-internal and external-to-external trips, this TCP scenario was anticipated to primarily impact inbound trips from the eastern quadrants, a phenomenon consistent with the STA results and preliminary investigation of the O-D demands for the DTA models. A comparison between the subnetwork demand extracted from the base scenario (full) network and the impact scenario (full) network revealed little to no change to the inbound demand along the western quadrants' boundary centroids.

For the northeast quadrant, external trips were grouped into the region's representative megacentroid and the boundary centroids located at the intersections of Martin Luther King Boulevard/Red River Street (Node ID #155197) and 15th Street/I-35 SB Frontage Road (#155780), as depicted in Figure 5.6 on page 155. All trips from the base subnetwork demand originating at the aforementioned boundary centroids were disaggregated into 15-minute intervals for the first two hours of simulation. Next, external travel times from the megacentroid to each boundary centroid were determined from VISTA trajectory outputs for the full network model. Internal travel times from the subnetwork base scenario results were then extracted for trips between each boundary centroid and every destination centroid for each time interval. The demand at each boundary centroid was then used to establish an existing proportion of external trips passing through these centroids bound for subnetwork destinations (internal or boundary).

From this information, the logit equation for external-to-internal trips was used to calculate the sensitivity parameter (θ) for each resultant O-D pair (r, s) using Excel's solver function. A sample of this process is shown below for destination centroid #200358 (22nd Street/San Gabriel Street) with a departure time of 900 seconds (second 15-minute interval, from 900 to 1800 seconds):

$$P_i^{rs,\tau} = \frac{e^{\theta[-(TT_{Internal}^{\tau} + TT_{External}^{\tau})]}}{\sum_{\forall j} e^{\theta[-(TT_{Internal}^{\tau} + TT_{External}^{\tau})]}}$$

$$P_{155197}^{NE-200358,900} = \frac{10\ trips}{11\ trips} = 0.91 = \frac{e^{\theta[-(2.86+4.20)]}}{e^{\theta[-(2.86+4.20)]} + e^{\theta[-(2.27+4.88)]}}$$

$$\theta = 24.3$$

$$P_{155780}^{NE-200358,900} = \frac{1\ trip}{11\ trips} = 0.09 = \frac{e^{\theta[-(7.15)]}}{e^{\theta[-(7.06)]} + e^{\theta[-(7.15)]}}$$

$$\theta = 24.3$$

After a representative sensitivity parameter was calculated for the boundary centroids for each O-D pair, they were used along with the updated internal travel times (highlighted in the equation below) extracted from the subnetwork impact scenario output to establish a new proportion of trips and subsequent demand passing through each boundary centroid. A sample of this process is shown below:

$$P_{155197}^{NE-200358,900} = \frac{e^{24.3[-(2.85+4.20)]}}{e^{24.3[-(2.85+4.20)]} + e^{24.3[-(3.42+4.88)]}}$$

$$P_{155197}^{NE-200358,900} = 1.00 \rightarrow 1.00 * 11\ trips = 11\ trips = demand_{155197}^{NE-200358,900}$$

$$P_{155780}^{NE-200358,900} = 1 - 1.00 = 0 \rightarrow 0 * 11\ trips = 0\ trips = demand_{155780}^{NE-200358,900}$$

For the above example, the resultant demand would be updated from 10 vehicles entering at boundary centroid #155197 and one vehicle at #155780 bound for destination centroid #200358 to 11 and 0 vehicles, respectively. This is based on the sensitivity parameter being large enough that travel time was found to be a valued utility in route selection for this O-D combination, and the increase in internal travel time for boundary centroid #155780 resulted in a decrease in demand for that entry point. Again this process was repeated for all O-D combinations for the boundary centroids in the northeast quadrant over all time periods. It was found that in some cases the value of the sensitivity parameter came out to be negative. This would indicate that a decrease in travel time actually has an adverse effect on choosing a particular route, a counterintuitive phenomenon inconsistent with the core principle of user equilibrium, as well as

assumptions relative to travel time utility used in the logit model (Koppelman and Bhat, 2006). Therefore, it was assumed that the demand would not change between the base and impact scenarios where this occurred and the base demand should not be adjusted.

Once the logit function was implemented and new proportions calculated for all O-D pairs, the new total demand for each boundary centroid was summed over all destinations. This resultant value was compared against the base demand, resulting in a net increase of 12 trips using boundary centroid #155197 (MLK/Red River) and a consequent decrease of 12 trips using boundary centroid #155780 (15th St/I-35 SBFR). This was then compared to the change in demand recorded from the subnetwork demands extracted from the full base and impact scenario networks, where the impact scenario demand represented the target value. Compared to the changes in total demand (aggregated over all time intervals) estimated from the full network extraction, this value was consistent in direction, but of a smaller magnitude.

The "Estimated Percent Change" in Table 5.5 represents the change in demand calculated using the logit formulation, while the column labeled "Target Percent Change" represents the change in demand from the impact scenario network for the northeast quadrant. It was found that the estimated change was not of the magnitude of the target difference in demand between the two scenarios, as extracted from the full network models. Nonetheless, the adjustment was more consistent than that found from the STA-based method where the demand was actually reduced for centroid #155197 and no change implemented for #155780, as shown in Table 5.3 on page 148.

Table 5.5 Subnetwork Boundary Total Demand Comparison for the Northeast Quadrant

Boundary Centroid	Centroid ID	Base Demand (Subnetwork)	Estimated Adjusted Demand (Logit)	Estimated Percent Change	Impact Demand (Subnetwork)	Target Percent Change
MLK/Red River	155197	2171	2183	0.6%	2210	1.8%
15th St/I-35 SBFR	155780	776	764	-1.5%	719	-7.3%

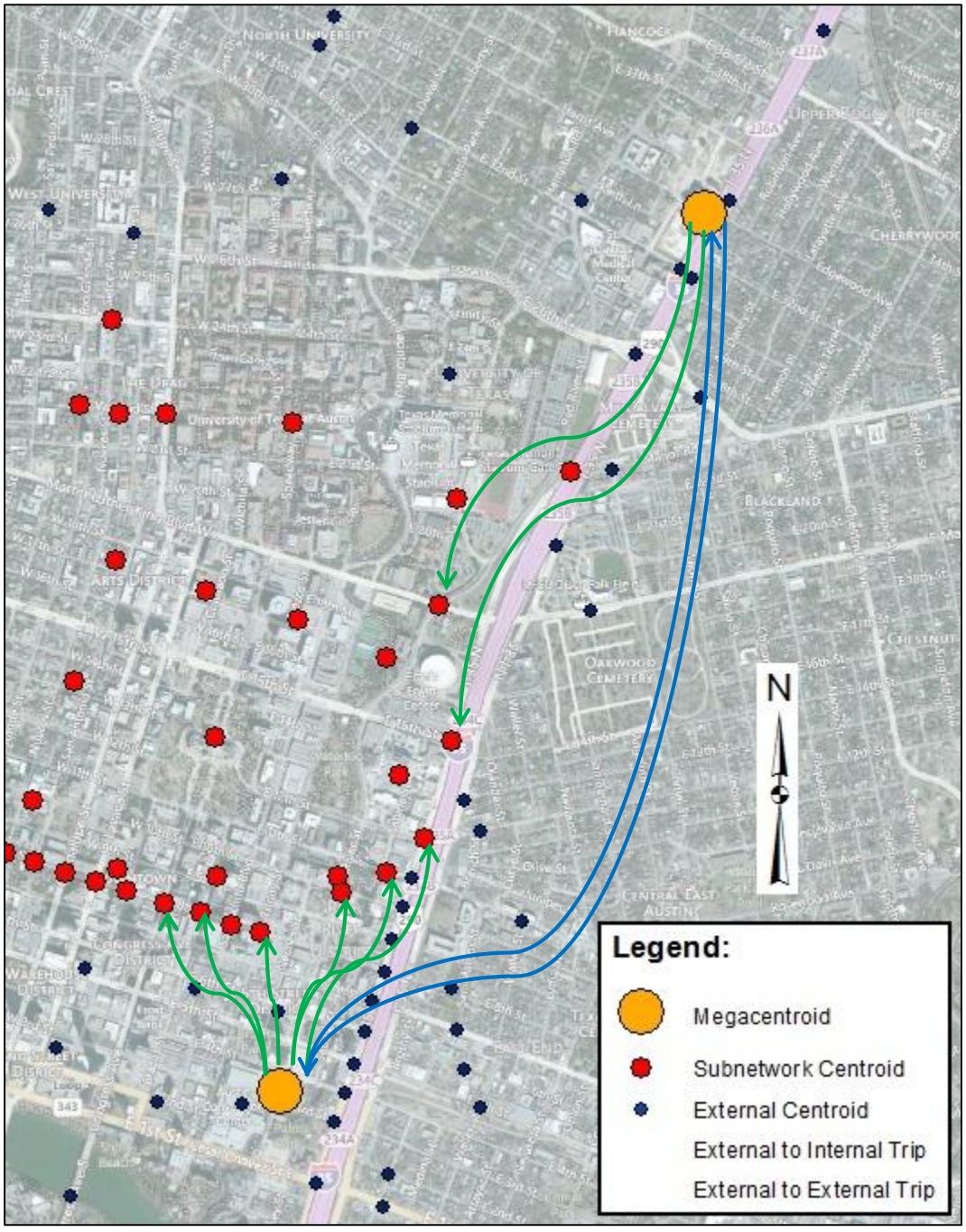

Figure 5.6 Trips Investigated as Part of Logit Methodology for 15th Street Scenario
(Basemap Source: BING © 2010 Microsoft and its Data Suppliers)

For the southeast quadrant, there were six viable boundary centroids, or entry points from the megacentroid into the subnetwork, as depicted in Figure 5.6 (two of the eight original boundary centroids are located at outbound one-way streets). The larger number of possible entry points resulted in a much different logit formulation than that used for the northeast quadrant. As such, many internal destinations had proportional demand from more than two possible boundary centroids (subnetwork origins). Furthermore, calculation of a representative sensitivity parameter value for each destination at a specific departure time interval where more than two origins had none-zero demand values was found to be infeasible.

Existing demands for these cases were not found to be distributed in a manner consistent with the principle of user equilibrium for the estimated total travel times (external plus internal). The aggregation of external travel times across all external centroids, represented by the travel time from the megacentroid to each boundary centroid, appeared to be an oversimplification of the travel time utility. In other words, assuming the choice of entry location can be based on the total travel time, including a fixed external travel time regardless of real trip origin, for a group of external centroids may be insufficient. In some cases, the base demand for a particular entry point appears consistent with the estimated total travel time (a larger travel time coupled with a lower demand), while in other cases, often for the same destination, a larger estimated travel time was coupled with a higher demand. A sample of this phenomenon with four utilized (per base demand) entry points, or boundary centroids, is represented below:

$$P_i^{rs,\tau} = \frac{e^{\theta[-(TT_{Internal}^{\tau} + TT_{External}^{\tau})]}}{\sum_{\forall j} e^{\theta[-(TT_{Internal}^{\tau} + TT_{External}^{\tau})]}}$$

$$P_{155772}^{SE-200377,1800} = \frac{8\ trips}{21\ trips} = 0.38$$

$$0.38 = \frac{e^{\theta[-(1.78+3.72)]}}{e^{\theta[-(1.78+3.72)]} + e^{\theta[-(1.65+3.22)]} + e^{\theta[-(2.26+1.90)]} + e^{\theta[-(1.41+2.66)]}}$$

$$\theta = -0.56$$

$$P_{162098}^{SE-200377,1800} = \frac{3\ trips}{21\ trips} = 0.14$$

$$0.14 = \frac{e^{\theta[-(4.87)]}}{e^{\theta[-(5.50)]} + e^{\theta[-(4.87)]} + e^{\theta[-(4.16)]} + e^{\theta[-(4.07)]}}$$

$$\theta = 1.37$$

$$P_{162734}^{SE-200377,1800} = \frac{7\ trips}{21\ trips} = 0.33$$

$$0.33 = \frac{e^{\theta[-(4.16)]}}{e^{\theta[-(5.50)]} + e^{\theta[-(4.87)]} + e^{\theta[-(4.16)]} + e^{\theta[-(4.07)]}}$$

$$\theta = 0.77$$

$$P_{163015}^{SE-200377,1800} = \frac{3\ trips}{21\ trips} = 0.14$$

$$0.14 = \frac{e^{\theta[-(4.07)]}}{e^{\theta[-(5.50)]} + e^{\theta[-(4.87)]} + e^{\theta[-(4.16)]} + e^{\theta[-(4.07)]}}$$

$$\theta = -0.78$$

Again, the negative values of the sensitivity parameter represent boundary centroid alternatives where the travel time to the destination is higher, and the associated volume is also higher than some of the other origins. This is represented above by the first boundary centroid #155772, which has the highest travel time to destination centroid #200377 (5.50 minutes), yet it has the highest demand of the four centroids, with 8 trips.

This example also shows how each boundary centroid yields a different sensitivity parameter when more than two centroids serve a particular destination. To be conservative in application, the minimum calculated value was used to determine the new demand proportions. In this particular case, since the minimum sensitivity parameter value was -0.78, the demand proportions were determined to remain unchanged between the base and impact scenarios, as discussed earlier with respect to negative parameter values. This was supported by the finding that the travel times remained nearly identical in the two scenarios as well, with the impact scenario yielding the following times: 5.53

min (+0.03) for #155772, 4.87 min (+0.0) for #162098, 4.26 min (+0.1) for #162734, and 4.07 min (+0.0) for #163015. This would also suggest that the demands remain approximately the same between the two scenarios.

The fluctuation in the sensitivity parameter values between the boundary centroids when more than two entry locations are considered is likely due to the fact that the external travel times are simplified for the megacentroid, resulting in an aggregated travel time over all external centroids in the quadrant. This generalization was likely influencing the overall travel time calculated in such a way that a general trend of decreasing demand with increasing travel time could not be established consistently. This is illustrated in the graph of the base demand as a function of the total estimated travel time (internal plus external) shown in Figure 5.7. The linear trend line indicates a general decreasing trend, but the extremely low R-squared value suggests this relationship is not statistically significant.

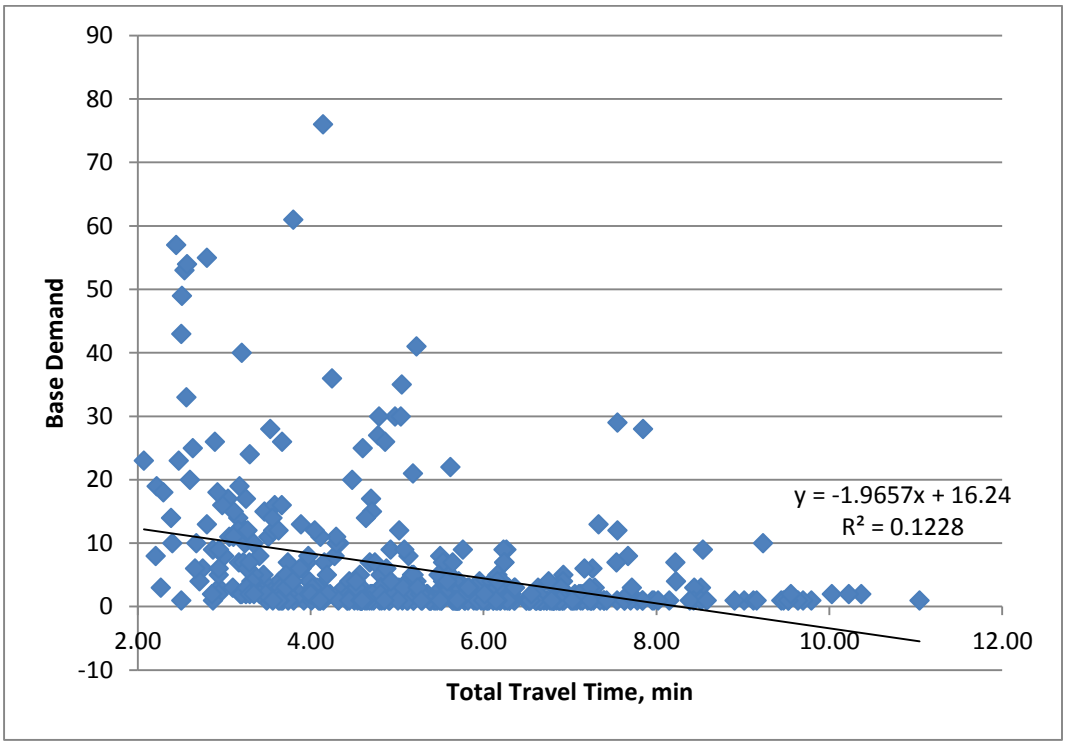

Figure 5.7 Base Demand as a Function of Estimated Total Travel Time (O-D Pair)

Nevertheless, some scenarios did yield fluctuations in demand proportions and the total demand at the boundary centroids did change for the southeast quadrant, albeit slightly. Only two boundary centroids exhibited a net change in demand, with #155732 (10th Street/Red River Street) increasing by one trip and #162734 (8th Street/Brazos Street) decreasing by one trip. For this quadrant, the results were not only lower in magnitude than those observed from the extracted demand from the full network impact scenario, but the increase for #155732 was opposite in direction, as shown in Table 5.6.

Table 5.6 Subnetwork Boundary Total Demand Comparison for the Southeast Quadrant

Boundary Centroid	Centroid ID	Base Demand (Subnetwork)	Estimated Adjusted Demand (Logit)	Estimated Percent Change	Impact Demand (Subnetwork)	Target Percent Change
10th St/Red River	155732	684	685	0.1%	620	-9.4%
12th St/I-35 SBFR	155772	543	543	0.0%	523	-3.7%
8th St/Congress	161381	212	212	0.0%	193	-9.0%
11th St/Sabine	162098	551	551	0.0%	630	14.3%
8th St/Brazos	162734	554	553	-0.2%	515	-7.0%
8th St/Trinity	163015	209	209	0.0%	215	2.9%

Overall, the absence of an estimated change in demand appears inconsistent with the magnitude of the changes identified from the extracted demand from the full network model for the impact scenario. The limited change in overall demand calculated by the logit formulation could be due to the fact that only the entry points with base demands were considered as alternatives for the demand adjustments. Since a base demand did not exist for certain O-D pairs with a boundary origin, no internal travel times for these pairs were available, and thus, the logit calculations could not be readily completed to establish new proportions for the TCP scenario (at these entry points).

Likewise, if only one boundary centroid had demand in the base scenario for a particular destination at a specific departure time interval, it was assumed that this demand would

remain unchanged (i.e. the demand would not be distributed among other potential entry points). However, it is likely some demand shifted to previously unused entry points as part of re-assignment in the full model impact scenario. While these would be extremely difficult to track manually, as done in this analysis, an estimation of these internal travel time changes could possibly be made available from the raw data if this process were to be automated by a developed JavaScript code.

In addition to evaluating the external-to-internal trips for the two quadrants independently, a manual assessment of external-to-external trips, as illustrated in Figure 4.13 on page 123, was also made. The travel time between the northeastern and southeastern megacentroids was evaluated to estimate demand fluctuations at the boundary to the subnetwork where trips between external centroids in each quadrant may have been likely to change from traversing the subnetwork to bypassing it, or vice-versa. This was done using the adjusted logit formulation for external-to-external trips identified in Chapter 4.

This process yielded a change of only two trips in the northeast quadrant avoiding boundary centroid #155780 (15th Street/I-35 SBFR). Nonetheless, the result was consistent with a decrease in demand found using this entry point in the full network impact scenario. The overall decrease was found to be 14 trips (-1.8 percent), 12 external-to-internal plus 2 external-to-external, when compared to the base demand. While consistent in direction, this decrease was still substantially lower than the target value (-7.3 percent) found from the full network model.

For the southeast quadrant, one trip was found to avoid boundary centroid #161381 (8th Street/Congress) in favor of bypassing the subnetwork, and one trip was found to move from an exclusive external route to traversing the subnetwork through boundary centroid #163015 (8th Street/Trinity Street). The overall decrease for boundary centroid #161381 was then determined to be one, or 0.5 percent, and the overall increase for boundary

centroid #163015 was also one, or 0.5 percent. While these changes were minimal, they were consistent with the change in direction for each entry point found in the full network impact scenario, with #161381 decreasing 9.0 percent and #163015 increasing 2.9 percent, as shown in Table 5.6 on page 159.

Overall, the direction of demand changes found using the logit formulation were fairly consistent with the DTA full model results, an encouraging outcome; however, the magnitude of these changes appeared largely underestimated. Preliminary testing revealed that additional modifications to the formulation and use of all potential entry points and subsequent internal travel times for evaluation, regardless of whether the boundary centroid is used in the base model for a particular destination, appear warranted. In addition, aggregating the external travel times over smaller groups may be needed to achieve more accurate analysis results.

Ultimately, two strategies were implemented for evaluating adjustments to demand at subnetwork boundaries caused by internal impacts from TCP scenarios. The first involved using STA model results to estimate respective changes to demand at the subnetwork boundaries for implementation with the DTA models. The second strategy involved using a logit formulation to estimate demand adjustments based on differences in internal travel times, and respective utilities of associated entry points at boundary centroids, between base and impact scenario subnetwork DTA models.

The results from the STA-based demand adjustments provide little evidence that the modifications yield improvements across all time intervals for the DTA subnetwork model. Even though the magnitudes of the volume changes appeared reasonable for adjusting subnetwork boundary demands compared to the full network impact scenario model, the location of these changes across the subnetwork boundary were noticeably different. This is where the logit formulation could possibly be used to improve the estimation of the subnetwork demand. Since the results showed that improvements to the

boundary demand are often in the right direction at appropriate locations when applying the logit models, application of this method on a larger scale was chosen.

Software Implementation of the Logit Formulation and Preliminary Testing

The logit formulation was ultimately chosen for large scale implementation and testing. To alleviate some of the issues relative to the time and effort required to apply the methodology and perform the calculations, the process was automated to the extent practical. In addition, an effort was made to overcome several issues encountered during the manual implementation described above. This included dividing the network and grouping external centroids into more than four regions to incorporate additional disaggregation deemed necessary for establishing estimates of external travel times. This involved reducing the number of centroids combined to generate these aggregate travel time estimates and using more intricate grouping strategies.

As identified previously, the purpose was to streamline the process of estimating external impacts and modifying the subnetwork boundary demand accordingly. The underlying procedure is based on the fact that any trips originating at a subnetwork boundary centroid have initially originated upstream of that centroid, since these boundary centroids are essentially artificial in nature (created by cutting the network). The demand at these centroids is subsequently based on the volume passing through these points as obtained from the full network base model run, which is required prior to completing this process. As such, the boundary centroid is merely an intermediate point along a used path. All trips passing through these points can be analyzed and potentially reallocated based on external travel time components (assumed to remain constant across all scenarios), as well as internal travel time components that may change between the base and impact scenarios.

Overall, this methodology assumes that the subnetwork has been developed sufficiently such that travel times beyond the boundary will not be changed due to the impact scenario. However, it is recognized that changes to link travel times occurring inside the subnetwork may influence route choice decisions and subsequent used paths extending beyond the boundary. Therefore, a user may alter their path upstream of the subnetwork due to congestion and resulting travel time increases generated within the subnetwork such that their entry point may also change between scenarios, or that a user may avoid the subnetwork altogether.

One primary goal is to provide a process for dividing the network into sections for which the external centroids can be grouped and the boundary centroids assigned appropriately. It was intended to test grouping the boundary centroids in accordance to both the origin of the demand passing into the subnetwork at those locations and the spatial relationship that exists among them. ArcGIS provides a number of useful tools that can be applied to perform this process. A second goal is to apply the logit formulas in a robust and efficient manner with the aid of computer software, in this case, Matlab. Therefore, the implemented method for adjusting the subnetwork demand includes two fundamental procedures, grouping the centroids and applying the logit models. The following describes, in detail, the process necessary for implementation and automation using model tools created in ArcGIS and software code written in Matlab.

Grouping the Centroids

The procedure for grouping the centroids is initiated in ArcGIS by creating a layer with a shape that divides the network into appropriately defined regions or sections. This process has been automated in ArcGIS using a series of developed software models. These models effectively execute an algorithm using a series of software tools joined in sequence. The primary purpose of these preliminary models is to create a polygon

shapefile separated into regions that encompasses the entire network. This shapefile is ultimately used to group centroids into those regions.

The polygon, centered at a chosen network link, is circular shaped and divided into pie-shaped slices. It is also oriented geometrically with respect to the modified link. That is to say the polygon is rotated so that a cut is made both directly along the link and exactly perpendicular to it. Two separate models were developed to provide a user the option to create either four or eight slices depending on what is deemed appropriate given the network layout. In addition, the model provides the user an option to further separate the slices into sections with circumferential cuts at designated radii. This functionality offers the freedom to apply a number of strategies for dividing the network into sections for grouping centroids.

The first step in implementing the model is for the user to select a link of interest, either representing a modified link or the middle of a series of modified links, within the link shapefile in ArcGIS. With this link selected, the user can choose the appropriate tool for creating the grouping polygon. Once the model is initiated, a dialogue box appears, as shown in Figure 5.8. Here, the user specifies the radius of the polygon (1) and any additional radii by which to further divide the polygon (2). The user also has the ability within the tool's dialogue box to specify the file name and path for storing the created shapefile (3).

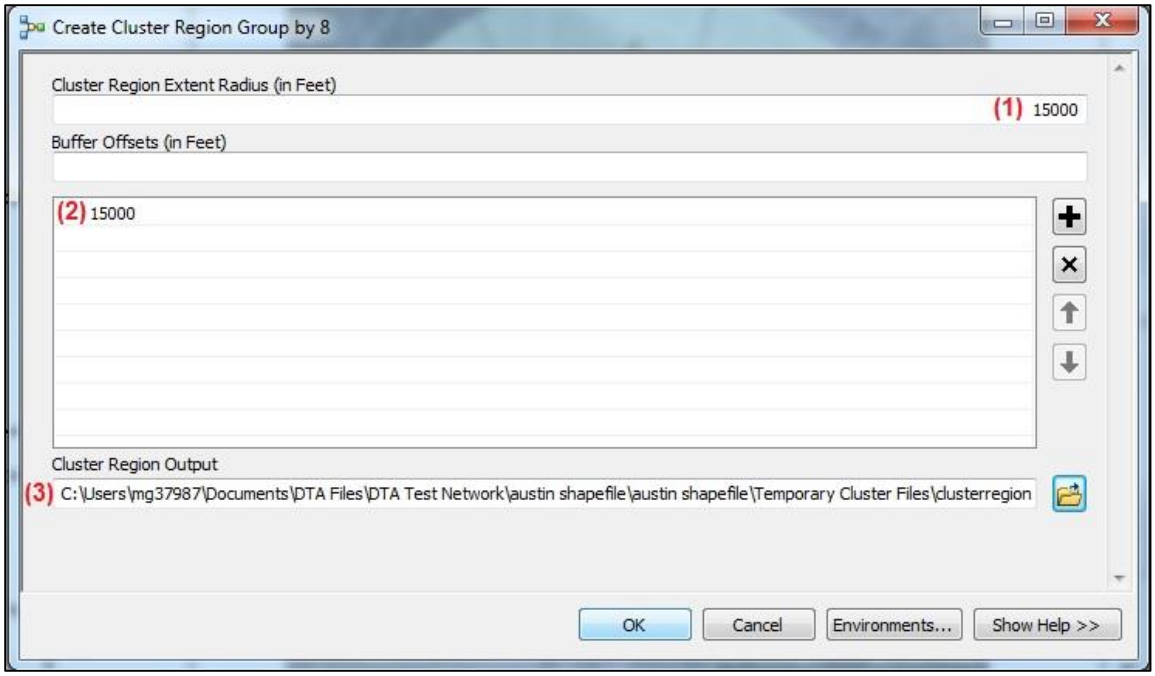

Figure 5.8 Input Prompt for Cluster Region Model

A layout of the model identifying the complex array of tools sequenced to produce the subsequent shapefile can be found in Appendix A, Figure A.4. Within the model, two submodels are embedded that calculate the center X-Y coordinates of the polygon based on an endpoint of the link selected. These submodels are shown in Figure A.4, as well.

After initiating the cluster-region creation tool, a polygon shapefile will be created and displayed in the ArcGIS map, as demonstrated in Figure 5.9. This figure represents the division of the network into regions extending from one of the modified links for a sample TCP scenario. The particular scenario identified involves adjusting the capacity of three links along Guadalupe Street in downtown Austin, between 6th Street and 9th Street. The link chosen for this example represents the central connection between 7th Street and 8th Street.

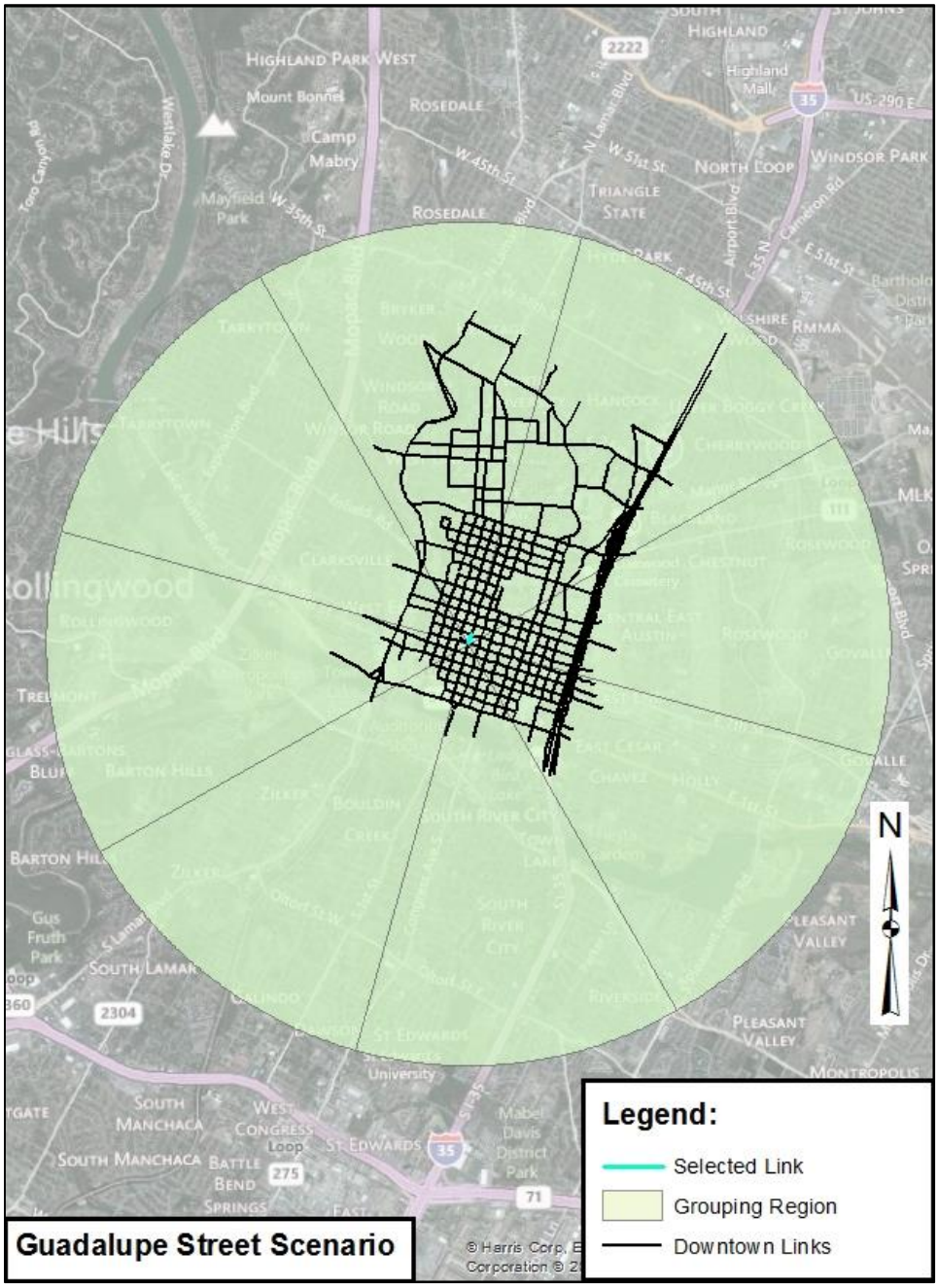

Figure 5.9 Sample Cluster Regions for Guadalupe Street Scenario (Basemap Source: BING © 2010 Microsoft and its Data Suppliers)

At this point, it is necessary to import several files into the ArcGIS project map that are required for grouping the external and boundary centroids. This includes shapefiles representing the full network and subnetwork centroids, along with an Excel file with the

demand, by time period, between each external centroid and subnetwork boundary centroid. This demand output is a product of a JavaScript code created to estimate the demand and average travel time between the external centroids and subnetwork boundary centroids for use with the logit formulation.

This script is run using VISTA files for the full network's centroids, the full network's vehicle trajectory output, and the subnetwork's link details table as inputs. The script identifies travel times for vehicles traversing external-to-internal paths relative to the subnetwork. To do this, it reads the vehicle trajectory output file for the regional network and determines whether or not vehicles originating at centroids enter the "physical" network along a link contained within the subnetwork. If so, they represent internal-to-external or internal-to-internal trips and are ignored. If they enter along a link outside of the subnetwork, the vehicles are flagged and travel times subsequently stored. These vehicles are monitored to determine if they enter the subnetwork, and if so, their travel times from beginning of trip to entry are saved.

Vehicles that do not enter the subnetwork prior to reaching their destination represent external-to-external trips and do not have their travel times saved. If a vehicle that has entered the subnetwork then leaves the subnetwork, the remaining external portion of their trip is also ignored. The output from the script can be converted from a text file to a database file and imported into the ArcGIS project map accordingly. The flow chart shown in Figure 5.10 illustrates the algorithm from which the script was built.

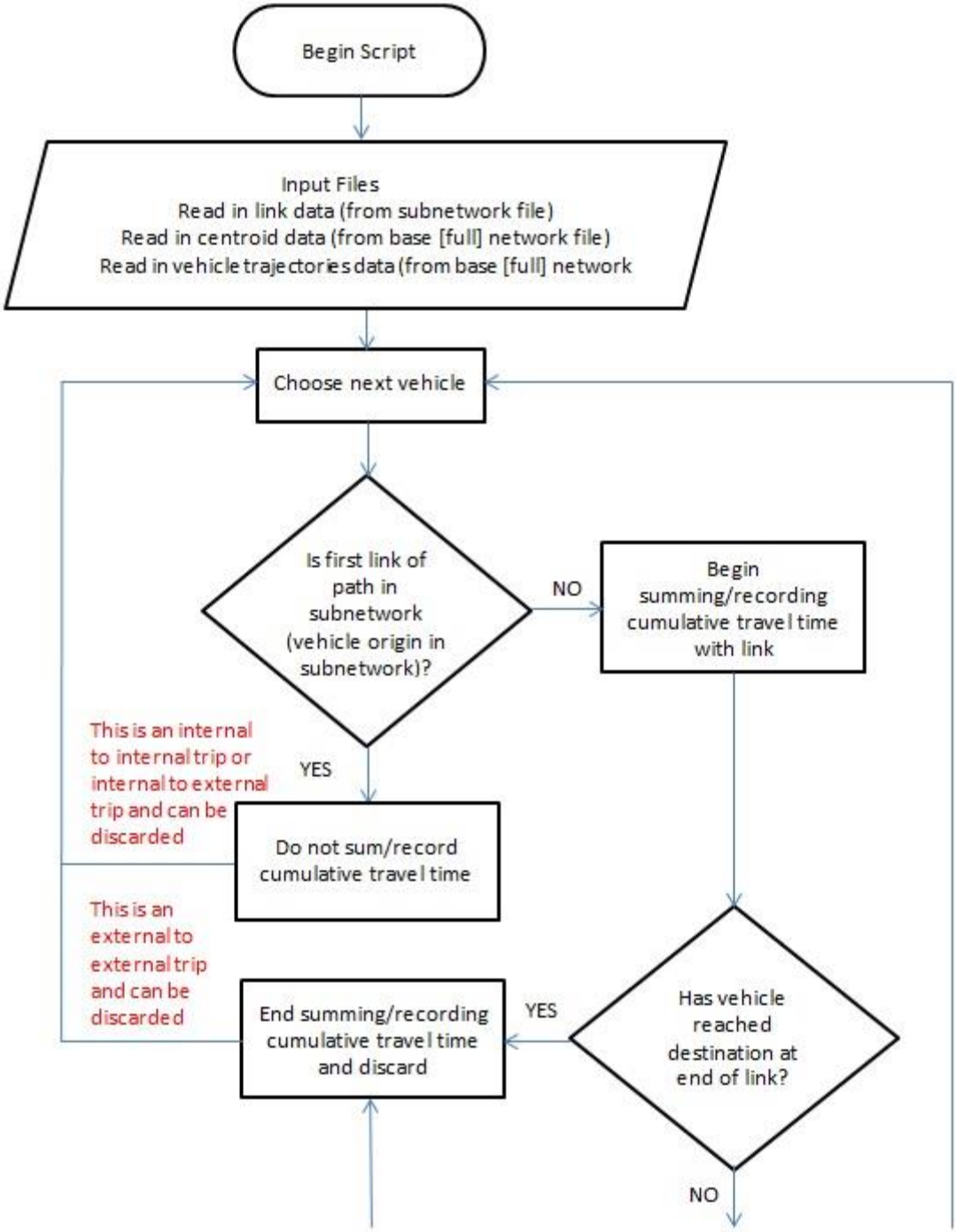

Figure 5.10 Flow Chart of Algorithm Used for External-to-Boundary Travel Time Script

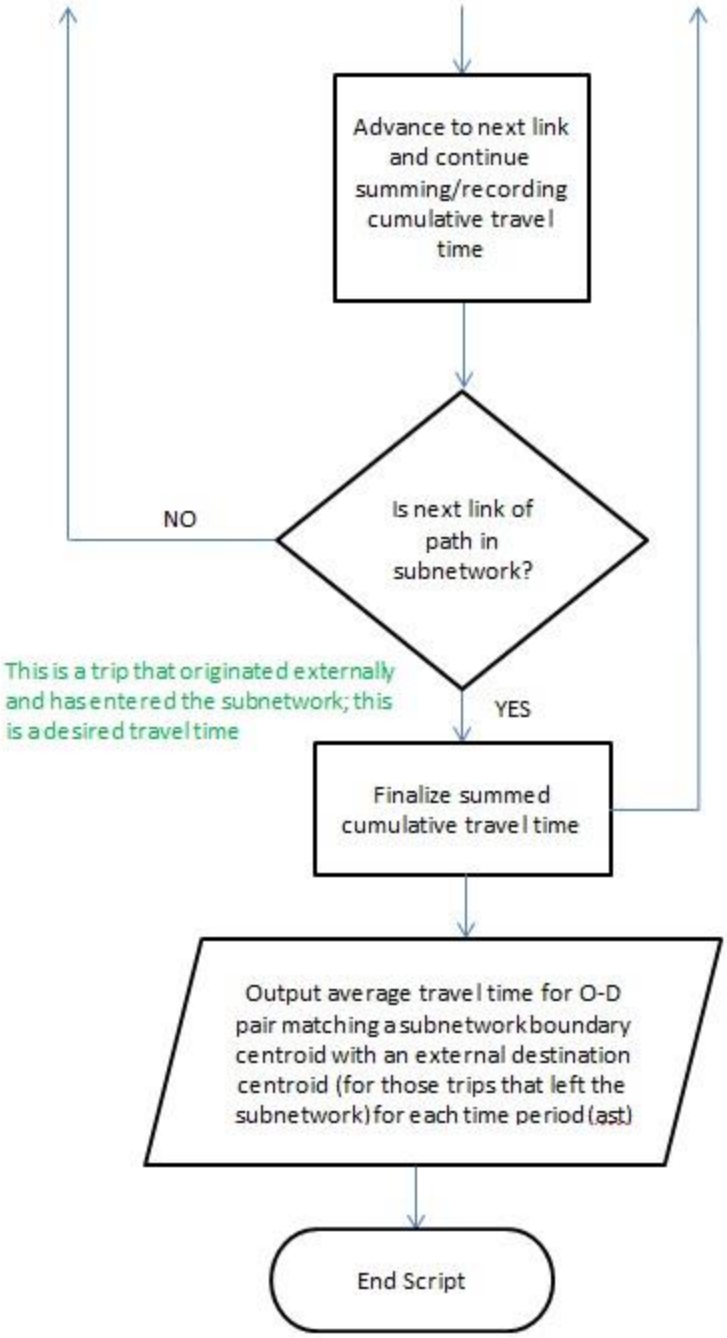

Figure 5.10 (Continued) Flow Chart of Algorithm Used for External-to-Boundary Travel Time Script

An excerpt from the script's output is provided in Table 5.7. It should be noted that the subnetwork entry point is identified by the boundary origin ID. This is particularly relevant to applying the grouping strategies for the subnetwork boundary centroids.

Table 5.7 Output from External-to-Boundary Travel Time Script

External Origin	Time Period	Subnetwork Boundary Origin	Average Travel Time (sec)	Demand
100361	0	156339	114.92	12
100361	0	163055	205.00	1
100361	1	156339	114.89	46
100361	1	163055	190.50	6
100361	2	156339	115.05	41
100361	2	163055	215.00	1
100361	3	156339	123.44	48
100361	3	163055	212.67	6
100361	4	156339	113.76	25
100361	4	163055	179.00	1

Producing the necessary centroid shapefiles involves accessing VISTA and extracting the coordinate information for the centroid elements. To do this, the centroids must be isolated from the other nodes using an SQL query in VISTA that selects nodes from the network's database with a type consistent with a centroid (100), as shown below:

Command:

```
SELECT id,x,y FROM nodes WHERE TYPE=100
```

This query generates a table with the centroid attributes for a network, including unique ID and X-Y coordinate information. The coordinate information can then be used to create a point shapefile in ArcGIS. This process includes assigning the appropriate global coordinate system for the shapefile and then adding it to the map. Once this has been completed, the centroids can be examined and the subsequent grouping process applied.

As part of testing the boundary demand adjustment using the logit formulation, a number of grouping strategies were developed. To provide a level of flexibility relative to grouping boundary centroids and to properly evaluate the methodology, three methods were created and implemented. The first strategy involves simply grouping the boundary centroids into the geographic regions represented by the created polygon. This method groups the centroids based on somewhat arbitrarily selected boundaries. It was anticipated that the process would oversimplify and perhaps bias the resultant travel time estimates, thus, an attempt was made to cluster the boundary centroids according to their spatial relationship with respect to originating demand location.

One of the two resulting demand-based strategies involves grouping these centroids by the region contributing the maximum proportion of their demand (entering flow). Those centroids receiving the majority of their demand from the same region are then grouped together. A second demand-based grouping strategy was developed to use the proportion of demand originating from each of the external regions that passes through the individual boundary centroids. This way, all of the external-to-internal demand is included in the grouping process.

The process of grouping the boundary centroids has been automated in ArcGIS using three different models representative of each strategy. These models are composed of a series of data management tools and created submodels. The submodels are specifically used for iterative procedures. For a model to be initiated, the user must specify inputs for the different files needed to perform the specified grouping analysis, as well as the final output file. The output file is formatted to be imported into Matlab to serve as input information for the automated logit formulation.

To group the centroids simply based on the originally formed region, the model requires inputs for the cluster region (polygon) shapefile (1) and the subnetwork centroids shapefile (2) as shown in Figure 5.11.

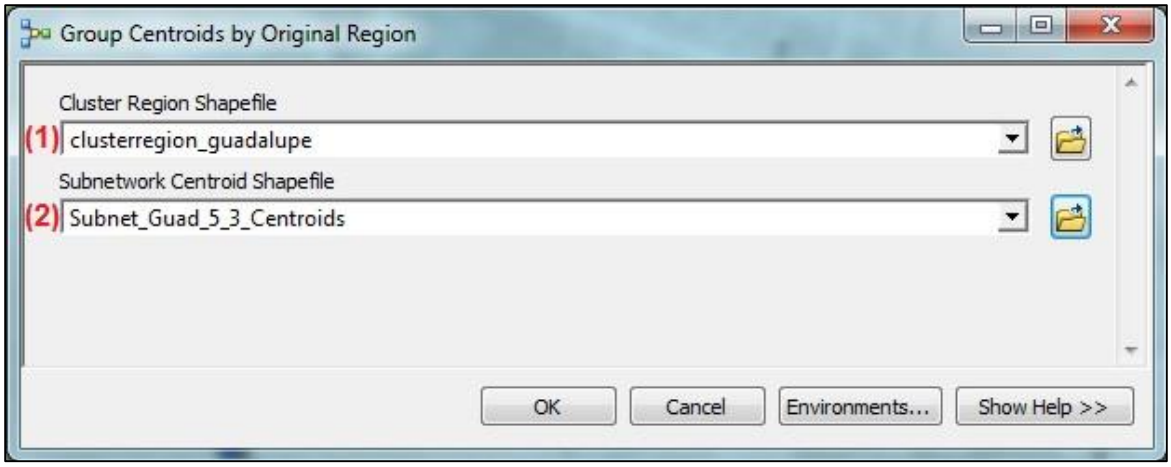

Figure 5.11 Input Prompt for Grouping by Region Model

The model directly groups both the origin and destination centroids along the boundary, encompassing this required input for the automated logit formulation. In Appendix A, Figure A.5 shows the model as constructed in ArcGIS. The associated iterative sub-routine that assigns the boundary centroids to each region sequentially can be found in Figure A.6. This model specifically assigns each subnetwork boundary centroid to its respective region (section) within the polygon created using the model described earlier. A sample illustration of this grouping strategy is provided in Figure 5.12.

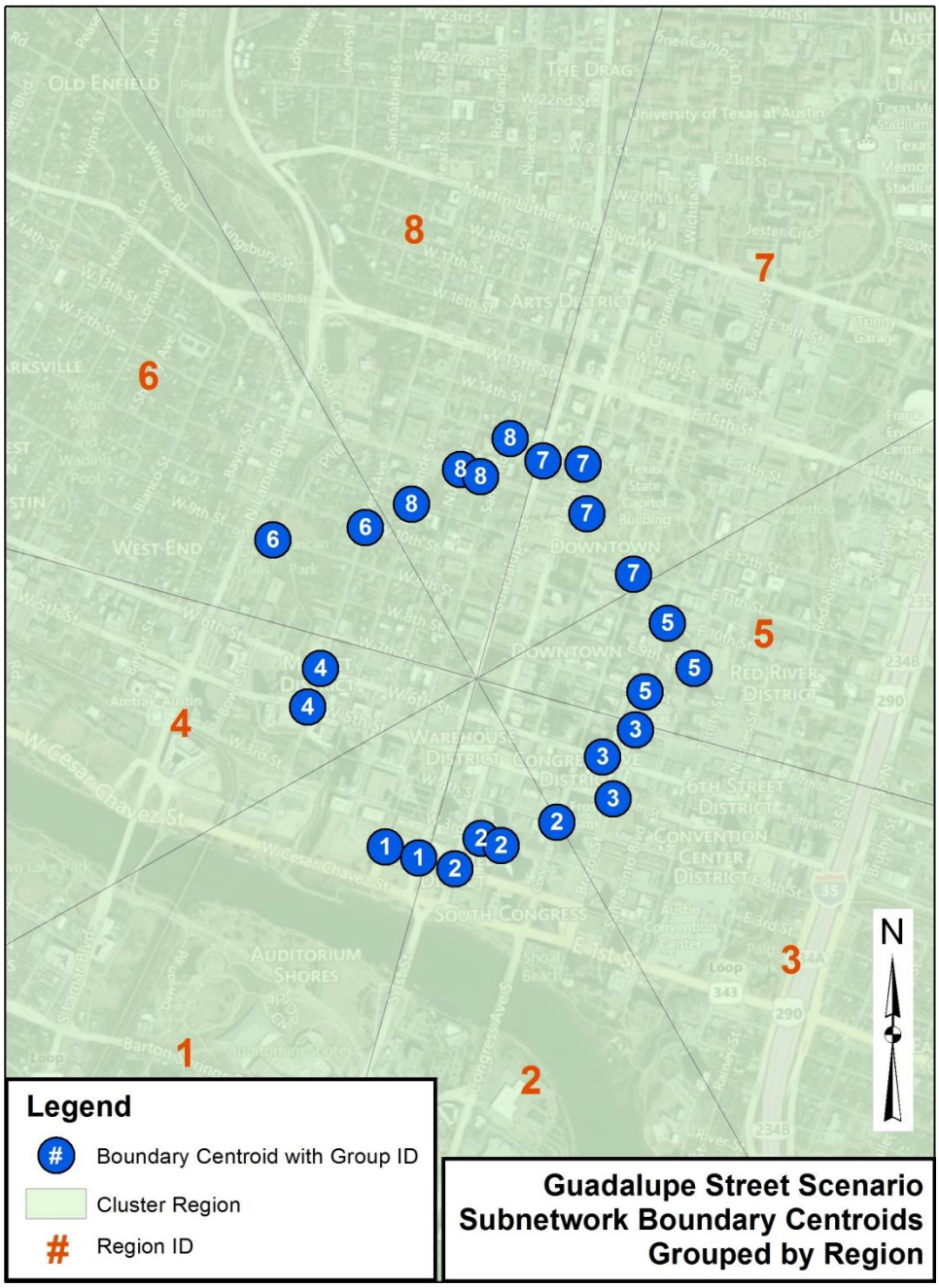

Figure 5.12 Sample Grouping of Boundary Centroids by Region (Basemap Source: BING © 2010 Microsoft and its Data Suppliers)

The second strategy involves a slightly more complicated grouping process that builds off the originally defined regions. Again, this demand-based grouping procedure assigns each of the boundary origins to a respective region associated with the maximum

contributing demand. Rather than grouping centroids by their geographic location, the method assigns boundary centroids specifically based on demand. This is done in ArcGIS using the boundary demand reported in the output for the external-to-boundary script identified earlier. Therefore, the origin centroids are grouped irrespective of location. While each group is likely to encompass many of the boundary centroids located within the same geographic region, it provides additional flexibility in the grouping assignment such that this need not always be the case.

Since the division of the original regions acts a limiting factor, it was decided that no additional constraint was needed for this grouping strategy. To designate the boundary destination centroids, the model contains a built-in routine that joins each destination to the nearest origin and assigns it the respective region ID. The associated model for this grouping strategy requires inputs for the centroid shapefile associated with the full network (1), the imported external-to-boundary demand database file (2), the subnetwork centroids shapefile (3), the cluster region (polygon) shapefile (4), and the output file name and path (5) as demonstrated in Figure 5.13.

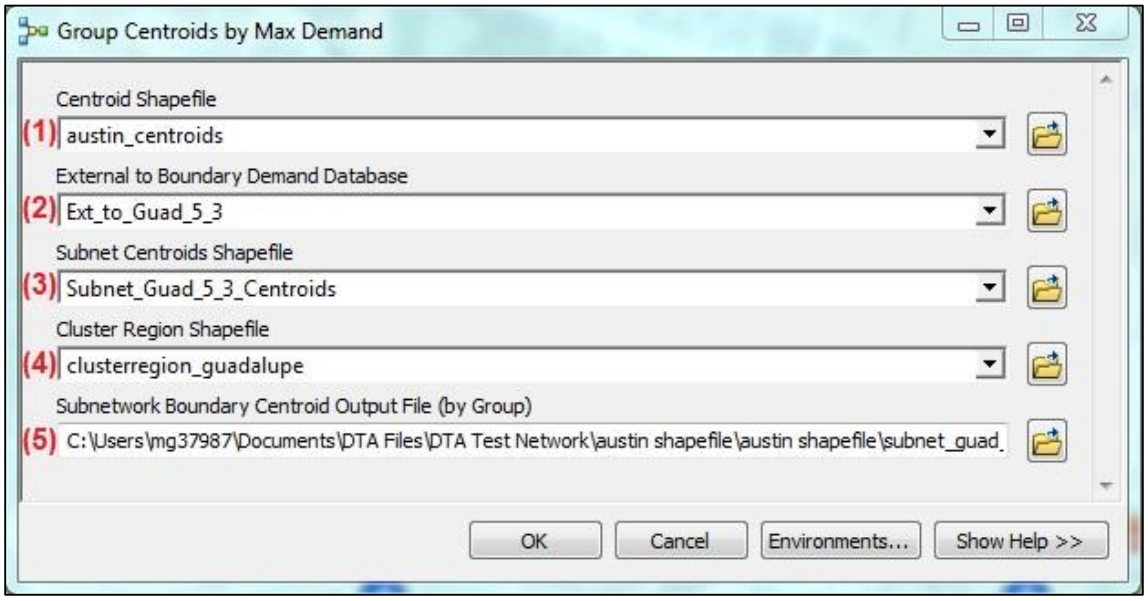

Figure 5.13 Input Prompt for Grouping by Maximum Demand Model

As mentioned, it was intended that the boundary centroids for the subnetwork be grouped based on the entire external demand passing through each centroid, as well as the spatial relationship among these centroids. In this manner, centroids that are likely to compete for associated external demand are grouped together and can be evaluated accordingly. To implement such a strategy, as with the maximum demand-based method, the boundary demand reported in the output for the external-to-boundary script is required. Once this information is imported into ArcGIS, models developed in the software can be applied to complete a statistical grouping analysis.

The second demand-based grouping strategy was developed to use the proportion of demand originating from each of the regions that passes through the individual boundary centroids. In many ways, this strategy operates like the maximum demand-based strategy except that it uses the demand from all of the regions for each centroid in the grouping process. It also adds a level of complexity in that it incorporates a specified spatial constraint. To some extent, it acts as a combination of the other two strategies. The inputs required for this model routine include the centroid shapefile associated with the full network (1), the imported external-to-boundary demand database file (2), the cluster region (polygon) shapefile (3), the subnetwork centroids shapefile (4), and the output file name and path (5) as shown in Figure 5.14.

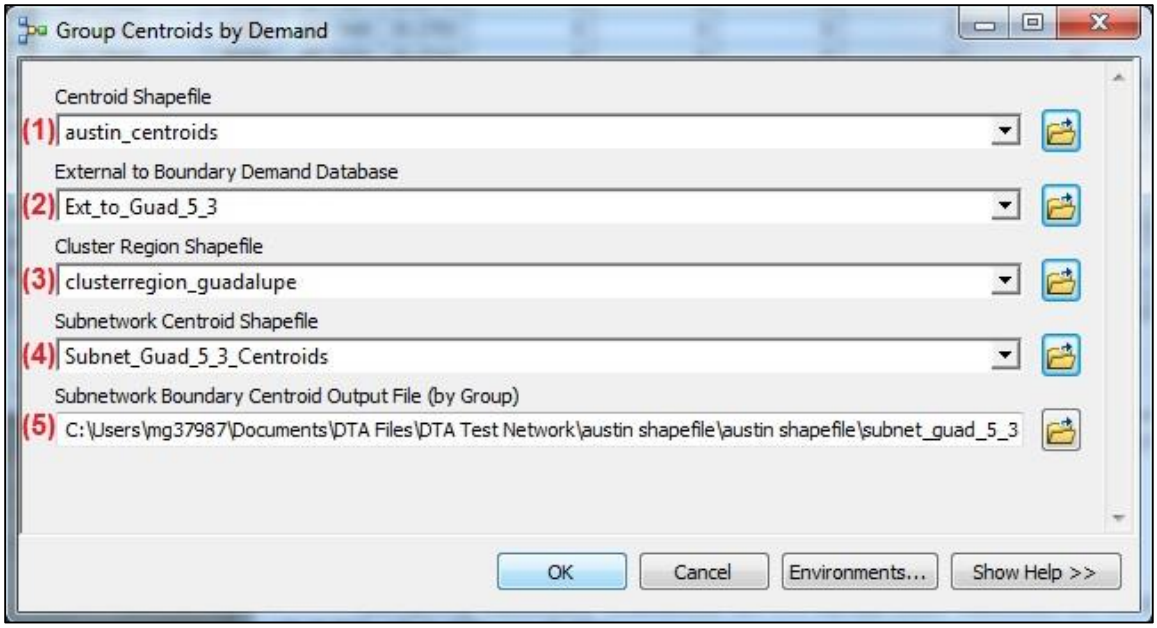

Figure 5.14 Input Prompt for Proportional Demand Model

The associated model routines for both demand-based strategies are provided in Appendix A, Figures A.7 and A.8, along with their associated iterative sub-models shown in Figures A.9-A.12. A number of the preliminary model processes are the same for both demand-based strategies and they require the same inputs. The models begin by first assigning each centroid within the full network to their respective region (section) within the polygon created using the aforementioned model. This is done using an iterative process similar to the one developed for grouping the boundary centroids by region identified earlier.

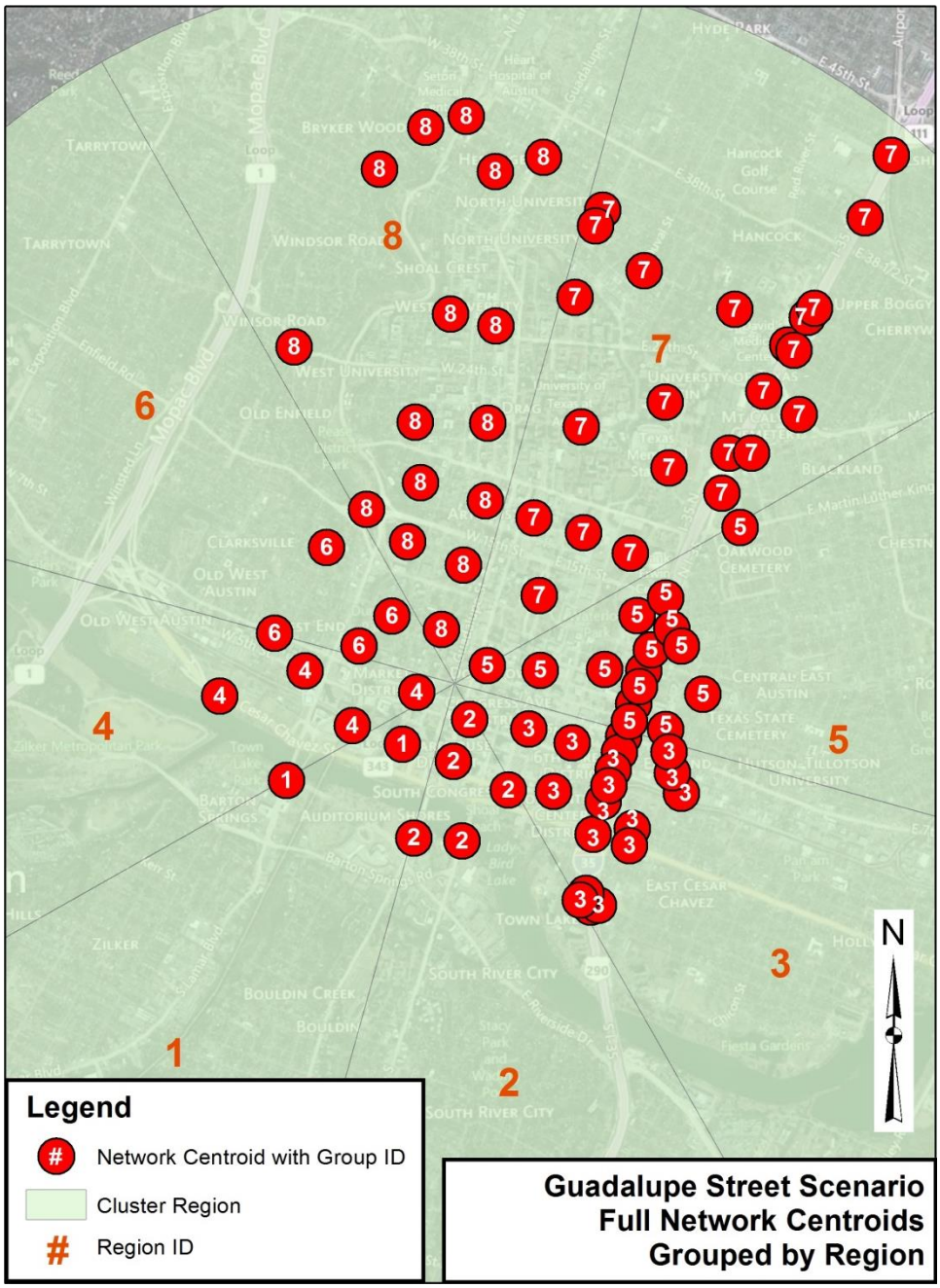

Figure 5.15 Sample Grouping of Full Network Centroids by Region (Basemap Source: BING © 2010 Microsoft and its Data Suppliers)

Once the full network centroids have been grouped, they are assigned an ID consistent with their parent region, as demonstrated in Figure 5.15. This "Region ID" is added to the external-to-internal demand/travel time file output from the JavaScript code that was

imported into the map database, as described above, using a join tool embedded in the model (see Appendix A, Figure A.9). Once this information has been joined, the total demand for each boundary centroid that originates from centroids in each region is summed. A sample excerpt of this information taken from an intermediate output of the model is provided in Table 5.8.

Table 5.8 ArcGIS Model Output with Demand Proportions for Each Boundary Centroid

Boundary Origin ID	Region ID	Demand From Region	Total Demand for Centroid	Demand Proportion
155581	1	121	1658	0.0730
155582	1	1	357	0.0028
160486	1	1	31	0.0323
162736	1	102	923	0.1105
163085	1	3	133	0.0226
163088	1	151	364	0.4148
163110	1	87	1696	0.0513
163153	1	19	675	0.0281
155582	2	312	357	0.8739
155750	2	237	258	0.9186
162734	2	165	1568	0.1052
163110	2	1174	1696	0.6922
163131	2	75	75	1.0000
155582	3	9	357	0.0252
155750	3	20	258	0.0775
155758	3	28	537	0.0521
162734	3	187	1568	0.1193
163137	3	282	454	0.6211
163165	3	2	2608	0.0008

With the regional demand values summed for each boundary origin, the total centroid demand and proportion of the demand from that region is then calculated and stored. Subsequently, each boundary origin can be assigned the region from which the majority of its demand originates, as well as the proportion of its total demand that originates in each region of the polygon. This is where the two demand-based strategies deviate. The

following paragraphs describe the process for implementing the maximum demand-based strategy.

The maximum demand and associated region ID for each boundary centroid is calculated using a descriptive statistics tool in ArcGIS. This tool is incorporated into the maximum demand-based model as the subsequent output is specifically required for that particular grouping strategy. A sample excerpt from the table produced by the model identifying the region that produces the most demand for a particular boundary origin, as well as that maximum demand, is shown in Table 5.9.

Table 5.9 ArcGIS Model Output with the Maximum Demand and Associated Region for Each Boundary Centroid

Boundary Origin ID	# Contributing Regions	Maximum Demand	Region ID
155431	1	18	4
155581	3	1400	4
155582	5	312	2
155750	3	237	2
155758	3	330	5
160486	4	16	4
162734	4	952	5
162736	6	617	8
163020	2	68	5
163025	2	3	1
163028	1	126	7
163085	5	78	8
163088	3	210	4
163110	3	1174	2
163131	1	75	2
163137	3	282	3
163153	5	540	8
163165	4	1582	7

Once these quantities have been calculated by the maximum demand-based model, the maximum demand and maximum demand region are joined to the subnetwork centroid

shapefile. This information is only available for boundary origins; therefore, the boundary destination centroids still need to be grouped accordingly. To do this, the model creates a duplicate region ID field and performs a procedure that identifies the nearest centroid. For the boundary centroids, origins and destinations are often stacked. This process assigns the unique centroid origin ID to the associated destination centroid. It is also a useful tool for assigning boundary destinations along outbound one-way streets. Since these roadways are often coupled with an inbound one-way street located nearby, the destinations centroids are paired up accordingly.

With this process completed, the subnetwork centroid table can be joined with itself to store the associated region ID for each nearest neighbor. In this manner, each boundary destination can be assigned the region ID, resulting from the maximum demand-based grouping analysis, associated with its nearest boundary origin. A region ID will thus be given to each boundary centroid, as demonstrated in the screenshot provided in Figure 5.16 (boundary origins have IDs greater than 150,000 and destinations are greater than 250,000).

Table

Subnet_Guad_5_3_Centroids

FID	Shape	id	x	y	MAX_SUM_De	Region	Unique	RegionID	NEAR_FID
22	Point	155431	-97.7463	30.2755	18	8	22	8	40
23	Point	155581	-97.751	30.2693	1400	4	23	4	34
24	Point	155582	-97.7487	30.2656	312	2	24	2	41
25	Point	155750	-97.7435	30.2662	237	2	25	2	45
26	Point	155758	-97.7411	30.2727	330	5	26	5	46
27	Point	160486	-97.7478	30.2746	16	4	27	4	47
28	Point	162734	-97.7408	30.2696	952	5	28	5	42
29	Point	162736	-97.752	30.2737	617	8	29	8	50
30	Point	163020	-97.7401	30.2714	68	5	30	5	51
31	Point	163025	-97.7448	30.2763	3	8	31	8	52
32	Point	163028	-97.7425	30.2743	126	7	32	7	53
33	Point	163085	-97.7492	30.274	78	8	33	8	54
34	Point	163088	-97.7506	30.2703	210	4	34	4	55
35	Point	163110	-97.7466	30.265	1174	2	35	2	36
36	Point	163131	-97.7458	30.2658	75	2	36	2	48
37	Point	163137	-97.7421	30.2679	282	3	37	3	44
38	Point	163153	-97.7457	30.2753	540	8	38	8	57
39	Point	163165	-97.7438	30.2757	1582	7	39	7	31
40	Point	255431	-97.7463	30.2755	0	0	40	8	22
41	Point	255582	-97.7487	30.2656	0	0	41	2	24
42	Point	255714	-97.7411	30.2686	0	0	42	5	28
43	Point	255727	-97.7393	30.2702	0	0	43	5	30
44	Point	255739	-97.7418	30.2668	0	0	44	3	37
45	Point	255750	-97.7435	30.2662	0	0	45	2	25
46	Point	255758	-97.7411	30.2727	0	0	46	5	26
47	Point	260486	-97.7478	30.2746	0	0	47	4	27
48	Point	260488	-97.7452	30.2656	0	0	48	2	36
49	Point	261081	-97.7426	30.2756	0	0	49	7	39
50	Point	262736	-97.752	30.2737	0	0	50	8	29
51	Point	263020	-97.7401	30.2714	0	0	51	5	30
52	Point	263025	-97.7448	30.2763	0	0	52	8	31
53	Point	263028	-97.7425	30.2743	0	0	53	7	32
54	Point	263085	-97.7492	30.274	0	0	54	8	33
55	Point	263088	-97.7506	30.2703	0	0	55	4	34
56	Point	263111	-97.7477	30.2653	0	0	56	2	24
57	Point	263153	-97.7457	30.2753	0	0	57	8	38

0 (0 out of 36 Selected)

Subnet_Guad_5_3_Centroids

Figure 5.16 ArcGIS Screenshot Demonstrating the Grouping by Region ID

For the last step, the model outputs a text file with the subsequent grouping assignment for use with the logit formulation. Again, the purpose of this model is to assign each boundary centroid to a respective region based on the maximum contributing demand. Figure A.7, in Appendix A, shows the model layout as constructed in ArcGIS. The iterative sub-routine that assigns the boundary centroids to the respective region that contributes its largest proportion of demand is shown in Figure A.10. An example

grouping of subnetwork boundary centroids using this strategy is illustrated in Figure 5.17. The figure demonstrates that the boundary centroids are not confined to groups based on geographic location (i.e. the region within which they are located).

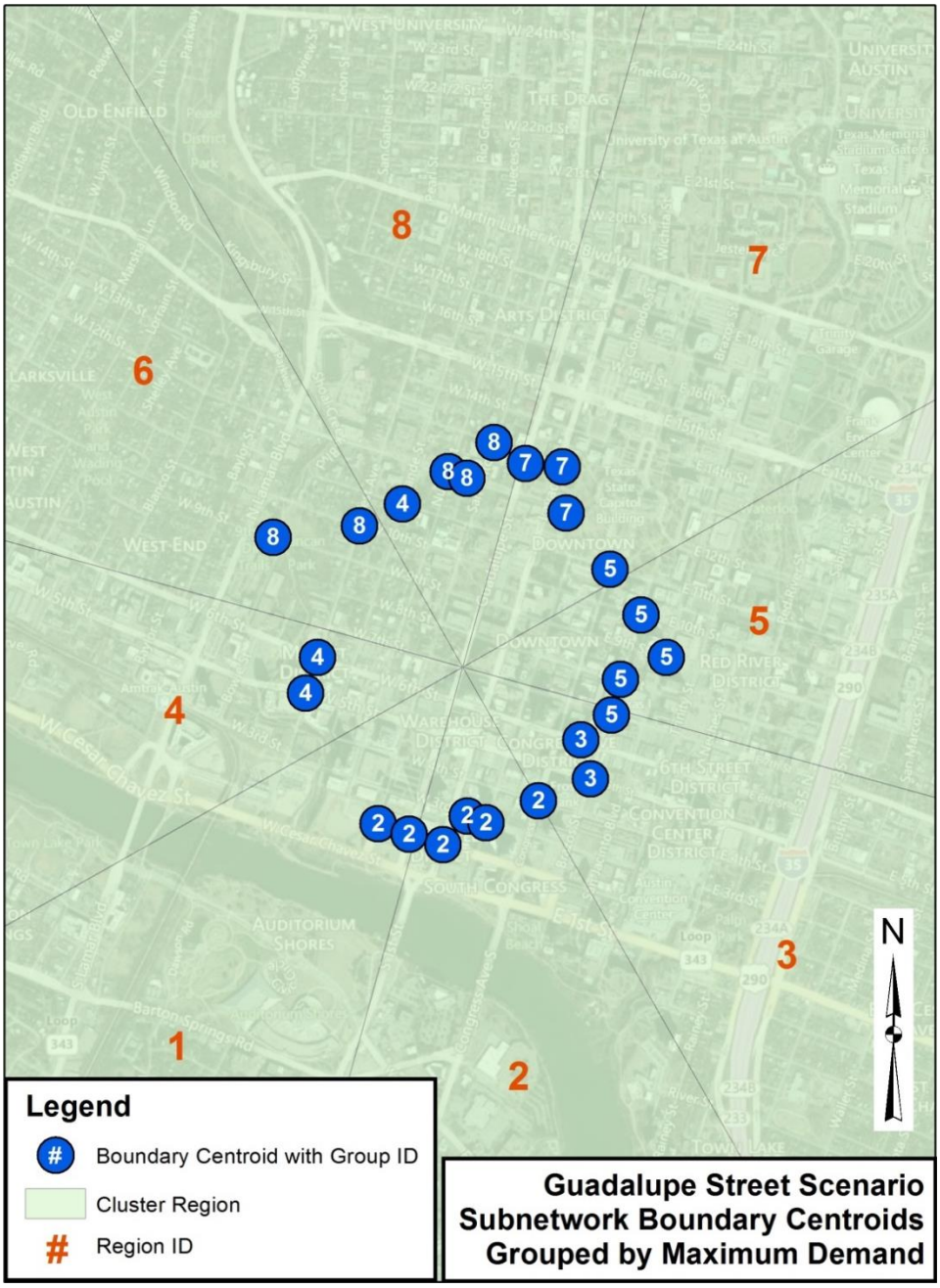

Figure 5.17 Sample Grouping of Boundary Centroids by Maximum Demand (Basemap Source: BING © 2010 Microsoft and its Data Suppliers)

For the proportional demand-based strategy, the regional demand proportions (as shown in Table 5.8 on page 178) are joined to the database associated with the subnetwork centroid shapefile and organized by region. This provides an overview of where the demand for a particular boundary centroid originated. The screenshot in Figure 5.18 illustrates how this information is organized for further evaluation in ArcGIS using the created model. As shown, the demand proportions across each row, representative of an individual boundary centroid, add up to one.

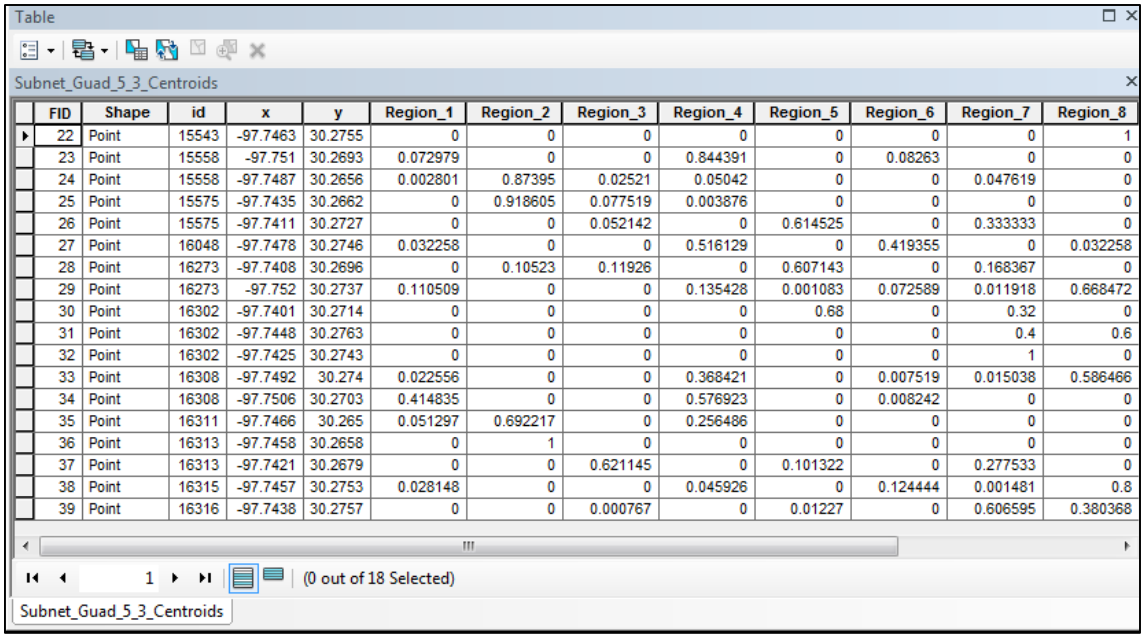

FID	Shape	id	x	y	Region_1	Region_2	Region_3	Region_4	Region_5	Region_6	Region_7	Region_8
22	Point	15543	-97.7463	30.2755	0	0	0	0	0	0	0	1
23	Point	15558	-97.751	30.2693	0.072979	0	0	0.844391	0	0.08263	0	0
24	Point	15558	-97.7487	30.2656	0.002801	0.87395	0.02521	0.05042	0	0	0.047619	0
25	Point	15575	-97.7435	30.2662	0	0.918605	0.077519	0.003876	0	0	0	0
26	Point	15575	-97.7411	30.2727	0	0	0.052142	0	0.614525	0	0.333333	0
27	Point	16048	-97.7478	30.2746	0.032258	0	0	0.516129	0	0.419355	0	0.032258
28	Point	16273	-97.7408	30.2696	0	0.10523	0.11926	0	0.607143	0	0.168367	0
29	Point	16273	-97.752	30.2737	0.110509	0	0	0.135428	0.001083	0.072589	0.011918	0.668472
30	Point	16302	-97.7401	30.2714	0	0	0	0	0.68	0	0.32	0
31	Point	16302	-97.7448	30.2763	0	0	0	0	0	0	0.4	0.6
32	Point	16302	-97.7425	30.2743	0	0	0	0	0	0	1	0
33	Point	16308	-97.7492	30.274	0.022556	0	0	0.368421	0	0.007519	0.015038	0.586466
34	Point	16308	-97.7506	30.2703	0.414835	0	0	0.576923	0	0.008242	0	0
35	Point	16311	-97.7466	30.265	0.051297	0.692217	0	0.256486	0	0	0	0
36	Point	16313	-97.7458	30.2658	0	1	0	0	0	0	0	0
37	Point	16313	-97.7421	30.2679	0	0	0.621145	0	0.101322	0	0.277533	0
38	Point	16315	-97.7457	30.2753	0.028148	0	0	0.045926	0	0.124444	0.001481	0.8
39	Point	16316	-97.7438	30.2757	0	0	0.000767	0	0.01227	0	0.606595	0.380368

Figure 5.18 ArcGIS Screenshot of the Calculated Demand Proportions for Each Centroid

With this step complete, a grouping analysis can be performed by initiating the respective tool available in ArcGIS. The grouping analysis evaluates values from a predefined set of fields (columns) in the database and groups features associated with the database based on these values. Essentially, if two features, for example boundary centroids, share similar values in the analysis field(s) then they are more likely to be grouped together than ones that don't. Typically, a grouping analysis is performed using one field. In this case, eight regions have been created and the proportion of the demand from each of these regions is available for analysis. The maximum demand-based procedure provides a

simple means of clustering the centroids by assigning them a group consistent with the original region IDs (i.e. eight groupings associated with eight original regions). However, the method ignores other potential relationships with respect to where the demand for the boundary centroids originates.

The second demand-based method attempts to account for this by grouping the centroids based on the proportion of their demand coming from each of the original regions. The purpose here is to group centroids together that have similar proportions of their demand originating from the same regions. So if two centroids have the vast majority of their demand originating from the same region(s), they are likely to be grouped together. If their demand is more dispersed, they may be grouped with centroids that share similar demand characteristics, or grouped by themselves. Therefore, demand proportions for each of the eight regions associated with the individual centroids are included in the analysis.

Another aspect of the ArcGIS grouping analysis is the optional spatial constraint. When incorporated, the spatial constraint applies limitations on which features can be grouped together based on their geographic relationship. The nature of this constraint can be chosen as part of the process. Common types of constraints include fixed distance, inverse distance, and 'K' nearest neighbor relationships. A short description of each is provided below:

- Fixed Distance – Only features within a specified distance of each other will be considered for a possible grouping
- Inverse Distance – The relationship between two features will diminish as the distance between them increases
- 'K' Nearest Neighbors – Only the nearest 'K' features will be considered for including in the same group

The options essentially set limitations on how far away another feature can be to still be considered as part of a particular group. The distance calculated between features can be specified as either Euclidean (straight-line) or Manhattan (right-angle). Once these and other options are specified, the analysis can be completed.

ArcGIS performs the grouping analysis using spatial statistics designed to generate clusters of features. The tool assigns a variable associated with each field included as part of the analysis and calculates a subsequent R-squared value for each variable (ESRI, 2013). This way, it can determine which variables provide the most effective means of dividing the groups. In the particular application where the demand proportions for each region are considered, the tool will determine which regions to consider when forming the centroid groups. In addition, the tool uses a statistical analysis process to determine the optimal number and size of each group.

Ultimately, the tool has the ability to evaluate different combinations of features and determine which grouping is the most effective. The grouping is optimized using the Calinski-Harabasz pseudo F-statistic, which assesses within-group similarity and between-group differences (ESRI, 2013). The pseudo F-statistic is a ratio calculated as a function of the individual R-squared values computed for each variable, or field included in the analysis. The interpretation follows that the higher the calculated F-statistic, the better the chosen grouping. Therefore, this F-statistic can be used to select the optimal number of groups to utilize. The option can be selected to have ArcGIS determine the optimal number of groups (from 2 to 15) and the proper assignment of features to those groups. This involves finding the combination of features with the most values in common within the selected analysis field(s), while conforming to the chosen spatial constraint. Again, combinations are evaluated based on the calculated F-statistic, and the optimal grouping is provided as the output.

As mentioned, there are a number of options available and inputs required for running a grouping analysis. Since the grouping analysis tool is a part of the larger model created, several of these options, along with the input files, are predefined to automate the process without requiring additional user input. Nonetheless, it is important to note the default inputs selected for this application. For a spatial constraint, the 'K' nearest neighbors option has been selected to constrain the grouping to the two closest neighbors. Therefore, the groupings do not skip adjacent boundary origins but remain contiguous. It was decided that this was a realistic constraint in order to provide consistent and reliable groupings along the boundary of the subnetwork.

The additional options available revolve around the number of groups that the program will consider. The exact number of groups can be defined by the user or the option selected to have ArcGIS choose the optimal number of groups based on the pseudo F-statistic, as discussed earlier. Selecting this option prompts ArcGIS to investigate the optimal number of groups ranging from 2 to 15. However, some discretion is necessary with respect to the level of disaggregation applied. For this analysis, the grouping optimization option has been selected as a default in the model; however, the maximum number of groups has been set to eight, or equal to the default number of original regions. Therefore, the analysis will be completed and the boundary centroids will be clustered in a manner that maximizes the pseudo F-statistic and results in no more groups than the number of regions used to divide the network.

To demonstrate the results of a grouping analysis, one of the subnetworks for the Guadalupe Street location has been chosen. Again, the impact scenario involves a capacity reduction across three links along Guadalupe Street between 6th Street and 9th Street. The subnetwork size for this sample analysis is associated with a connected order of 5. Figure 5.19 shows the attribute table for the subnetwork boundary centroids with Region 2 highlighted. Again, the proportion of the total demand for each boundary centroid originating in Region 2 is listed in the column.

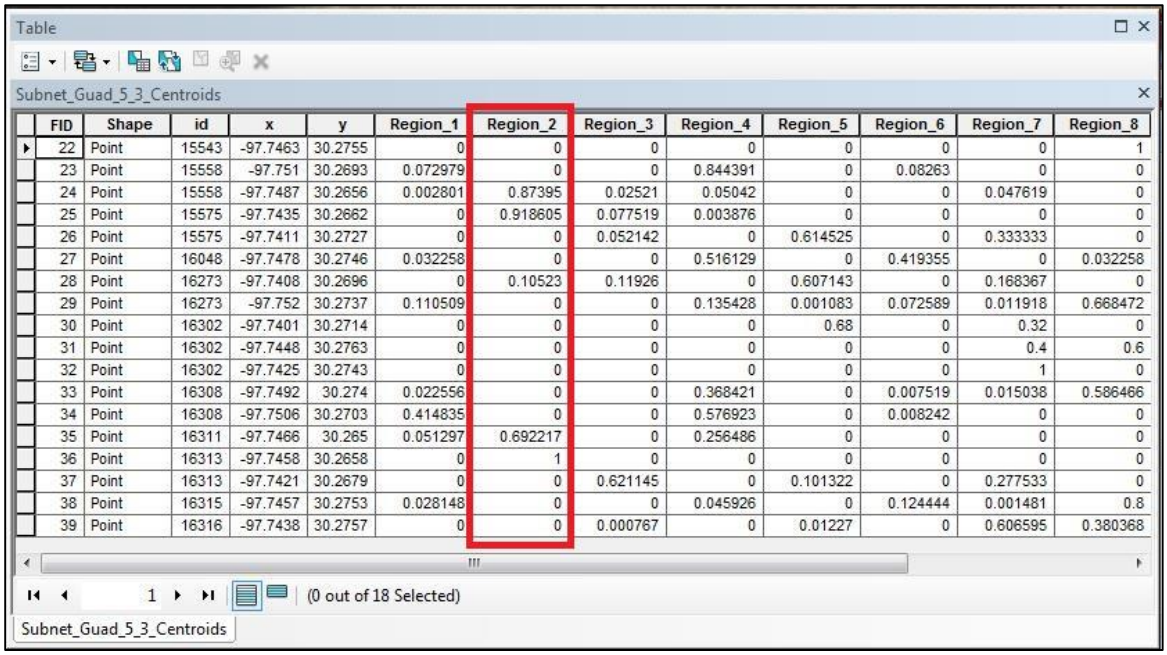

FID	Shape	id	x	y	Region_1	Region_2	Region_3	Region_4	Region_5	Region_6	Region_7	Region_8
22	Point	15543	-97.7463	30.2755	0	0	0	0	0	0	0	1
23	Point	15558	-97.751	30.2693	0.072979	0	0	0.844391	0	0.08263	0	0
24	Point	15558	-97.7487	30.2656	0.002801	0.87395	0.02521	0.05042	0	0	0.047619	0
25	Point	15575	-97.7435	30.2662	0	0.918605	0.077519	0.003876	0	0	0	0
26	Point	15575	-97.7411	30.2727	0	0	0.052142	0	0.614525	0	0.333333	0
27	Point	16048	-97.7478	30.2746	0.032258	0	0	0.516129	0	0.419355	0	0.032258
28	Point	16273	-97.7408	30.2696	0	0.10523	0.11926	0	0.607143	0	0.168367	0
29	Point	16273	-97.752	30.2737	0.110509	0	0	0.135428	0.001083	0.072589	0.011918	0.668472
30	Point	16302	-97.7401	30.2714	0	0	0	0	0.68	0	0.32	0
31	Point	16302	-97.7448	30.2763	0	0	0	0	0	0	0.4	0.6
32	Point	16302	-97.7425	30.2743	0	0	0	0	0	0	1	0
33	Point	16308	-97.7492	30.274	0.022556	0	0	0.368421	0	0.007519	0.015038	0.586466
34	Point	16308	-97.7506	30.2703	0.414835	0	0	0.576923	0	0.008242	0	0
35	Point	16311	-97.7466	30.265	0.051297	0.692217	0	0.256486	0	0	0	0
36	Point	16313	-97.7458	30.2658	0	1	0	0	0	0	0	0
37	Point	16313	-97.7421	30.2679	0	0	0.621145	0	0.101322	0	0.277533	0
38	Point	16315	-97.7457	30.2753	0.028148	0	0	0.045926	0	0.124444	0.001481	0.8
39	Point	16316	-97.7438	30.2757	0	0	0.000767	0	0.01227	0	0.606595	0.380368

Figure 5.19 ArcGIS Screenshot Highlighting Demand Proportions for Region 2

The demand originating from Region 2 that is destined for each boundary centroid is associated with the external origins located in that region. In Figure 5.20, the corresponding boundary centroids with demand from the external origins in that region are identified along with their respective proportions, illustrating how the process of assigning demand is implemented. As shown in the figure, four of the boundary centroids have significant proportions of their demand originating in Region 2.

Additionally, each of these boundary origins is located in the same vicinity. It would be realistic to suggest that these boundary centroids be grouped accordingly. However, the grouping analysis must also take into account the proportions of the demand originating from each of the remaining seven regions.

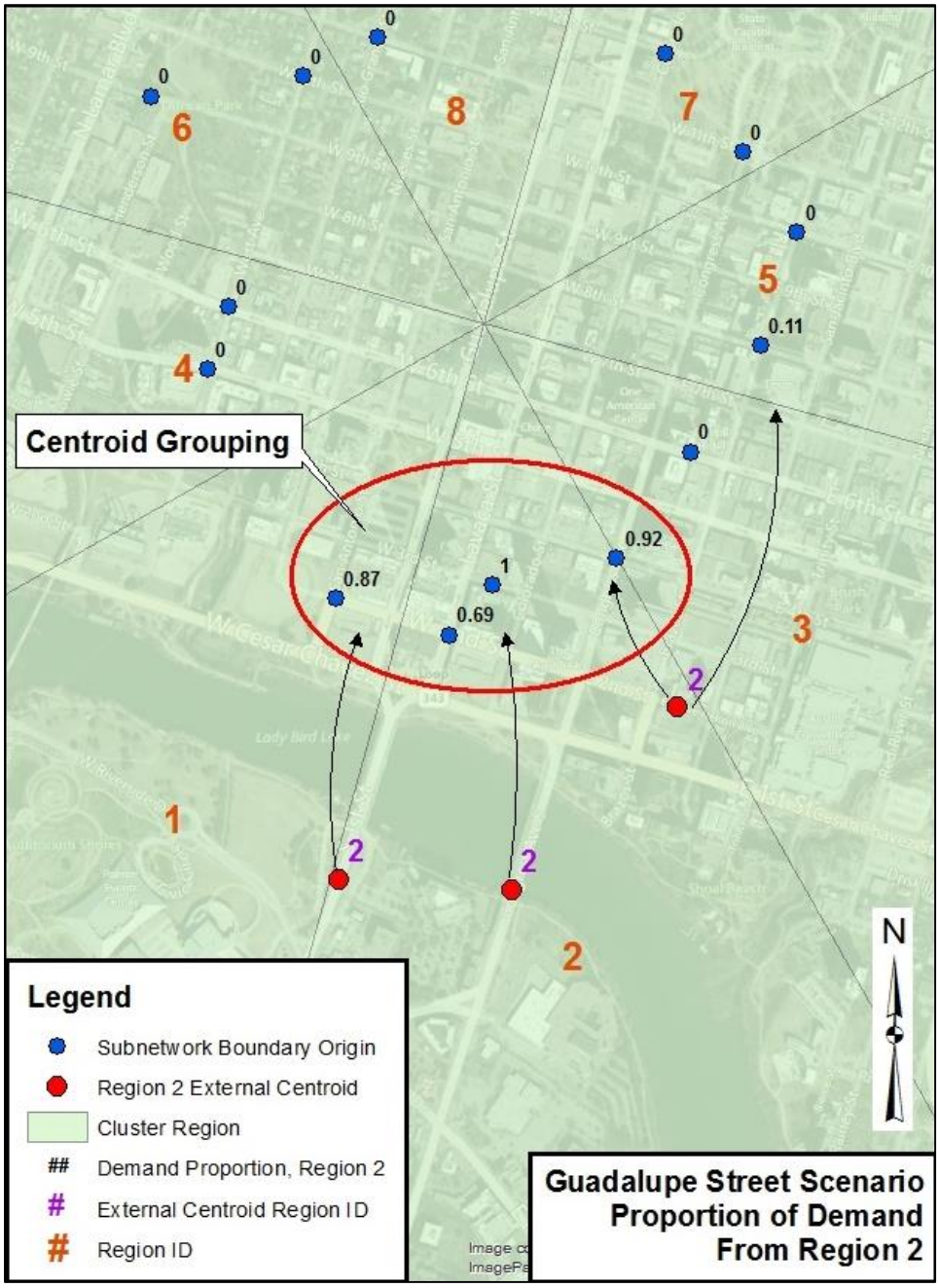

Figure 5.20 Sample Distribution of Region's Demand Across Boundary Centroids (Basemap Source: BING © 2010 Microsoft and its Data Suppliers)

The grouping analysis for the subnetwork boundary centroids was completed resulting in eight groups. The ID associated with each group has been joined to the subnetwork centroid attribute table as part of the model. This is illustrated in Figure 5.21, where the

“Group ID” is the last field in the table. The boundary centroids for Group 1 have been identified to demonstrate how the group was chosen.

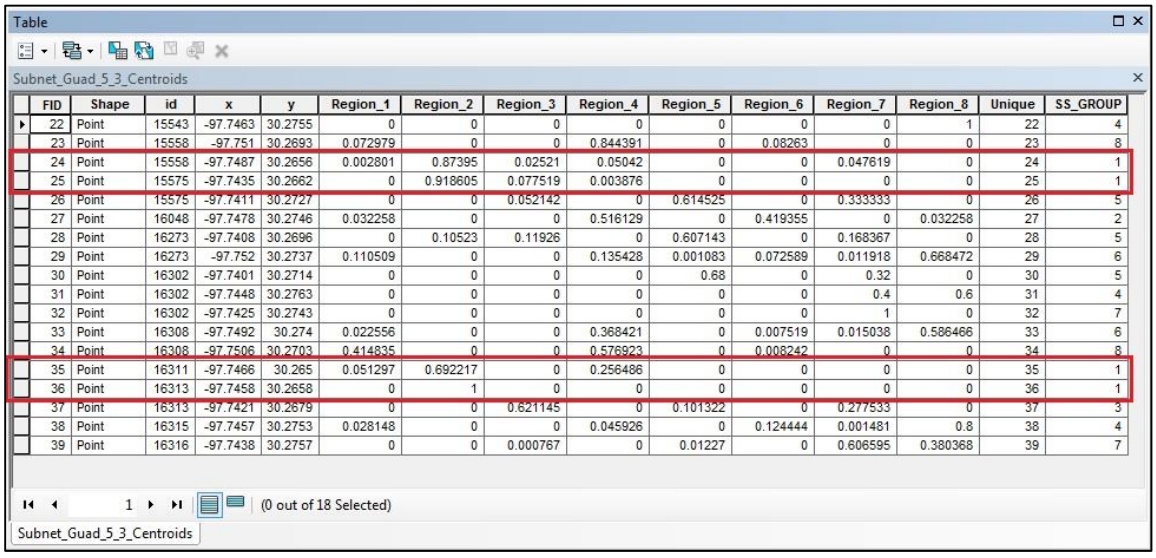

FID	Shape	id	x	y	Region_1	Region_2	Region_3	Region_4	Region_5	Region_6	Region_7	Region_8	Unique	SS_GROUP
22	Point	15543	-97.7463	30.2755	0	0	0	0	0	0	0	1	22	4
23	Point	15558	-97.751	30.2693	0.072979	0	0	0.844391	0	0.08263	0	0	23	8
24	Point	15558	-97.7487	30.2656	0.002801	0.87395	0.02521	0.05042	0	0	0.047619	0	24	1
25	Point	15575	-97.7435	30.2662	0	0.918605	0.077519	0.003876	0	0	0	0	25	1
26	Point	15575	-97.7411	30.2727	0	0	0.052142	0	0.614525	0	0.333333	0	26	5
27	Point	16048	-97.7478	30.2746	0.032258	0	0	0.516129	0	0.419355	0	0.032258	27	2
28	Point	16273	-97.7408	30.2696	0	0.10523	0.11926	0	0.607143	0	0.168367	0	28	5
29	Point	16273	-97.752	30.2737	0.110509	0	0	0.135428	0.001083	0.072589	0.011918	0.668472	29	6
30	Point	16302	-97.7401	30.2714	0	0	0	0	0.68	0	0.32	0	30	5
31	Point	16302	-97.7448	30.2763	0	0	0	0	0	0	0.4	0.6	31	4
32	Point	16302	-97.7425	30.2743	0	0	0	0	0	0	1	0	32	7
33	Point	16308	-97.7492	30.274	0.022556	0	0	0.368421	0	0.007519	0.015038	0.586466	33	6
34	Point	16308	-97.7506	30.2703	0.414835	0	0	0.576923	0	0.008242	0	0	34	8
35	Point	16311	-97.7466	30.265	0.051297	0.692217	0	0.256486	0	0	0	0	35	1
36	Point	16313	-97.7458	30.2658	0	1	0	0	0	0	0	0	36	1
37	Point	16313	-97.7421	30.2679	0	0	0.621145	0	0.101322	0	0.277533	0	37	3
38	Point	16315	-97.7457	30.2753	0.028148	0	0	0.045926	0	0.124444	0.001481	0.8	38	4
39	Point	16316	-97.7438	30.2757	0	0	0.000767	0	0.01227	0	0.606595	0.380368	39	7

Figure 5.21 ArcGIS Screenshot Highlighting Boundary Centroids Assigned to Group 1

As anticipated, the four centroids identified for their substantial demand proportion originating from Region 2, identified in Figures 5.19 and 5.20, along with their close proximity were chosen as a group. Several other similarities relative to their demand exist among centroids within the group, indicating that these centroids are highly correlated. The tool assigns group IDs in accordance with the results of the grouping analysis. As with the maximum demand-based grouping strategy, this method only provides group IDs for the boundary origins.

As before, the boundary destination centroids need to be grouped separately. To do this, the model creates a duplicate group ID field and populates it using a process similar to that identified earlier for the maximum demand-based strategy. Boundary destinations are thus given the same group ID as their nearest neighboring boundary origin. As a result, a group ID is assigned to each boundary centroid, as demonstrated in the screenshot provided in Figure 5.22.

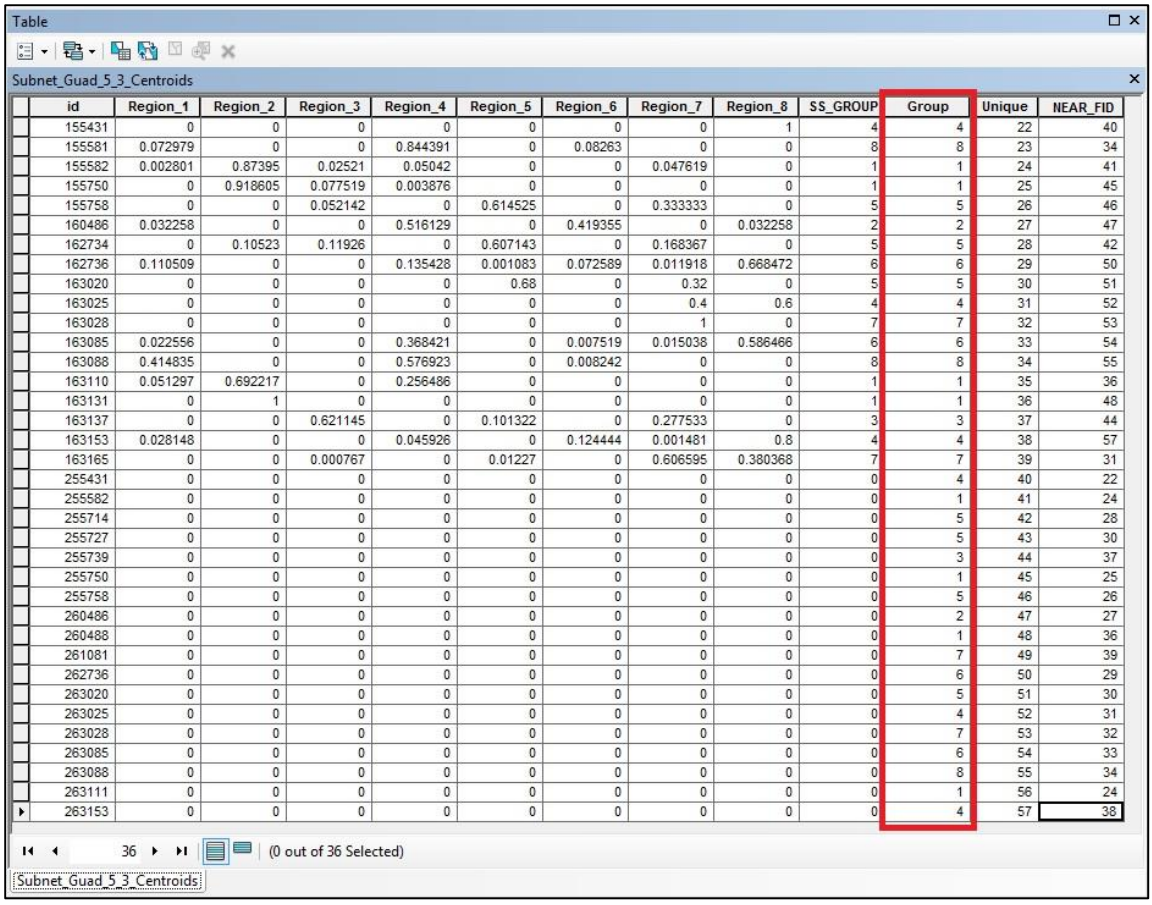

id	Region_1	Region_2	Region_3	Region_4	Region_5	Region_6	Region_7	Region_8	SS_GROUP	Group	Unique	NEAR_FID
155431	0	0	0	0	0	0	0	1	4	4	22	40
155581	0.072979	0	0	0.844391	0	0.08263	0	0	8	8	23	34
155582	0.002801	0.87395	0.02521	0.05042	0	0	0.047619	0	1	1	24	41
155750	0	0.918605	0.077519	0.003876	0	0	0	0	1	1	25	45
155758	0	0	0.052142	0	0.614525	0	0.333333	0	5	5	26	46
160486	0.032258	0	0	0.516129	0	0.419355	0	0.032258	2	2	27	47
162734	0	0.10523	0.11926	0	0.607143	0	0.168367	0	5	5	28	42
162736	0.110509	0	0	0.135428	0.001083	0.072589	0.011918	0.668472	6	6	29	50
163020	0	0	0	0	0.68	0	0.32	0	5	5	30	51
163025	0	0	0	0	0	0	0.4	0.6	4	4	31	52
163028	0	0	0	0	0	0	1	0	7	7	32	53
163085	0.022556	0	0	0.368421	0	0.007519	0.015038	0.586466	6	6	33	54
163088	0.414835	0	0	0.576923	0	0.008242	0	0	8	8	34	55
163110	0.051297	0.692217	0	0.256486	0	0	0	0	1	1	35	36
163131	0	1	0	0	0	0	0	0	1	1	36	48
163137	0	0	0.621145	0	0.101322	0	0.277533	0	3	3	37	44
163153	0.028148	0	0	0.045926	0	0.124444	0.001481	0.8	4	4	38	57
163165	0	0	0.000767	0	0.01227	0	0.606595	0.380368	7	7	39	31
255431	0	0	0	0	0	0	0	0	0	4	40	22
255582	0	0	0	0	0	0	0	0	0	1	41	24
255714	0	0	0	0	0	0	0	0	0	5	42	28
255727	0	0	0	0	0	0	0	0	0	5	43	30
255739	0	0	0	0	0	0	0	0	0	3	44	37
255750	0	0	0	0	0	0	0	0	0	1	45	25
255758	0	0	0	0	0	0	0	0	0	5	46	26
260486	0	0	0	0	0	0	0	0	0	2	47	27
260488	0	0	0	0	0	0	0	0	0	1	48	36
261081	0	0	0	0	0	0	0	0	0	7	49	39
262736	0	0	0	0	0	0	0	0	0	6	50	29
263020	0	0	0	0	0	0	0	0	0	5	51	30
263025	0	0	0	0	0	0	0	0	0	4	52	31
263028	0	0	0	0	0	0	0	0	0	7	53	32
263085	0	0	0	0	0	0	0	0	0	6	54	33
263088	0	0	0	0	0	0	0	0	0	8	55	34
263111	0	0	0	0	0	0	0	0	0	1	56	24
263153	0	0	0	0	0	0	0	0	0	4	57	38

Figure 5.22 ArcGIS Screenshot Demonstrating the Grouping by Group ID

As before, the model outputs a text file with the subsequent grouping assignment for use with the logit formulation. Figure A.8, in Appendix A, shows the model constructed in ArcGIS. The iterative sub-routines embedded in the model to create fields for each region and assign the associated proportional demand to each boundary centroid are shown in Figures A.10 through A.12. An example grouping of subnetwork boundary centroids using this strategy is illustrated in Figure 5.23.

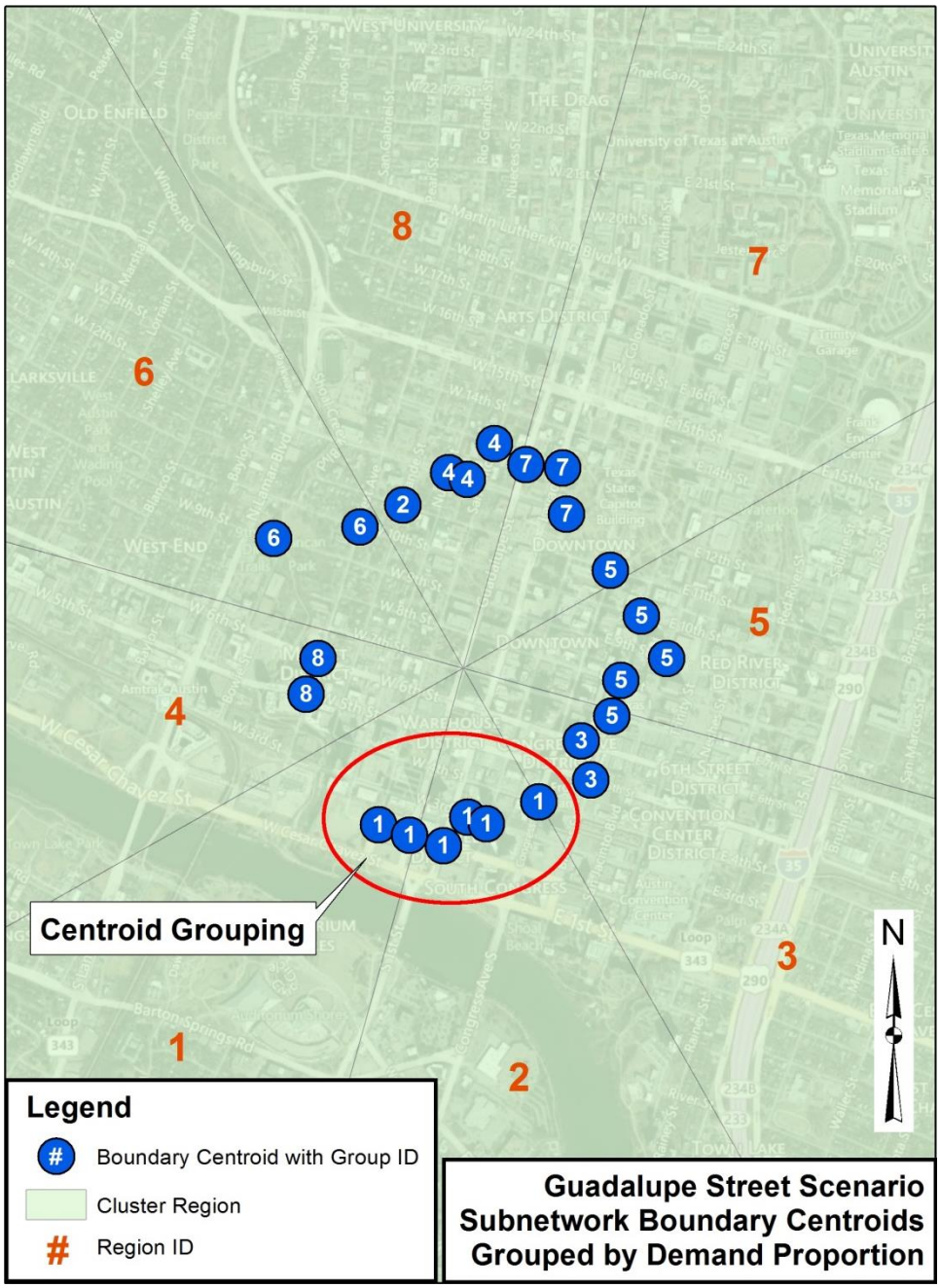

Figure 5.23 Sample Grouping of Boundary Centroids by Demand Proportion (Basemap Source: BING © 2010 Microsoft and its Data Suppliers)

Note here that the group IDs do not correspond to the region IDs. The grouping analysis performed takes into account the value of the proportional demand from each region, not the region ID itself. Therefore, these groups are created and assigned independently of

the region. Again, it is important to point out that the groupings do not conform to the regional extents within which the boundary centroids are located. This emphasizes the value of grouping centroids, not simply based on locations established by arbitrary divisions of the network, but by where their demand originates.

Ultimately, this serves as a means to help overcome the artificial boundaries, and associated limitations, created by assigning centroids to subjectively selected regions. Furthermore, this strategy takes into account spatial constraints that are intuitive, but are not incorporated in the maximum demand-based strategy. A sample grouping that exemplifies the characteristic differences between the three grouping methods discussed, along with the associated regional boundaries, is shown in Figure 5.24.

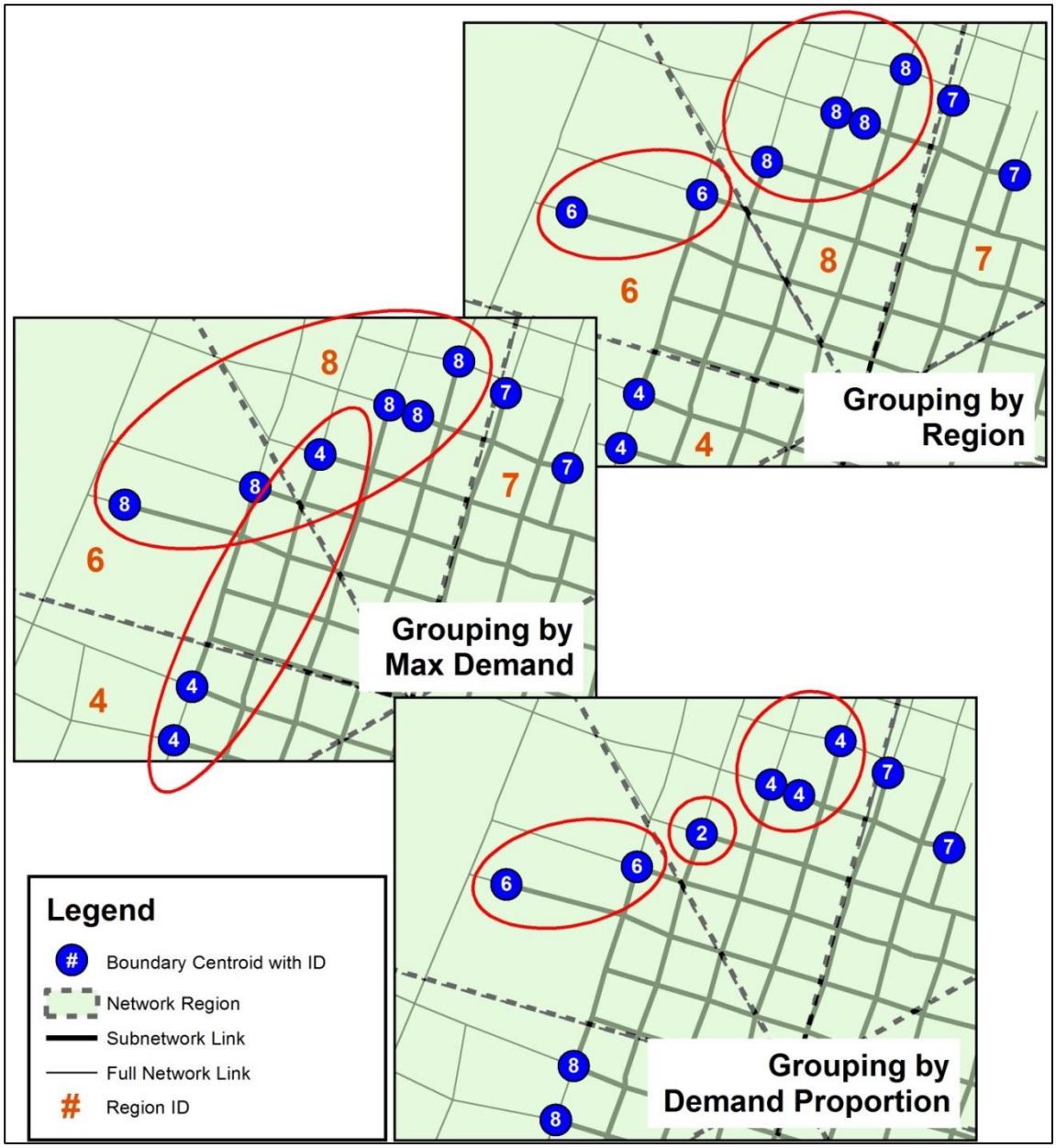

Figure 5.24 Grouping Methods for Subnetwork Boundary Origins

In addition to grouping the boundary centroids, two strategies were investigated for grouping the external centroids. The first method involves grouping the external centroids simply based on the region within which they are located. This is the same process as that applied as part of the first strategy identified for grouping the boundary centroids.

Assigning a region ID for the full network centroids is completed as a sub-process as part of the models for the demand-based grouping strategies for the boundary centroids. It was not able to be coded as part of the first boundary grouping strategy due to complications with the built-in iterator.

ArcGIS does not allow multiple iterative processes to be completed within the same model. The solution of implementing both as submodels caused issues as well. Since both submodels complete a very similar task of iterating through the regions and assigning IDs accordingly, the process of assigning a region ID for the first centroid group (boundary) caused the final region ID extracted from the iterator to be input for the second centroid group (external). Therefore, only centroids in the final region (e.g. region 8) received an ID number. However, the (sub)model that assigns region IDs to the full network centroids can be run independently as needed. This model layout is shown in Appendix A, Figure A.9.

Due to the potential limitations caused by grouping simply based on the arbitrarily assigned regions, another strategy was investigated. The second method implemented is to group the external centroids based on the source of the boundary demand. With the boundary groups previously defined, this strategy clusters external centroids together that contribute demand to any boundary centroid within a group. This resembles the concept introduced with clustering the boundary centroids, grouping based on demand and not solely geographic location. Figure 5.25 illustrates the conceptual difference between "Grouping by Region" and "Grouping by Boundary Centroids".

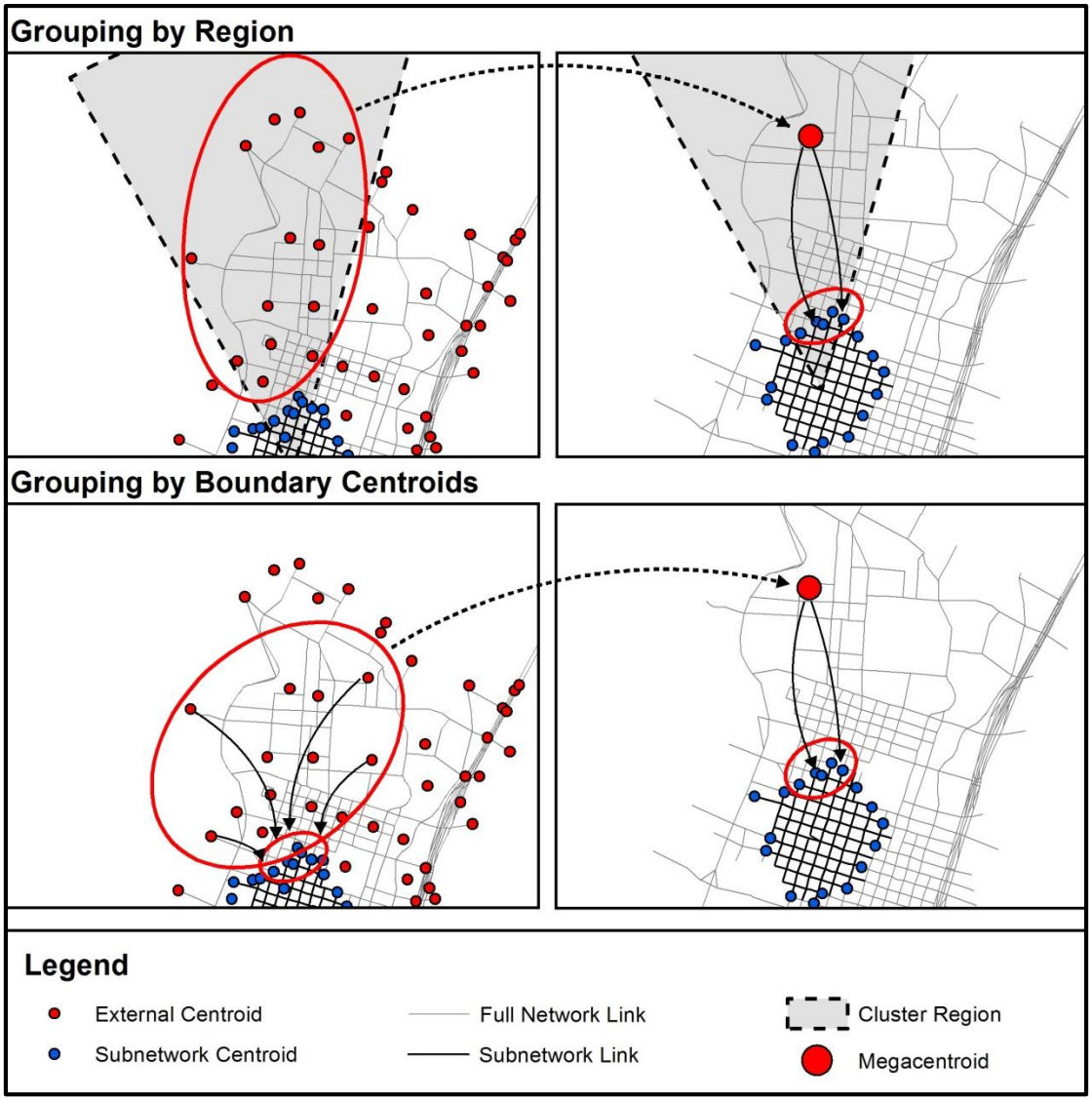

Figure 5.25 Conceptual Difference Between External Centroid Grouping Methods

Although the geographic location is taken into account indirectly due to the nature of the distribution of external centroids that would contribute to a boundary centroid's demand, it does not serve as a specific constraint on the process. The strategy effectively neutralizes the artificial boundaries created in the earlier process of dividing the network into regions. Any centroid from any part of network that contributes demand to a boundary centroid group is then assigned that group's associated ID value (see bottom half of Figure 5.25). In this way, external centroids may be assigned to multiple groups

associated with the boundary centroids. However, this is not a limitation since the external travel time components provided for the logit model are associated with the O-D pair for a specific grouping. Furthermore, removing the constraint imposed by the selected regional boundaries was considered a potential enhancement to the process.

Grouping the external centroids is important as it facilitates provision of the external travel time components required to implement the logit formulation. With the process of grouping the boundary and external centroids complete, tables output from ArcGIS, exported from the created models, corresponding to the boundary centroids and their grouping can be imported into Matlab as matrix variables. These variables are some of the required inputs for the developed Matlab code that applies the developed logit formulas.

Applying the Logit Formulation

To apply the logit formulation outlined in Chapter 4 and automate the process of evaluating trips between representative megacentroids, Matlab was used. A series of scripts were written using the software to evaluate ODT combinations and redistribute demand based on changes to internal travel times between base and impact scenarios. These codes complete successive algorithms that process data imported from ArcGIS, VISTA, and JavaScript code outputs. It should be noted that adjustments are only made with respect to external-to-external and external-to-internal trips. Trips originating inside the subnetwork and subsequent modifications to the demand were not assessed because these trips can be accounted for directly by the subnetwork model.

For external-to-external trips, the applied logit model is used to estimate a change in proportion of users that choose to traverse or bypass the subnetwork due to variations in internal travel times. These travel time changes can also be used to determine if a specific entry point (boundary centroid) becomes more or less appealing, and can then be used to

adjust the boundary demand for external-to-internal trips. To provide these assessments, the centroid grouping tables are required from ArcGIS and demand and travel time information must be extracted from VISTA.

To analyze representative O-D pairs for each time interval, the logit methodology requires one run of the full network and two runs of the subnetwork in VISTA. The full network run is for the base scenario and is used to establish external travel times, as well as demand proportions extracted for the subnetwork boundary centroids. Once this has been completed, a subnetwork model is also run under base conditions to produce internal travel times for the given proportional splits along the subnetwork boundary. The second subnetwork run incorporates the proposed modifications to the network, providing new internal travel times for the impact scenario. These new travel times are then used to adjust demand along the subnetwork boundary using the logit formulas.

Essentially, VISTA data are used to generate most of the inputs for the logit code created in Matlab. This includes the subnetwork's dynamic O-D table, as extracted from the full network base model, along with the full network's dynamic O-D table for the base scenario. These files are exported directly from tables available for download in the VISTA GUI for these respective networks. An example of one of these demand outputs is provided in Table 5.10.

Table 5.10 Sample Dynamic O-D Table Exported from VISTA

Demand ID	Vehicle Type	Origin ID	Destination ID	Demand (veh)	Time Period
1	1	162668	255711	9	0
1	1	162668	255711	2	1
1	1	162668	200404	14	2
1	1	162668	200405	4	6
1	1	162668	200404	14	3
1	1	162668	200405	2	7
1	1	162668	200404	31	0
1	1	162668	200405	7	4
1	1	162668	200404	18	1
1	1	162668	200405	7	5

In addition to the demand, the travel time information necessary to compile the travel time input components is also required. These inputs include external-to-boundary, boundary-to-boundary, and boundary-to-external travel time components for traversing trips (see left side of Figure 4.13 on page 123), as well as external-to-external (bypassing) travel times for the external-to-external logit formula derived in Chapter 4. Additionally, the external-to-internal trip evaluation requires external (external-to-boundary) and internal travel time components (see right side of Figure 4.13). Therefore, the code requires the external-to-internal demand/travel time information used in the centroid grouping process described in the previous section. It also requires representative external-to-external (bypass), boundary-to-external, and internal travel times (boundary-to-internal and/or boundary-to-boundary).

The internal travel times are extracted directly from the VISTA subnetwork model outputs produced from running the base and impact scenarios, similarly to the base demand tables identified earlier. This is done using the following SQL query in the VISTA GUI:

Command:

select a.origin, a.dest, ast, avg(sim_exittime-sim_departure) as average_tt_sec, count (*) as volume from vehicle_path a, vehicle_path_time b, demand c where b.sim_path=a.id and c.id=b.id and a.origin>=150000 group by a.origin, a.dest, ast

The above command specifically compiles volumes and average travel times (in seconds) for trips originating at a boundary centroid (ID greater than or equal to 150,000) and groups them by origin, destination, and time period (departure interval). The resulting table is saved for import into Matlab.

The boundary-to-external component and external-to-external (bypassing) travel times are compiled using developed JavaScript codes similarly to the one for the external-to-boundary demand/travel times identified earlier. The scripts also use VISTA files for the full network's centroids and vehicle trajectory output data, along with the subnetwork's link details table, as inputs. Outputs from all of these scripts are text files that can be directly imported into Matlab for analysis. For the boundary-to-external script, the process again involves investigating individual vehicle paths identified in the vehicle trajectory output file.

This file is processed by the script to determine if, at any time, a vehicle exits the subnetwork along its path. If a vehicle exits the subnetwork, the script begins storing the vehicle's external travel time. This time is cumulated until the vehicle reaches its destination. Vehicles that exit and re-enter the subnetwork are ignored. Average travel times between boundary centroids and external destinations are compiled and stored, along with the number of vehicles contributing to the calculation for each time period. The flow chart shown in Figure 5.26 illustrates the algorithm from which the script was built.

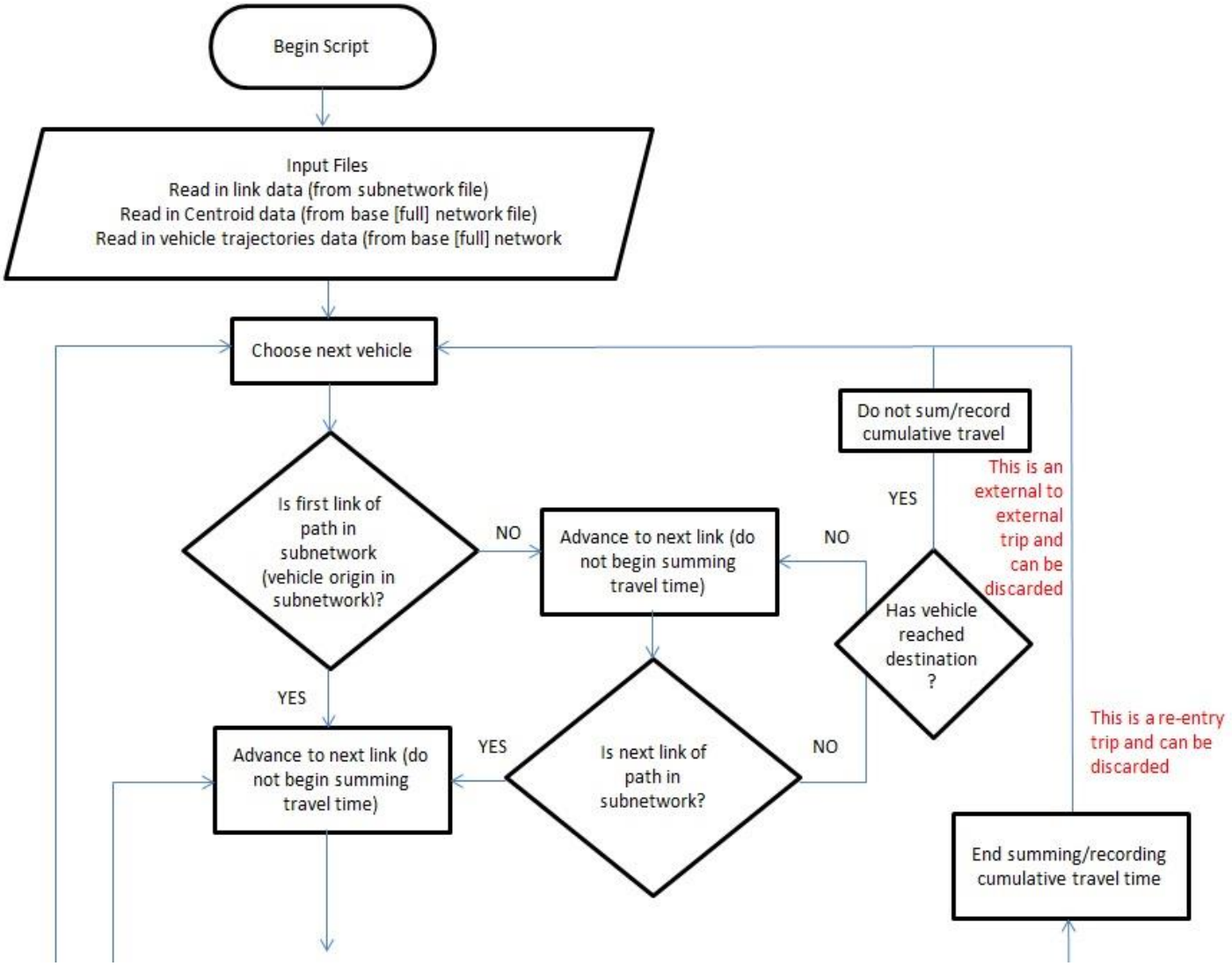

Figure 5.26 Flow Chart of Algorithm Used for Boundary-to-External Travel Time Script

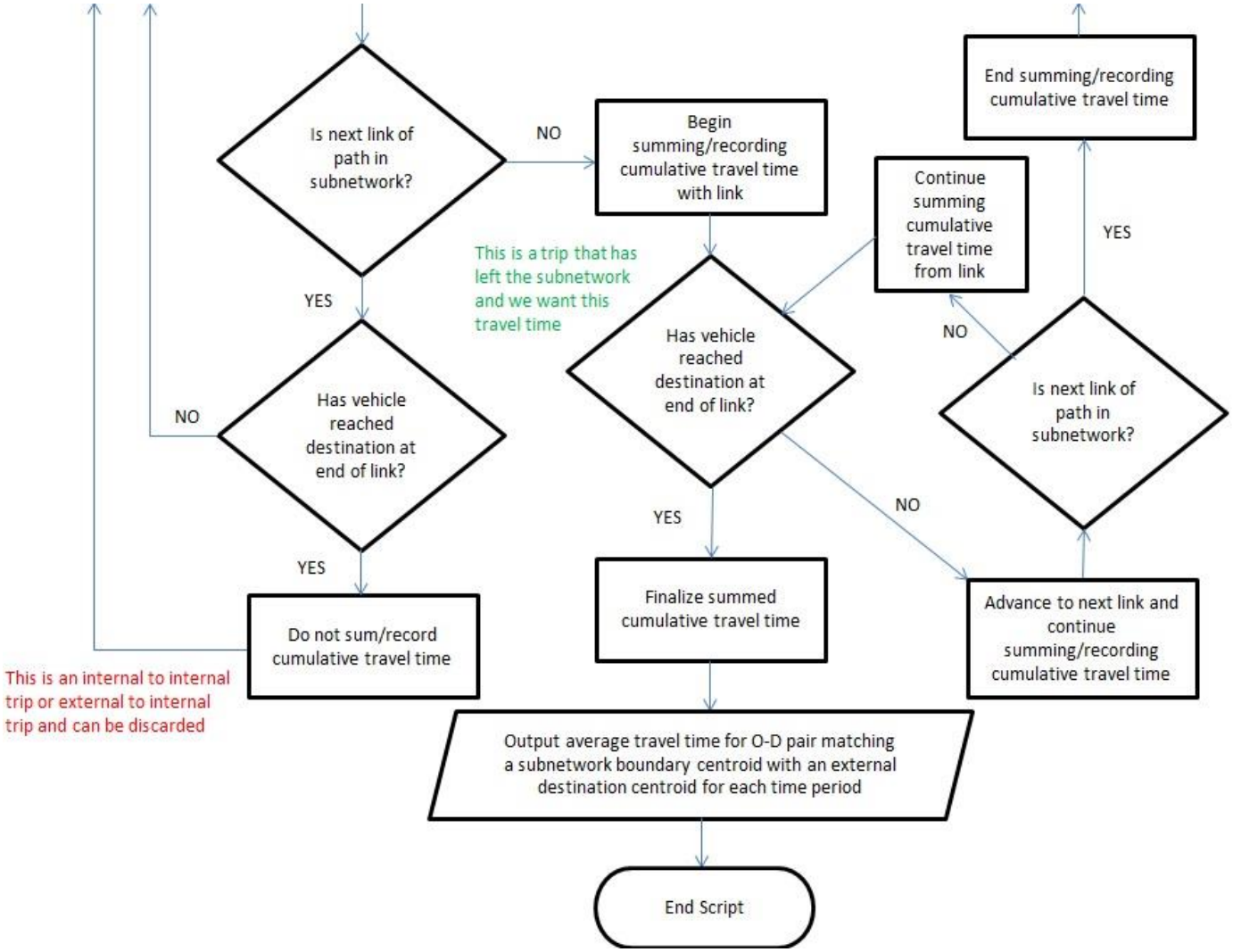

Figure 5.26 (Continued) Flow Chart of Algorithm Used for Boundary-to-External Travel Time Script

For the external-to-external bypassing travel time script, the vehicle trajectory information is processed in a similar manner. The first step is to determine if a vehicle begins its trip in the subnetwork. If so, the vehicle is traveling on an internal-to-external or internal-to-internal path and is subsequently ignored. If a vehicle begins its trip outside of the subnetwork, the script stores the travel time beginning with the first traversed link. The script flags the vehicle and monitors it to determine if at any time it enters the subnetwork. If it does, the vehicle and travel time for that trip is ignored. Vehicles that never enter the subnetwork are stored along with their cumulative trip travel times. The subsequent output is organized to provide the demand and average travel time for each external O-D pair and time period. The algorithm used to create this script is shown in Figure 5.27.

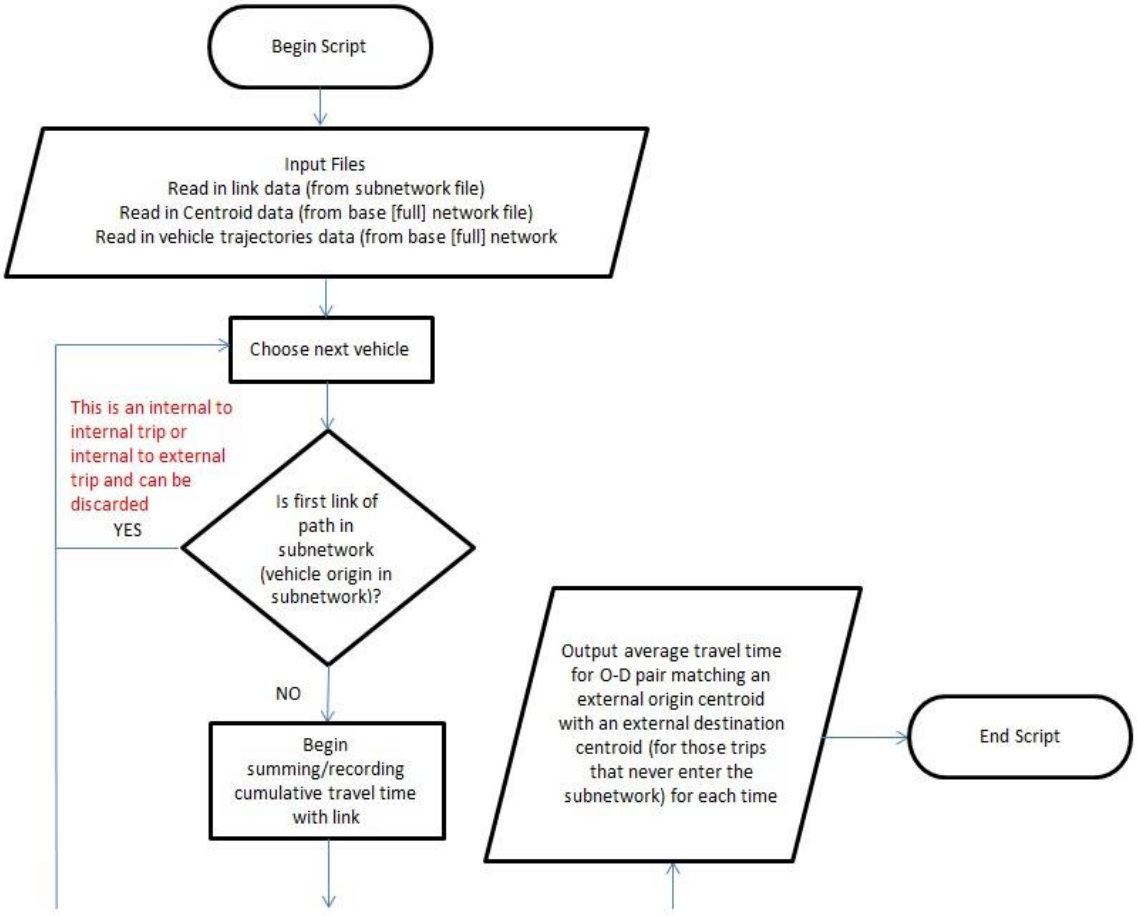

Figure 5.27 Flow Chart of Algorithm Used for Bypassing Travel Time Script

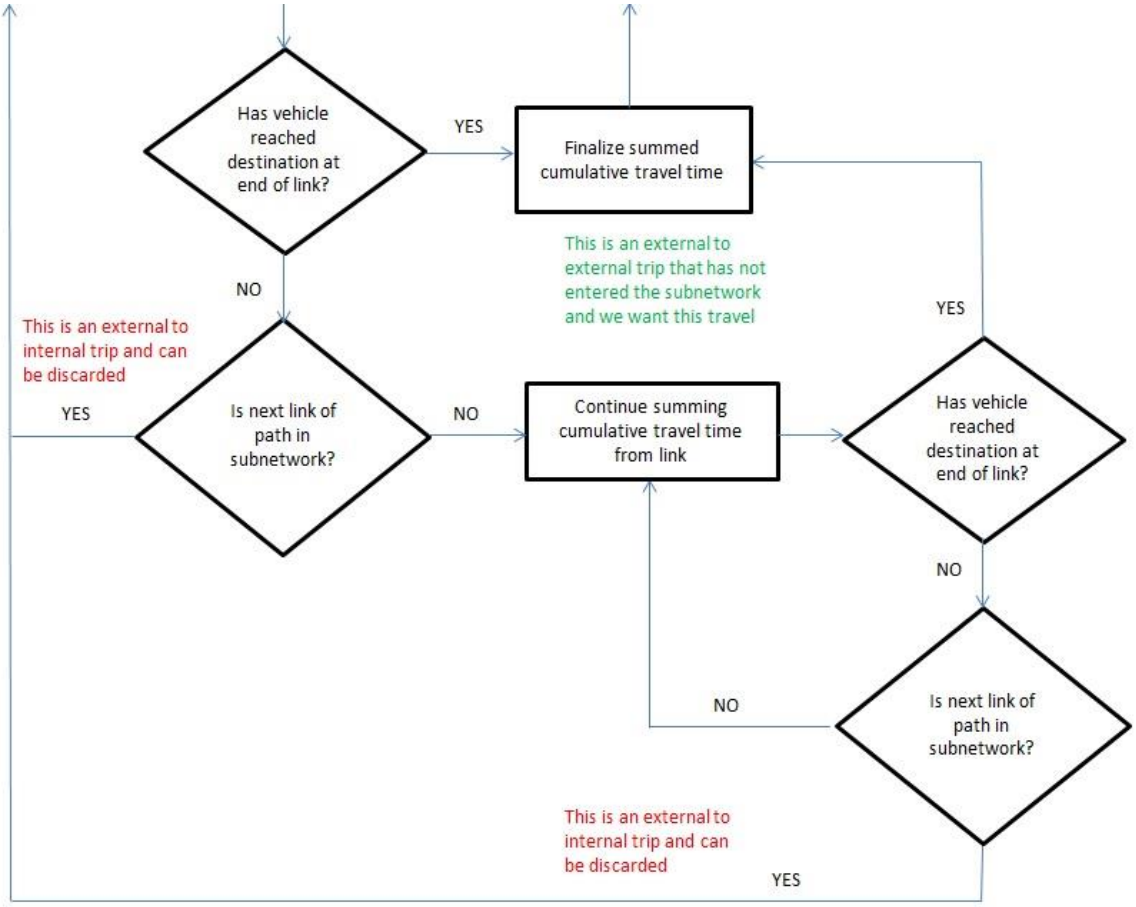

Figure 5.27 (Continued) Flow Chart of Algorithm Used for Bypassing Travel Time Script

The output files for both scripts are formatted similar to that shown in Table 5.7 on page 170. Even though the files are in text format, Matlab has the capability to read them in as inputs and reformat them accordingly. This involves storing the origin, destination, time period, average travel time, and demand data in matrix format. In fact, all of the input files can be stored as matrices to provide a consistent data format for manipulation by the code. This includes the output files for the centroid grouping process completed using ArcGIS. The grouping file is comma delimited and imported into Matlab with columns for x-coordinate, y-coordinate, (boundary) centroid ID, and group ID. An example of one of these files in the format necessary for input in Matlab is provided in Figure 5.28.

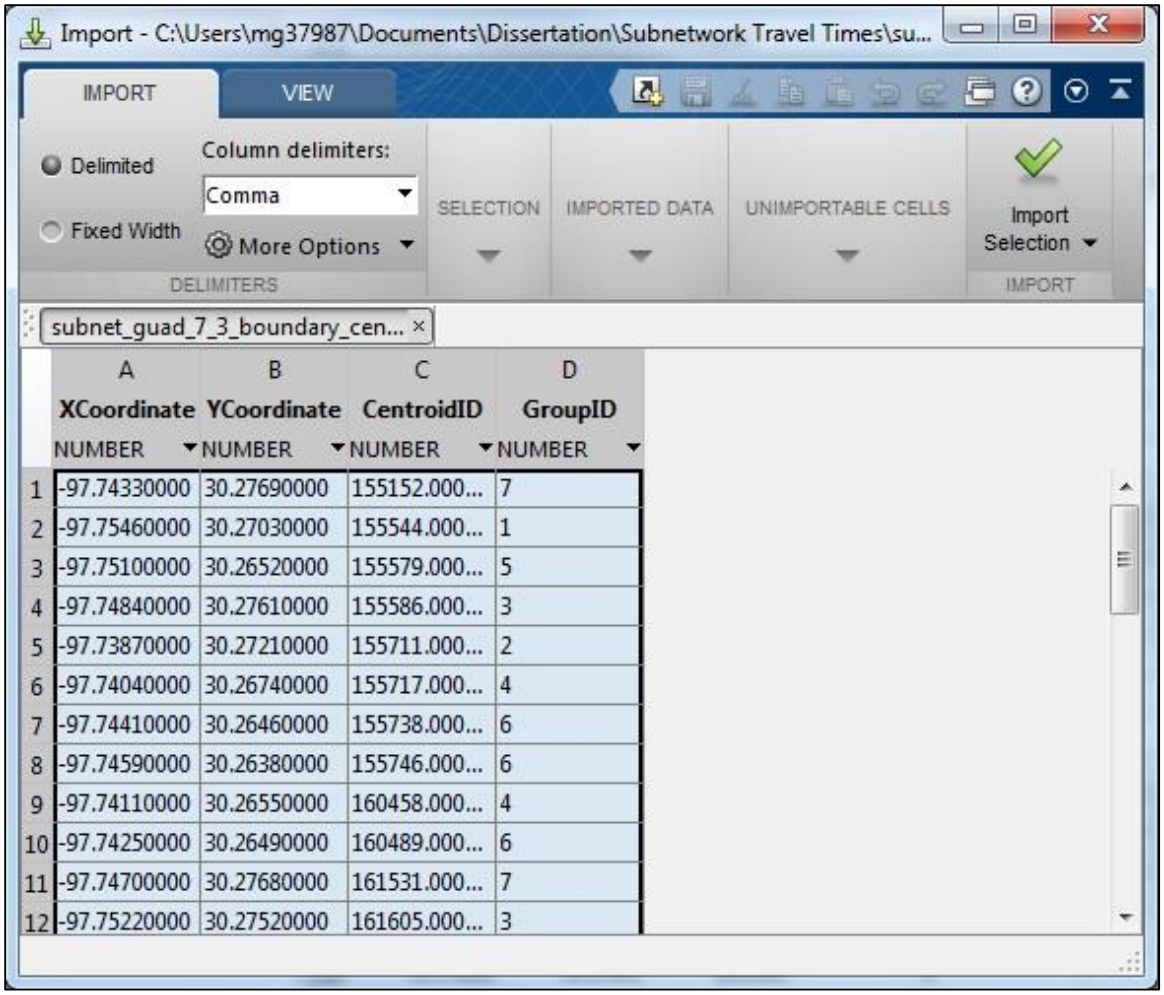

Figure 5.28 Importing Grouping File for Use in Matlab

To apply the logit formulas in Matlab and perform the demand adjustments, two scripts were created, one for the external-to-external trip assessment and another for external-to-internal trips. The developed scripts are designed to run sequentially with the external-to-external demand adjustment performed first. As such, the second script is coded to read in the output from the former.

For the script completing the first demand adjustment based on external-to-external trips, the following tabular variables are required as inputs:

- Boundary Centroids with Grouping IDs (Exported from ArcGIS)
- Full Network Centroids with Grouping IDs (optional for use when grouping based on regions) (Exported from ArcGIS)
- Full Network (Base) Dynamic O-D Table (Exported from VISTA)
- Subnetwork (Base) Dynamic O-D Table (Exported from VISTA)
- External-to-Boundary ODT Demands/Travel Times (Exported from VISTA via JavaScript code)
- Boundary-to-External ODT Demands/Travel Times (Exported from VISTA via JavaScript code)
- External-to-External Bypassing ODT Demands/Travel Times (Exported from VISTA via JavaScript code)
- Subnetwork (Base) Internal Demands/Travel Times (Exported from VISTA)
- Subnetwork (Impact) Internal Demands/Travel Times (Exported from VISTA)

The external-to-external Matlab code performs a detailed array of tasks to compile the imported data and apply the logit formulas. The following provides a summary list of the steps performed by the code:

1) The boundary centroids, both origins and destinations, are separated into their respective groups based on the provided group ID
2) The full network centroids are grouped based on the boundary centroid grouping [Option 1) external centroid IDs contributing demand to a boundary centroid within a group are given the same group designation or, Option 2) based on geographic location (i.e. region ID as imported from ArcGIS)]
3) The full network dynamic O-D table is reduced to only those ODT combinations involving external origins
4) A two-dimensional “external” matrix is created and populated with ODT combinations with origins matching a specific, chosen group number (iterated over all groups)

5) A three-dimensional "internal" matrix is created to store ODT combinations for each boundary centroid grouping
6) Each page (3rd dimension) of the "internal" matrix represented by an individual group is populated with entries from the subnetwork dynamic O-D table that match boundary centroids for that group
7) External-to-external bypassing travel times are compiled for ODT combinations matching those found in the "external" matrix
8) Representative external-to-external travel times between groups, or megacentroids, are determined by computing an average travel time across origins from one group to destinations in another group weighted by demand (from the external-to-external bypassing demand/travel time input)
9) Representative external-to-boundary travel times from a megacentroid to its associated boundary group are determined using a weighted (by demand) average travel time compiled across the grouped external and boundary centroids (from the external-to-boundary demand/travel time input)
10) Representative boundary-to-boundary (internal) travel times between boundary groups is determined using a weighted (by demand) average travel time for both the base and impact scenario (from the internal demand/travel time inputs)
11) Representative boundary-to-external travel times from a boundary group to an associated megacentroid are determined using a weighted (by demand) average travel time across the grouped boundary and external centroids (from the boundary-to-external demand/travel time input)
12) External-to-boundary, internal, and boundary-to-external travel times for an origin group are summed for each applicable destination group compiling a total traversing travel time for both the base and impact scenario and then matched with representative bypassing travel times for the same ODT combination
13) The total traversing and bypassing demand between external megacentroids is determined, along with the representative proportions for each

14) The binary logit formula for the external-to-external demand adjustment is applied:
    a) A check is made and any ODT combination missing a travel time component is not considered for possible demand adjustment
    b) A nested solver is used to calculate a sensitivity parameter for each passing ODT combination using the base traversing travel time versus the bypassing travel time and the associated demand proportions using the logit formula
    c) The sensitivity parameter is evaluated and ODT combinations resulting in negative values are not considered for possible demand adjustment (counterintuitive result)
    d) The logit formula is used again for ODT combinations with a positive sensitivity parameter; this value along with the impact traversing travel time is input to determine an adjusted demand proportion
    e) The traversing demand proportion is multiplied by the total demand for the external megacentroid ODT combination to provide an adjusted traversing demand; those ineligible for adjustment retain their original demand value
15) The boundary centroids within each grouping are evaluated to determine the proportion of the traversing demand that each contributes for a representative ODT combination (i.e. the composition of the boundary group to boundary group demand is assessed to determine how much each individual boundary centroid is contributing)
16) This centroid demand proportion is multiplied by the updated (where applicable) total traversing demand to calculate the adjusted demand for an individual centroid

The above process is iterated across each group and a final subnetwork OD table is produced with both the original and adjusted demand provided for comparison. Rather

than using a single centroid, the model is applied to a representative cluster so resultant changes to the demand are assessed across all boundary centroids contained in a group consistent with the proportion of demand that each contributes to the group. For example, if the logit formula resulted in a change in demand of five vehicles across a group of centroids and an individual centroid contributes 20 percent of the group's demand for a particular departure time interval, then the demand would be adjusted by one vehicle for that individual centroid.

Even though the boundary demand is updated after each iteration, extracting the demand proportions contributed by each centroid when making the adjustments effectively fixes the demand representation within a group across all iterations, regardless of whether the original or an adjusted demand value is applied. This ensures that subsequent adjustments are made appropriately, without bias to earlier adjustments. The corresponding Matlab code for the external-to-external demand adjustment is provided in Appendix B.

For the script completing the second demand adjustment based on external-to-internal trips, the following tabular variables are required as inputs:

- Boundary Centroids by Group (resulting from the external-to-external script)
- Full Network Centroids by Group (resulting from the external-to-external script)
- Adjusted Subnetwork Dynamic O-D Table (resulting from the external-to-external script)
- External-to-Boundary ODT Demands/Travel Times (Exported from VISTA via JavaScript code)
- Subnetwork (Base) Internal Demands/Travel Times (Exported from VISTA)
- Subnetwork (Impact) Internal Demands/Travel Times (Exported from VISTA)

The external-to-internal Matlab code performs a separate list of tasks to compile both the imported data and output from the external-to-external demand adjustment script and

applies its own logit formula and adjustment. The following provides a summary list of the steps performed by the code (see Appendix B for Matlab code):

1) A three-dimensional "internal" matrix is created to store ODT combinations for each boundary centroid grouping
2) Each page (3rd dimension) of the "internal" matrix represented by an individual group is populated with entries from the adjusted subnetwork dynamic O-D table that match boundary centroids for that group
3) The ODT combinations for a boundary centroid group are sorted by subnetwork destination and those with only one boundary origin are removed (no competing demand/travel time is available to compare)
4) The proportion of the demand for each destination attributable to each boundary origin within the grouping is calculated and stored
5) Representative external-to-boundary (external component) travel times to the chosen boundary centroid grouping from its associated external megacentroid are determined using a weighted (by demand) average travel time compiled across the grouped external and boundary centroids (from the external-to-boundary demand/travel time input)
6) Representative external component travel times are combined with internal travel times between boundary origins and respective subnetwork destinations to form total external-to-internal travel times for both the base and impact scenario (from the internal demand/travel time inputs)
7) The binary logit formula for the external-to-internal demand adjustment is applied (iterated over each destination and time period):
    a) A check is made and any ODT combination missing a travel time component is not considered for possible demand adjustment
    b) For a destination and time period, a list of associated boundary origins is extracted

c) A pairwise comparison of each boundary origin to every other boundary origin in the list is performed:
    i) The total demand is calculated for each boundary centroid pairing
    ii) The contributing demand proportion for each boundary centroid is computed
    iii) A nested solver is used to calculate a sensitivity parameter for each boundary origin using its base travel time and associated demand proportion versus the travel time and the associated demand proportion for each and every other paired boundary origin using the logit formula
    iv) The pair producing the largest sensitivity parameter (representing the highest sensitivity to travel time changes) is selected
    v) The logit formula is used again for the selected boundary origins by inputting the associated sensitivity parameter and impact travel times to determine adjusted demand proportions for the two origins
    vi) The new demand proportion is multiplied by the total demand for the two boundary centroids to provide an adjusted demand

8) The process is repeated for each destination and time period for a specific boundary origin grouping

The above process is iterated across each group and a subnetwork O-D table is produced with only the final, adjusted demand. This table can be exported to a text file and imported into VISTA for DTA analysis.

Implementation of the logit methodology was evaluated using a sample case study selected from the test scenarios discussed earlier. The corridor selected for the network modification was Guadalupe Street and the chosen test scenario involved closing three roadway segments between 6th Street and 9th Street (100 percent capacity reduction). The

case study involved testing a relatively small subnetwork, consistent with a connected order of five, such that perceptible changes along the boundary would occur.

With the logit model formulas and software processes in place, the demand adjustment along the boundary of the subnetwork was assessed. The demand adjustment analysis included evaluation of the scenario using several variations of the centroid grouping strategies to determine which combination provided the most accurate demand adjustments. The demand adjustments resulting from the proposed process were evaluated with respect to the demand extracted from a full network model for the impact scenario. Therefore, the full network impact scenario model is used as the baseline for the analysis.

It was speculated that a network modification as severe as the one on Guadalupe Street would result in a decrease in overall subnetwork demand (at the size used in this study) as a result of route diversions, but a preliminary investigation revealed that the total demand for the subnetwork increased. Further examination revealed that the subnetwork "demand" was larger for the impact scenario due to an increase in the number of vehicles re-entering along the boundary. This is likely due to traffic moving away from the modified links and closer to the boundary, resulting in more flow fluctuation in its vicinity.

Since the boundary demand is extracted from the full network traffic flow, each time a vehicle re-enters, it is recorded as an individual trip. Therefore, the demand table originally assessed represented the total number of trips traversing the subnetwork, not the distinct number of vehicles. To better assess the true demand for the subnetwork, the JavaScript code used to compile the subnetwork boundary demand was modified to extract vehicles only once, recording their first entry point and their final destination. This way, the demand could be more adequately compared between base and impact conditions.

Assessing the difference in demand revealed that 677 less vehicles were using the subnetwork in the impact scenario, a decrease of approximately 3 percent. The modified demand tables revealed that the adjustment strategy also resulted in a decrease in demand regardless of the method applied. The results for the different variations in applied strategy are provided in Table 5.11.

Table 5.11 Demand Assessment for Guadalupe Street Impact Scenario

Scenario	Boundary Centroid Grouping Strategy	External Centroid Grouping Strategy	Total Demand	Total Demand Error	RMSE	
					Complete Subnetwork Demand Table	Boundary Origins Only
Impact	-		22,536	-	-	-
Base	-		23,213	3.0%	12.61	13.05
Ext to Ext Only	Demand Proportion	Boundary Centroids	22,757	1.0%	12.07	12.06
Ext to Int Only					12.61	13.05
Both					12.06	12.04
Ext to Ext Only	Max Demand	Boundary Centroids	22,713	0.8%	12.05	12.02
Ext to Int Only					12.61	13.05
Both					12.04	12.01
Ext to Ext Only	Max Demand	Region	23,034	2.2%	12.43	12.73
Ext to Int Only					12.64	13.10
Both					12.46	12.78
Ext to Ext Only	Region	Region	22,994	2.0%	12.18	12.27
Ext to Int Only					12.45	12.77
Both					12.10	12.12

The table provides an assessment of the total demand for each scenario, the error relative to the demand extracted from the impact scenario (full network), and the RMSE for both the complete subnetwork demand table and the boundary origin demand only. The RMSE was calculated to collectively compare each ODT combination in the demand table. Investigating only the boundary origins provides a more explicit evaluation of the candidate ODT pairs. It was used exclusively based on the findings for the subnetwork size evaluation where the RMSE proved to be more useful than the MCAPE or SSIM index.

The results indicate that grouping the boundary centroids based on the origin of contributing demand, and external centroids by the associated boundary centroids, provided the most accurate adjustment (as highlighted in the table). In combination with the external-to-external modification, the external-to-internal demand adjustment appeared to have a more modest effect. When combined, all of the methods resulted in an improved assessment of the overall demand for the subnetwork. Although none of the proposed strategies exhibited substantial improvements in terms of the overall accuracy relative to the impact scenario, the results were promising.

Summary of Demand Adjustment Process Using the Logit Formulation

The strategy for adjusting the demand involves the derivation of appropriate logit models, grouping analysis in ArcGIS, DTA model runs using VISTA, and implementation of the mathematical formulas and computation in Matlab. A summary list of the steps required is provided below:

1) Run full network DTA model in VISTA under base conditions
2) Select subnetwork elements in ArcGIS using specified subnetwork selection tool
3) Extract list of nodes and centroids and list of links and connectors for subnetwork
4) Run JavaScript code to create subnetwork in VISTA
5) Extract demand for subnetwork using JavaScript code from full base model
6) Import base demand and create dynamic O-D table for subnetwork
7) Run selected subnetwork DTA model in VISTA under *base* conditions and extract travel times using VISTA SQL query
8) Run selected subnetwork DTA model in VISTA under *impact* conditions and export travel times using VISTA SQL query
9) Extract external travel times from full network model using developed JavaScript codes (including external-to-boundary, boundary-to-external, and external-to-external bypassing travel times)

10) Group centroids in ArcGIS using developed grouping tool for selected method
11) Extract full network and subnetwork dynamic O-D tables from VISTA database in GUI
12) Import centroid grouping, travel time, and demand information into Matlab
13) Run developed Matlab codes implementing logit formulas to adjust boundary demand

Cognizant of the goal to reduce the time required to complete a subnetwork analysis relative to running a full network model for an impact scenario, the process of interfacing between software programs has been streamlined and numerous within-software functions automated, as discussed, to efficiently implement the proposed methodology. Each of the above steps, with the exception of running the full model, requires mere minutes to complete. This is opposed to re-running the full model, which may take many hours or days to reach an acceptable level of convergence.

Presentation of Results

Once the analysis methodology has been implemented, subnetworks have been selected, and DTA models have been processed appropriately, the results can be assembled and analyzed. This includes taking model outputs and compiling results for evaluating subnetwork sizes and demand adjustments across multiple scenarios, as well as interfacing with other software programs. The following steps provide the basis for using DTA to evaluate the impacts of network modifications on area traffic conditions.

Relevant Outputs for Scenario Comparison

One of the primary purposes of the aforementioned methodology is to compile relevant outputs for comparing the base network conditions with different work zone and construction impact scenarios identified as part of TCPs or other modification scenarios.

With the results obtained from the models, the subnetworks can be analyzed and multiple scenarios evaluated. The following sections detail the process for compiling and analyzing performance measures for network elements.

Network Element Performance Measures

The vehicle trajectory information produced by DTA models can be used to generate a number of resultant performance measures for further evaluation and analysis. The fundamental quantities readily extracted from the model are volume and average travel time for a link or path over a specified time interval. These values, along with individual link attributes, can be used to calculate a number of additional performance measures, including speed, density, and flow rate.

The following process outlines the steps necessary to obtain link volumes and average travel times for a specified time interval from the DTA model results. The methods for extracting these quantities require use of scripts created by CTR that extract vehicle trajectory data from the VISTA output file. One script executed after running the DTA model is used to obtain the link volume and volume-to-capacity (V/C) ratio. This particular script is run to create a function, called "compute_v_over_c", within the network database. The resultant function can be called using a query within VISTA and is used to output the following information:

- Link ID
- Start time, in seconds, from the beginning of the simulation at which the code begins compiling output information
- End time, in seconds, from the beginning of the simulation at which the code stops compiling output information
- Link volume
- Link V/C

The function produces output data for all links in the network organized by link ID. The query used to call the function requires the user to input the time interval over which to aggregate the output data, start time, and end time, as demonstrated with the command line shown below:

select * from compute_v_over_c (*aggregation*, *start_time*, *end_time*)

To extract the link travel time information, a JavaScript code can be copied into the folder where the network outputs are stored. The next step is to make user-specified edits to the JavaScript code to ensure the desired values are generated. Before compiling the code, the user can make edits to the code that specifies the following:

- Start time
- End time
- Aggregation: length, in seconds, of the individual periods in which the data will be compiled and output
- Input file name: the DTA model output file name with the vehicle trajectory information
- Output file name: the specified name of the text file where the data for link travel times will be stored

The output text file contains information identifying each link ID, along with the associated period's begin and end time, vehicle volume over which the time was estimated, average travel time, and turning movement volume and average travel times for each movement, including destination link IDs. Table 5.12 provides an example of this output file opened as an Excel spreadsheet.

Table 5.12 Sample from Link Volume and Travel Time Output File

Link ID	From (sec)	To (sec)	Count	Avg TTime (sec)	Dest Link1	Count	Avg TTime (sec)	Dest Link2	Count	Avg TTime (sec)
2	3600	7200	1377	27.65	18	1377	27.65			
3	3600	7200	657	32.05	361225	593	30.76	47380	64	43.97
5	3600	7200	157	36.19	7	157	36.19			
6	3600	7200	353	74.77	370078	32	74.25	9	118	74.85
7	3600	7200	159	30.91	370078	14	30.00	9	49	31.10
8	3600	7200	40	48.00	361331	40	48.00			
9	3600	7200	210	49.06	8	23	49.04	47013	146	49.27
13	3600	7200	29	36.00	47408	29	36.00			
14	3600	7200	360	212.45	34	56	211.71	147041	46	211.30
15	3600	7200	126	84.67	47041	122	84.69	370080	4	84.00
17	3600	7200	232	17.51	147385	179	18.97	47352	53	12.57
16	3600	7200	31	18.00	47390	31	18.00			
19	3600	7200	662	114.00	47366	662	114.00			
18	3600	7200	1380	42.00	47375	1380	42.00			
21	3600	7200	87	12.00	47356	87	12.00			
20	3600	7200	146	24.00	59211	146	24.00			
23	3600	7200	151	18.08	21	87	18.00	47394	64	18.19
24	3600	7200	158	18.00	47362	158	18.00			

Those entries with multiple destination links infer the existence of a multi-leg intersection at the downstream end of the link. This information can be used to identify turning movement proportions. The exact output volumes from this script are somewhat arbitrary since they represent only the total number of vehicles over which the average travel time was estimated. Therefore, these vehicles must have completely traversed the link during the compiled time period and is not necessarily a true representation of the number of vehicles on a link. This is the basis for using the above function to provide this output information.

Once link volume and travel time estimates have been compiled for the chosen time period, they can be imported into ArcGIS and joined with a link shapefile attribute table. This requires setting up the Excel spreadsheet, similar to the example above, and

preparing it for import into ArcGIS. For additional evaluation of results, data queries can be entered into VISTA to generate path volumes and travel times. To generate these path measures, grouped by path ID, origin, and destination, the following query is used:

select sim_path,origin,dest,count(*),ast,avg(sim_exittime-sim_departure) as ttime from vehicle_path_time a, demand b where b.id=a.id group by origin,dest,ast,sim_path

This query was developed to select the simulated path, origin, destination, number of vehicles, time period, and calculated average travel time (for each time period) from the output table for the vehicle trajectories, matched with the O-D demand table, and group these values by origin, destination, time period, and simulated path. It should be noted that the time periods, by default, are set to 15-minute intervals in the VISTA models. To compile additional travel time information, the resultant table created using the above query can be downloaded and opened with Excel.

In this file, a new column can be created and titled for a specific time period of interest (e.g. the second hour of simulation). This can be called “Average TT Hour 2” or similar. It is necessary to then sort the spreadsheet by Path ID. Next, the following formula (shown here with generic cell entries) can be entered into the first cell under the new column header:

=IF(*sim_pathcell=sim_pathcell*,AVERAGEIFS(*ttimecolumn, sim_pathcolumn,sim_pathcell,astcolumn*,"*>lowerlimitperiod*", *astcolumn*,"*<upperlimitperiod*"))

The lower-limit period identified in the formula should coincide with the beginning 15-minute period of the range of time one wants to collect average travel time information for (i.e. 0 = first 15 min, 1 = second 15 min, etc.) and the upper-limit period should coincide with the last period of that range. For example, setting the lower-limit entry to

“>3” and the upper-limit to “<8”, the formula will average the travel time between the fourth and seventh periods, or between one hour and two hours into the simulation.

With the formula entered to average the path travel time over the appropriate interval, the formula can be extended to cover all rows of the spreadsheet. The user can also filter out the unwanted time periods, and subsequent path IDs that do not have times for the periods of interest to clean up the spreadsheet, if so desired. These results can also be imported into ArcGIS and combined with path attribute tables (from created path shapefiles) for further evaluation.

The outputs, particularly those compiled for individual links, can be used to generate performance measures in order to evaluate network or subnetwork traffic conditions. Based on the HCM 2010, speed is an appropriate automobile performance measure for freeway facilities, basic freeway segments, freeway merge and diverge segments, multilane and two-lane highways, and urban street segments (HCM, 2010). In addition, density is identified as an automobile performance measure for freeway facilities, basic freeway segments, freeway weaving segments, freeway merge and diverge segments, and multilane highways. Therefore, it is important to calculate these measures from DTA outputs to evaluate the results and compare scenarios.

Furthermore, measures of link speed and density can be used to assess the LOS of these network elements. This can be done by calculating speed ratios of average speed versus free-flow speed for urban streets and densities for freeway segments, specifically for each link, and comparing them to the A-F scales provided in tables for each roadway classification in the HCM 2010. For reference, these LOS scales are provided for the two types of roadways most commonly encountered in the Austin downtown network, urban streets and weaving (merge-diverge) freeway segments, as shown in Tables 5.13 and 5.14.

Table 5.13 Automobile LOS Criteria for Urban Streets (HCM, 2010)

Total speed as a % of base free-flow speed (%)	
% (Range)	LOS
> 85	A
> 67 - 85	B
> 50 - 67	C
> 40 - 50	D
> 30 - 40	E
≤ 30	F

Table 5.14 Automobile LOS Criteria for Weaving (Merge-Diverge) Freeway Segments (HCM, 2010)

Density, pc/mi/ln	LOS
≤ 10	A
> 10 - 20	B
> 20 - 28	C
> 28 - 35	D
> 35 - 45	E
> 45*	F

* Note: LOS F criteria for freeway weaving/merging/diverging segments is specified as v/c > 1; however, since the DTA results will not produce a v/c greater than 1, the criteria for "basic freeway segments" was assumed for the threshold between LOS E and F (density > 45 pc/mi/ln).

For the purpose of evaluating results for the Austin downtown network, all links input in VISTA with a free-flow speed of less than 55 mph have been assumed to be urban streets with the appropriate LOS criteria established. All links with a free-flow speed of 55 mph or more have been assumed to be freeway segments within a weaving area, consistent with conditions along I-35 through the downtown network, with the intent to evaluate them accordingly. It was assumed that none of the segments in the downtown network would be considered basic due to the high number of access points in the area. Figure 5.29 illustrates a portion of I-35 within the downtown network, including the abundance of ramps connecting the mainlanes and frontage roads that contribute to the common occurrence of weaving sections.

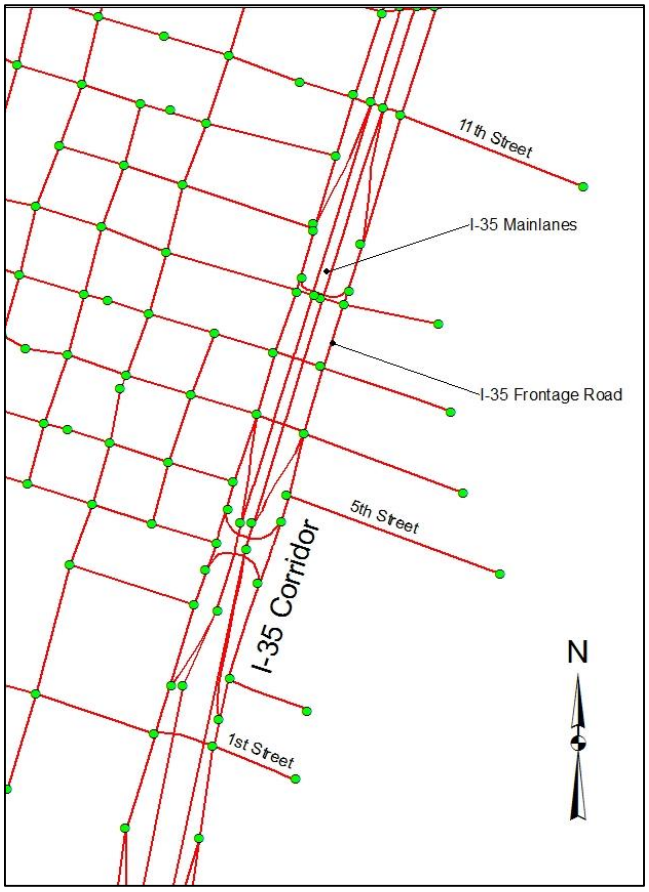

Figure 5.29 I-35 Corridor Within the Downtown Austin Network in ArcGIS

Compiling Results

To compile the performance measures necessary to evaluate network conditions, the VISTA outputs can be imported into ArcGIS to perform the necessary calculations. At this point, it is necessary to determine the simulated link lengths. This is different than the link length reported in the link details table in VISTA. The link details table includes the link length as measured in the field or using appropriate mapping and measurement tools. The simulated length is based on the division of the links into discrete cells (rounded to the nearest integer) for the CTM, and the subsequent sum of all of these individual cell lengths. Since this value is based on rounding the discrete number of cells to the nearest integer, the resultant link length (simulated) may be noticeably different

than the actual link length. The sum of the individual cell lengths is required to provide average link speeds since the resultant simulated link lengths are used in the DTA model's simulation for determining vehicle trajectories via the CTM. The simulated link lengths for all links in the network can be obtained using the following query in VISTA:

select a.id,count(*)*speed*3*5280/60 as sim_length from linkdetails a,celldata b where b.link=a.id group by a.id,a.speed order by a.id

The table created using the above query can be downloaded and saved in Excel format. Then, the simulated link lengths can be imported along with the output link volumes and travel times from the developed scripts, as discussed earlier, into ArcGIS. This can be done by joining the link attribute table (for the link shapefile) in ArcGIS with the created Excel spreadsheets. This is accomplished by matching the respective columns in each database for "Link ID". Once this has been completed, the steps for calculating link speed, density, flow rate, and LOS can be performed using the processes outlined below.

First, the average link speed is calculated based on the average travel time and simulated link length. In the link attribute table in ArcGIS, the first step is to create a new field (column) for average link speed (e.g. "Avg_Speed"). The ArcGIS "Field Calculator" can then be used to perform the necessary calculation for speed (in mph) using the simulated length field and dividing this entry by 5280 to convert feet to miles, then dividing by the travel time column and multiplying by 3600 to convert the denominator from seconds to hours. An example of the command prompt is provided below:

'"austin_links.sim_length"/5280/"austin_links.ttime"*3600'.

The field for average speed will now be populated with the average link speed in miles per hour. Next, the hourly flow rate is calculated in order to derive the link density. This involves creating fields for both attributes (e.g. "Flow_Rate" and "Density"). Similar to

the above process, the “Field Calculator” is used to obtain the quantities for link flow rate and density. To do this, the volume field is multiplied by the number of time periods aggregated in the output file that occur during the course of one hour (e.g. “1” for a one-hour aggregation, “2” for a 30-minute aggregation, etc.), then dividing by the number of lanes field. An example of the command prompt is provided below for a 30-minute aggregation:

’”link_volume$.volume”*2/”austin_links.LANES”’.

The field for flow rate is then populated with the link flow rate in passenger cars per hour per lane (pcphpl) for the link. Next, the field for density can be calculated by dividing the flow rate by speed. This is done using the “Python” script editor by inputting the following code in the box titled “Pre-Logic Script Code:”:

```
def density(flow_rate, speed):
  if speed == 0:
    return 0
  if speed > 0:
    density = (flow_rate/speed)
    return density
```

In the bottom command window, titled “*shapefilename.columnname* =” (e.g. austin_links.Density =”), the following code is entered:

Command:

density(*linkflowratefield*, *averagelinkspeedfield*)

The field for density will now be populated with the link density in passenger cars per mile per lane (pc/mi/ln). The resultant average speed from the DTA model and the free-flow speed for the link can then be used to establish LOS for the links classified as urban streets, and the link density can be used for links classified as freeway segments, based

on the HCM 2010 LOS criteria identified earlier. The link average speed and density can both be calculated in ArcGIS using the above process, and the free-flow speed is already included in the DTA model as part of the link characteristics. Therefore, the free-flow speed field already exists in the link attributes table in ArcGIS.

The first step for obtaining link LOS is to create a text field for the service measure ("LOS"). The field for "LOS" can then be populated using the "Field Calculator" while again using the "Python" script editor by entering the following code:

```
def Level(speed,limit,density):
  ratio = (speed*100/limit)
  if limit<55:
    if ratio>85:
      return 'A'
    elif ratio>67 and ratio<=85:
      return 'B'
    elif ratio>50 and ratio<=67:
      return 'C'
    elif ratio>40 and ratio<=50:
      return 'D'
    elif ratio>30 and ratio<=40:
      return 'E'
    elif ratio<=30:
      return 'F'
  else:
    if density <=10:
      return 'A'
    elif density >10 and density <=20:
      return 'B'
    elif density >20 and density <=28:
      return 'C'
    elif density >28 and density <=35:
      return 'D'
    elif density >35 and density <=45:
      return 'E'
    else:
      return 'F'
```

This above code is used to establish the LOS rating for each link based on the criteria provided in the HCM 2010. Again, links with free-flow speeds less than 55 mph are assumed to be urban streets, with those at or above 55 mph classified as freeway sections. The code includes a threshold check based on the free-flow speed column value in order to make the distinction between which criteria to use. This threshold can be modified in the above code by changing the defined "limit", if deemed necessary. In the bottom command window, titled "*shapefilename.columnname* =" (e.g. austin_links.LOS ="), the following code is entered:

Command:

Level(*averagelinkspeedfield*, *linkspeedlimitfield*, *linkdensityfield*)

The field for LOS will now be populated with the appropriate letter rating based on the corresponding A-F scale presented in the HCM 2010 and in Tables 5.13 and 5.14 on page 220. Figure 5.30 shows a screenshot from ArcGIS depicting the link attribute table with the performance measures calculated.

LINKID	SPEED_MPH	CAPACITY	LANES	sim_length	count	SPEED	DENSITY	FLOWRATE	LOS
5124	45	1800	2	792	176	45	2.011111	90.5	A
5125	35	1500	2	307.999832	172	15.968161	5.385717	86	D
5126	45	1800	1	792	262	41.048159	7.844444	322	A
5129	45	1800	2	594	438	38.891753	6.466667	251.5	A
5134	45	1800	3	396	114	45	1	54	A
5136	35	1200	4	307.999832	424	14.56375	6.385718	93	D
5138	30	1300	2	396	221	19.47408	7.394444	144	C
5139	30	1300	4	264	147	19.830508	1.966667	39	C
5140	30	1100	3	396	250	13.074324	8.77037	114.666667	D
5145	40	1500	3	528.000252	232	40.000019	1.633333	65.333333	A
5146	40	1500	4	352.000168	873	9.969295	19.334366	192.75	F
5148	35	1200	4	307.999832	619	11.401732	12.739293	145.25	E
5149	35	1200	4	307.999832	339	8.102989	8.11429	65.75	F
5150	40	1500	1	704.000336	451	18.707458	25.337488	474	D
5153	40	1500	1	352.000168	376	36.963714	7.574996	280	A
5158	65	2300	3	1143.996517	1490	64.999802	6.953867	452	A
5159	45	1800	1	792	520	42.793087	11.894444	509	A
5165	30	1300	4	264	318	30	2	83	A

Figure 5.30 Sample from the Link Attributes Table with Calculated Performance Measures in ArcGIS

Additional link and network performance measures can be calculated using a similar method to the one outlined above. Once all of the desired performance measures are calculated and organized, the next step is to run other network or subnetwork models to create additional outputs for different impact scenarios. Once these model outputs are extracted and imported into ArcGIS, along with the performance measures calculated for evaluation, the results can be compared between the base and impact conditions.

This is done by first completing simple calculations in ArcGIS, such as travel time, volume, and density differences for the links in the network. Once fields have been populated with these differentials, the shapefiles can be created with an appropriate symbology for identifying network links by their attribute values. This can be accomplished using symbology representative of different volume and travel time ranges or LOS values. This is very helpful for identifying links in the network that are most impacted by a particular construction project or TCP scenario.

Visualization of Results Using GIS Software

As noted earlier, the VISTA Java-based editor tool can be utilized to create, edit, and visualize network elements in a GIS environment associated with the DTA software. This feature allows the user to select and visually examine individual elements by specific attributes using a query or the selection tool. Simulated vehicles can also be animated over a specified time interval to provide a rough overview of the movement of vehicles through the network. This animation can also be used to visualize the estimated LOS of links throughout the network and how this performance changes with time. Graphs can also be opened in the editor tool to view the change in flow and select performance measures over time for individual links.

While these visual aids are good for examining geometric elements and basic performance measures, the editor tool is limited in its capabilities and doesn't allow the

user to adjust the element symbologies or other display options. However, by exporting the VISTA results into Excel files, one can use this data to create visual elements in GIS software. Once network or subnetwork elements have been created in VISTA, shapefiles can be exported for visualization in ArcGIS. Output tables with volume and average travel time information can then be manipulated in Excel and imported and joined with these shapefiles in ArcGIS. This process was utilized to visualize paths using a specific link, as shown in Figure 4.6 on page 98, as well as to compare DTA model results between scenarios.

When output information has been imported into ArcGIS and joined with the shapefiles, performance measures, such as those described above, can be calculated and compared. For example, travel times for both base and impact conditions can be attached to the link attribute table and the difference calculated in ArcGIS. The new field created with this difference can have a symbology assigned based on the range of recorded values. A color ramp can be used to establish a color coding scheme for changes in travel time that exceed a set of threshold values. Figure 5.31 illustrates this use of symbology.

Figure 5.31 Sample Change in Travel Time Visualization in ArcGIS (Basemap Source: BING © 2010 Microsoft and its Data Suppliers)

In the figure, those travel times that are reduced in the impact scenario or have no change are coded in green, while those that increase are divided into categories of 15 second intervals ranging from yellow to red in color. This provides a useful means of determining where the most critical disruptions in terms of travel time are occurring. A similar methodology can be used to visualize changes in volume, speed, density, LOS and other aforementioned link performance measures. If specific thresholds are established for these performance measures to determine which are performing

substantially worse in the impact scenario, those links can be color coded for ready identification.

It should be noted that since VISTA creates a link for each direction of flow, many roadway segments have two representative links in the shapefile, one on top of the other. Links in the westbound and southbound directions have an ID less than 100,000 (e.g. 18134). Corresponding links in the eastbound and northbound directions have an ID equal to the opposite direction ID plus 100,000 (e.g. 118134). As such, these links have IDs greater than 100,000. Since links in opposite directions have the same endpoint coordinates, they are stacked in the shapefile and directions are difficult to visualize in ArcGIS without some manipulation. To separate the directions, the link shapefile can be split into group layers, one for each set of directions based on the corresponding range of IDs (i.e. one for link IDs less than 100,000 and one for link IDs greater than 100,000).

Once group layers have been created, the appropriate symbology can be applied. Each group layer can have a color ramp established for coding ranges of performance measures, and directional indicators, such as arrows, can be used as line types. Links representing the westbound and southbound directions (with IDs less than 100,000) can be offset by a specified value so that they appear separately from the eastbound and northbound directions, with the arrows pointing in the appropriate direction of flow, as illustrated in Figure 5.31. These layer properties and symbology adjustments are represented in the ArcGIS menus shown in Figure 5.32.

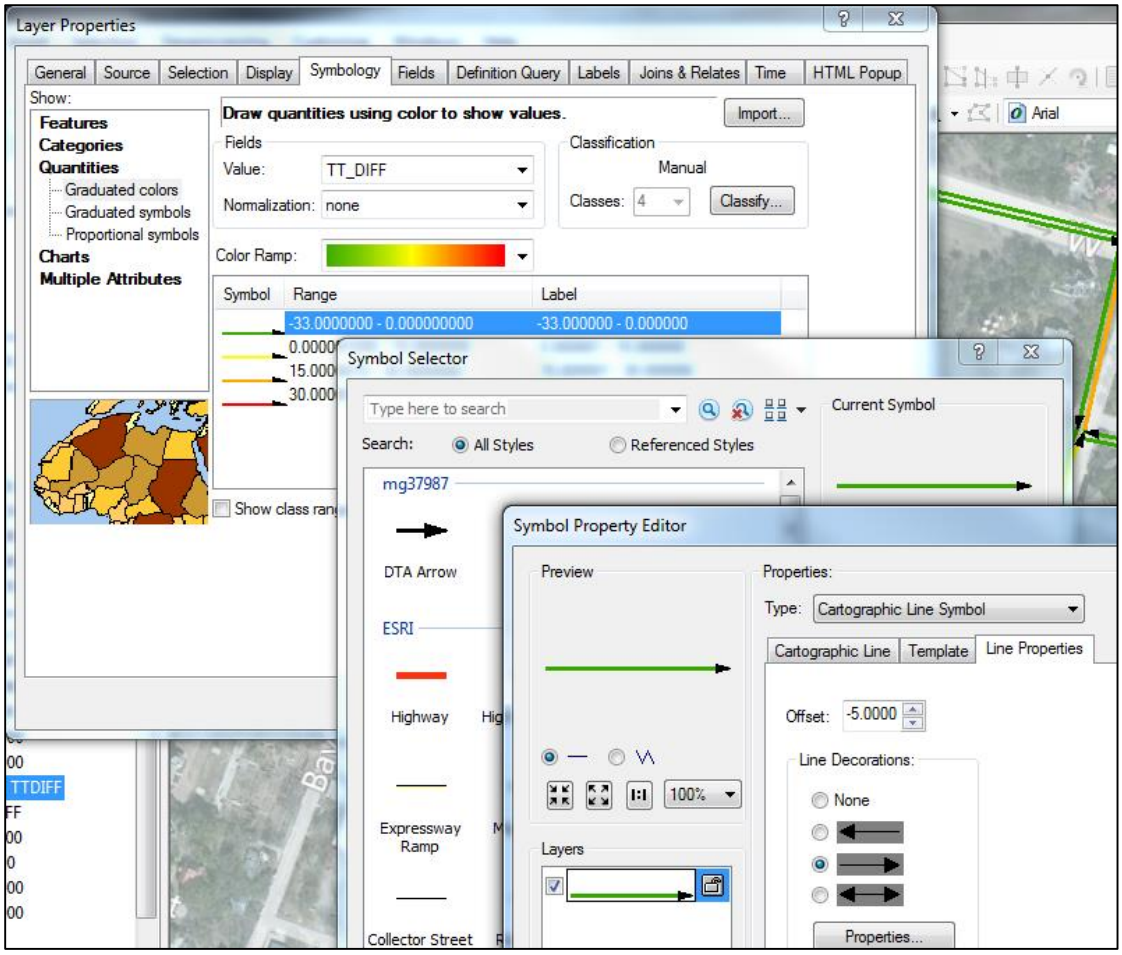

Figure 5.32 Sample Symbology Menus for Line Properties in ArcGIS

Once layers and symbology preferences have been established for one set of performance measures, they can be used for establishing visuals for others. This can be done by copying the shapefiles, selecting the associated field that the symbology is intended to reference, and modifying the thresholds for the color ramp accordingly. Using this process, a number of useful visuals can be efficiently created for evaluating impact scenarios and identifying problem areas.

Importing the DTA outputs from VISTA into ArcGIS also enables one to evaluate results beyond the roadway network. Many planners use GIS software to evaluate the impact of transportation projects on the spatial environment, visualizing transportation elements

relative to different demographics and land uses. Shapefiles representative of these spatial elements can be imported into ArcGIS and used to further evaluate the DTA results. This enables one to investigate not only what roadways are impacted by construction activity, but who is impacted.

There are many possibilities for using ArcGIS to visualize DTA results and evaluate TCPs with respect to a multitude of performance measures and impact scenarios. GIS software enables one to evaluate impacts with respect to the roadway network, as well as the spatial environment. Furthermore, this process demonstrates how VISTA outputs can be used to interface with other software programs and provide tools for planners and engineers alike. Ultimately, the results are utilized for comparing subnetwork sizes, evaluating subnetwork demand estimation (including adjustments), and analyzing relevant performance measures, all necessary for providing a comprehensive and efficient tool used for reviewing TCP or other network modification scenarios. Implementation of the outlined processes for accomplishing these tasks, including the subnetwork analysis of multiple TCP scenarios, is detailed in the following chapter.

6. ANALYSIS RESULTS AND DISCUSSION

Following development and preliminary implementation of the defined methodology, subnetwork analyses were performed on multiple networks. This included using the downtown Austin network as a prototype for additional review of the proposed methodology across a vast array of impact scenarios. A subnetwork analysis was also performed on a regional network to demonstrate the value of evaluating a portion of a much larger network to assess impacts of a network modification as a means of saving time and effort. The trade-offs associated with implementing subnetwork analyses, introduced earlier, are demonstrated by gains in efficiency both computationally and on behalf of the user versus loss of accuracy and coverage relative to use of full network models. The benefits and drawbacks of implementing subnetworks of varying size to analyze network modification scenarios are discussed herein.

The following sections provide results relative to several important objectives, including use of subnetwork analysis to save computational time, space, and effort. The analyses demonstrate large-scale implementation of the described methodology using a number of subnetwork applications. This involved analysis of network modifications to a large regional network, continued evaluation of subnetwork sizes using multiple impact scenarios, and further assessment of demand adjustments using the logit formulation for several of the selected scenarios. The goal of these analyses was to demonstrate the need for using subnetworks to review network modifications, implement and evaluate the proposed methodology, and provide valuable guidance relative to subnetwork selection and analysis.

Dallas-Fort Worth Regional Network Case Study

Implementation of a subnetwork analysis using a large regional network was anticipated to provide consequential results. It was determined that the Dallas-Fort Worth (DFW)

regional network would be a valuable candidate for evaluation. It is much larger and more complex than the Austin downtown or regional networks, and presents some unique challenges in terms of DTA analysis and assessment. Furthermore, it involves implementing a different process for running a DTA model than a smaller regional network or subnetwork. As noted in Chapter 4, using VISTA to perform a DTA analysis on a network of substantial size requires each process, or module, in VISTA to be run independently and manually.

Network Description and Preparation

The DTA model in VISTA for the DFW regional network contains 71,721 links, including 21,414 connectors, and 31,364 nodes, including 10,772 centroids (origin and destination). The network comprises Dallas and Fort Worth, as well as the joining and surrounding suburbs. It spans approximately 115 miles from south to north, encompassing the entire IH 35E and IH 35W freeway sections, and 120 miles from west to east, from US Highway 281 in the west to about 10 miles west of Texas Highway 19 in the east. Figure 6.1 displays a map for the entire DFW regional network.

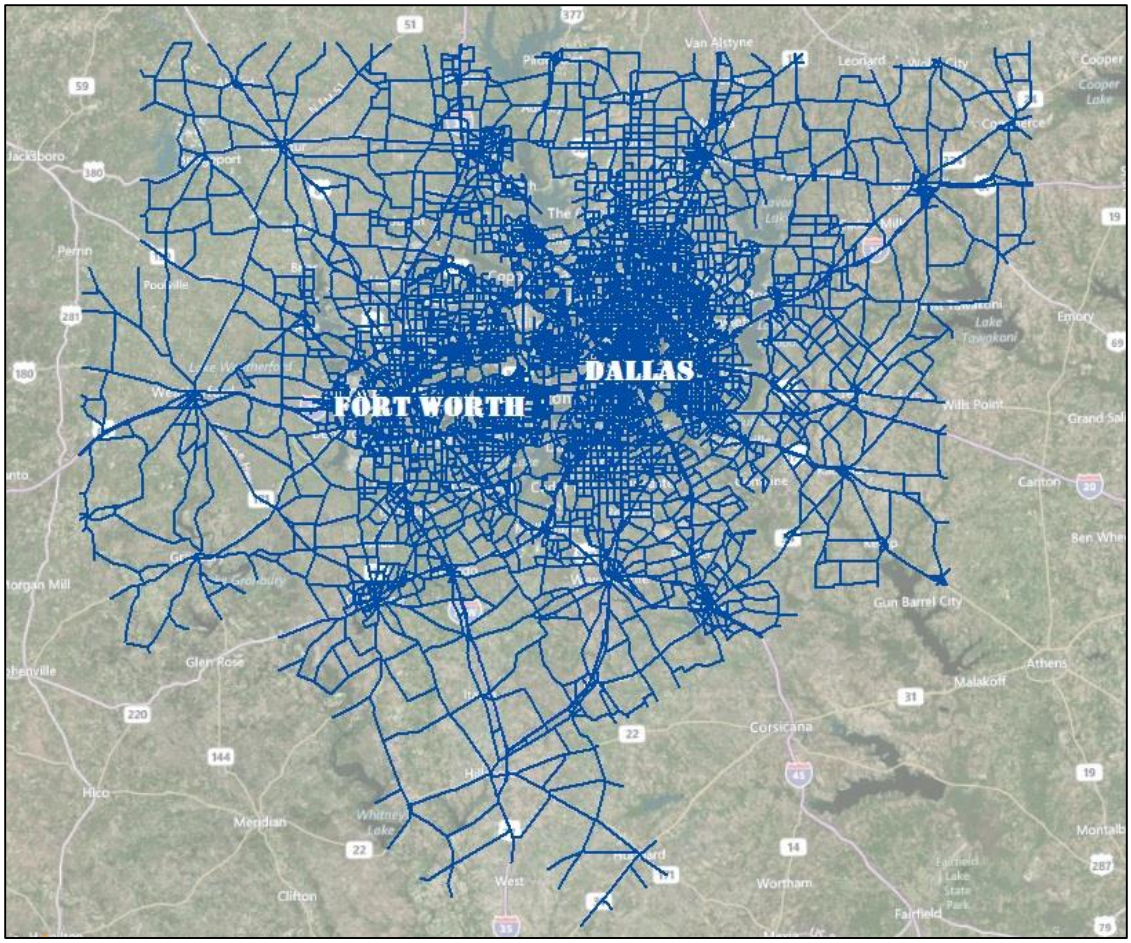

Figure 6.1 Extents of the Dallas-Fort Worth Regional Network (Basemap Source: BING © 2010 Microsoft and its Data Suppliers)

The modules used for manually completing a DTA analysis in VISTA include preparing the network elements and demand, as well as running path generation and dynamic user equilibrium (DUE) processes. The latter two modules are run using inputs for multiple parameters, and are typically completed multiple times in an alternating pattern until an acceptable gap is achieved. This process is initiated using a series of path generation iterations so that multiple paths are created and evaluated between O-D pairs to establish preliminary shortest path sets. These path sets are produced using simplicial decomposition and vehicles are assigned accordingly.

The process continues until the maximum number of iterations input by the user is reached, or no additional path sets can be created that result in lower travel times given the provided parameters. Next, a series of DUE iterations are completed to reassign vehicles across the path sets created by the path generation module in an attempt to improve the gap measure. Vehicles are assigned different paths based on the results of the previous iteration, without creating any new paths, and the resulting travel times are evaluated for subsequent iterations and vehicle assignments. The DUE iterations are completed until the maximum number input by the user is reached or no improvement across the available paths is achieved between subsequent iterations. The module is thus terminated and the resultant gap measure is presented in the software output for each completed iteration.

Another process imperative to a network the size of Dallas-Fort Worth is the identification and evaluation of signalized intersections. While VISTA treats unsignalized intersections using the CTM with priority given to vehicles leaving upstream cells based on the number of entering lanes, signalized intersections function based on input signal timing plans. If the signal timing plans implemented in the field are not available, a signal optimization tool can be applied using a developed JavaScript code.

The script reads a list of nodes identified to represent signalized intersections via text file and evaluates candidate timing plans based on several user inputs, including minimum and maximum cycle length and minimum green time per phase, and allocates green time for each phase proportional to entering volumes from each approach. The optimization tool is typically initiated between runs of the DUE module. It is often run several times during the process to better optimize the signal timing plans for the current assignment based on the most recent DUE iteration. It also helps establish the best possible traffic assignment given the available path sets for successive DUE and path generation module processes.

Review and preparation of the DFW network revealed that the existing model and inputs were outdated. Therefore, the most recent available static O-D table was obtained from the North Central Texas Council of Governments (NCTCOG) planning group, a 2012 version with passenger car and truck trip totals for each O-D pair in the network. As with the original model, the AM peak period trip table was utilized. It was found that the O-D pairs matched those from the existing model and that the centroids from that model were consistent with the updated trip table.

The resulting 2012 demand table was imported into VISTA yielding a total demand for the network of 2,512,462 vehicles. This demand included 2,427,126 cars and 83,636 trucks (approximately 3.3 percent network-wide). It should be noted that the static O-D table contained fractional trip values, including a substantially large number of O-D pairs with less than one trip. Consideration was made to round the trip values in an attempt to reduce to file size and eliminate the O-D pairs with less than 0.5 trips. However, using a conventional rounding method, it was discovered that approximately 1 million total trips were rounded out of the table due in large part to these small values. Since VISTA is able to utilize fractional values input as part of a static O-D table, it was decided to leave the values as-is and rely on VISTA to manipulate the data during creation of a dynamic O-D table.

In order to create the dynamic O-D table, VISTA uses both the static O-D table and a demand profile. The demand profile establishes the distribution of trips in the static O-D table over the time period analyzed in 10-minute intervals. With the lack of detailed information about the demand profile for the DFW network, and given the large scale of the region modeled, likely resulting in distribution patterns varying by location, a simple distribution was chosen. This resulted in an even division of trips over the first two hours of the model run-time (12, 10-minute intervals), representing the AM peak period and the pattern of loading vehicles onto the network utilized by the model.

In addition, VISTA uses a random number generator to round trips to the nearest integer, allowing it to take into account fractions uploaded into the static O-D table. This process randomly chooses a fraction and if that value is larger than the fraction in the table, the value in the table is rounded down to the nearest integer. If the random value is larger, the fraction in the table is rounded up. This process, coupled with a 2-hour demand profile, yielded a dynamic O-D table with approximately 2.51 million vehicles. This number was subsequently utilized due to its consistency with the original total from the NCTCOG trip table.

As part of the effort taken to improve the model, an in-depth review of network elements was performed using ArcGIS. This involved creating shapefiles for the links, nodes, centroids, and centroid connectors for the model. In addition, an updated network shapefile was obtained from NCTCOG to check against the VISTA network shapefiles. It was determined that the existing network in VISTA had relatively good coverage for the region with the exception of a few select areas. A detailed review at several spot-check locations revealed that verifying the network link attributes, including direction, number of lanes, speed limit, and length, would be necessary.

Notably, the TxDOT Dallas District enlisted CTR to utilize the subnetwork analysis process to review a select alternative for a major interstate reconstruction project in the downtown Dallas area. Due to the nature and location of the project scenario, special attention was given to verifying network elements and checking the coverage in the vicinity of the project. Since the alternative was likely to impact freeways and major highways in the Dallas area, these elements were carefully reviewed. Additional detail was provided to include arterial and collector roadways in the vicinity of the project site to account for alternative routes to and from nearby centroid locations.

Furthermore, a review of the treatment of signalized intersections was undertaken. Due to the fact that the DFW model encompasses the jurisdictions of many municipalities and

transportation agencies, signal timing plans have not been obtained for the entire network. Therefore, the JAVA-based signal optimization tool was applied to create the signal timing plans in VISTA, including approximately 3,590 signals throughout the network. The signal optimization was performed after several rounds of path generation and DUE were completed on the network so that reliable approach volumes would be established prior to implementing the timing plans. In addition, several DUE runs were completed after optimization to redistribute vehicles accordingly.

In all, 105 DTA processes were run on three versions of the base model for the DFW region. Fixing connectivity issues with the network, updating demand tables, and trouble-shooting errors required new versions of the network and rerunning processes. Over 1,700 hours of computational time were required, totaling nearly 71 days of run-time. For the final model alone, 32 DTA processes were run requiring approximately 1,000 hours or 42 days of computational time to reach an acceptable level of convergence. This included five path generation processes totaling eight completed iterations, 11 DUE processes totaling 36 completed iterations, three traffic simulation modules, and two signal optimization procedures. With some periodic trouble-shooting, the process of developing and finalizing the results took nearly 47 calendar days to complete. In the end, the final gap achieved was just under 13 percent.

Subnetwork Selection and Analysis

The goal of the analysis was to evaluate the impact of a modification to the Dallas inner freeway loop on the area transportation network. However, running a single DTA model on the entire DFW network was estimated to take at least four weeks based on the time required to run the final base model. As such, the use of a subnetwork, encompassing the area most likely impacted by the project scenario(s) was proposed for implementation to save on the time and resources required for the analysis.

Discretion was used with respect to implementing a subnetwork analysis large enough to contain the primary impacts of such a substantial impact scenario in order to maintain the integrity of the model results, while small enough to save time and effort. A review of the network surrounding the project limits was performed for the purpose of choosing an appropriately sized subnetwork in which to analyze in detail. The objective of this analysis was to compare the base and impact scenarios to determine the magnitude of the traffic impact within the subnetwork.

It was anticipated that a modification to the inner freeway loop would substantially impact traffic using the freeway system surrounding the Dallas CBD. It was also speculated that any capacity reduction implemented as part of a TCP would inhibit area through traffic, subsequently affecting other circumferential routes in the area likely to be used as alternatives. Major highway and freeway loops in the Dallas area expected to be impacted included Loop 12 and IH 635/IH 20. Therefore, the area within the outer IH 635/IH 20 loop was chosen as the subnetwork for analysis. Figure 6.2 illustrates the extents of this subnetwork, along with the inner freeway loop.

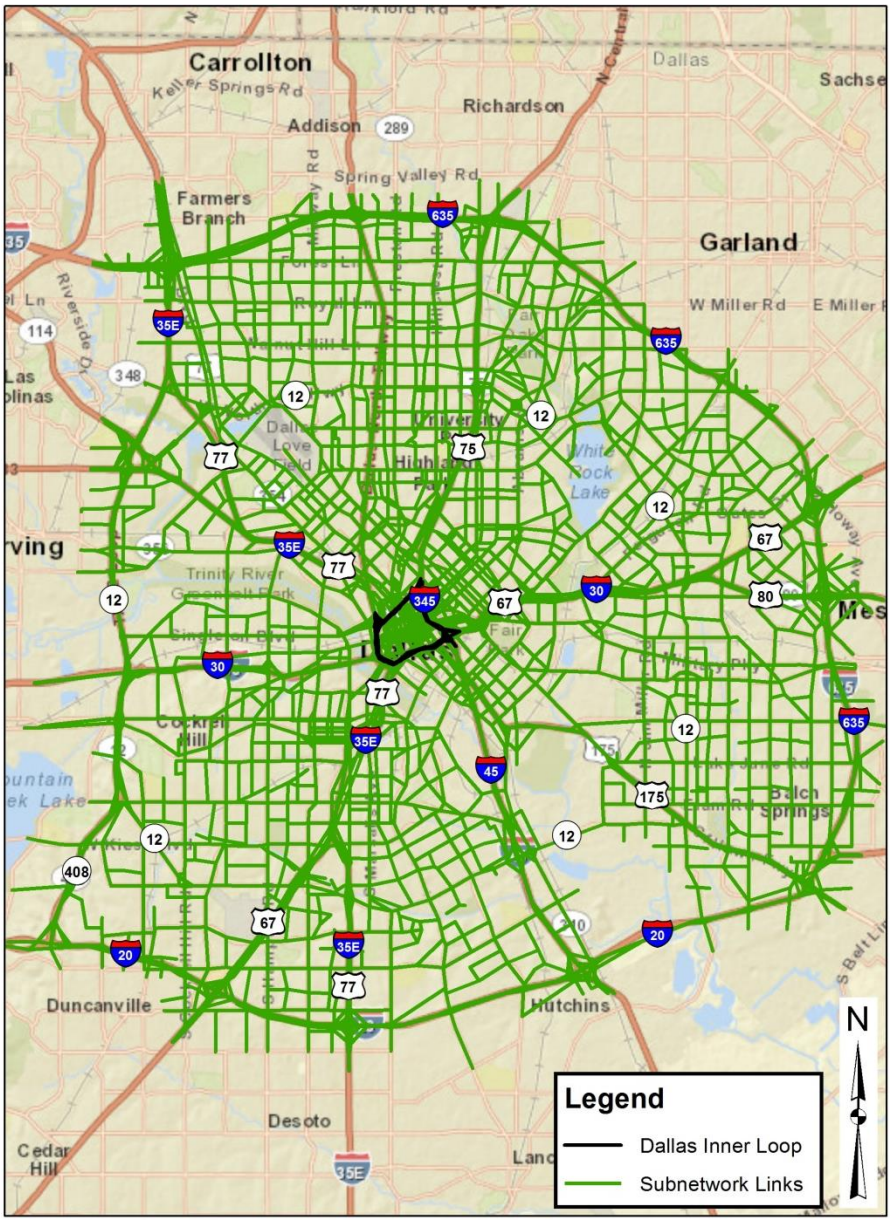

Figure 6.2 Extents of the Selected Subnetwork for the Dallas Project Scenario (Basemap Source: Esri, DeLorme, NAVTEQ, USGS, Intermap, iPC, NRCAN, METI, TomTom, 2013)

Once all of the elements were selected manually in ArcGIS, the network components were imported to create the subnetwork model in VISTA. The base subnetwork contains 16,434 links, including 5,728 connectors, and 7,408 nodes, including 2,942 centroids, amounting to approximately one-fourth of the original regional network. After creation of

the subnetwork, the boundary volumes and internal O-D demand information extracted from the base model were integrated to create the subnetwork dynamic O-D table. The resultant subnetwork demand consisted of 858,613 vehicles, including 814,312 cars and 44,301 trucks, totaling just over one-third of the full network demand.

Unlike the full regional model, the subnetwork model could be evaluated using the JavaScript code created by CTR implementing MSA and the ODT path sorting option as described in Chapter 4. This script was used to run 10 iterations of path generation followed by 10 iterations of DUE, 10 more iterations of path generation, and 20 additional iterations of DUE. These 50 iterations were able achieve a gap of approximately 9 percent. Notably, all of these iterations were completed in around 40 hours of computational time. After the script was run, additional DUE iterations were completed in an attempt to reduce the gap further. Three processes and 10 iterations were completed over another 30 hours of computation time, reducing the gap to just over 7 percent. In all, 15 processes totaling approximately 72 hours, or three days, of computational time over five calendar days were required.

Once the subnetwork model results were compiled, the link volumes were checked against available traffic counts. For many of the count locations the model volumes matched the counts particularly well, and others did not. It was speculated that this was due to some of the links being uncongested during all or part of the time interval over which the model volumes were extracted. When links are uncongested, the DUE process may move trips on and off of routes somewhat arbitrarily since travel times do not vary with an increase in volume (if links are operating at FFS). For this reason, count data do not always provide the best validation for a DTA model. Therefore, an effort was made to validate the subnetwork using travel times to and from the area of interest, as well as between boundary points. Travel time contour maps were created to perform this validation. A sample contour map is provided in Figure 6.3 which shows travel times to the downtown Dallas CBD.

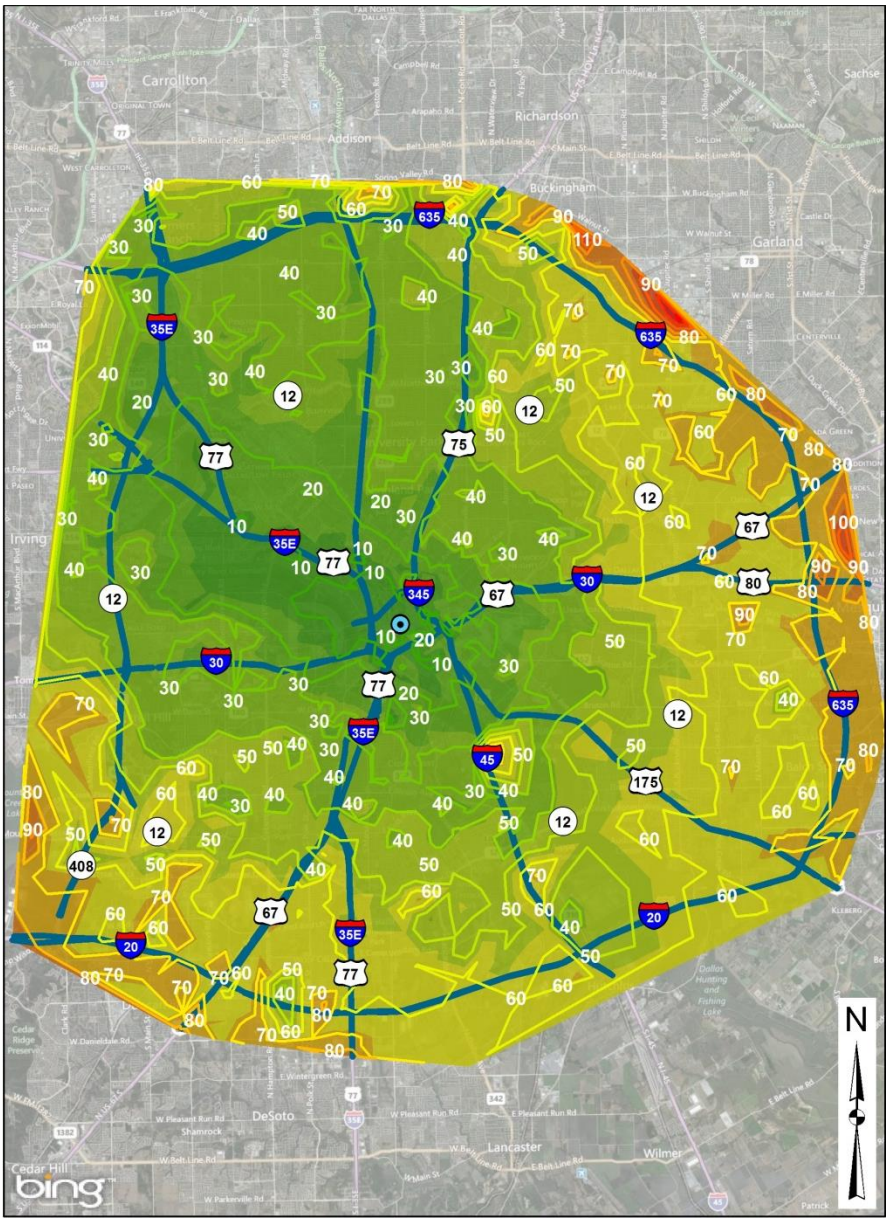

Figure 6.3 Sample Travel Time Contour Map for Travel to Downtown CBD (Basemap Source: BING © 2010 Microsoft and its Data Suppliers)

The map above shows travel times from origins throughout the subnetwork to the downtown area, distinguished by the blue dot at the center of the map. The subnetwork is color-coded to show the travel time from low (0-30 min), in green, to high (90+ min), in red. Furthermore, the travel time contours are labeled in 10-minute increments.

The travel time evaluation revealed that the subnetwork model was providing consistent results with respect to real-world observations and expectations. After validating the base subnetwork model through a review of the travel times, it was determined that a sample modification scenario could be examined. Therefore, a copy of the base subnetwork was created to implement network modifications consistent with capacity adjustments to multiple freeway links along the inner loop. Once these modifications were implemented, the subnetwork impact scenario model was run using the same DTA process as that for the base model. This required 12 processes totaling approximately 74 hours of computational time over five calendar days. The gap achieved for the impact scenario model was approximately 7.8 percent.

The purpose of the aforementioned subnetwork models was to evaluate the impact of significant modifications to the freeway network in the downtown Dallas area. However, through implementation of these models, the use of subnetworks to save computational time, effort, and space was thoroughly demonstrated. Further analyzing a base subnetwork extracted from a regional model also provided the capability of achieving better convergence. This is due to the fact that more path generation and DUE iterations could be completed on the subnetwork. Additionally, the DFW regional model is too large to implement the JavaScript code used to automate and streamline the DTA process. The ability to use the script in place of only manual processes resulted in additional savings in terms of the user time and effort required to implement DTA.

Notwithstanding, manual processes can be used to supplement the script if needed or deemed warranted, as demonstrated in this application. The following tables summarize the savings in terms of time and effort achieved using a subnetwork analysis for the inner freeway loop modification scenario.

Table 6.1 Performance Specifications for DFW Network Models (I)

Network	DTA Analysis Processes	Path Generation Iterations	DUE Iterations	Time to Complete Analysis (hours)	Calendar Days to Complete
Full DFW Network	32	8	36	1,022.3	47
Dallas Subnetwork - Base	15	20	40	72.2	5
Dallas Subnetwork - Impact	12	20	40	73.8	5

Table 6.1 shows that the subnetworks required fewer DTA processes and much less time to complete, but were able to accommodate more path generation and DUE iterations due to use of the script. Notably, the subnetwork models each took more than 40 fewer days to complete than the full network model revealing that many days or weeks could be saved implementing subnetwork analyses for reviewing multiple impact scenarios. Since the subnetwork required fewer DTA processes and could be implemented in fewer user steps, the burden on the user was also substantially less. This is further emphasized by the number of calendar days saved, demonstrating the improvement in efficiency achieved by implementing a subnetwork analysis.

In addition to time savings, both in terms of user and computational effort, a reduction in the amount of computer space required to store network-related files can be achieved. Table 6.2 compares the full network and subnetwork attributes and related file sizes. The table shows that the file sizes for the two subnetworks combined are far less than the full network for the base scenario alone.

Table 6.2 Performance Specifications for DFW Network Models (II)

Network	Number of Links	Number of Nodes	Number of Vehicles	Final Gap Measure	Total File Space Required
Full DFW Network	71,721	31,364	2,512,462	13.00	57.24 GB
Dallas Subnetwork – Base	16,434	7,408	858,613	7.15	9.73 GB
Dallas Subnetwork - Impact	16,414	7,394	858,613	7.80	10.17 GB

To demonstrate the importance of using subnetworks to analyze the impact of modifications within a large network, a sample case study was examined using the DFW regional DTA model. The DFW case study serves as a valuable example that stresses the need for an efficient and accurate subnetwork analysis process. However, selection of the subnetwork implemented was somewhat arbitrary. Additional assessment of subnetwork sizes relative to impact scenarios within a prototype network and evaluation of demand changes at the boundary of a subnetwork is warranted. Again, these steps can be used to establish recommendations for selection and treatment of a subnetwork in order to provide a more adequate analysis of a network modification.

Assessment of Subnetwork Sizes for Multiple Impact Scenarios

In Chapter 5, an investigation of different subnetwork sizes relative to multiple network modification scenarios was introduced. The proposed method assessed the difference in subnetwork boundary demand between the base and impact scenarios using several statistical measures including the RMSE, MCAPE, and SSIM index. The preliminary results revealed that the RMSE provided the best means of assessing the error in demand estimation relative to subnetwork size.

A number of scenarios involving all three locations where assessed in the previous chapter. The project locations and extents of applicable subnetworks are identified in Chapter 5, Figure 5.1 on page 131. In addition, a diverse group of scenarios was

evaluated. Attention was paid to select scenarios such that the location was fixed for three scenarios covering the full range of impacts (1-link, 25-percent capacity reduction to 3-link, 100-percent capacity reduction) and to fix a scenario across all three locations (50-percent reduction to 2 links).

For this subsequent evaluation, all of the remaining scenarios have been assessed for each location. This included 25-percent, 50-percent, and 100-percent capacity reductions across 1, 2, or 3 consecutive links. While Figure 5.1 shows the location of the scenarios relative to the entire downtown network, more detailed visuals of each location are provided below.

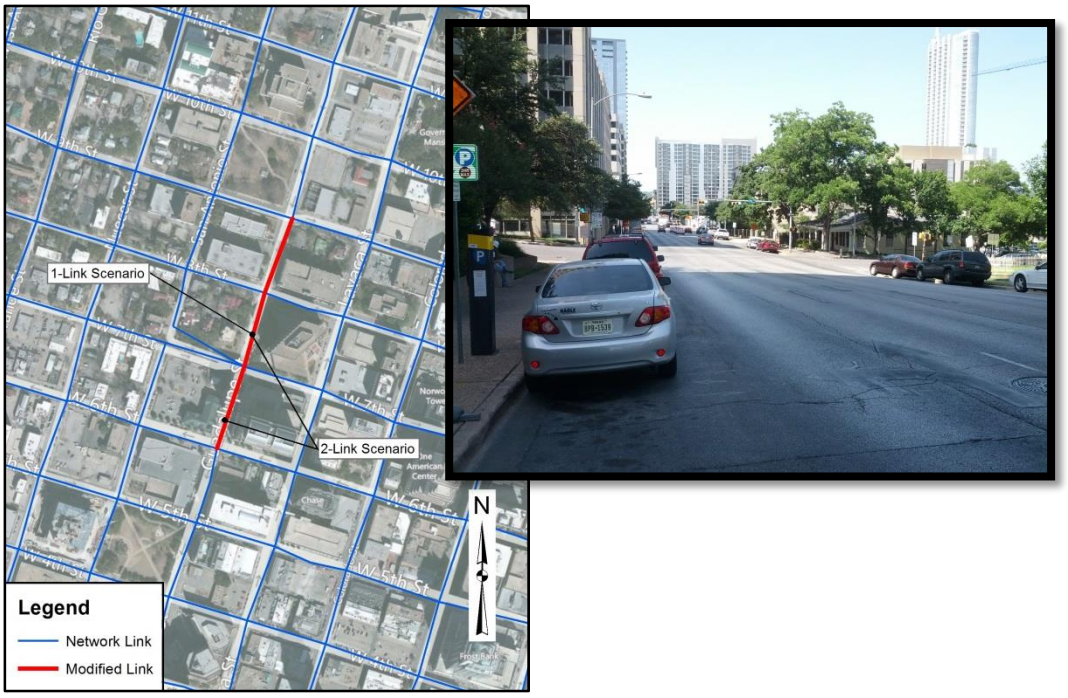

Figure 6.4 Guadalupe Street Project Site Location and Photo: Facing South Between 8th and 9th Streets (Basemap Source: BING © 2010 Microsoft and its Data Suppliers)

Figure 6.4 identifies the project location chosen for the Guadalupe Street scenarios. As shown in the photograph on the right, Guadalupe Street is a 4-lane southbound one-way arterial. The 1-link scenarios represent modifications to the roadway between 7th Street

and 8th Street. The 2-link scenarios represent modifications between 6th Street and 8th Street and the 3-link scenarios between 6th Street and 9th Street.

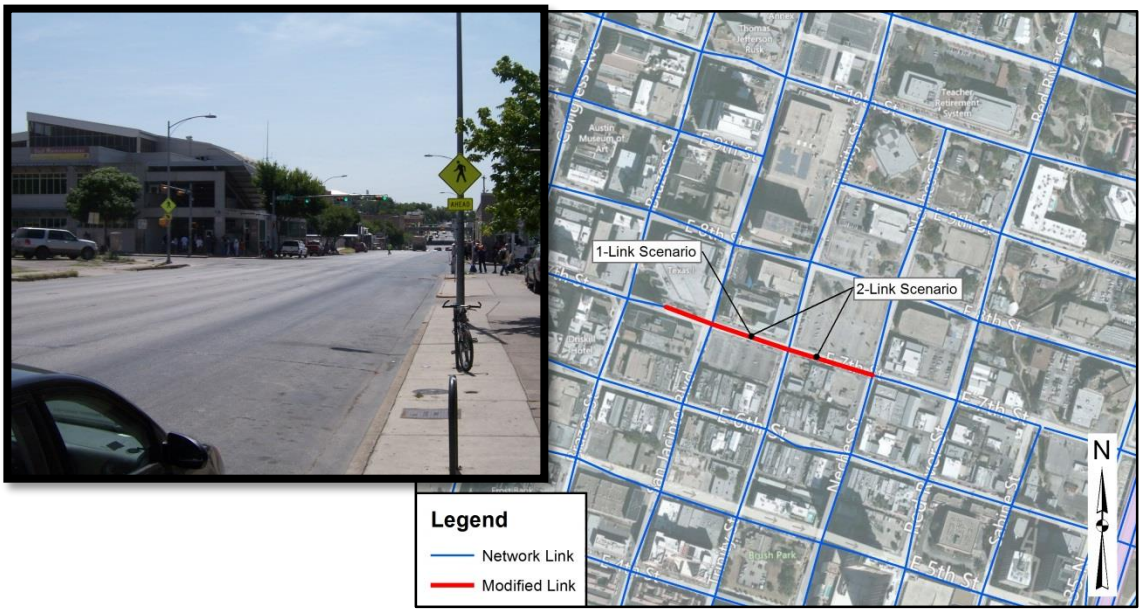

Figure 6.5 Seventh Street Project Site Location and Photo: Facing East Between Trinity and Neches Streets (Basemap Source: BING © 2010 Microsoft and its Data Suppliers)

The project location for the 7th Street scenarios is shown in Figure 6.5. Seventh Street is a 4-lane eastbound one-way arterial, as shown in the photograph on the left. The 1-link scenarios represent modifications to the roadway between San Jacinto Boulevard and Trinity Street. The 2-link scenarios represent modifications between San Jacinto Boulevard and Neches Street and the 3-link scenarios from the midblock location between Brazos Street and San Jacinto Boulevard to Neches Street.

Figure 6.6 Fifteenth Street Project Site Location and Photo: Facing West Between Guadalupe and San Antonio Streets (Basemap Source: BING © 2010 Microsoft and its Data Suppliers)

Figure 6.6 identifies the project location for the 15th Street scenarios. Fifteenth Street is a 6-lane two-way (east/west) arterial. The 1-link scenarios represent modifications to the westbound direction (shown in the photograph on the right) between Guadalupe Street and San Antonio Street. The 2-link scenarios represent modifications between Lavaca Street and San Antonio Street and the 3-link scenarios between Lavaca Street and Nueces Street.

For the subnetwork size evaluation, assessing the random differences between model runs involving the same network and scenario were important. It was necessary to capture random variation in order to determine where statistically significant differences could be found between modeled scenarios when a modification was imposed on the network. Therefore, the inputs were set using the provided JavaScript code used to run the DTA process incorporating MSA, identified in Chapter 4, so that randomness would occur in the models. The JavaScript code was subsequently assigned to perform 20 iterations of path generation followed by 30 DUE-only iterations. This sequence was chosen as part of

an extensive evaluation of preliminary model results and recommendations provided by CTR staff.

Taking into account the preliminary investigation, where 10 model runs for each scenario were evaluated, an effort was made to simplify and expedite the evaluation process. Using 10 individual models for each selected scenario would require nearly 300 runs of the full network. Originally, it was intended to use the prediction interval to streamline the review, requiring only one run of each impact scenario as described in Chapter 4. Unfortunately, the results obtained using the prediction interval, identified in the preliminary results obtained in Chapter 5, were inconsistent with the hypothesis test.

It was anticipated that if an impact scenario run resulted in a demand measure falling within the base prediction interval, the null hypothesis would not be rejected. However, in some cases, the null hypothesis was rejected even if one or more impact run values fell within this interval. Therefore, it was concluded that a hypothesis test would be required for all locations and scenarios to properly assess the results. Rather than using 10 impact runs for each scenario, as done in the preliminary evaluation, it was anticipated that two runs would be adequate to provide the sample needed for this test.

For a hypothesis test with only two impact runs, the threshold t-statistic identified in Chapter 4 was modified for consistency with the adjusted sample size. For a significance level (α) of 0.05 and 10 degrees of freedom, the threshold t-statistic for a two-tailed test is $t_{0.025,10} = 2.228$ instead of 2.101 as identified in Chapter 4. For a prediction interval for the two impact runs, a t-statistic of $t_{0.025,1} = 12.706$ was used. The t-statistic for the 10 base runs remained 2.262. Additionally, a new critical F-value was used for the equal variance test. It should be noted that normality tests cannot be completed using Matlab for sample sizes of less than four. Therefore, these tests were not completed on the remaining impact scenarios.

The results obtained from implementing the hypothesis test across the 81 scenarios evaluated are summarized in the tables below. The demand comparisons used in the analysis were extracted from a one-hour and two-hour period representative of the peak hour and peak period, respectively, during the DTA simulation. This includes demand values for 15-minute intervals beginning 30 minutes from the start of the simulation. Tables 6.3, 6.4, and 6.5 show the summarized hypothesis test results of the subnetwork size evaluation based on the boundary demand assessment for the 1-link, 2-link, and 3-link scenarios, respectively. The results are based on a comparison of base and impact conditions using the RMSE.

Table 6.3 Hypothesis Test Results for 1-Link Scenarios

Location	Subnetwork Size (Order)	Capacity Reduction (%)	1-Hour Hypothesis Test*	2-Hour Hypothesis Test*
Guadalupe St	5	25	Y	Y
Guadalupe St	7	25	Y	Y
Guadalupe St	9	25	Y	Y
7th St	5	25	Y	N
7th St	7	25	Y	N
7th St	9	25	Y	Y
15th St	5	25	Y	Y
15th St	7	25	Y	Y
15th St	9	25	Y	Y
Guadalupe St	5	50	Y	Y
Guadalupe St	7	50	Y	Y
Guadalupe St	9	50	Y	Y
7th St	5	50	Y	Y
7th St	7	50	Y	Y
7th St	9	50	Y	Y
15th St	5	50	Y	N
15th St	7	50	Y	Y
15th St	9	50	Y	Y
Guadalupe St	5	100	N	N
Guadalupe St	7	100	N	N
Guadalupe St	9	100	Y	Y
7th St	5	100	N	N
7th St	7	100	N	N
7th St	9	100	Y	Y
15th St	5	100	N	N
15th St	7	100	Y	Y
15th St	9	100	Y	Y

* Y = Accept H_o: $\mu_1 = \mu_2$; N = Reject H_o, conclude H_a: $\mu_1 \neq \mu_2$

Table 6.4 Hypothesis Test Results for 2-Link Scenarios

Location	Subnetwork Size (Order)	Capacity Reduction (%)	1-Hour Hypothesis Test*	2-Hour Hypothesis Test*
Guadalupe St	5	25	Y	Y
Guadalupe St	7	25	Y	Y
Guadalupe St	9	25	Y	Y
7th St	5	25	Y	Y
7th St	7	25	Y	Y
7th St	9	25	Y	Y
15th St	5	25	Y	N
15th St	7	25	Y	N
15th St	9	25	Y	Y
Guadalupe St	5	50	Y	Y
Guadalupe St	7	50	Y	Y
Guadalupe St	9	50	Y	Y
7th St	5	50	N	N
7th St	7	50	N	N
7th St	9	50	Y	Y
15th St	5	50	N	N
15th St	7	50	Y	Y
15th St	9	50	Y	Y
Guadalupe St	5	100	N	N
Guadalupe St	7	100	N	N
Guadalupe St	9	100	Y	N
Guadalupe St	11	100	N	N
7th St	5	100	N	N
7th St	7	100	N	N
7th St	9	100	Y	N
7th St	11	100	Y	Y
15th St	5	100	N	N
15th St	7	100	Y	N**
15th St	9	100	Y	N
15th St	11	100	Y	N

* Y = Accept H_o: $\mu_1 = \mu_2$; N = Reject H_o, conclude H_a: $\mu_1 \neq \mu_2$
** Result with outlier removed

Table 6.5 Hypothesis Test Results for 3-Link Scenarios

Location	Subnetwork Size (Order)	Capacity Reduction (%)	1-Hour Hypothesis Test*	2-Hour Hypothesis Test*
Guadalupe St	5	25	Y	Y
Guadalupe St	7	25	Y	Y
Guadalupe St	9	25	Y	Y
7th St	5	25	Y	Y
7th St	7	25	Y	N
7th St	9	25	Y	Y
15th St	5	25	Y	N
15th St	7	25	Y	Y
15th St	9	25	Y	Y
Guadalupe St	5	50	Y	Y
Guadalupe St	7	50	Y	Y
Guadalupe St	9	50	Y	Y
7th St	5	50	N	N
7th St	7	50	Y	Y
7th St	9	50	Y	Y
15th St	5	50	Y	Y
15th St	7	50	Y	Y
15th St	9	50	Y	Y
Guadalupe St	5	100	N	N
Guadalupe St	7	100	N	N
Guadalupe St	9	100	Y	N
Guadalupe St	11	100	N	N
7th St	5	100	N	N
7th St	7	100	N	N
7th St	9	100	N	N
7th St	11	100	Y	Y
15th St	5	100	N	N
15th St	7	100	Y	N
15th St	9	100	Y	Y
15th St	11	100	Y	Y

* Y = Accept H_o: $\mu_1 = \mu_2$; N = Reject H_o, conclude H_a: $\mu_1 \neq \mu_2$

The hypothesis test results (N) highlighted in the table represent a rejection of the null hypothesis that the sample means are equal. This implies that there exists a statistically significant difference in the boundary demand between the base and impact runs for a particular location and scenario. Initially, subnetwork sizes consistent with a connected order of 5, 7, or 9 were used. The intent was to limit the size relative to the full network and to adhere to prior research. Nonetheless, for the more extensive 2-link and 3-link, 100-percent capacity reduction scenarios, where many of the results indicated that a connected order of 9 was inadequate, a connected order of 11 was also reviewed.

For several of the scenarios, a connected order of 11 was sufficient; however, for others it was not. It was determined unnecessary to go beyond 11 since this would have required selection of substantially more than half of the downtown network. The findings support the assertion that a scenario requiring the full closure of multiple successive links along a major arterial would result in far-reaching impacts to the surrounding network during the peak period.

The above tables indicate that the results were similar between the time periods examined, although some inconsistencies were found. Where different, the 1-hour results appeared to show that a smaller subnetwork size was adequate when compared to the 2-hour period; however, this could have been influenced by the examination of a shorter time period representing half the number of 15-minute intervals. This finding is accentuated by the 2-link, 100 percent capacity reduction scenario for 15th Street shown near the bottom of Table 6.4. A few other minor inconsistencies were also discovered.

Originally for the 2-link, 100-percent capacity reduction scenario along 15th Street, the results for a subnetwork size of 7 (accept null) were inconsistent with the results for sizes 5 and 9 (reject null) using the 2-hour time period. An in-depth investigation revealed that an outlier within the base results caused a failure to reject the null hypothesis for the connected order of size 7 subnetwork. With the outlier removed, the null hypothesis was

rejected and the results indicated that a statistically significant difference in boundary demand existed for this subnetwork size.

Several minor inconsistencies also persisted across scenarios for 7th Street (2-hour) and Guadalupe Street (1-hour). For 7th Street, the tests resulted in a rejection of the null hypothesis for the 1-link, 25-percent reduction scenario at subnetwork sizes of 5 and 7, but not for the 1-link, 50-percent reduction scenario at these sizes. For Guadalupe Street, the 100-percent capacity reduction scenarios indicated that a subnetwork of order 9 was adequate, but 11 was not. When compared with the 2-hour results, the hypothesis tests for a connected order of 11 exhibited better consistency. Where these issues occurred at both locations, the results appeared to be on the borderline between rejecting and not rejecting the null hypothesis (for detailed results, see Appendix D). In other words, the result is somewhat ambiguous for a few of the scenarios where discrepancies occurred.

In addition to the tables above, the detailed results, including the outcome of the equal variance and normality tests for all applicable scenarios as well as the prediction intervals for both base and impact model runs, are provided in Appendix D, Tables D.1 through D.18. As with the preliminary assessment discussed in Chapter 5, the results of the equal variance and normality tests were generally good, but revealed some inconsistencies as well. Many scenarios failed the equal variance test, though this was likely a result of demand fluctuations caused by the impact scenarios. The normality test results were much more conclusive, determining that the data is largely normally distributed.

Though some fluctuations relative to the hypothesis tests exist across the locations and scenarios, the results can be interpreted appropriately. Based on the hypothesis test conclusions summarized in Tables 6.3, 6.4, and 6.5, as well as Appendix D, a recommended subnetwork size required to contain the majority of traffic impacts can be ascertained. Though not all possible scenarios are represented, applicable sizes can be interpolated, using a measure of engineering judgment, from the results. The

recommended subnetwork sizes established using the test results for the 81 scenarios are provided in Table 6.6. These recommendations are consistent with arterial classification or lower throughout a downtown/urban area, representative of a well-connected grid network.

Table 6.6 Recommended Subnetwork Sizes by Scenario

Scenario		Interpretation	
# Links Impacted	% Capacity Reduction	Applicable Range	Recommended Subnetwork Size
1	25	5-7	5
1	50	5-7	7
1	100	7-9	9
2	25	5-7	5
2	50	5-7	7
2	100	9-11+	10+
3	25	5-7	7
3	50	5-7	7
3	100	9-11+	10+

The table presents an applicable range of subnetwork connected order sizes relative to each scenario. This is based on a more general interpretation of the results in Tables 6.3, 6.4, and 6.5. For many of the scenarios, a subnetwork size of 7 appears adequate unless a 100-percent capacity reduction is involved. When a link is completely closed along a well-traveled corridor, such as those tested, a subnetwork size equivalent to a connected order of at least 9 is recommended. Again, one should be cautioned about going beyond a connected order of 10. It has been suggested that a subnetwork used to test the impact of disabling a link not exceed 10 (Chen et al., 2011), though closing multiple links in succession may justify an exception (as suggested by the results in Tables 6.4 and 6.5). A visual representation of the results compiled in Table 6.6 is shown in Figure 6.7. The figure provides a recommended subnetwork size for a scenario from lining up the number of links impacted and the capacity reduction imposed.

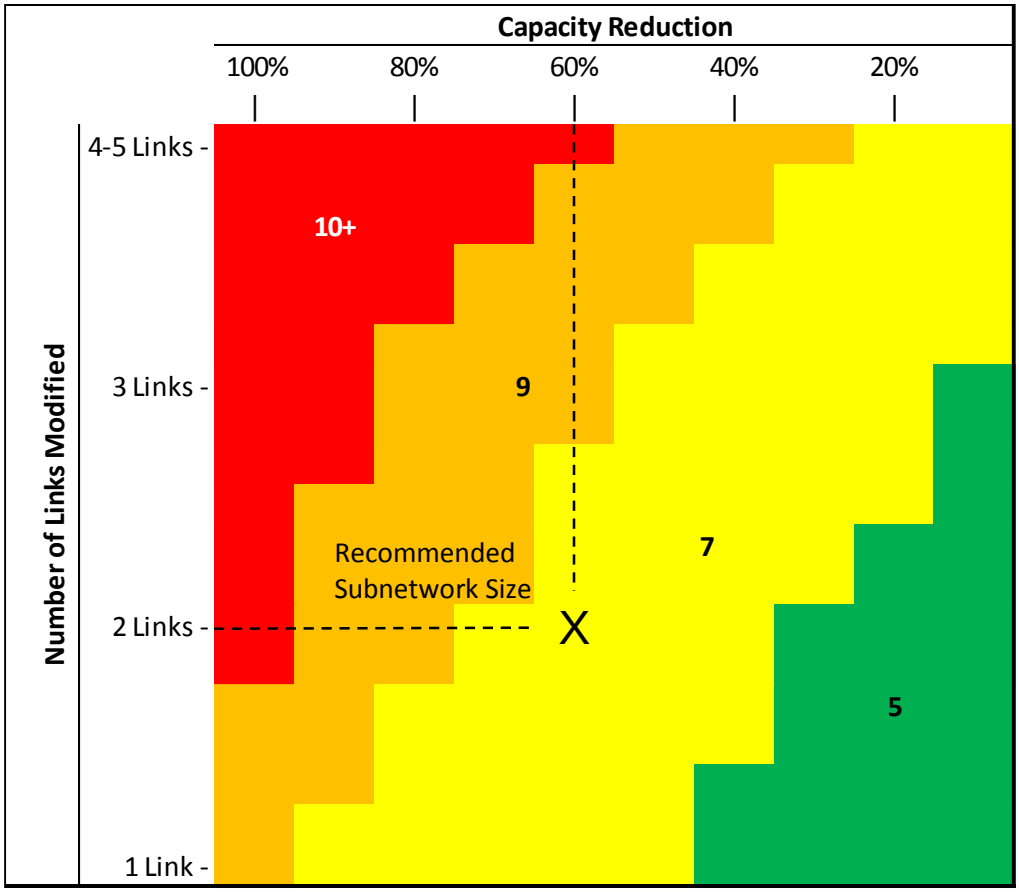

Figure 6.7 Recommended Subnetwork Size Based on Scenario Characteristics (with Example)

If a scenario appears to require a subnetwork beyond a connected order of 10, a review of the subnetwork size relative to the full network should be undertaken to determine if a subnetwork analysis is still adequate. At this size, care should be taken to choose a representative boundary that takes advantage of natural borders, breaks, or general changes in connectivity that can be found in the surrounding network or geographical makeup of the area. Choosing an area with more natural boundaries, independent of connected order, such as that used for the DFW network may be more adequate. Scenarios likely to substantially impact traffic in an area certainly rely on in-depth review of the greater network and considerable engineering judgment.

Evaluation of the Logit Formulation for Adjusting Subnetwork Demand

The preliminary review of strategies for adjusting subnetwork boundary demand revealed that using the logit formulation could improve the subnetwork demand estimation. It was shown that applying adjustments to external-to-external trips, as well as external-to-internal trips based on changes to internal travel times proved beneficial. Therefore, as a follow-up to the subnetwork size evaluation and to the preliminary investigation of the methodology outlined in Chapter 5, the logit formulation was implemented across an array of impact scenarios.

In addition, through an evaluation of different centroid grouping strategies it was found that grouping boundary centroids based on the demand origin performed better than grouping based on arbitrarily selected regions. Grouping external centroids was also found to influence the results, with a grouping strategy consistent with the boundary centroid groups being superior to grouping based simply on geographically-defined regions. However, this conclusion was derived from a limited sample of scenarios for one location. To further evaluate the proposed grouping strategies, all four methods were implemented for the remaining scenarios.

The tested scenarios included all three locations reviewed as part of the subnetwork size evaluation: Guadalupe Street, 7th Street, and 15th Street. Since the need to adjust the boundary demand is more explicitly demonstrated with larger-scale network modifications, those scenarios were the focus for evaluation of the logit formulation. It was further speculated that a review inclusive of scenarios and respective subnetwork sizes that consistently yielded statistically significant differences in boundary demand, as observed in the subnetwork size evaluation, would be especially beneficial. This included many of the 100-percent capacity reduction scenarios, as well as several 50-percent reductions. Since the 25-percent capacity reduction scenarios were rarely found to demonstrate statistically significant differences in boundary demand between the base

and impact models, these scenarios were excluded from the logit evaluation. As a result, all scenarios involving a 50- or 100-percent capacity reduction were included in the review. This included 54 of the 81 scenarios used in the subnetwork size assessment.

For the subnetwork size evaluation, assessing the random differences between model runs involving the same network and scenario were important. It was necessary to capture random variation in order to determine where statistically significant differences could be found. Therefore, the script inputs were set so that randomness would occur in the models. However, for the logit evaluation, isolating the change in subnetwork demand attributable to a network modification is ideal such that the true differences between base and impact scenarios can be identified. Therefore, an effort was made to capture only the effects of a network modification on the surrounding network, including travel times and boundary demands.

To do this, the developed JavaScript code implementing MSA as described in Chapter 4 was modified to allow the random seed to be fixed. This option forces the model to fix decisions involving random number generators between runs of the same network, thus yielding the same results when the same inputs are used. Due to limitations with respect to implementing the modified JavaScript code, different input parameters than those used for the subnetwork size evaluation were required. The differences are relatively minor and involve the number of assigned path generation iterations.

Instead of applying 20 path generation followed by 30 DUE-only iterations, all 50 iterations were run with the full path generation/DUE process. Therefore, paths were created by the model at every iteration. While this takes longer computationally than the DUE-only iterations, the uniformity of the process allows the user to initiate the code only once (instead of twice for a path generation and DUE-only sequence). As discussed in Chapter 5, the process of implementing the logit formulation necessitated running the full base model, as well as the base and impact subnetwork models to supply the proper

inputs for the created Matlab code. Once all of the travel time and demand information was input into Matlab for a particular scenario, the code was run and the results extracted.

The detailed results from the analysis can be found in Appendix E, Tables E.1 through E.3. The scenarios where an improvement was found are documented in Table E.4. Table E.4 also identifies if a statistically significant difference was found between the base and impact scenario, from the subnetwork size evaluation, for a particular location and modification scenario. In addition, Table 6.7 summarizes results for the different scenarios disaggregated by location: Guadalupe Street, 7th Street, and 15th Street, as well as across all locations and scenarios. The table identifies the number of times an improvement was found at each location and the subsequent percent of the total scenarios for which the adjustment was applied for each category. The table also notes the improvements found relative to where a statistically significant difference in boundary demand was found from the subnetwork size evaluation.

Table 6.7 Improvement Found from Implementation of Boundary Demand Adjustment

Category	Total Scenarios	Total Demand Estimation		Demand RMSE	
		# Improved	% Improved	# Improved	% Improved
Guadalupe Street/All Scenarios					
Overall	18	10	56%	9	50%
Statistically Different	8	5	63%	6	75%
7th Street/All Scenarios					
Overall	18	9	50%	0	0%
Statistically Different	11	4	36%	0	0%
15th Street/All Scenarios					
Overall	18	7	39%	0	0%
Statistically Different	7	3	43%	0	0%
All Locations/All Scenarios					
Overall	54	26	48%	9	17%
Statistically Different	26	12	46%	6	23%

Again, 54 of the 81 scenarios were evaluated since the 25-percent capacity reduction cases were excluded. The adjustment strategy was evaluated against the demand extracted from each impact scenario implemented on the full network (benchmark). The overall results indicate that with respect to the total demand estimation, the adjustment strategy appeared to have a positive impact roughly half of the time. This simply compares the total demand for the subnetwork as extracted from the impact and base scenarios for the full network, as well as the total demand after the external-to-external demand adjustment was implemented. It should be noted that when an improvement was not found, the demand estimation achieved from the adjustment strategy was worse than the base demand (unadjusted).

When the boundary demand was evaluated using the RMSE, the overall results indicate that the adjustment strategy was less effective on a disaggregate level. Specifically, the RMSE compares the individual demand values across all ODT combinations from the Matlab output (adjusted demand) versus the baseline values extracted from the full network under impact conditions (benchmark). This demand comparison, as identified in Table 6.7, uses only the boundary centroids in the assessment since the remaining centroids are not adjusted by the code. The assessment of all centroids is nonetheless provided in Appendix E, Tables E.1 through E.3. Notably, the Guadalupe Street location, utilized in the preliminary assessment of the strategy in Chapter 5, performed relatively well. An improvement was achieved 75-percent of the time where a statistically significant difference was found in the subnetwork size evaluation.

To provide a more disaggregate assessment of the results, performance summaries for each of the four centroid grouping strategies are presented in the tables below. Since each of the four strategies outlined in Chapter 5 were evaluated in the analysis, the results are categorized accordingly. Table 6.8 summarizes the results for the four grouping strategies relative to each location. In addition to the number and percent that showed improvement over the base demand, the percent of the time a particular grouping strategy performed

the best, relative to the other three, for each category is also documented. The values indicative of the best performance among the scenarios evaluated are highlighted in green.

Table 6.8 Performance of the Grouping Strategies by Scenario Location

Grouping by Demand Proportion (Boundary) and Boundary Centroid (External)							
		Total Demand Estimation			Demand RMSE		
Category	Total Scenarios	# Improved	% Improved	% Best Performing	# Improved	% Improved	% Best Performing
Guadalupe Street/All Scenarios							
Overall	18	3	17%	11%	4	22%	17%
Stat Diff	8	3	38%	13%	3	38%	13%
7th Street/All Scenarios							
Overall	18	7	39%	17%	0	0%	33%
Stat Diff	11	2	18%	18%	0	0%	27%
15th Street/All Scenarios							
Overall	18	2	11%	22%	0	0%	22%
Stat Diff	7	0	0%	14%	0	0%	29%
All Locations/All Scenarios							
Overall	54	12	22%	19%	4	7%	24%
Stat Diff	26	5	19%	15%	3	12%	23%
Grouping by Max Demand (Boundary) and Boundary Centroid (External)							
		Total Demand Estimation			Demand RMSE		
Category	Total Scenarios	# Improved	% Improved	% Best Performing	# Improved	% Improved	% Best Performing
Guadalupe Street/All Scenarios							
Overall	18	6	33%	22%	5	28%	17%
Stat Diff	8	3	38%	13%	3	38%	13%
7th Street/All Scenarios							
Overall	18	6	33%	22%	0	0%	17%
Stat Diff	11	2	18%	9%	0	0%	18%
15th Street/All Scenarios							
Overall	18	3	17%	28%	0	0%	6%
Stat Diff	7	1	14%	29%	0	0%	14%
All Locations/All Scenarios							
Overall	54	15	28%	24%	5	9%	13%
Stat Diff	26	6	23%	15%	3	12%	15%

Table 6.8 (Continued) Performance of the Grouping Strategies by Scenario Location

Grouping by Max Demand (Boundary) and Region (External)							
		Total Demand Estimation			Demand RMSE		
Category	Total Scenarios	# Improved	% Improved	% Best Performing	# Improved	% Improved	% Best Performing
Guadalupe Street/All Scenarios							
Overall	18	10	56%	61%	4	22%	17%
Stat Diff	8	5	63%	63%	3	38%	13%
7th Street/All Scenarios							
Overall	18	7	39%	39%	0	0%	6%
Stat Diff	11	3	27%	45%	0	0%	0%
15th Street/All Scenarios							
Overall	18	2	11%	28%	0	0%	0%
Stat Diff	7	1	14%	29%	0	0%	0%
All Locations/All Scenarios							
Overall	54	19	35%	43%	4	7%	7%
Stat Diff	26	9	35%	46%	3	12%	4%
Grouping by Region (Boundary and External)							
		Total Demand Estimation			Demand RMSE		
Category	Total Scenarios	# Improved	% Improved	% Best Performing	# Improved	% Improved	% Best Performing
Guadalupe Street/All Scenarios							
Overall	18	4	22%	6%	8	44%	50%
Stat Diff	8	4	50%	13%	6	75%	63%
7th Street/All Scenarios							
Overall	18	6	33%	22%	0	0%	44%
Stat Diff	11	3	27%	27%	0	0%	55%
15th Street/All Scenarios							
Overall	18	4	22%	28%	0	0%	72%
Stat Diff	7	2	29%	29%	0	0%	57%
All Locations/All Scenarios							
Overall	54	14	26%	19%	8	15%	56%
Stat Diff	26	9	35%	23%	6	23%	58%

The results indicate that the grouping strategy involving the maximum demand region for the boundary centroids, and the geographic region for the external centroids performed the best for the overall demand estimation. Grouping both the boundary and external

centroids by region also performed well in this category. This grouping strategy also performed the best with respect to the RMSE assessment. Again, it is evident that the demand adjustment resulted in an improvement for the Guadalupe Street scenario, but not for the other locations. Table 6.9 summarizes the results in a similar manner categorized by subnetwork size: connected order 5, 7, and 9.

Table 6.9 Performance of the Grouping Strategies by Subnetwork Size

Grouping by Demand Proportion (Boundary) and Boundary Centroid (External)							
		Total Demand Estimation			Demand RMSE		
Category	Total Scenarios	# Improved	% Improved	% Best Performing	# Improved	% Improved	% Best Performing
Subnetwork Connected Order Size 5/All Scenarios							
Overall	18	3	17%	11%	3	17%	11%
Stat Diff	13	2	15%	8%	2	15%	8%
Subnetwork Connected Order Size 7/All Scenarios							
Overall	18	4	22%	28%	1	6%	17%
Stat Diff	8	2	25%	25%	1	13%	25%
Subnetwork Connected Order Size 9/All Scenarios							
Overall	18	5	28%	22%	0	0%	44%
Stat Diff	5	1	20%	20%	0	0%	60%
Grouping by Max Demand (Boundary) and Boundary Centroid (External)							
		Total Demand Estimation			Demand RMSE		
Category	Total Scenarios	# Improved	% Improved	% Best Performing	# Improved	% Improved	% Best Performing
Subnetwork Connected Order Size 5/All Scenarios							
Overall	18	8	44%	22%	3	17%	17%
Stat Diff	13	3	23%	23%	2	15%	15%
Subnetwork Connected Order Size 7/All Scenarios							
Overall	18	3	17%	33%	1	6%	17%
Stat Diff	8	1	13%	13%	1	13%	25%
Subnetwork Connected Order Size 9/All Scenarios							
Overall	18	4	22%	17%	1	6%	6%
Stat Diff	5	2	40%	0%	0	0%	0%

Table 6.9 (Continued) Performance of the Grouping Strategies by Subnetwork Size

Grouping by Max Demand (Boundary) and Region (External)							
		Total Demand Estimation			Demand RMSE		
Category	Total Scenarios	# Improved	% Improved	% Best Performing	# Improved	% Improved	% Best Performing
Subnetwork Connected Order Size 5/All Scenarios							
Overall	18	8	44%	50%	3	17%	11%
Stat Diff	13	5	38%	46%	2	15%	8%
Subnetwork Connected Order Size 7/All Scenarios							
Overall	18	5	28%	39%	1	6%	11%
Stat Diff	8	3	38%	63%	1	13%	0%
Subnetwork Connected Order Size 9/All Scenarios							
Overall	18	6	33%	39%	0	0%	0%
Stat Diff	5	1	20%	20%	0	0%	0%
Grouping by Region (Boundary and External)							
		Total Demand Estimation			Demand RMSE		
Category	Total Scenarios	# Improved	% Improved	% Best Performing	# Improved	% Improved	% Best Performing
Subnetwork Connected Order Size 5/All Scenarios							
Overall	18	5	28%	17%	4	22%	61%
Stat Diff	13	4	31%	23%	3	23%	69%
Subnetwork Connected Order Size 7/All Scenarios							
Overall	18	3	17%	6%	2	11%	56%
Stat Diff	8	2	25%	0%	2	25%	50%
Subnetwork Connected Order Size 9/All Scenarios							
Overall	18	6	33%	33%	2	11%	50%
Stat Diff	5	3	60%	60%	1	20%	40%

Again, grouping by region performed the best, similarly to the results identified in Table 6.8. It also appeared, at least with respect to the RMSE assessment, that subnetworks of connected order 5 had the highest propensity for improvement as a result of the demand adjustment. The rate of improvement seemed to increase as the subnetwork size decreased. This is a positive result since smaller subnetworks are associated with more substantial impacts across the boundary, as demonstrated in the subnetwork size evaluation, and a greater need to provide demand adjustments. Next, the results were

categorized by number of consecutive links modified: 1, 2, or 3, across all locations and capacity reduction scenarios in Table 6.10.

Table 6.10 Performance of the Grouping Strategies by Number of Links Modified

Grouping by Demand Proportion (Boundary) and Boundary Centroid (External)							
		Total Demand Estimation			Demand RMSE		
Category	Total Scenarios	# Improved	% Improved	% Best Performing	# Improved	% Improved	% Best Performing
3-Link Scenarios							
Overall	18	4	22%	22%	2	11%	44%
Stat Diff	9	2	22%	33%	2	22%	44%
2-Link Scenarios							
Overall	18	4	22%	11%	2	11%	17%
Stat Diff	11	1	9%	9%	1	9%	18%
1-Link Scenarios							
Overall	18	4	22%	22%	0	0%	11%
Stat Diff	6	2	33%	0%	0	0%	0%
Grouping by Max Demand (Boundary) and Boundary Centroid (External)							
		Total Demand Estimation			Demand RMSE		
Category	Total Scenarios	# Improved	% Improved	% Best Performing	# Improved	% Improved	% Best Performing
3-Link Scenarios							
Overall	18	7	39%	39%	2	11%	17%
Stat Diff	9	3	33%	22%	2	22%	11%
2-Link Scenarios							
Overall	18	6	33%	28%	1	6%	17%
Stat Diff	11	2	18%	9%	0	0%	27%
1-Link Scenarios							
Overall	18	2	11%	11%	2	11%	6%
Stat Diff	6	1	17%	33%	1	17%	0%

Table 6.10 (Continued) Performance of the Grouping Strategies by Number of Links Modified

Grouping by Max Demand (Boundary) and Region (External)							
		Total Demand Estimation			Demand RMSE		
Category	Total Scenarios	# Improved	% Improved	% Best Performing	# Improved	% Improved	% Best Performing
3-Link Scenarios							
Overall	18	7	39%	22%	2	11%	6%
Stat Diff	9	4	44%	22%	2	22%	0%
2-Link Scenarios							
Overall	18	5	28%	39%	2	11%	6%
Stat Diff	11	2	18%	45%	1	9%	9%
1-Link Scenarios							
Overall	18	7	39%	61%	0	0%	11%
Stat Diff	6	3	50%	67%	0	0%	0%
Grouping by Region (Boundary and External)							
		Total Demand Estimation			Demand RMSE		
Category	Total Scenarios	# Improved	% Improved	% Best Performing	# Improved	% Improved	% Best Performing
3-Link Scenarios							
Overall	18	5	28%	17%	3	17%	33%
Stat Diff	9	4	44%	22%	3	33%	44%
2-Link Scenarios							
Overall	18	5	28%	28%	4	22%	61%
Stat Diff	11	3	27%	36%	2	18%	45%
1-Link Scenarios							
Overall	18	4	22%	11%	1	6%	72%
Stat Diff	6	2	33%	0%	1	17%	100%

As identified previously, grouping by region performed the best, though grouping by maximum demand region performed a little better here. The table indicates that the best performances were a little more widely distributed, as all strategies led in at least one evaluated category. It also appeared the majority of the more substantial improvements were found for the 2-link and 3-link scenarios. Since these involve larger, more substantial network modifications and subsequent impacts, this is another positive result. These scenarios represent those where an improvement in the demand estimation would

be most desirable. Finally, Table 6.11 summarizes the results categorized by capacity reduction: 50 percent or 100 percent.

Table 6.11 Performance of the Grouping Strategies by Capacity Reduction

Grouping by Demand Proportion (Boundary) and Boundary Centroid (External)							
		Total Demand Estimation			Demand RMSE		
Category	Total Scenarios	# Improved	% Improved	% Best Performing	# Improved	% Improved	% Best Performing
50-Percent Capacity Reduction/All Locations							
Overall	27	7	26%	19%	1	4%	15%
Stat Diff	5	0	0%	0%	0	0%	0%
100-Percent Capacity Reduction/All Locations							
Overall	27	5	19%	22%	3	11%	33%
Stat Diff	21	5	24%	19%	3	14%	29%
Grouping by Max Demand (Boundary) and Boundary Centroid (External)							
		Total Demand Estimation			Demand RMSE		
Category	Total Scenarios	# Improved	% Improved	% Best Performing	# Improved	% Improved	% Best Performing
50-Percent Capacity Reduction/All Locations							
Overall	27	10	37%	33%	2	7%	15%
Stat Diff	5	1	20%	0%	0	0%	20%
100-Percent Capacity Reduction/All Locations							
Overall	27	5	19%	15%	3	11%	11%
Stat Diff	21	5	24%	19%	3	14%	14%
Grouping by Max Demand (Boundary) and Region (External)							
		Total Demand Estimation			Demand RMSE		
Category	Total Scenarios	# Improved	% Improved	% Best Performing	# Improved	% Improved	% Best Performing
50-Percent Capacity Reduction/All Locations							
Overall	27	9	33%	41%	1	4%	11%
Stat Diff	5	0	0%	40%	0	0%	0%
100-Percent Capacity Reduction/All Locations							
Overall	27	10	37%	44%	3	11%	4%
Stat Diff	21	9	43%	48%	3	14%	5%
Grouping by Region (Boundary and External)							
		Total Demand Estimation			Demand RMSE		
Category	Total Scenarios	# Improved	% Improved	% Best Performing	# Improved	% Improved	% Best Performing
50-Percent Capacity Reduction/All Locations							
Overall	27	4	15%	19%	2	7%	89%
Stat Diff	5	1	20%	60%	0	0%	80%
100-Percent Capacity Reduction/All Locations							
Overall	27	10	37%	19%	6	22%	78%
Stat Diff	21	8	38%	14%	6	29%	52%

The table shows that the strategy involving grouping by region once again performed the best. Scenarios involving 100-percent capacity reductions yielded more improvements than the 50-percent scenarios. This is consistent with the link-based evaluation, where demand adjustments for the more substantial impact scenarios performed better. Again, since these are associated with more significant demand changes, and a greater need for adjustment, this result is promising.

In addition to the more substantial network modifications, the adjustment strategy appeared to perform better for the Guadalupe Street scenario (see Table 6.8 on page 262-263). The inconsistency of the results relative to the other locations, and the lack of more widespread improvement signified that a more detailed review of the results may be necessary. Primarily, the logit-based demand adjustments were applied with respect to both external-to-external and external-to-internal trips. However, to investigate the impact of each adjustment individually, the processes were implemented and reviewed independently. This was done to further investigate the influence (positive or negative) of each adjustment process, and to determine if additional improvements could be achieved or other noticeable differences would be observed using one alone.

To accomplish this review, a number of scenarios were examined in more detail. For Guadalupe Street, the three scenarios involving a 100-percent capacity reduction across 3 links within subnetwork sizes of 5, 7 and 9 were chosen. The following table shows the detailed results obtained from the analysis of these scenarios. The results for these scenarios are shown in Tables 6.12, 6.13, and 6.14.

Table 6.12 Evaluation of 3-Link, 100-Percent Capacity Reduction Scenario for Guadalupe Street: Subnetwork of Size 5

Scenario	Boundary Centroid Grouping	External Centroid Grouping	Demand	Total Demand Diff	Total Demand Error	RMSE	
						Full Subnetwork Demand	Boundary Origins Only
Impact	-	-	22,536	-	-	-	-
Base	-	-	23,213	677	3.0%	12.61	13.05
Ext to Ext Only	Demand Prop	Boundary Centroids	22,757	221	1.0%	12.07	12.06
Ext to Int Only						12.61	13.05
Both						12.06	12.04
Ext to Ext Only	Max Demand	Boundary Centroids	22,713	177	0.8%	12.05	12.02
Ext to Int Only						12.61	13.05
Both						12.04	12.01
Ext to Ext Only	Max Demand	Region	23,034	498	2.2%	12.43	12.73
Ext to Int Only						12.64	13.10
Both						12.46	12.78
Ext to Ext Only	Region	Region	22,994	458	2.0%	12.18	12.27
Ext to Int Only						12.45	12.77
Both						12.10	12.12

Table 6.13 Evaluation of 3-Link, 100-Percent Capacity Reduction Scenario for Guadalupe Street: Subnetwork of Size 7

Scenario	Boundary Centroid Grouping	External Centroid Grouping	Demand	Total Demand Diff	Total Demand Error	RMSE	
						Full Subnetwork Demand	Boundary Origins Only
Impact	-	-	37,060	-	-	-	-
Base	-	-	37,302	242	0.0%	10.75	13.59
Ext to Ext Only	Demand Prop	Boundary Centroids	37,034	-268	0.7%	10.59	13.31
Ext to Int Only						10.79	13.66
Both						10.61	13.35
Ext to Ext Only	Max Demand	Boundary Centroids	36,978	-324	0.9%	10.58	13.30
Ext to Int Only						10.87	13.81
Both						10.63	13.39
Ext to Ext Only	Max Demand	Region	37,206	-96	0.3%	10.68	13.47
Ext to Int Only						10.80	13.68
Both						10.70	13.51
Ext to Ext Only	Region	Region	37,178	-124	0.3%	10.67	13.45
Ext to Int Only						10.81	13.69
Both						10.67	13.46

Table 6.14 Evaluation of 3-Link, 100-Percent Capacity Reduction Scenario for Guadalupe Street: Subnetwork of Size 9

Scenario	Boundary Centroid Grouping	External Centroid Grouping	Demand	Total Demand Diff	Total Demand Error	RMSE	
						Full Subnetwork Demand	Boundary Origins Only
Impact	-	-	50,763	-	-	-	-
Base	-	-	51,162	399	0.8%	8.99	12.70
Ext to Ext Only						8.99	12.70
Ext to Int Only	Demand Prop	Boundary Centroids				9.00	12.72
Both			51,166	403	0.8%	9.00	12.72
Ext to Ext Only						8.97	12.65
Ext to Int Only	Max Demand	Boundary Centroids				9.03	12.76
Both			51,050	287	0.6%	8.99	12.70
Ext to Ext Only						9.04	12.77
Ext to Int Only	Max Demand	Region				9.03	12.76
Both			50,950	187	0.4%	9.07	12.83
Ext to Ext Only						8.97	12.66
Ext to Int Only	Region	Region				9.02	12.74
Both			51,087	324	0.6%	8.99	12.70

The more detailed results exemplify how improvements could be achieved for the Guadalupe location, particularly for scenarios involving network modifications of substantial magnitude. It should be pointed out that although the adjustment strategy was able to improve the demand estimation, the benefits of implementation were modest. This is important to note since the grouping process and logit formulation took considerable time and effort to implement.

Furthermore, inconsistencies among the results are evident here. Though grouping the boundary centroids based on maximum-demand region and the external centroids by boundary group performs the best relative to the RMSE assessment, grouping the external centroids by region performed the best relative to the total demand estimation. Additionally, applying only the external-to-external adjustment yields the best results for two of the subnetwork sizes, while using both processes works best for a subnetwork of size 5. This would suggest that there is no clear answer to what combination of grouping strategies will yield the best results; there appears to be no robust process. With little

improvement even where one does exist, it raises the concern that none of the strategies are worth the effort. This is more evident at the other locations.

Although no improvements were found relative to the RMSE evaluation for the 7th Street and 15th Street locations for any scenario, several examples were chosen for further review at these locations as well. The scenarios chosen for 7th Street included the 3-link 100-percent capacity reduction, the 1-link 100-percent reduction, and the 1-link 50-percent reduction, all for subnetworks of connected order size 5. These scenarios were chosen as candidates because some level of improvement was anticipated based on the earlier evaluation. Tables 6.15, 6.16, and 6.17 provide the detailed results for these scenarios.

Table 6.15 Evaluation of 3-Link, 100-Percent Capacity Reduction Scenario for 7th Street: Subnetwork of Size 5

Scenario	Boundary Centroid Grouping	External Centroid Grouping	Demand	Total Demand Diff	Total Demand Error	RMSE	
						Full Subnetwork Demand	Boundary Origins Only
Impact	-	-	30,823	-	-	-	-
Base	-	-	31,108	285	0.9%	5.31	3.39
Ext to Ext Only	Demand Prop	Boundary Centroids	30,424	-399	1.3%	16.45	21.59
Ext to Int Only						5.40	3.65
Both						16.47	21.63
Ext to Ext Only	Max Demand	Boundary Centroids	29,566	-1,257	4.1%	9.81	11.80
Ext to Int Only						5.38	3.59
Both						9.85	11.86
Ext to Ext Only	Max Demand	Region	30,638	-185	0.6%	6.40	5.96
Ext to Int Only						5.33	3.43
Both						6.41	5.98
Ext to Ext Only	Region	Region	31,070	247	0.8%	5.31	3.37
Ext to Int Only						5.36	3.54
Both						5.36	3.52

Table 6.16 Evaluation of 1-Link, 100-Percent Capacity Reduction Scenario for 7th Street: Subnetwork of Size 5

Scenario	Boundary Centroid Grouping	External Centroid Grouping	Demand	Total Demand Diff	Total Demand Error	RMSE	
						Full Subnetwork Demand	Boundary Origins Only
Impact	-	-	21,000	-	-	-	-
Base	-	-	21,226	226	1.1%	7.34	4.25
Ext to Ext Only	Demand Prop	Boundary Centroids	21,100	100	0.5%	7.53	4.82
Ext to Int Only						7.40	4.42
Both						7.58	4.97
Ext to Ext Only	Max Demand	Boundary Centroids	20,979	-21	0.1%	7.43	4.52
Ext to Int Only						7.42	4.49
Both						7.50	4.74
Ext to Ext Only	Max Demand	Region	21,106	106	0.5%	7.39	4.41
Ext to Int Only						7.39	4.41
Both						7.44	4.56
Ext to Ext Only	Region	Region	21,170	170	0.8%	7.36	4.31
Ext to Int Only						7.34	4.23
Both						7.37	4.33

Table 6.17 Evaluation of 1-Link, 50-Percent Capacity Reduction Scenario for 7th Street: Subnetwork of Size 5

Scenario	Boundary Centroid Grouping	External Centroid Grouping	Demand	Total Demand Diff	Total Demand Error	RMSE	
						Full Subnetwork Demand	Boundary Origins Only
Impact	-	-	21,201	-	-	-	-
Base	-	-	21,226	25	0.1%	3.10	2.25
Ext to Ext Only	Demand Prop	Boundary Centroids	21,220	19	0.1%	3.16	2.38
Ext to Int Only						3.18	2.45
Both						3.23	2.57
Ext to Ext Only	Max Demand	Boundary Centroids	21,192	-9	0.0%	3.10	2.24
Ext to Int Only						3.24	2.57
Both						3.23	2.56
Ext to Ext Only	Max Demand	Region	21,208	7	0.0%	3.11	2.26
Ext to Int Only						3.21	2.51
Both						3.21	2.52
Ext to Ext Only	Region	Region	21,224	23	0.1%	3.10	2.25
Ext to Int Only						3.10	2.25
Both						3.10	2.25

The results of an in-depth review of scenarios for 7th Street revealed that some improvements, although extremely minimal, could indeed be obtained for this location. Achieving this required a different combination of grouping strategies for each scenario, and one that was inconsistent with the best performing for the total demand estimation. Notably, the largest improvement was attained with a stand-alone demand adjustment process, though there was no consistency across the three scenarios evaluated. Two performed better with only the external-to-external adjustment and one with the external-to-internal adjustment alone. Again, this highlights the inconsistent performance of the strategies between different scenarios.

The scenarios chosen for the 15th Street location included the 3-link 100-percent capacity reduction for a subnetwork of size 5, the 2-link 50-percent reduction for a subnetwork of size 9, and the 1-link 100-percent reduction for subnetwork of size 9. Like before, these

scenarios were chosen based on a perceived prospect for improvement. The tables below provide results for the three scenarios.

Table 6.18 Evaluation of 3-Link, 100-Percent Capacity Reduction Scenario for 15th Street: Subnetwork of Size 5

Scenario	Boundary Centroid Grouping	External Centroid Grouping	Demand	Total Demand Diff	Total Demand Error	RMSE	
						Full Subnetwork Demand	Boundary Origins Only
Impact	-	-	19,706	-	-	-	-
Base	-	-	19,799	93	0.5%	4.70	5.43
Ext to Ext Only	Demand Prop	Boundary Centroids	19,281	-425	2.2%	4.76	5.51
Ext to Int Only						5.35	6.40
Both						5.38	6.44
Ext to Ext Only	Max Demand	Boundary Centroids	19,155	-551	2.8%	4.93	5.77
Ext to Int Only						5.75	6.98
Both						5.90	7.19
Ext to Ext Only	Max Demand	Region	18,726	-980	5.0%	9.06	11.62
Ext to Int Only						6.44	7.98
Both						10.05	12.98
Ext to Ext Only	Region	Region	18,526	-1180	6.0%	7.57	9.57
Ext to Int Only						6.19	7.61
Both						8.23	10.48

Table 6.19 Evaluation of 2-Link, 50-Percent Capacity Reduction Scenario for 15th Street: Subnetwork of Size 9

Scenario	Boundary Centroid Grouping	External Centroid Grouping	Demand	Total Demand Diff	Total Demand Error	RMSE	
						Full Subnetwork Demand	Boundary Origins Only
Impact	-	-	36,206	-	-	-	-
Base	-	-	36,266	60	0.2%	2.69	2.46
Ext to Ext Only	Demand Prop	Boundary Centroids	36,251	45	0.1%	2.69	2.46
Ext to Int Only						3.86	4.81
Both						3.86	4.81
Ext to Ext Only	Max Demand	Boundary Centroids	36,254	48	0.1%	2.69	2.45
Ext to Int Only						3.86	4.81
Both						3.86	4.80
Ext to Ext Only	Max Demand	Region	36,237	31	0.1%	2.69	2.46
Ext to Int Only						3.86	4.80
Both						3.85	4.80
Ext to Ext Only	Region	Region	36,308	102	0.3%	2.74	2.57
Ext to Int Only						3.53	4.21
Both						3.57	4.28

Table 6.20 Evaluation of 1-Link, 100-Percent Capacity Reduction Scenario for 15th Street: Subnetwork of Size 9

Scenario	Boundary Centroid Grouping	External Centroid Grouping	Demand	Total Demand Diff	Total Demand Error	RMSE	
						Full Subnetwork Demand	Boundary Origins Only
Impact	-	-	32,631	-	-	-	-
Base	-	-	32,593	-38	0.1%	2.50	2.71
Ext to Ext Only	Demand Prop	Boundary Centroids	33,097	466	1.4%	4.20	5.49
Ext to Int Only						11.07	15.47
Both						11.59	16.22
Ext to Ext Only	Max Demand	Boundary Centroids	33,365	734	2.2%	3.43	4.28
Ext to Int Only						11.07	15.47
Both						11.36	15.89
Ext to Ext Only	Max Demand	Region	32,400	-231	0.7%	2.93	3.46
Ext to Int Only						10.97	15.33
Both						11.06	15.46
Ext to Ext Only	Region	Region	32,387	-244	0.7%	2.85	3.33
Ext to Int Only						10.97	15.33
Both						11.06	15.45

Again, it was found that using an adjustment for only one type of trip could provide an improvement in the demand adjustment. Only one scenario showed an actual improvement with the applied processes, though some strategies were shown to yield much better results than others. This suggests that some adjustment strategies can actually make the demand estimation much worse depending on the scenario, and that making no adjustment may be the best option. This is especially true for scenarios where no significant difference in the boundary demand was found between the base and impact scenario obtained from the subnetwork size evaluation, indicating that the subnetwork size selection may be the more important consideration.

The fact that improvements, though sparse, could be obtained for both the 7th Street and 15th Street locations indicates that the logit adjustment strategy can work even when it would seem unlikely to provide useful results following preliminary investigation. In some cases, the results initially implied the strategy had a detrimental impact on the

demand estimation, but after further review it was revealed that beneficial adjustments could be achieved. The results, though currently inconsistent, support the idea that a refined strategy, building upon the foundation established, could work more effectively and produce valuable subnetwork demand estimates in the future.

Overall, the evaluation appeared to indicate that demand-based grouping results in a very minimal, if any, improvement to the adjustment results relative to grouping by geographically assigned region, even though these regions were somewhat arbitrarily assigned. In particular, grouping by demand proportion did not provide a noticeable improvement relative to grouping simply based on the region supplying the maximum demand for a boundary centroid. The grouping of external centroids by region performed much better than clustering by boundary centroid group.

This signifies that a simplified grouping strategy performs better, and that demand-based grouping of boundary centroids is not necessary, nor especially beneficial for use with the logit formulation. Implementing a demand-based strategy may not be worth the additional effort required, and the time may be better spent reviewing the subnetwork selection and forming the geographic regions used to group the centroids. The results from the evaluation across different subnetwork sizes (Table 6.9 on pages 264-265) further emphasize that as a subnetwork size increases, it is less meaningful to use specialized grouping strategies, as the impacts themselves are minimized.

Nonetheless, the models used in ArcGIS to group boundary centroids based on the origin of their demand may still be beneficial for visualization purposes. It could prove helpful in the general assessment of geographic-based grouping regions and provide a basic understanding of where the demand originates for an individual boundary centroid or grouping. Furthermore, demand-based grouping may be better for larger, regional networks where centroids are more spread out and the impact of forming geographical regions arbitrarily may have more of an adverse impact on the results.

From the evaluation of the logit formulation, it is notable that the adjustment strategy performed the best for the Guadalupe Street location since it was chosen for the preliminary evaluation. Had it not been chosen, the logit-based adjustment strategy may have been abandoned, as it did not perform nearly as well at the other locations. While the Guadalupe Street assessment is encouraging, the overall results raise a few concerns.

There appears to be an inconsistency between improvements in the overall demand adjustment and the detailed adjustment across individual boundary centroids, as evaluated using the RMSE. While the overall demand adjustment revealed some relatively widespread improvements across scenarios and locations, the more detailed assessment revealed little or no benefit. This is especially evident for the 7th Street and 15th Street locations, where no improvement relative to RMSE was found for any subnetwork size or scenario.

When considering 7th Street and 15th Street, the adjustment initially appeared to have an adverse effect on the demand adjustment. Since the network modifications were fixed across the locations, this suggests some inherent differences between them. Looking at the network, these locations may have had more options for users to avoid the route, resulting in more fluctuation in demand.

However, an in-depth review of the results reveals that the base demand provided a better estimate for the impact scenario at these two locations than at Guadalupe Street (see Appendix E). This indicates that there wasn't a large margin for potential improvement. Many of the scenarios resulted in a small change to the overall demand and a relatively low RMSE across the boundary. Perhaps the results are indicative of the difficulty in assessing demand changes within a well-connected portion of a network, such as the downtown area. When travelers have many options to complete a trip, it may be difficult to predict route changes based solely on estimated travel times. The connectivity of the network is likely to result in numerous fluctuations in demand or travel time within the

model. Some of these changes may be overestimated or underestimated using this type of strategy, which aims to generalize the shift in demand in order to save time and effort.

There are a number of identified limitations related to implementation of the logit formulation that appear likely to have negatively influenced the results. These include the following:

- The internal travel times are based on running the subnetwork for the base and impact scenario using the base (unadjusted) subnetwork demand – It is likely that impacts extending beyond the boundary that would change the demand would also influence the internal travel times. These changes are not captured here. Furthermore, running the subnetwork for the base scenario refines the results beyond what was achieved prior to the demand extraction, which could unduly influence the travel time assessment.
- The treatment of re-entering vehicles is simplified such that only their initial entry point and final destination are considered. This influences the demand assessment and creates some inconsistency with what was actually modeled.
- The centroids are grouped and assigned a weighted travel time for each component of a trip. This generalization results in a change in the assessed travel time associated with an individual O-D pair and results in demand adjustments made across an entire group that may not be consistent with an individual centroid.
- Travel times for routes not utilized for trips originating within a group of centroids are not evaluated as they are not available. Therefore, a comprehensive assessment of options available to users does not exist.

It is worth noting that the treatment of re-entering vehicles may have unduly influenced the results in some manner. The high number of re-entering vehicles found for many of the subnetworks resulted in the need to assess the boundary demand differently (as

outlined in Chapter 5). It further indicated that the subnetwork selection may have been inadequate and caused some unintended consequences in the analysis. Eliminating the re-entries in the demand assessment using the described JavaScript code may have subsequently biased the results. This may be substantiated by improvements found with the overall demand estimation even though they were absent at the more disaggregate level (RMSE). In other words, the adjusted subnetwork demand was closer to the impact scenario in many cases than the base demand, but the changes applied to the individual centroids were inconsistent. A degree of fuzziness is created along the boundary when vehicles are re-entering the network that influences the demand estimation and internal travel times. The adjusted code, that counts these vehicles only once, tries to cut through some of the muddle, but it also fails to capture some of the true impacts that would require a more adequate subnetwork selection.

In addition, issues associated with grouping the boundary centroids could be apparent here. Applying a reduction across all centroids within a group could result in an overgeneralization of the impact. Wholesale changes across multiple centroids are likely to be inconsistent with the real results. A close review of the results substantiates this claim. In some cases, a demand change to a centroid within a group is consistent with the impact scenario while another centroid within the same group should experience no change or move in the opposite direction. It was attempted to dampen this effect by proportionally changing demand based on the amount contributed, as well as disaggregating by destination centroid, but the individual results indicate that this strategy is still somewhat deficient.

Clearly, the more influential limitations relate to grouping the centroids. The development and evaluation of multiple grouping strategies was used to find the approach that best mitigated any resultant issues. Understanding that grouping centroids and assigning them the same travel time components would be a constraint, it was attempted to more intelligently group them so that unrelated centroids, either by demand origin or

location (or both), would not be grouped together. Ultimately, the results indicate that grouping by geographic location is the most effective. This is reasonable since centroids that may have the same demand origin may be located far apart; grouping and assigning them the same travel time components is predictably erroneous. That is why the demand-based grouping strategy for the proportional demand uses a spatial constraint.

Nonetheless, problems persist related to using groups within the framework of the logit formulation. As discussed, grouping was used to both simplify the calculations and overcome the limitation that a travel time for an individual O-D pair is only available for any used path. Since used paths must be equal and minimal within the construct of DUE, this likely results in only one path. Grouping origins allows for multiple alternative routes to a destination to be extracted; however, these options are associated with the collective group, not an individual centroid. CTR researchers are currently working on code to extract travel times for unused routes between nodes, but this is not currently available. Again, a proper assessment of alternatives would be more disaggregate, and this information would facilitate a means to properly evaluate individual O-D pairs using the logit formulas.

While the limitations are evident, the foundation is in place to improve upon using additional information extracted from the DTA model outputs. In general, the results show some promising signs. A modification scenario, particularly one of smaller magnitude, may actually result in an increase in demand for a subnetwork, as shown in the detailed results in Appendix E, even without counting re-entering vehicles more than once. It was found that the demand adjustment could capture these increases at least part of the time, indicating that the use of internal travel times to adjust demand has some merit. Furthermore, the adjustment strategy appeared to perform better relative to smaller subnetworks, where the impacts are more acute, and for larger magnitude modifications to the network (multiple link and 100-percent capacity reduction). These are all scenarios

where applying adjustments to the boundary demand would be more desirable as the subnetwork size chosen may be inadequate to contain the majority of the impacts.

The logit evaluation provides an additional means of assessing the adequacy of different subnetwork sizes. To supplement the travel time assessment obtained from the subnetwork size evaluation outlined in the previous section, the error in the demand estimation was collected here. Table 6.21 summarizes the average error in the demand estimation associated with using the base demand extracted from the full network for each scenario relative to subnetwork size.

Table 6.21 Evaluation of the Error in Demand Estimation Relative to Subnetwork Size and Scenario

Subnetwork Size	Number of Links	% Capacity Reduction	By Scenario		By # Links		By Capacity Reduction			By Subnetwork Size	
			Avg. Demand Error	Avg. RMSE	Avg. Demand Error	Avg. RMSE		Avg. Demand Error	Avg. RMSE	Avg. Demand Error	Avg. RMSE
5	3	100	1.5%	7.3	0.9%	5.4	100%	1.0%	5.9	0.8%	5.0
		50	0.4%	3.4							
	2	100	0.6%	5.3	0.7%	5.6					
		50	0.7%	5.8			50%	0.5%	4.1		
	1	100	0.9%	5.1	0.6%	4.1					
		50	0.3%	3.1							
7	3	100	0.3%	6.7	0.3%	4.9	100%	0.3%	4.6	0.4%	4.2
		50	0.3%	3.0							
	2	100	0.1%	3.5	0.6%	4.6					
		50	1.1%	5.7			50%	0.5%	3.9		
	1	100	0.4%	3.5	0.3%	3.2					
		50	0.2%	2.9							
9	3	100	0.3%	6.0	0.2%	4.2	100%	0.2%	3.7	0.2%	3.6
		50	0.1%	2.3							
	2	100	0.2%	2.5	0.4%	4.2					
		50	0.6%	5.9			50%	0.3%	3.5		
	1	100	0.1%	2.7	0.1%	2.5					
		50	0.1%	2.3							

Several trends are evident from the table. It is clear that as the subnetwork size increases, the error in the demand estimation decreases. Interestingly, the error in total demand estimation is halved going from a subnetwork with a connected order of size 5 to size 7 (0.8 percent to 0.4 percent), and is halved again going from size 7 to 9 (0.4 percent to 0.2 percent). A decrease in the RMSE for the boundary demand is evident across the change in subnetwork size as well.

This generally decreasing trend is also found relative to the number of links modified, particularly when going from two or more links to one link. Less apparent is a decrease in error relative to total demand estimation as the capacity reduction goes from 100 percent to 50 percent. A decreasing trend appears for a subnetwork of size 5, but does not exist for the other sizes. All trends relative to the RMSE assessment are more consistent and distinct. In addition to a decrease in error as the subnetwork size increases, the RMSE decreases as the network modification becomes less extensive (2 or 3 links to 1 and 100 percent to 50 percent capacity reduction).

An extensive review of the results obtained from implementing the logit-based demand estimation indicates that the formula may or may not yield an improved estimate in terms of the total subnetwork demand or the disaggregate boundary demand. Though yielding an improved estimate of the total subnetwork demand about 50 percent of the time, more often than not, the adjustment has an adverse impact on the boundary demand estimation as measured by RMSE. This impact was speculated to mainly result from grouping both external and boundary centroids in the implementation of the formulae.

Four combinations of grouping strategies were tested and it was found that grouping centroids by geographic region is the most effective, and the additional effort required to group based on the origin of boundary demand does not appear justified. While the results indicate that the limitations associated with the method adversely impact the results, a number of observations suggest the method still has potential. With a few

modifications, including a more disaggregate assessment of individual O-D pairs facilitated by code under development, the method could prove successful on a more consistent basis. Though the method in its current form proved to be minimally effective, assessment of the logit formulation across 54 scenarios provided valuable information important for the evaluation of different subnetwork sizes. The results indicated that as subnetwork sizes increase and the modification scenario becomes less extensive, the error relative to the subnetwork demand estimation decreases noticeably.

Real-World Example Applications Using the Downtown Austin Network

Throughout the subnetwork analysis and evaluation process hereto discussed, a number of important lessons were learned regarding subnetwork selection and assessment. To effectively demonstrate what was learned, the subnetwork selection process was applied to several real-world scenarios. Since one of the primary objectives was to determine the proper size of subnetwork to select and analyze relative to an impact scenario, this was determined to be paramount to the research. It was also found that evaluation of the subnetwork size provided more reliable results and recommendations than that obtained from evaluation of subnetwork demand adjustment strategies designed to account for impacts beyond the subnetwork.

Throughout the Austin downtown network there are a number of ongoing construction projects. On June 28, 2013, a short tour of the area was taken and 10 projects involving lane closures were identified. Note that this number is not meant to be inclusive of all downtown projects, but to provide a sample assortment of construction projects that would be commonly encountered by travelers in the area. The discovery accentuates the importance of using DTA to analyze the impact of TCPs on this network, as well as the adequacy of subnetwork analysis. Not only is the downtown network congested during peak periods, but construction projects involving network modifications and associated

TCPs in the area are common. The map in Figure 6.8 identifies the project locations observed.

Project	Roadway	Direction	Location	Scenario
1	Guadalupe Street	SB	Btwn 4th St and 6th St	1 lane closed; 2 links*, 25% capacity reduction
2	5th Street	EB	Btwn Brazos St and Trinity St	2 lanes closed; 3 links*, 50% capacity reduction
3a	Colorado Street	SB	Btwn 4th St and 6th St	3 lanes closed; 2 links, 75% capacity reduction
3b	5th Street	EB	Btwn Lavaca St and Colorado St	2 lanes closed; 2 links*, 50% capacity reduction
4a	5th Street	EB	Btwn Rio Grande St and San Antonio St	2 lanes closed; 2 links*, 50% capacity reduction
4b	Nueces Street	NB/SB	Btwn 5th St and 6th St	Narrow lanes; 2 links**, 25% capacity reduction
5	Lavaca Street	NB	Btwn 4th St and 7th St	1 lane closed; 3 links*, 25% capacity reduction
6	Red River Street	SB	Btwn 3rd St and 4th St	Narrow lane; 1 link, 25% capacity reduction
7	Trinity Street	NB	Btwn 1st St and 3rd St	1 lane closed; 2 links*, 50% capacity reduction
8a	Guadalupe Street	SB	Btwn 7th St and 10th St	1 lane closed; 1 link*, 25% capacity reduction 2 lanes closed; 2 links*, 50% capacity reduction
8b	8th Street	EB	Btwn San Antonio St and Guadalupe St	2 lanes closed; 1 link, 100% capacity reduction
9	8th Street	WB	Btwn Colorado St and Congress Ave	3 lanes closed; 2 links, 75% capacity reduction
10	Colorado Street	SB	Btwn 7th St and 9th St	2 lanes closed; 2 links*, 50% capacity reduction

* Includes taper extending beyond link where work area is located

** One link in each direction

Figure 6.8 Construction Project Locations Identified in the Downtown Austin Area (Basemap Source: BING © 2010 Microsoft and its Data Suppliers)

The table below the map in the figure identifies the roadway, direction of travel impacted, and location along the roadway corresponding to each project location. Each identified

project also includes a description of the type of impact in a format similar to that used for the test scenarios outlined in the subnetwork size evaluation process. Notably, the majority of the real-world impact scenarios are very comparable in scope to those tested.

To further evaluate the subnetwork size selection procedure using real-world scenarios, five of the above projects were selected for review. This includes the following locations:

1) Southbound Guadalupe Street between 4th Street and 6th Street – 2 links, 25-percent capacity reduction
2) Northbound Lavaca Street between 4th Street and 7th Street – 3 links, 25-percent capacity reduction
3) Eastbound 5th Street between Brazos Street and Trinity Street – 3 links, 50-percent capacity reduction
4) Westbound 8th Street between Colorado Street and Congress Avenue – 2 links, 75-percent capacity reduction
5) Southbound Guadalupe Street between 7th Street and 10th Street – 1 link, 25-percent capacity reduction and 2 links, 50-percent capacity reduction; Eastbound 8th Street between San Antonio Street and Guadalupe Street – 1 link, 100-percent capacity reduction

The above scenarios represent a broad array of locations and impact scenarios consistent with common construction projects in the downtown area. They are intended to demonstrate how DTA subnetwork analysis can be applied to assess the impact of real-world TCPs or other network modification scenarios.

The first scenario involves closure of one lane along Guadalupe Street between 4th Street and 6th Street (midblock). Since Guadalupe Street is a 4-lane one-way arterial, this represents a 25-percent capacity reduction (approx.) to the roadway. Two links are impacted here due to a taper beginning south of 6th Street near the midblock location

approaching 5th Street. Figure 6.9 illustrates the impact conditions as observed in the field.

Figure 6.9 Southbound Guadalupe Street South of 6th Street (Photo Taken 6/28/13)

The second scenario involves closure of one lane along Lavaca Street between 5th Street and 7th Street. Lavaca Street is another 4-lane one-way arterial, so this again represents a 25-percent capacity reduction (approx.) to the roadway. Three links are impacted here because of the taper beginning south of 5th Street. Figure 6.10 illustrates the impact conditions as observed in the field.

Figure 6.10 Northbound Lavaca Street South of 5th Street (Photo Taken 6/28/13)

The third scenario involves closure of two lanes along 5th Street between Brazos Street and Trinity Street. Fifth Street is also a 4-lane one-way arterial and this scenario represents a 50-percent capacity reduction (approx.) to the roadway. Again, three links are impacted due to a taper beginning west of San Jacinto Boulevard and the fact that the roadway between Brazos Street and San Jacinto Boulevard is divided midblock by a connector. So even though only two city blocks are impacted by the work zone, three links need to be modified. Figure 6.11 illustrates the impact conditions as observed in the field.

Figure 6.11 Eastbound 5th Street West of San Jacinto Boulevard (Photo Taken 6/28/13)

The fourth scenario involves closure of three lanes along 8th Street between Colorado Street and Congress Avenue. At this location, 8th Street is a 4-lane one-way arterial and this scenario represents a 75-percent capacity reduction (approx.) to the roadway. Only one city block is impacted due to the reconfiguration of turn lanes upstream of the site location, east of Congress Avenue (no taper deployed). However, two links in the model are affected due to another connector dividing the roadway at the midblock location. Figure 6.12 illustrates the impact conditions as observed in the field.

Figure 6.12 Westbound 8th Street at Congress Avenue (Photo Taken 6/28/13)

Finally, the fifth scenario involves closure of one lane along Guadalupe Street between 9th Street and 10th Street, two lanes along Guadalupe Street between 7th Street and 9th Street, and full closure of eastbound 8th Street between San Antonio Street and Guadalupe Street. Again, in this area, Guadalupe Street is a 4-lane arterial and this scenario is a combination of a 25-percent capacity reduction (approx.) for one lane and a 50-percent capacity reduction (approx.) for two lanes. At this location, 8th Street is a 4-lane two-way collector and this scenario represents a 100-percent capacity reduction to the roadway in the eastbound direction. In total, four city blocks are impacted due to tapers upstream of the work area along Guadalupe Street represented by four links in the model. Figures 6.13 and 6.14 illustrate impact conditions along Guadalupe Street and 8th Street, respectively, as observed in the field.

Figure 6.13 Southbound Guadalupe Street at 9th Street (Photo Taken 6/28/13)

Figure 6.14 Eastbound 8th Street at Guadalupe Street (Photo Taken 6/28/13)

The next task is to select a subnetwork size for each scenario consistent with the recommendations put forth in the evaluation conducted earlier. For the first scenario,

involving a 25-percent capacity reduction across two links, the recommended subnetwork from Table 6.6 on page 256, or using Figure 6.7 on page 257, is consistent with a connected order of size 5. For the second scenario, involving a 25-percent capacity reduction across three links, the recommended subnetwork from the figure is consistent with a connected order of size 7. For the third scenario, involving a 50-percent capacity reduction across two links, the recommended subnetwork is also consistent with a connected order of size 7.

For the fourth scenario, involving a 75-percent capacity reduction to two links, Table 6.6 must be interpolated using engineering judgment. The recommended sizes for 50-percent and 100-percent capacity reduction scenarios involving one link are 7 and 10+, respectively. Noting that the applicable range extends from 5 to more than 10 for these scenarios, and that 8th Street does not appear to be a critical link at this location, a subnetwork of size 7 is chosen. The need to interpolate the table for certain scenarios demonstrates the value of Figure 6.7.

The fifth and final scenario again involves a combination of a 25-percent capacity reduction to one link, a 50-percent capacity reduction to two links, and a 100-percent capacity reduction to one link. The 100-percent capacity reduction appears to be the controlling factor and yields a recommended subnetwork size, according to the table, consistent with a connected order of 9. The recommended subnetwork sizes for the five scenarios are identified in Figure 6.15.

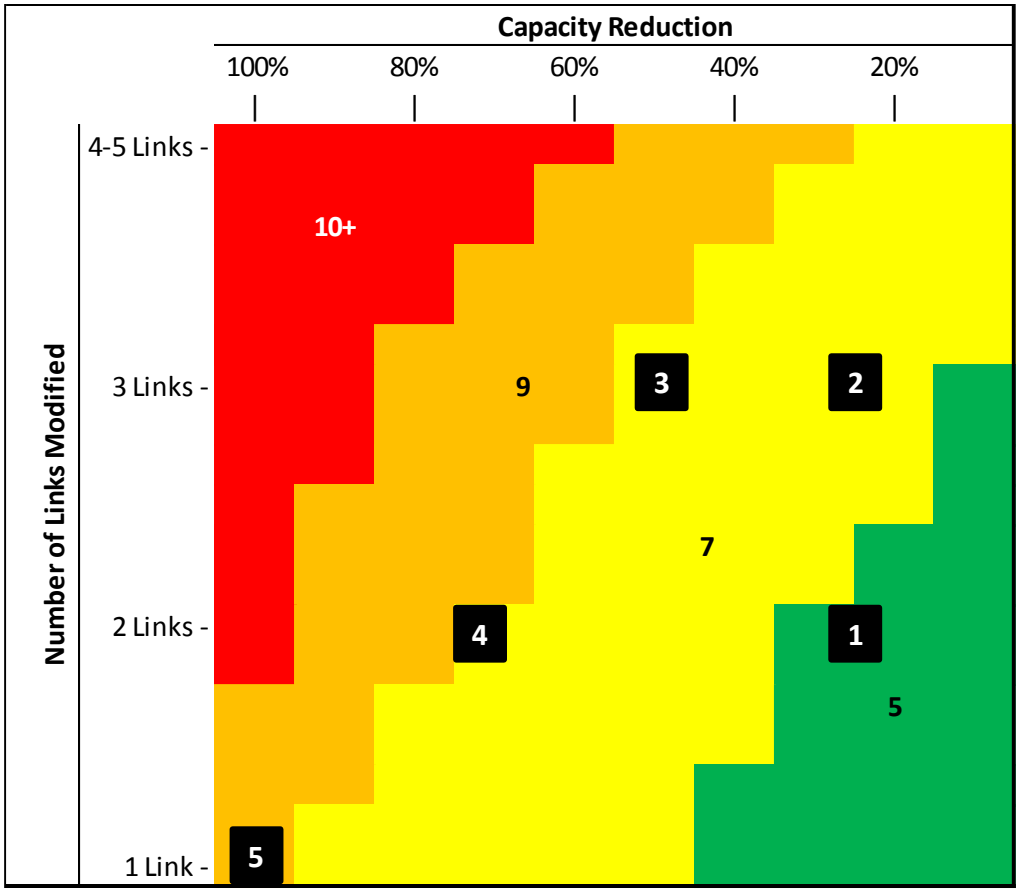

Figure 6.15 Recommended Subnetwork Sizes for Each Real-World Scenario

To evaluate the effectiveness of the subnetworks selected, the boundary demand was compared between base and impact conditions using a similar process to that outlined in the subnetwork size evaluation. A hypothesis test was conducted to determine if each chosen subnetwork was adequate. The test was applied for a sample size of 10 base runs and 10 impact runs for each TCP scenario. Again, the chosen subnetworks are consistent with the recommendations provided earlier. The results of this analysis for one-hour (peak hour) and two-hour (peak period) intervals, respectively, are summarized in Tables 6.22 and 6.23.

Table 6.22 Hypothesis Test Results for Real-World Scenarios: 1-Hour Period

					Hypothesis Testing				Prediction Interval			
						Normality Test						
Scenario	Location	Subnetwork Size (Order)	Impact Size	Capacity Reduction	Equal Variance*	Lilliefor**	A-D**	Equal Mean***	Lower Bound	Upper Bound	Range	Alternate Runs Within
Base	Guadalupe St	5	2	25		Y	Y		1.54	4.20	2.66	10
Treatment	Guadalupe St	5	2	25	N	Y	Y	Y	2.15	3.33	1.18	7
Base	Lavaca St	7	3	25		Y	Y		1.84	4.57	2.72	10
Treatment	Lavaca St	7	3	25	Y	Y	Y	Y	1.95	4.60	2.65	10
Base	5th St	7	3	50		N	Y		1.02	2.81	1.80	10
Treatment	5th St	7	3	50	Y	Y	Y	Y	1.37	2.62	1.25	9
Base	8th St	7	2	75		Y	Y		1.38	3.59	2.22	9
Treatment	8th St	7	2	75	Y	Y	Y	Y	1.23	4.00	2.77	10
Base	Guadalupe St	9	4	25-50-100		Y	Y		0.67	2.59	1.93	10
Treatment	Guadalupe St	9	4	25-50-100	Y	Y	Y	Y	1.10	2.13	1.03	9

* Y = Accept H_o: $\sigma_1^2 = \sigma_2^2$; N = Reject H_o, conclude H_a: $\sigma_1^2 \neq \sigma_2^2$ (at the 95-percent confidence level)
** Y = Accept H_o: Distribution is normal; N = Reject H_o, conclude H_a: Distribution is not normal (at the 95-percent confidence level)
*** Y = Accept H_o: $\mu_1 = \mu_2$; N = Reject H_o conclude H_a: $\mu_1 \neq \mu_2$ (at the 95-percent confidence level)

Table 6.23 Hypothesis Test Results for Real-World Scenarios: 2-Hour Period

					Hypothesis Testing				Prediction Interval			
						Normality Test						
Scenario	Location	Subnetwork Size (Order)	Impact Size	Capacity Reduction	Equal Variance*	Lilliefor**	A-D**	Equal Mean***	Lower Bound	Upper Bound	Range	Alternate Runs Within
Base	Guadalupe St	5	2	25		Y	Y		1.50	3.74	2.24	10
Treatment	Guadalupe St	5	2	25	N	Y	Y	Y	2.14	3.19	1.04	7
Base	Lavaca St	7	3	25		Y	Y		1.95	4.23	2.28	10
Treatment	Lavaca St	7	3	25	Y	Y	Y	Y	2.03	4.18	2.15	9
Base	5th St	7	3	50		Y	Y		1.01	2.56	1.55	10
Treatment	5th St	7	3	50	Y	Y	Y	Y	1.33	2.40	1.07	10
Base	8th St	7	2	75		Y	Y		1.38	3.49	2.11	9
Treatment	8th St	7	2	75	Y	Y	Y	Y	1.08	4.20	3.12	10
Base	Guadalupe St	9	4	25-50-100		Y	Y		0.95	2.36	1.41	10
Treatment	Guadalupe St	9	4	25-50-100	Y	Y	Y	Y	1.05	2.29	1.24	10

* Y = Accept H_o: $\sigma_1^2 = \sigma_2^2$; N = Reject H_o, conclude H_a: $\sigma_1^2 \neq \sigma_2^2$ (at the 95-percent confidence level)
** Y = Accept H_o: Distribution is normal; N = Reject H_o, conclude H_a: Distribution is not normal (at the 95-percent confidence level)
*** Y = Accept H_o: $\mu_1 = \mu_2$; N = Reject H_o conclude H_a: $\mu_1 \neq \mu_2$ (at the 95-percent confidence level)

The results indicate that the subnetwork sizes chosen for each modification scenario were adequate for containing the network impacts relative to boundary demand. The null hypothesis was chosen for the hypothesis test of equal means between the base and impact conditions for each scenario. The interpretation stands that the measure of the boundary demand for each modification scenario was not statistically different from the base conditions for the subnetwork sizes implemented. This result was supported by the

finding that the vast majority of the error measures for each model run fell within the prediction interval for the alternate conditions (base versus impact).

Nearly all of the equal variance and normality checks passed their respective hypothesis tests as well. The equal variance test failed only at the smallest of subnetworks analyzed. The one-hour and two-hour results were also very comparable, reflecting a consistency in the analysis measures beyond what was seen in the evaluation of the test scenarios. By in large, the subnetworks analyzed appeared adequate for all five of the respective real-world scenarios. Analysis of the error measures was also encouraging, as shown in Table 6.24. The error measures were generally lower than those reported for the test scenarios with the exception of the larger Guadalupe Street/8th Street scenario that impacted four links, more than any tested.

Table 6.24 Evaluation of Error Measures for Real-World Scenarios

	Error					
	Demand		Link Travel Time (sec)		Link Volume	
Network (Size)	Total	RMSE	MCAPE	RMSE	MCAPE	RMSE
Full Networks	-	-	-	-	-	-
Guadalupe Subnetwork (5)	0.0%	2.8	14.9%	5.8	18.5%	13.0
8th Subnetwork (7)	0.0%	3.1	14.0%	5.8	18.2%	11.4
5th Subnetwork (7)	0.2%	2.3	14.4%	5.6	18.8%	17.4
Lavaca Subnetwork (7)	0.3%	3.4	12.0%	5.9	20.3%	13.3
Guadalupe Subnetwork (9)	0.0%	2.2	12.3%	14.7	22.1%	17.1
Size 7 Subnetworks	*0.2%*	*2.9*	*13.5%*	*5.8*	*19.1%*	*14.0*
All Subnetworks	**0.1%**	**2.8**	**13.5%**	**7.6**	**19.6%**	**14.4**

Table 6.24 shows the RMSE relative to the subnetwork boundary demand, as well as the travel times and volumes for the links across each subnetwork analyzed, including averages for the size 7 subnetworks and across all of the subnetworks. In addition, the MCAPE values are reported for the link travel times and volumes. The demand error measures were noticeably low, and the travel time measures were also favorable (less than 6 seconds per link).

While the error measures for the link volumes were relatively high, this is not necessarily indicative of poor results. A change in link volume along uncongested links does not influence the subsequent free-flow speed or travel time and thus, does not always affect the path selection process. Therefore, fluctuations do not necessarily indicate that the analysis is faulty, just that differences in assignment have occurred. Outbound links along the boundary of the subnetworks also function at free flow since the boundary centroids act as an artificial sink at these locations. These are likely contributing factors to the reported differences in both travel time and volume and may impact the route assignment for outbound trips. To reiterate, the error measures are reported relative to the analysis of the network modification using the full network. The full network results provide a benchmark, or a baseline for evaluation, but do not represent absolute truth.

In addition to the subnetwork size validation, the real-world scenarios were evaluated using the logit-based demand adjustment. This required selecting subnetworks smaller than those recommended for each scenario. As such, the Lavaca Street, 5th Street, 8th Street, and Guadalupe Street/8th Street scenarios were evaluated using subnetworks consistent with a connected order of 5. The larger Guadalupe Street/8th Street scenario was also evaluated with a subnetwork of size 7. Since the smaller Guadalupe Street scenario (2-link, 25-percent capacity reduction) already resulted in a recommended subnetwork of size 5, it was not evaluated with the demand adjustment.

Unlike the test cases, the subnetworks for the real-world scenarios were chosen such that the number of re-entering vehicles would be minimized. This involved the selection of additional links, beyond those chosen using the (automated) selection tool, to close gaps along the boundary. Therefore, supplemental to an evaluation of the demand adjustment, the subnetwork models with the modified boundary demands could be run using VISTA, and additional results compared with the baseline model.

Evaluation of the five real-world scenarios revealed that the logit-based demand adjustment did not improve the estimation of the boundary demand compared to a fixed demand table. This was relatively consistent with the test scenario evaluation. Nonetheless, to determine if the demand adjustment improved the capability of a subnetwork model to assess a particular impact scenario, the link volumes and travel times were evaluated using the RMSE and MCAPE with the full network impact scenario results as the baseline. A comparison was made between running the subnetwork model without an adjusted demand versus implementing the adjustment strategies described earlier involving different centroid grouping methods. The results of this assessment are summarized in Table 6.25.

The highlighted cells in the table indicate where an RMSE or MCAPE value was lower for the subnetwork model run with the corresponding demand adjustment implemented when compared to results using a fixed demand table. As shown before, there was little to no consistency in terms of the performance of the different grouping methods. No strategy appeared to uniformly yield better results when compared to the other strategies, including the fixed demand table. Where identified, the improvements were generally modest and little consistency was found in terms of performance with respect to the error measure assessed.

Notably, improvements in terms of link travel times were more common than link volumes. This is a favorable result, as improvements in terms of link travel times are more attractive than link volumes. As noted earlier, volume fluctuations are common in the DUE process and do not always result in a change in travel time (e.g. when links are operating at FFS). Therefore, link travel times are generally more valuable in the assessment of model performance.

Table 6.25 Evaluation of Link Travel Time and Volume Error Measures for Real-World Scenarios

Network	Subnetwork Size (Order)	Scenario		Grouping Strategy*	RMSE		MCAPE	
		# Links	% Capacity Reduction		Travel Time	Volume	Travel Time	Volume
Lavaca Street	5	3	25	None	5.83	20.70	15.30	22.73
				Grouping 1	5.73	25.77	15.18	25.15
				Grouping 2	5.65	20.99	15.16	23.34
				Grouping 3	5.44	21.87	15.10	24.37
				Grouping 4	5.57	21.07	15.17	22.99
5th Street	5	3	50	None	9.28	16.67	19.07	18.53
				Grouping 1	9.09	15.72	18.37	18.53
				Grouping 2	9.39	16.46	19.37	19.56
				Grouping 3	9.21	14.82	19.47	18.05
				Grouping 4	9.26	16.42	19.57	18.92
8th Street	5	2	75	None	6.09	11.08	17.51	15.25
				Grouping 1	6.18	11.29	17.31	16.32
				Grouping 2	5.92	11.54	16.89	15.40
				Grouping 3	6.11	12.85	17.61	15.98
				Grouping 4	6.19	12.38	17.26	16.79
Guadalupe Street	5	4	25-100	None	6.40	17.37	14.14	26.72
				Grouping 1	6.44	17.05	14.08	26.57
				Grouping 2	6.59	18.72	14.30	27.79
				Grouping 3	6.56	16.83	13.94	26.53
				Grouping 4	6.94	17.39	14.41	27.57
Guadalupe Street	7	4	25-100	None	24.79	22.36	17.20	25.63
				Grouping 1	26.82	23.55	16.80	27.17
				Grouping 2	28.22	24.11	16.60	27.62
				Grouping 3	20.86	22.99	16.90	26.67
				Grouping 4	24.12	24.31	17.08	27.25

* Grouping 1 – Boundary centroids by proportional demand and external centroids by boundary centroids
Grouping 2 – Boundary centroids by maximum demand and external centroids by boundary centroids
Grouping 3 – Boundary centroids by maximum demand and external centroids by region
Grouping 4 – Boundary centroids by region and external centroids by region

Additional Assessment of Computational Effort and Error Measures

In a final assessment of the viability of using subnetworks to analyze impacts of network modifications, typical network attributes and file sizes, along with computational times were compiled and compared to the models for the full downtown Austin network. In addition, the error measures associated with different subnetwork sizes in terms of demand estimation and link travel time and volume measures for 27 different subnetworks were evaluated. Four copies of the entire downtown network were used in the comparison to represent the full network. The computational time and space required to produce the models and complete the DTA runs evaluated using the JavaScript code are summarized in the tables below. Other relevant performance measures are also shown.

Table 6.26 Typical Network Performance Specifications (I)

Network	# Links	# Nodes	# Vehicles	Gap Measure	% Imp	Output File Size (MB)	% of Full Network
Full Network	1,578	717	97,606	1.6	-	21.3	-
Subnetwork Size 5	267	145	23,521	0.4	74%	3.0	14%
Subnetwork Size 7	435	218	38,767	0.7	57%	5.2	24%
Subnetwork Size 9	616	301	46,415	1.6	-1%	7.7	36%

Table 6.26 identifies the typical network sizes in terms of the number of links, nodes, and vehicles. These values are the same for all versions of the full network, but vary for the subnetworks based on location and scenario within each size category. Nine samples of each subnetwork size ranging between a connected order of 5 and 9 were used to compile average values for the network elements. The values for the connected order of 11 are not reported since only a small subset was used in the analysis.

Eighty-four subnetwork runs and 21 full network runs were used to compile the performance specifications in the table. These runs were taken from evaluation of the

logit formulation where the random seeds were fixed. These model results were used to maintain as much consistency as possible between the full network and subnetwork model runs. The convergence measures are based on the average relative gap achieved for each of the model runs for a particular size. The percent improvement is also documented to compare the performance of subnetworks to the full network runs with respect to convergence. The average gap level achieved appears to increase with subnetwork size, indicating that it is more difficult for the larger models to reach convergence within the same number of iterations.

As expected, the output file sizes for the full network were much larger than that produced by the subnetwork models, though these increase with subnetwork size. Table 6.27 shows a similar trend with respect to the computational time required to complete 50 model iterations of the DTA process (path generation and DUE) using the developed JavaScript code.

Table 6.27 Typical Network Performance Specifications (II)

Network	Time to Complete 50 Iterations (min)	% of Full Network	Error					
			Demand		Link Travel Time (sec)		Link Volume	
			Total	RMSE	MCAPE	RMSE	MCAPE	RMSE
Full Network	139.1	-	-	-	-	-	-	-
Subnetwork Size 5	50.5	36%	0.8%	5.0	18.4%	8.8	24.1%	19.7
Subnetwork Size 7	53.1	38%	0.4%	4.2	16.9%	15.2	24.7%	19.1
Subnetwork Size 9	56.5	41%	0.2%	3.6	13.8%	11.6	21.1%	19.3

The table reveals that the subnetwork models took, on average, less than half the time to complete than a full network model. This was true of all sizes, which vary somewhat within each category between the 1-link and 3-link scenarios, with the subnetworks associated with a connected order of 5 taking just over one-third of the computational time compared to a full network model.

The table also summarizes the average error values associated with using each size of subnetwork based on the results reported in the previous sections. Essentially, this establishes a measure of the anticipated error associated with a choice of subnetwork size for a given impact scenario consistent with those tested. These measures are included here to demonstrate the trade-off between the performance benefits achieved using a subnetwork with the cost in terms of accuracy relative to a full network analysis. For example, for a subnetwork of size 5, though the computational savings are attractive, the subnetwork boundary demand has a RMSE of five vehicles.

The error measures for link travel time and volume may appear large on the surface. It is important to reiterate that the error measures are relative to the full network analyses, not real-world conditions. Therefore, the results indicate that the subnetwork analysis is different, though not necessarily wrong. In many ways, as demonstrated by the convergence measures, the subnetwork analysis is more refined and should be expected to vary compared with the full model results. This is substantiated by the error in demand estimation. It should be anticipated that differences in the demand at the boundary of the subnetwork, as reported, would influence the assignment process. With path generation initiated for all 50 model iterations, any divergence in assignment would be amplified. As noted earlier, the uncongested portions of the network, including outbound links along the boundary, are also expected to influence the results and contribute to these differences.

It was anticipated that the type of modification scenario would influence the accuracy of the results relative to the full network models. Therefore, a comparison of the error measures across different scenarios was conducted similar to that undertaken for the error in demand estimation provided in Table 6.21 on page 285. The error measures were compiled based on the number of links impacted and the percent capacity reduction imposed. As shown in Tables 6.28 and 6.29, as the scope of the scenario increases, the error generally increases as well.

Table 6.28 Evaluation of Error Measures by Number of Links Impacted

Links Impacted	Travel Time (sec)		Link Volume	
	MCAPE	RMSE	MCAPE	RMSE
1 Link	14.4%	9.9	20.8%	16.9
2 Links	16.8%	12.8	22.9%	20.3
3 Links	17.5%	13.0	24.5%	21.2

Table 6.29 Evaluation of Error Measures by Percent Capacity Reduction

Capacity Reduction	Travel Time (sec)		Link Volume	
	MCAPE	RMSE	MCAPE	RMSE
25 Percent	13.4%	6.9	19.8%	14.3
50 Percent	15.8%	12.6	22.5%	18.7
100 Percent	18.2%	12.3	26.7%	23.5

Some encouraging results were found with respect to the analysis of real-world scenarios. Tables 6.30 and 6.31 show the network performance specifications for the five scenarios chosen for analysis, as well as averages for the three subnetworks of size 7 and all of the subnetworks combined. Many of the same trends identified with the test scenarios are demonstrated here. A much better convergence was achieved except for the larger Guadalupe Street scenario. Substantially smaller output file sizes and lower computational times were also found.

Table 6.30 Network Performance Specifications for Real-World Scenarios (I)

Network	# Links	# Nodes	# Vehicles	Gap Measure	% Imp	Output File Size (MB)	% of Full Network
Full Networks	1,578	717	97,606	1.5	-	21.4	-
Guadalupe (5) Subnet	245	124	25,455	0.2	85%	3.4	16%
8th (7) Subnet	430	218	35,593	0.2	89%	5.0	23%
5th (7) Subnet	456	233	47,219	0.2	85%	6.9	32%
Lavaca (7) Subnet	498	228	38,797	0.3	80%	6.0	28%
Guadalupe (9) Subnet	698	311	48,116	3.2	-115%	8.1	38%
Size 7 Subnetworks	*461*	*226*	*40,536*	*0.2*	*85%*	*6.0*	*28%*
All Subnetworks	**465**	**223**	**39,036**	**0.8**	**45%**	**5.9**	**28%**

In a noticeable deviation from the test scenario findings, the error measures with respect to boundary demand and link travel times and volumes were lower (Table 6.31). Again, with exception to the larger Guadalupe Street scenario, the subnetwork results appeared to be closer to those obtained from the full network models than what was found with the test scenarios (Table 6.27 on page 303). Generally, the error measures were lower for the larger subnetworks, particularly with respect to MCAPE, though this trend was less apparent for RMSE. This is likely due to the fact that only one size was evaluated for each real-world scenario based on the recommendations, whereas all three reported sizes were examined for each test scenario.

Table 6.31 Network Performance Specifications for Real-World Scenarios (II)

Network	Time to Complete 50 Iterations (min)	% of Full Network	Error					
			Demand		Travel Time (sec)		Link Volume	
			Total	RMSE	MCAPE	RMSE	MCAPE	RMSE
Full Networks	107.6	-	-	-	-	-	-	-
Guadalupe (5) Subnet	39.7	37%	0.0%	2.8	14.9%	5.8	18.5%	13.0
8th (7) Subnet	36.0	33%	0.0%	3.1	14.0%	5.8	18.2%	11.4
5th (7) Subnet	37.7	35%	0.2%	2.3	14.4%	5.6	18.8%	17.4
Lavaca (7) Subnet	26.2	24%	0.3%	3.4	12.0%	5.9	20.3%	13.3
Guadalupe (9) Subnet	46.0	43%	0.0%	2.2	12.3%	14.7	22.1%	17.1
Size 7 Subnetworks	*33.3*	*31%*	*0.2%*	*2.9*	*13.5%*	*5.8*	*19.1%*	*14.0*
All Subnetworks	**37.1**	**35%**	**0.1%**	**2.8**	**13.5%**	**7.6**	**19.6%**	**14.4**

Overall, the savings associated with computational time and effort is well-documented in the tables above. Though the performance for the downtown Austin network does not offer as stark a contrast as that identified in the evaluation of the DTA models for the DFW regional network, where nearly 950 computational hours were saved, a substantial reduction in the computational time and space required was achieved using the implemented subnetworks. Notably absent in the downtown assessment is the substantial benefit in terms of the effort on the part of the analyst. The more than 40 calendar days saved using a subnetwork analysis for the DFW network demonstrates the burden associated with running the DTA processes manually.

This advantage is not apparent with respect to the downtown Austin network since the script can be implemented for the full network model. Provision of a regional network/subnetwork comparison fully exhibits the potential benefits of incorporating subnetwork analyses, particularly when multiple scenarios require review. Nonetheless, demonstrating the advantages of using a subnetwork within a smaller full network, especially where the automated process can be used, lends additional support for the use of subnetworks.

7. CONCLUSIONS AND RECOMMENDATIONS FOR FUTURE RESEARCH

The subnetwork analysis capability is intended to allow a user to run a traffic simulation model on a specific portion of a large network. For this application, subnetwork analysis is intended to enable one to complete a detailed DTA model of only the roadways surrounding a TCP or other network modification to take into account traffic impacts in an efficient and accurate manner. Implementation of subnetwork analyses have been shown to greatly reduce the computational resources and effort required to run multiple DTA models and provide practical results for the software user in a timely fashion.

As part of this study, subnetworks were extracted from both a large-scale regional model, Dallas-Fort Worth, and a more compact network, downtown Austin. The use of subnetwork DTA models within these networks on opposite ends of the spectrum effectively demonstrated their benefit with respect to reducing the amount of computational time, effort, and space required to complete a DTA analysis. For the subnetworks extracted from the downtown Austin network, file sizes were reduced to approximately a third of that of the full network, or less, depending on the subnetwork size selected. For all tested sizes, computational times were reduced by more than half and gap measures were also reduced in most cases. These benefits were accentuated with respect to the DFW regional network.

For this network, file sizes were reduced by approximately two-thirds and computational times by more than 90 percent. Furthermore, the amount of time required to run the DTA model was reduced by approximately 42 days. This exemplified a decrease in the level of effort required on the part of the analyst. The reduced burden was largely due to the fact that smaller networks, including the evaluated subnetworks, can be modeled using a JavaScript code that automates application of the DTA processes within the VISTA software that would otherwise have to be performed manually.

It should be noted that there are trade-offs when using a subnetwork analysis, notably with respect to the accuracy achieved by the model. When using a subnetwork model, the error in estimated demand for the subnetwork and travel time measures obtained within it, with respect to analysis of an impact scenario, increase as the subnetwork size decreases. These assessed error measures were reported relative to re-analysis of the full network under impact conditions in the study. Therefore, the results indicate that a subnetwork analysis is noticeably different and, as demonstrated by the convergence measures, often more refined. Due to a number of influential factors identified, including estimation of boundary demand and consideration of uncongested portions of the subnetwork, the subnetwork analysis should be expected to vary compared with the full model results. It is important to point out these trade-offs since understanding a model's limitations can aid in the proper selection of a subnetwork for analyzing the impact of a particular network modification. For instance, knowing the anticipated error relative to a subnetwork size for a given scenario, one can determine a subnetwork's adequacy for completing the planned analysis.

In addition to demonstrating the computational benefit of implementing a subnetwork analysis, along with identifying the trade-offs in terms of accuracy relative to a full network model, this research set out to answer a number of important questions facing engineers tasked with reviewing TCPs or other types of network modifications. To answer these questions, subnetwork selection strategies, sizes, and demand estimation procedures were developed and evaluated. As part of this process, three sample project locations and 81 impact scenarios were evaluated, incorporating subnetworks of varying sizes within the downtown Austin network. To increase the efficiency of implementation and facilitate timely evaluation, components of the methodology were automated. Numerous software scripts and models were developed to complete this task using available software programs, including ArcGIS and Matlab.

The use of ArcGIS proved essential for providing a visual representation of network elements and compiling vital attributes in an accompanying database, as well as developing models required for selection of subnetwork elements and implementation of proposed strategies. Additionally, Matlab facilitated the means of extracting, manipulating, and organizing large quantities of data, as well as performing repetitive and complex calculations over vast datasets. These programs were used in conjunction with each other, along with the DTA analysis software VISTA, to implement the proposed strategies, perform the DTA analyses, and output results in an efficient manner for review.

The primary objectives of the research centered on evaluating subnetwork sizes to determine the appropriate extents required to analyze network modifications and developing a strategy to account for impacts extending beyond the subnetwork boundary. The first objective was accomplished through an in-depth review of subnetwork sizes relative to multiple impact scenarios. The evaluation was conducted on 81 impact scenarios across three locations within the downtown Austin network. A combination of network modifications varying with respect to roadway capacity reduction, ranging from 25 percent to 100 percent, and project length, ranging from one to three links, were used to assess a variety of possible impact scenarios. A field review of area construction activity indicated that these sample scenarios were appropriate.

Three statistical measures were implemented to evaluate the adequacy of subnetwork sizes relative to the designated impact scenarios based on an assessment of boundary demand. These measures included the root mean squared error (RMSE), mean censored absolute percentage error (MCAPE), and the structural similarity (SSIM) index. These measures have all been proven through previous research to be effective for evaluating network demand tables relative to a target O-D matrix. For this study, the average subnetwork demand extracted from multiple runs of the full network under base conditions was established as the target or benchmark. Demands extracted from the full

network under impact conditions along the boundary of different subnetwork sizes were compared to the benchmark values to determine when statistically significant differences occurred and a subnetwork size was deemed inadequate. In the subsequent evaluation, the RMSE proved to be the most reliable indicator of where, or at what subnetwork size, an impact scenario exhibited a statistically significant deviation in demand compared to the base scenario.

Although the MCAPE and SSIM index did not provide as valuable of results, these tools are still useful for comparing model runs. Additional modifications to the strategy for applying the SSIM index could prove fruitful since this measure is effective for evaluating O-D matrices, and assessing demand is such an important element of subnetwork analysis. Ultimately, the RMSE evaluation was used successfully to provide a series of recommended subnetwork sizes associated with an array of possible impact scenarios. These recommendations were validated, and application of the proposed methodology demonstrated, using five scenarios selected from real-world network modifications observed in the field. Future research can be used to extend this evaluation to a larger network, including locations where the surrounding area exhibits less connectivity.

While the primary effects of a network modification can often be contained within a properly selected subnetwork boundary, some modification scenarios may be of a large enough scope that a reasonably sized subnetwork cannot contain these critical impacts, or circumstances dictate that an adequately sized subnetwork cannot be employed. For these instances, accounting for impacts beyond the subnetwork is of great interest. Failing to do so, or ignoring potential inadequacies, could adversely affect DTA analysis results and potentially lead to erroneous conclusions.

When a network is altered, the impact on traffic flow and route choice behavior extends outward from the modified element(s). When a subnetwork is not large enough to contain

this impact, the goal is to capture related fluctuations at the subnetwork boundary, the farthest extent for which the impact can be accounted for in the model. When impacts to inbound trips pass beyond the boundary, there is a change in flow at this location that can be represented by a change in the demand assigned to the subnetwork at each entry point.

Therefore, two strategies for adjusting the demand at subnetwork boundaries were implemented and evaluated. The first strategy involved using STA model results to estimate respective changes to demand at the subnetwork boundaries for implementing with DTA models. The second strategy involved using a logit formulation to estimate demand adjustments based on differences in internal travel times, and respective utilities of associated entry points at boundary centroids, between base and impact scenario subnetwork DTA models.

Preliminary results from the STA-based demand adjustments provided little evidence that the modifications yield noticeable improvements for the accompanying DTA subnetwork model. One of the major limitations associated with this strategy is the assumption that the changes observed from the STA models occur during all time intervals of the DTA model. Even if some predefined distribution is assigned to these results, there is no way to truly account for the time varying effects with this strategy. Even though the magnitudes of volume changes appeared reasonable for adjusting subnetwork boundary demands compared to the full network impact scenario model, the location of these changes across the subnetwork boundary were noticeably different. This led to the conclusion that another strategy sensitive to changes in travel time within the subnetwork due to a network modification may be more appropriate.

It was speculated that a logit formulation could be used to improve the estimation of the subnetwork demand, specifically along the boundary. Since preliminary results showed that improvements to the boundary demand could be achieved when applying the logit method, this strategy was selected for large-scale implementation and testing. Fifty-four

of the 81 originally selected scenarios, inclusive of all three locations and the more substantial modification scenarios, were chosen for thorough evaluation.

Application of the logit model relied on an assessment of the utility of route choices with respect to travel times and the derivation of appropriate formulas. This process was then employed to assess both external-to-external and external-to-internal trips so that the impact of changes to internal travel times on traffic flow entering the subnetwork could be determined. Implementing the proposed methodology involved simplifying the network representation and grouping centroids based on similar attributes. Centroids were grouped in order to streamline subsequent calculations and to provide an adequate array of route choices for evaluation using the formulas. Due to limitations anticipated with this approach, four alternate strategies for grouping external and boundary centroids based on a combination of demand- and location-based methods were evaluated in detail.

An in-depth performance review revealed that strategies involving the grouping of centroids simply by geographic region performed the best, and that demand-based grouping of boundary centroids may not be necessary or especially beneficial for use with the logit formulation. The accompanying examination of the results showed that application of the logit model could provide an improved estimate of subnetwork boundary demand compared to use of a fixed demand table extracted from the base model. However, not all of the scenarios exhibited an actual improvement with the applied processes, though some strategies were shown to yield much better results than others. This suggests that some adjustment strategies can actually make the demand estimation worse depending on the scenario, and that making no adjustment may be the best option. This is especially true for scenarios where no significant difference in the boundary demand was found between the base and impact scenario as obtained from the subnetwork size evaluation, indicating that the subnetwork size selection may be the more important consideration.

In addition to the subnetwork size validation, the real-world scenarios were evaluated using the logit-based demand adjustment. Unlike the test cases, the subnetworks for the real-world scenarios were chosen such that the number of re-entering vehicles would be minimized, enabling the subnetwork models with the modified boundary demands to be run using VISTA. Evaluation of the five real-world scenarios revealed that the logit-based demand adjustment did not improve the estimation of the boundary demand compared to a fixed demand table; however, improvements in terms of link travel times and volumes were found from the subnetwork analysis results suggesting that the demand adjustment could improve the accuracy of model results with respect to the full network analysis. Nonetheless, where identified, the improvements were generally modest and little consistency was found in terms of performance with respect to the error measure assessed or centroid grouping strategy implemented.

The inconsistent performance of the logit formulation in large-scale implementation highlights the limitations of the methodology as applied for this study. However, the results suggest that a refined strategy that builds on the foundation established could work more effectively, producing valuable subnetwork demand estimates and subsequent link performance measures in the future. The goal would be to overcome the limitations of the tested methodology, which aimed to simplify the process in order to save time. This simplification appears to have a tendency to negatively impact the demand estimation. Overcoming this limitation may be facilitated using a software code currently under development at CTR that will enable the compilation of travel times for unused routes between individual O-D pairs, thus eliminating the need to group centroids in order to provide adequate route alternatives. Automating the calculations required to implement a refined strategy based on the Matlab code already established could be used to retain some of the efficiency achieved with the implemented methodology.

With any strategy, understanding the constraints that exist relative to using a contracted network is important. The logit method, or any other developed strategy, cannot be

expected to correctly predict all impacts extending beyond the subnetwork or the magnitude of the effect on the boundary demand due to subsequent assumptions that must be made regarding the external component of entering trips. Further investigation of this issue appears warranted as overcoming this limitation is likely a rewarding goal.

Ultimately, choice of a subnetwork may be dependent on what questions the analyst would like answered. One should always be cognizant of constraints relative to the availability of time to complete the analysis, as well as the area of influence. The analyst or stakeholders may be concerned with a particular portion of the network, perhaps roadways for which they have jurisdiction or where they can apply strategies to mitigate impacts, communicate with travelers, or divert or detour traffic. In this sense, the goal may be to investigate impacts that are critical from a practical standpoint. While an automated subnetwork selection process was largely demonstrated in this study, in some cases, such as the one used for the DFW regional network, manual subnetwork selection may be more appropriate.

The DFW network case study demonstrated the use of this type of analysis to encompass an area important to stakeholders. The automated process of selecting subnetwork elements based on the provided recommendations may then be used as a basis, or a minimum selection area to include. It is extremely important that any subnetwork selection take into account the nature of the scenario, the network elements being modified, and the composition of the surrounding network. Therefore, engineering judgment remains an important part of the subnetwork selection and analysis process.

Overall, this research was used to provide recommendations for selecting and analyzing subnetworks using DTA for an array of common impact scenarios involving network modifications. The trade-offs between improved efficiency and reduced accuracy associated with using subnetworks were thoroughly demonstrated. This valuable information has been provided as a product of implementing the proposed methodology,

designed to meet a series of project objectives. Several software programs were utilized and a number of tools were created and refined to enable the proper application and assessment of the derived procedures. Finally, the use of subnetwork selection and DTA analysis was effectively demonstrated using a series of real-world network modification scenarios. In addition to the recommendations and results provided relative to subnetwork analysis using DTA, the lessons learned and tools developed can be used as a strong foundation from which to build upon as part of future research.

APPENDIX A

ArcGIS Models

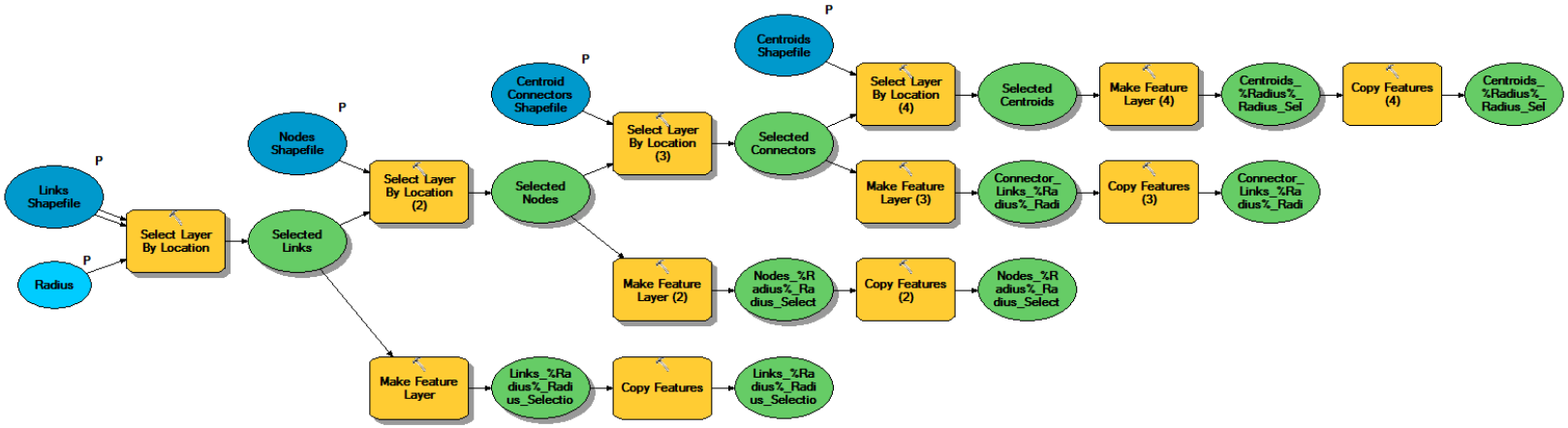

Figure A.1 ArcGIS Model for Performing Radius Selection of Network Elements

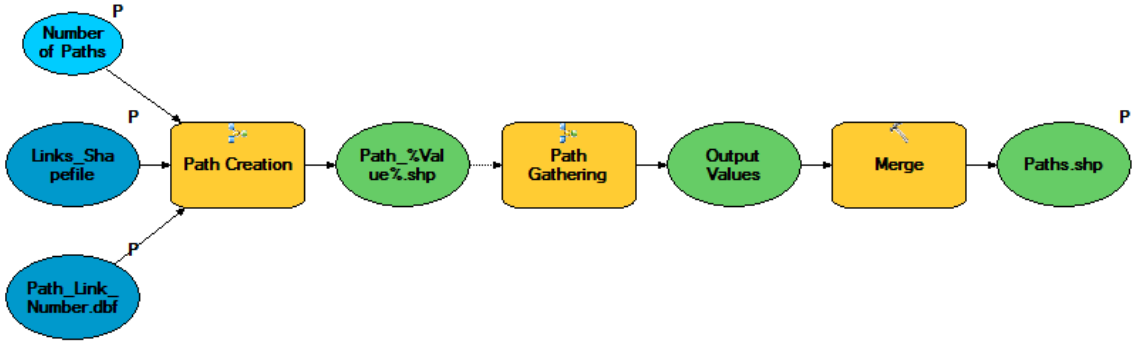

Figure A.2 ArcGIS Model for Creating a Path Shapefile Based on Extracted Links

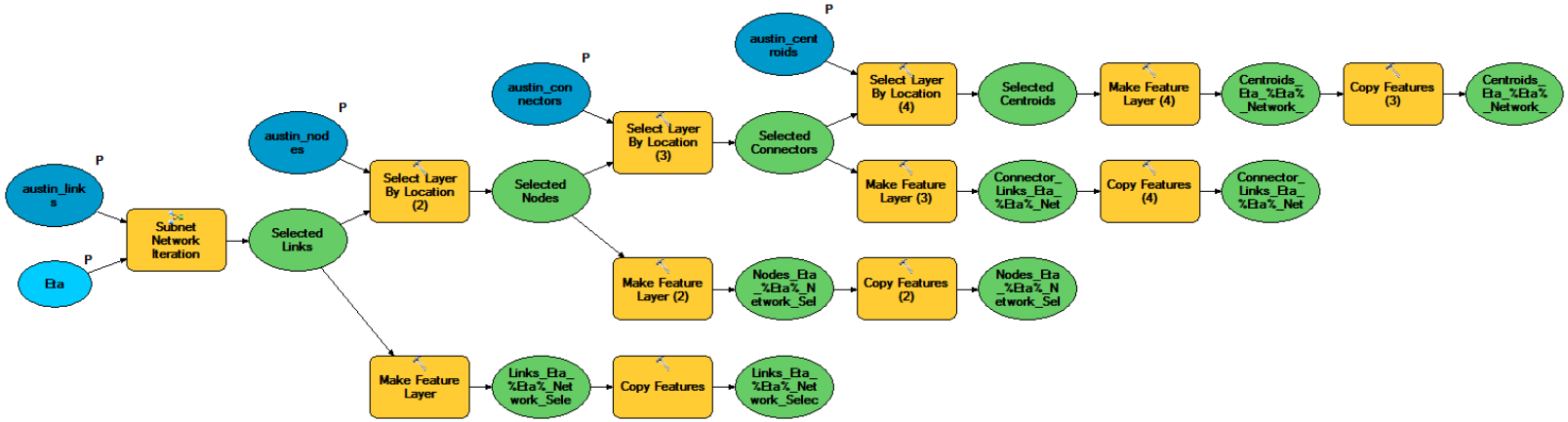

Figure A.3 ArcGIS Model for Performing Connected Order Selection of Network Elements

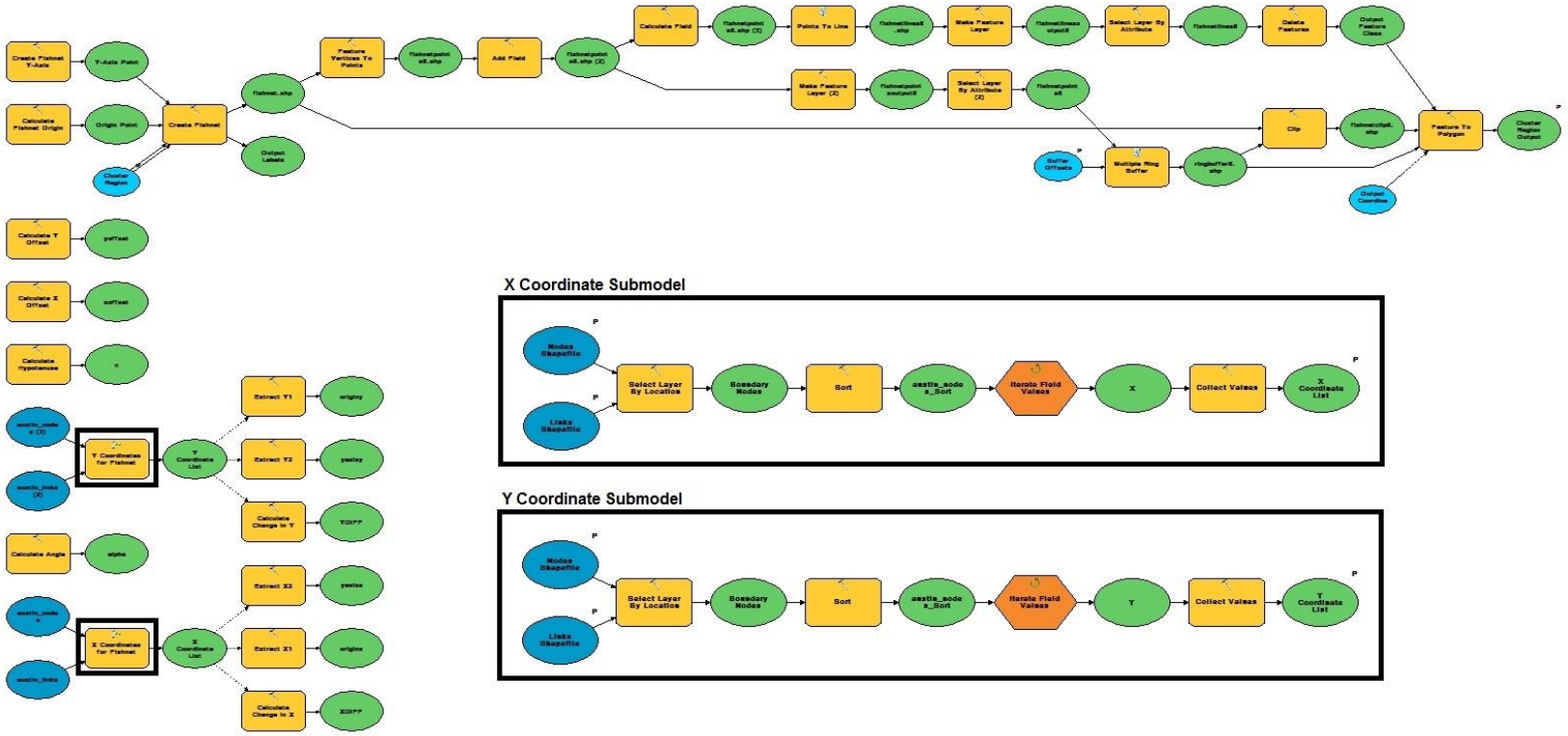

Figure A.4 ArcGIS Model for Cluster Region Tool

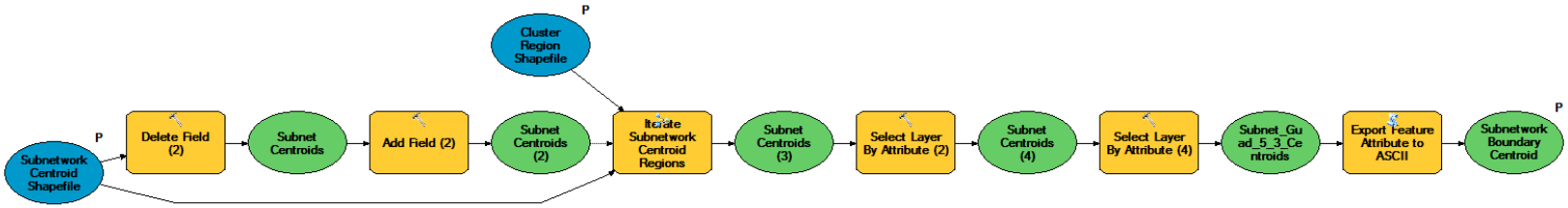

Figure A.5 ArcGIS Model for Grouping Boundary Centroids by Region

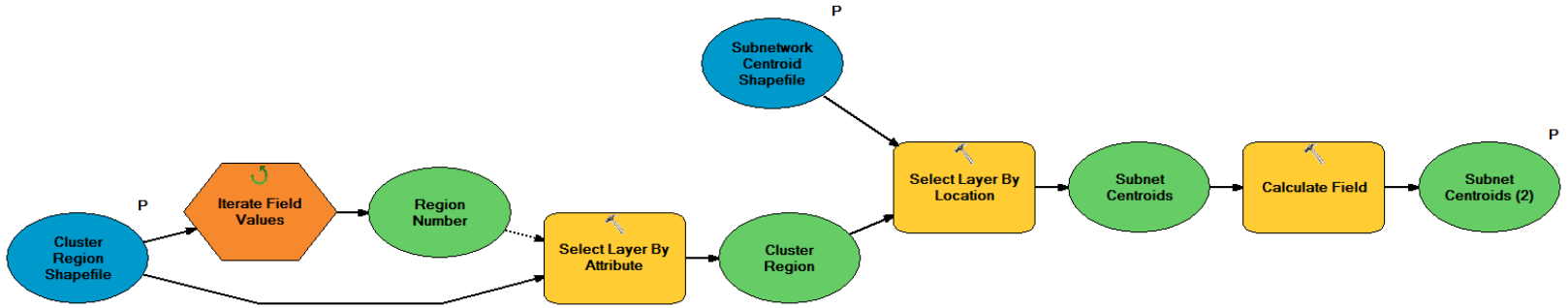

Figure A.6 Iterative Submodel Embedded to Facilitate Grouping Boundary Centroids by Region

Figure A.7 ArcGIS Model for Grouping Boundary Centroids by Maximum Demand

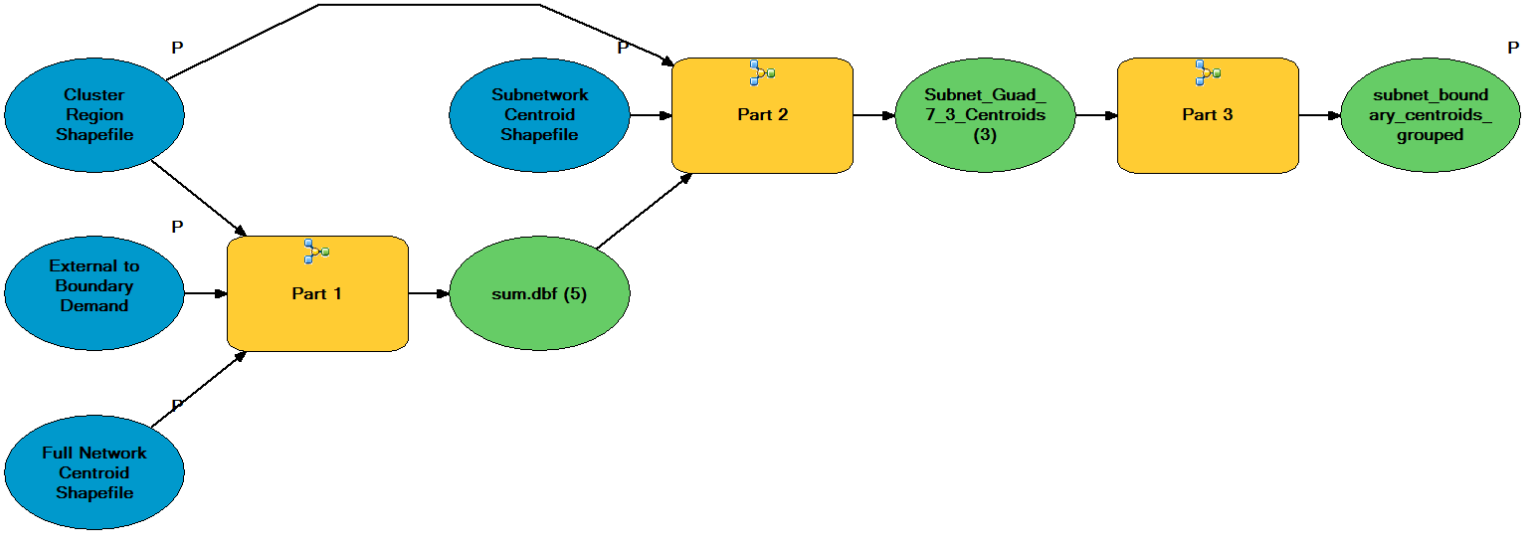

Figure A.8 ArcGIS Model for Grouping Boundary Centroids by Demand Proportions

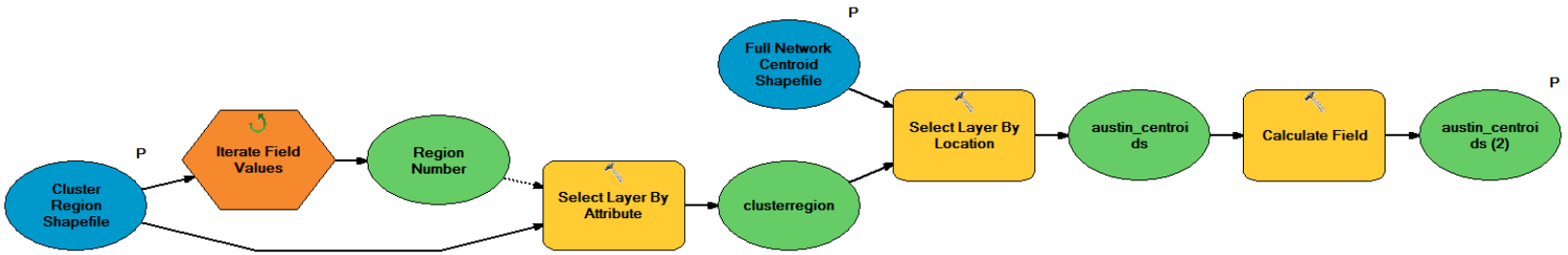

Figure A.9 Iterative Submodel Embedded to Facilitate Grouping Full Network Centroids by Region

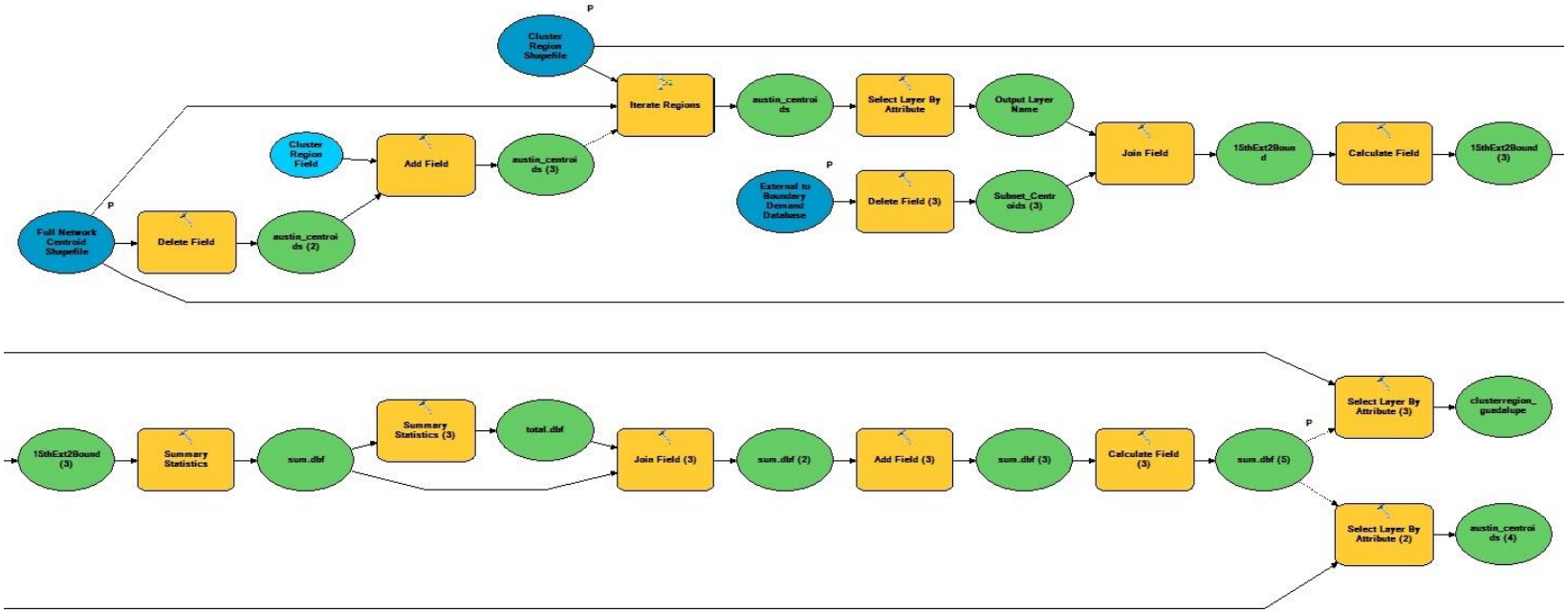

Figure A.10 Iterative Submodel Embedded to Facilitate Calculating Demand Proportions for each Region (Part 1)

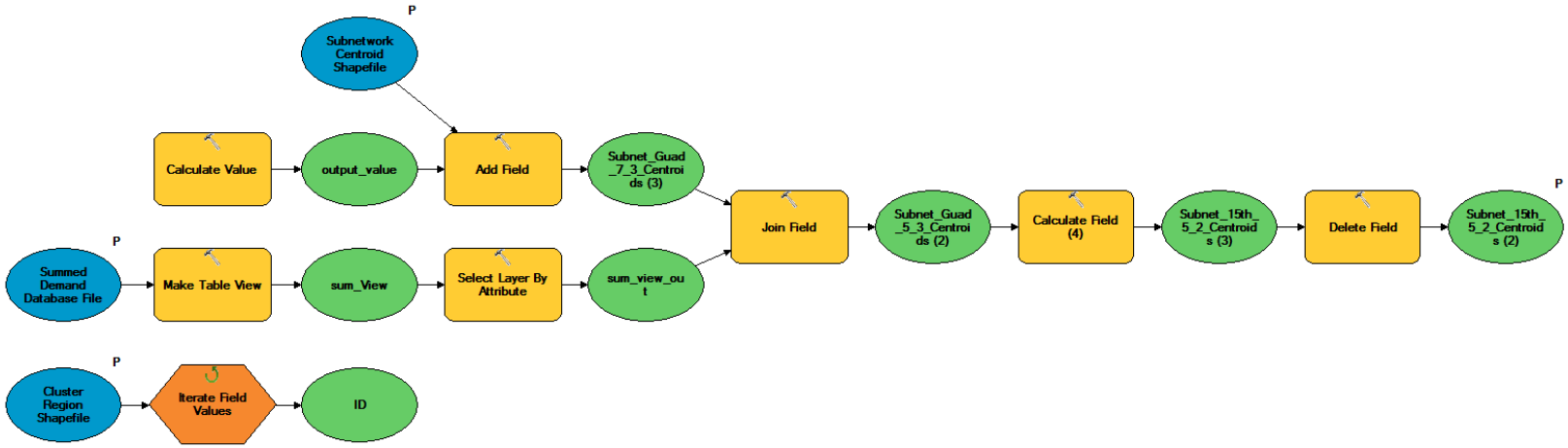

Figure A.11 Iterative Submodel Embedded to Add Demand Proportions for Each Region to Centroid Attribute Table (Part 2)

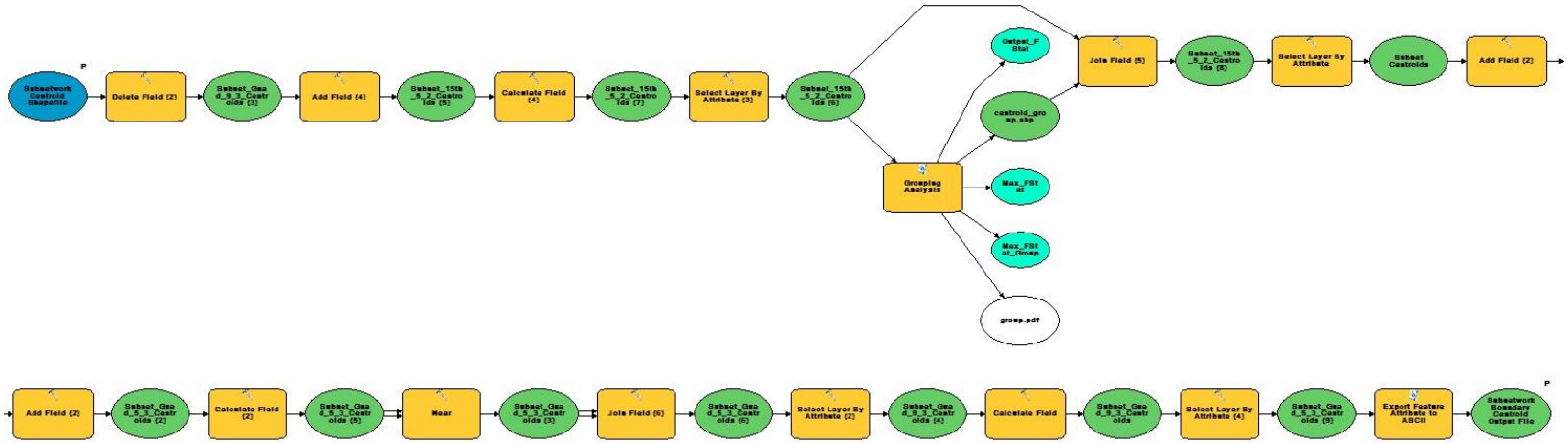

Figure A.12 Iterative Submodel Embedded to Perform Grouping Analysis (Part 3)

APPENDIX B

Matlab Code

Import O-D Matrix Script

```
%This code imports base and impact ODT matrices exported from VISTA
%and compiled in Excel
for z = 1:20
    test = xlsread('"O-D Matrix Filename".xlsx',z);
for i=1:length(test)
    test(i,7)=str2num(sprintf('%-1d',[test(i,3),test(i,4),test(i,6)]));
end
    test(:,[1 2])=[];

    if z==1
        base1=test;
    elseif z==2
        base2=test;
    elseif z==3
        base3=test;
    elseif z==4
        base4=test;
    elseif z==5
        base5=test;
    elseif z==6
        base6=test;
    elseif z==7
        base7=test;
    elseif z==8
        base8=test;
    elseif z==9
        base9=test;
    elseif z==10
        base10=test;
    elseif z==11
        impact1=test;
    elseif z==12
        impact2=test;
    elseif z==13
        impact3=test;
    elseif z==14
        impact4=test;
    elseif z==15
        impact5=test;
    elseif z==16
        impact6=test;
    elseif z==17
        impact7=test;
    elseif z==18
        impact8=test;
    elseif z==19
        impact9=test;
    elseif z==20
        impact10=test;
     end
```

```
end
```

Join O-D Matrix Script

```
%This code joins two ODT matrices by matching their unique ID, which is
%the concatenated origin, destination, and time period IDs.

for z = 1:9
    if z==1
        Base1=base1;
        Base2=base2;
    elseif z==2
        Base1=Joined_OD;
        Base2=base3;
    elseif z==3
        Base1=Joined_OD;
        Base2=base4;
    elseif z==4
        Base1=Joined_OD;
        Base2=base5;
    elseif z==5
        Base1=Joined_OD;
        Base2=base6;
    elseif z==6
        Base1=Joined_OD;
        Base2=base7;
    elseif z==7
        Base1=Joined_OD;
        Base2=base8;
    elseif z==8
        Base1=Joined_OD;
        Base2=base9;
    elseif z==9
        Base1=Joined_OD;
        Base2=base10;
    end

%Initialize index for matching unique IDs
n=1;
%Compare matrix unique IDs based on origins to reduce computation time
o=sort(unique(Base1(:,1)));
for i=1:length(o)
    index=find(Base1(:,1)==o(i));
    index2=find(Base2(:,1)==o(i));
    for j=1:length(index)
        for k=1:length(index2)
            if Base1(index(j),5)==Base2(index2(k),5)
                %Indices of each matrix match stored to combine later
                Base1_index(n,1)=index(j);
                Base2_index(n,1)=index2(k);
                n=n+1;
            end
        end
```

```
    end
end
%Append matrices where unique IDs match
Joined_OD=horzcat(Base1(Base1_index,:),Base2(Base2_index,3));
%Prepare the matrices to be appended to matching IDs, values of other
%matrix demand are set to zero
Base1_NoMatch=Base1;
Base1_NoMatch(Base1_index,:)=[];
Base1_NoMatch=horzcat(Base1_NoMatch,zeros(length(Base1_NoMatch),1));
Base2_NoMatch=Base2;
Base2_NoMatch(Base2_index,:)=[];
Base2_NoMatch=horzcat(Base2_NoMatch,zeros(length(Base2_NoMatch),z));
Base2_NoMatch=Base2_NoMatch(:,[1 2 5+z 4:4+z 3]);
%Join matches with ODTs that don't match
Joined_OD=vertcat(Joined_OD,Base1_NoMatch,Base2_NoMatch);

clear Base1
clear Base1_NoMatch
clear Base1_index
clear Base2
clear Base2_NoMatch
clear Base2_index
clear index
clear index2
clear i
clear j
clear k
clear n
clear o
clear z
end

Joined_OD(:,15)=mean(Joined_OD(:,[3 6:14]),2);
true_base=Joined_OD(:, [1 2 15 4 5]);

for z = 1:10
    if z==1
        Base1=true_base;
        Base2=base1;
    elseif z==2
        Base1=true_base;
        Base2=base2;
    elseif z==3
        Base1=true_base;
        Base2=base3;
    elseif z==4
        Base1=true_base;
        Base2=base4;
    elseif z==5
        Base1=true_base;
        Base2=base5;
    elseif z==6
```

```
        Base1=true_base;
        Base2=base6;
    elseif z==7
        Base1=true_base;
        Base2=base7;
    elseif z==8
        Base1=true_base;
        Base2=base8;
    elseif z==9
        Base1=true_base;
        Base2=base9;
    elseif z==10
        Base1=true_base;
        Base2=base10;
    end

%Initialize index for matching unique IDs
n=1;
%Compare matrix unique IDs based on origins to reduce computation time
o=sort(unique(Base1(:,1)));
for i=1:length(o)
    index=find(Base1(:,1)==o(i));
    index2=find(Base2(:,1)==o(i));
    for j=1:length(index)
        for k=1:length(index2)
            if Base1(index(j),5)==Base2(index2(k),5)
                %Indices of each matrix match stored to combine later
                Base1_index(n,1)=index(j);
                Base2_index(n,1)=index2(k);
                n=n+1;
            end
        end
    end
end

%Append matrices where unique IDs match
Joined_OD=horzcat(Base1(Base1_index,:),Base2(Base2_index,3));
%Prepare the matrices to be appended to matching IDs, values of other
%matrix demand are set to zero
Base1_NoMatch=Base1;
Base1_NoMatch(Base1_index,:)=[];
Base1_NoMatch=horzcat(Base1_NoMatch,zeros(length(Base1_NoMatch),1));
Base2_NoMatch=Base2;
Base2_NoMatch(Base2_index,:)=[];
Base2_NoMatch=horzcat(Base2_NoMatch,zeros(length(Base2_NoMatch),1));
Base2_NoMatch=Base2_NoMatch(:,[1 2 6 4 5 3]);
%Join matches with ODTs that don't match
Joined_OD=vertcat(Joined_OD,Base1_NoMatch,Base2_NoMatch);

    if z==1
        Base1Joined=Joined_OD;
    elseif z==2
```

```
        Base2Joined=Joined_OD;
    elseif z==3
        Base3Joined=Joined_OD;
    elseif z==4
        Base4Joined=Joined_OD;
    elseif z==5
        Base5Joined=Joined_OD;
    elseif z==6
        Base6Joined=Joined_OD;
    elseif z==7
        Base7Joined=Joined_OD;
    elseif z==8
        Base8Joined=Joined_OD;
    elseif z==9
        Base9Joined=Joined_OD;
    elseif z==10
        Base10Joined=Joined_OD;
    end

clear Base1
clear Base1_NoMatch
clear Base1_index
clear Base2
clear Base2_NoMatch
clear Base2_index
clear index
clear index2
clear i
clear j
clear k
clear n
clear o
clear z
end

for z = 1:10
    if z==1
        Base1=true_base;
        Base2=impact1;
    elseif z==2
        Base1=true_base;
        Base2=impact2;
    elseif z==3
        Base1=true_base;
        Base2=impact3;
    elseif z==4
        Base1=true_base;
        Base2=impact4;
    elseif z==5
        Base1=true_base;
        Base2=impact5;
    elseif z==6
```

```
        Base1=true_base;
        Base2=impact6;
    elseif z==7
        Base1=true_base;
        Base2=impact7;
    elseif z==8
        Base1=true_base;
        Base2=impact8;
    elseif z==9
        Base1=true_base;
        Base2=impact9;
    elseif z==10
        Base1=true_base;
        Base2=impact10;
    end

%Initialize index for matching unique IDs
n=1;
%Compare matrix unique IDs based on origins to reduce computation time
o=sort(unique(Base1(:,1)));
for i=1:length(o)
    index=find(Base1(:,1)==o(i));
    index2=find(Base2(:,1)==o(i));
    for j=1:length(index)
        for k=1:length(index2)
            if Base1(index(j),5)==Base2(index2(k),5)
                %Indices of each matrix match stored to combine later
                Base1_index(n,1)=index(j);
                Base2_index(n,1)=index2(k);
                n=n+1;
            end
        end
    end
end

%Append matrices where unique IDs match
Joined_OD=horzcat(Base1(Base1_index,:),Base2(Base2_index,3));
%Prepare the matrices to be appended to matching IDs, values of other
%matrix demand are set to zero
Base1_NoMatch=Base1;
Base1_NoMatch(Base1_index,:)=[];
Base1_NoMatch=horzcat(Base1_NoMatch,zeros(length(Base1_NoMatch),1));
Base2_NoMatch=Base2;
Base2_NoMatch(Base2_index,:)=[];
Base2_NoMatch=horzcat(Base2_NoMatch,zeros(length(Base2_NoMatch(:,1)),1)
);
Base2_NoMatch=Base2_NoMatch(:,[1 2 6 4 5 3]);
%Join matches with ODTs that don't match
Joined_OD=vertcat(Joined_OD,Base1_NoMatch,Base2_NoMatch);

    if z==1
        Impact1Joined=Joined_OD;
```

```
    elseif z==2
        Impact2Joined=Joined_OD;
    elseif z==3
        Impact3Joined=Joined_OD;
    elseif z==4
        Impact4Joined=Joined_OD;
    elseif z==5
        Impact5Joined=Joined_OD;
    elseif z==6
        Impact6Joined=Joined_OD;
    elseif z==7
        Impact7Joined=Joined_OD;
    elseif z==8
        Impact8Joined=Joined_OD;
    elseif z==9
        Impact9Joined=Joined_OD;
    elseif z==10
        Impact10Joined=Joined_OD;
    end

clear Base1
clear Base1_NoMatch
clear Base1_index
clear Base2
clear Base2_NoMatch
clear Base2_index
clear index
clear index2
clear i
clear j
clear k
clear n
clear o
clear z
end
```

RMSE and MCAPE Calculation Script

```
%This code calculates the RMSE and MCAPE for the boundary demand
%comparison for each base and impact run

RMSE_Base=zeros(20,1);
MCAPE_Base=zeros(20,1);
for z = 1:20
    if z==1
        Comparison=Base1Joined;
    elseif z==2
        Comparison=Base2Joined;
    elseif z==3
        Comparison=Base3Joined;
    elseif z==4
        Comparison=Base4Joined;
    elseif z==5
        Comparison=Base5Joined;
    elseif z==6
        Comparison=Base6Joined;
    elseif z==7
        Comparison=Base7Joined;
    elseif z==8
        Comparison=Base8Joined;
    elseif z==9
        Comparison=Base9Joined;
    elseif z==10
        Comparison=Base10Joined;
    elseif z==11
        Comparison=Impact1Joined;
    elseif z==12
        Comparison=Impact2Joined;
    elseif z==13
        Comparison=Impact3Joined;
    elseif z==14
        Comparison=Impact4Joined;
    elseif z==15
        Comparison=Impact5Joined;
    elseif z==16
        Comparison=Impact6Joined;
    elseif z==17
        Comparison=Impact7Joined;
    elseif z==18
        Comparison=Impact8Joined;
    elseif z==19
        Comparison=Impact9Joined;
    elseif z==20
        Comparison=Impact10Joined;
    end

Comparison=Comparison(find(Comparison(:,1)>=150000),:);
%The following two lines set the time period range to be analyzed
```

```
Comparison=Comparison(find(Comparison(:,4)>=2),:);
Comparison=Comparison(find(Comparison(:,4)<=9),:);
Comparison(:,7)= (Comparison(:,3)-Comparison(:,6)).^2;
Comparison(:,8)= min(100,abs((Comparison(:,3)-
Comparison(:,6))./Comparison(:,3)*100));
MCAPE_Base(z,1)=mean(Comparison(:,8));
RMSE_Base(z,1)=(mean(Comparison(:,7)))^.5;
end
```

SSIM Index Calculation Script

```
%This code receives a dynamic Origin-Destination table from cell form
%from VISTA and turns it into a Matrix to be used for the SSIM
%calculator. OD should be a table with the columns: Origin,
%Destination, Time Period, Demand 1, and Demand 2

for z = 1:20
    if z==1
        Comparison=Base1Joined;
    elseif z==2
        Comparison=Base2Joined;
    elseif z==3
        Comparison=Base3Joined;
    elseif z==4
        Comparison=Base4Joined;
    elseif z==5
        Comparison=Base5Joined;
    elseif z==6
        Comparison=Base6Joined;
    elseif z==7
        Comparison=Base7Joined;
    elseif z==8
        Comparison=Base8Joined;
    elseif z==9
        Comparison=Base9Joined;
    elseif z==10
        Comparison=Base10Joined;
    elseif z==11
        Comparison=Impact1Joined;
    elseif z==12
        Comparison=Impact2Joined;
    elseif z==13
        Comparison=Impact3Joined;
    elseif z==14
        Comparison=Impact4Joined;
    elseif z==15
        Comparison=Impact5Joined;
    elseif z==16
        Comparison=Impact6Joined;
    elseif z==17
        Comparison=Impact7Joined;
    elseif z==18
        Comparison=Impact8Joined;
    elseif z==19
        Comparison=Impact9Joined;
    elseif z==20
        Comparison=Impact10Joined;
    end

Comparison=Comparison(find(Comparison(:,1)>=150000),:);
Comparison=Comparison(find(Comparison(:,4)>=2),:);
```

```
Comparison=Comparison(find(Comparison(:,4)<=5),:);

OD=double(Comparison(:,[1 2 4 6 3]));
Origin = OD(:,1);
Destination = OD(:,2);
Time = OD(:,3);

%Creates a list of origin (row headers) and destination (column
%headers); Counts the number of time periods
o=Boundary_Origins;
d=sort(unique(Destination));
d=setdiff(d,Boundary_Destinations);
d=vertcat(Boundary_Destinations,d);
t=length(sort(unique(Time)));

a=length(o);
b=length(d);
c=length(Origin); %Counter for number of rows in original OD table

%Creates matrices for both demands with rows as the number of origins,
%columns as the number of destinations, and pages as the number of time
%periods
m1=zeros(a,b,t);
m2=zeros(a,b,t);
for i=1:c
    for j=1:a
        for k=1:b
            for l=1:t
if OD(i,1)==o(j) && OD(i,2)==d(k) && OD(i,3)==l-1
m1(j,k,l)=OD(i,4);
m2(j,k,l)=OD(i,5);
end
end
end
end
end

%Creates parameters for the SSIM matlab code and call code for each
time
%period OD and each windowing method
time=length(m1(1,1,:));
Base_1_SSIM_Cross=zeros(time,1);
Base_1_SSIM_Vert=zeros(time,1);
Base_1_SSIM_Normal=zeros(time,1);
Base_1_SSIM_Ones=zeros(time,1);

for t=1:time
L=max(max(max(m1(:,:,t)),max(max(m2(:,:,t)))));
K= [0.01,0.03];
window=[0 1/6 0; 1/6 1/3 1/6; 0 1/6 0];
[Base_1_SSIM_Cross(t,1), ssim_map] = ssim_index(m1(:,:,t), m2(:,:,t),
K, window, L);
```

```
end
SSIM_Cross(z,1)=mean(Base_1_SSIM_Cross);

for t=1:time
L=max(max(max(m1(:,:,t)),max(max(m2(:,:,t)))));
K= [0.01,0.03];
window=[0 .25 0; 0 .5 0; 0 .25 0];
[Base_1_SSIM_Vert(t,1), ssim_map] = ssim_index(m1(:,:,t), m2(:,:,t), K,
window, L);
end
SSIM_Vert(z,1)=mean(Base_1_SSIM_Vert);

for t=1:time
L=max(max(max(m1(:,:,t)),max(max(m2(:,:,t)))));
K= [0.01,0.03];
window=fspecial('gaussian', 3, .55);
[Base_1_SSIM_Normal(t,1), ssim_map] = ssim_index(m1(:,:,t), m2(:,:,t),
K, window, L);
end
SSIM_Normal(z,1)=mean(Base_1_SSIM_Normal);

for t=1:time
L=max(max(max(m1(:,:,t)),max(max(m2(:,:,t)))));
K= [0.01,0.03];
window=ones(3);
[Base_1_SSIM_Ones(t,1), ssim_map] = ssim_index(m1(:,:,t), m2(:,:,t), K,
window, L);
end
SSIM_Ones(z,1)=mean(Base_1_SSIM_Ones);

end

%Time periods in the created matrix will be one plus the original time
%period
```

Hypothesis Test and Prediction Interval Calculation Script

```
%This code initiates a function file and performs calculations
%necessary to evaluate all hypothesis tests and compilation of
%applicable prediction intervals for subnetworks of size 5, 7 and 9.
%Code can be adjusted accordingly to assess different sample sizes
%(default is 10) and number/size of subnetwork

for i=1:9
    if i ==1
        error=MCAPE_Base_5;
    elseif i == 2
        error=MCAPE_Base_7;
    elseif i == 3
        error=MCAPE_Base_9;
    elseif i == 4
        error=RMSE_Base_5;
    elseif i == 5
        error=RMSE_Base_7;
    elseif i == 6
        error=RMSE_Base_9;
    elseif i == 7
        error=SSIM_Cross_5;
    elseif i == 8
        error=SSIM_Cross_7;
    elseif i == 9
        error=SSIM_Cross_9;
    end

%The following initiates the associated function

    [ Lower_Base, Upper_Base, Alt_Runs_Within, Lower_Impact,
Upper_Impact, Base_Runs_Within, Base_L_Test, Base_AD_Test,
Impact_L_Test, Impact_AD_Test, Eq_Var_Test, t, p, ci,stat ] =
Pred_Int_Hyp_Test( error );

%The following is the function initiated by the above code block

function [ Lower_Base, Upper_Base, Alt_Runs_Within, Lower_Impact,
Upper_Impact, Base_Runs_Within, Base_L_Test, Base_AD_Test,
Impact_L_Test, Impact_AD_Test, Eq_Var_Test, t, p, ci,stat ] =
Pred_Int_Hyp_Test(error)

%This code produces the prediction interval, equal variance tests,
%normality tests, and a two sample t-test for the base vs. impact
%runs of a given scenario and error statistic.

x=mean(error(1:10,1));
t=2.262;
s=std(error(1:10,1));
n=length(error(1:10,1));
```

```
Lower_Base=x-t*s*(1+1/n)^.5;
Upper_Base=x+t*s*(1+1/n)^.5;
Alt_Runs_Within = histc(error(11:20,1),[Lower_Base Upper_Base]);

x=mean(error(11:20,1));
t=2.262;
s=std(error(11:20,1));
n=length(error(11:20,1));
Lower_Impact=x-t*s*(1+1/n)^.5;
Upper_Impact=x+t*s*(1+1/n)^.5;
Base_Runs_Within = histc(error(1:10,1),[Lower_Impact Upper_Impact]);

Base_L_Test=lillietest(error(1:10,1));
Base_AD_Test = adtest(error(1:10,1));

Impact_L_Test=lillietest(error(11:20,1));
Impact_AD_Test = adtest(error(11:20,1));

v1=var(error(1:10,1));
v2=var(error(11:20,1));
Fstar=max(v1,v2)/min(v1,v2);
Fcrit=4.026;
if Fstar<=Fcrit
    Eq_Var_Test=0;
else
    Eq_Var_Test=1;
end

[t,p,ci,stat] = ttest2((error(1:10,1)),error(11:20,1));

end

%The following continues to compile the test results from the function

    if i==1
        MCAPE_Results(1,1) = Eq_Var_Test;
        MCAPE_Results(1,2) = Base_L_Test;
        MCAPE_Results(1,3) = Base_AD_Test;
        MCAPE_Results(1,4) = t;
        MCAPE_Results(1,5) = Lower_Base;
        MCAPE_Results(1,6) = Upper_Base;
        MCAPE_Results(1,7) = Upper_Base-Lower_Base;
        MCAPE_Results(1,8) = Alt_Runs_Within(1,1);
        MCAPE_Results(2,1) = Eq_Var_Test;
        MCAPE_Results(2,2) = Impact_L_Test;
        MCAPE_Results(2,3) = Impact_AD_Test;
        MCAPE_Results(2,4) = t;
        MCAPE_Results(2,5) = Lower_Impact;
        MCAPE_Results(2,6) = Upper_Impact;
        MCAPE_Results(2,7) = Upper_Impact-Lower_Impact;
        MCAPE_Results(2,8) = Base_Runs_Within(1,1);
```

```
elseif i==2
    MCAPE_Results(3,1) = Eq_Var_Test;
    MCAPE_Results(3,2) = Base_L_Test;
    MCAPE_Results(3,3) = Base_AD_Test;
    MCAPE_Results(3,4) = t;
    MCAPE_Results(3,5) = Lower_Base;
    MCAPE_Results(3,6) = Upper_Base;
    MCAPE_Results(3,7) = Upper_Base-Lower_Base;
    MCAPE_Results(3,8) = Alt_Runs_Within(1,1);
    MCAPE_Results(4,1) = Eq_Var_Test;
    MCAPE_Results(4,2) = Impact_L_Test;
    MCAPE_Results(4,3) = Impact_AD_Test;
    MCAPE_Results(4,4) = t;
    MCAPE_Results(4,5) = Lower_Impact;
    MCAPE_Results(4,6) = Upper_Impact;
    MCAPE_Results(4,7) = Upper_Impact-Lower_Impact;
    MCAPE_Results(4,8) = Base_Runs_Within(1,1);

elseif i==3
    MCAPE_Results(5,1) = Eq_Var_Test;
    MCAPE_Results(5,2) = Base_L_Test;
    MCAPE_Results(5,3) = Base_AD_Test;
    MCAPE_Results(5,4) = t;
    MCAPE_Results(5,5) = Lower_Base;
    MCAPE_Results(5,6) = Upper_Base;
    MCAPE_Results(5,7) = Upper_Base-Lower_Base;
    MCAPE_Results(5,8) = Alt_Runs_Within(1,1);
    MCAPE_Results(6,1) = Eq_Var_Test;
    MCAPE_Results(6,2) = Impact_L_Test;
    MCAPE_Results(6,3) = Impact_AD_Test;
    MCAPE_Results(6,4) = t;
    MCAPE_Results(6,5) = Lower_Impact;
    MCAPE_Results(6,6) = Upper_Impact;
    MCAPE_Results(6,7) = Upper_Impact-Lower_Impact;
    MCAPE_Results(6,8) = Base_Runs_Within(1,1);

elseif i==4
    RMSE_Results(1,1) = Eq_Var_Test;
    RMSE_Results(1,2) = Base_L_Test;
    RMSE_Results(1,3) = Base_AD_Test;
    RMSE_Results(1,4) = t;
    RMSE_Results(1,5) = Lower_Base;
    RMSE_Results(1,6) = Upper_Base;
    RMSE_Results(1,7) = Upper_Base-Lower_Base;
    RMSE_Results(1,8) = Alt_Runs_Within(1,1);
    RMSE_Results(2,1) = Eq_Var_Test;
    RMSE_Results(2,2) = Impact_L_Test;
    RMSE_Results(2,3) = Impact_AD_Test;
    RMSE_Results(2,4) = t;
    RMSE_Results(2,5) = Lower_Impact;
    RMSE_Results(2,6) = Upper_Impact;
```

```
    RMSE_Results(2,7) = Upper_Impact-Lower_Impact;
    RMSE_Results(2,8) = Base_Runs_Within(1,1);

elseif i==5
    RMSE_Results(3,1) = Eq_Var_Test;
    RMSE_Results(3,2) = Base_L_Test;
    RMSE_Results(3,3) = Base_AD_Test;
    RMSE_Results(3,4) = t;
    RMSE_Results(3,5) = Lower_Base;
    RMSE_Results(3,6) = Upper_Base;
    RMSE_Results(3,7) = Upper_Base-Lower_Base;
    RMSE_Results(3,8) = Alt_Runs_Within(1,1);
    RMSE_Results(4,1) = Eq_Var_Test;
    RMSE_Results(4,2) = Impact_L_Test;
    RMSE_Results(4,3) = Impact_AD_Test;
    RMSE_Results(4,4) = t;
    RMSE_Results(4,5) = Lower_Impact;
    RMSE_Results(4,6) = Upper_Impact;
    RMSE_Results(4,7) = Upper_Impact-Lower_Impact;
    RMSE_Results(4,8) = Base_Runs_Within(1,1);

elseif i==6
    RMSE_Results(5,1) = Eq_Var_Test;
    RMSE_Results(5,2) = Base_L_Test;
    RMSE_Results(5,3) = Base_AD_Test;
    RMSE_Results(5,4) = t;
    RMSE_Results(5,5) = Lower_Base;
    RMSE_Results(5,6) = Upper_Base;
    RMSE_Results(5,7) = Upper_Base-Lower_Base;
    RMSE_Results(5,8) = Alt_Runs_Within(1,1);
    RMSE_Results(6,1) = Eq_Var_Test;
    RMSE_Results(6,2) = Impact_L_Test;
    RMSE_Results(6,3) = Impact_AD_Test;
    RMSE_Results(6,4) = t;
    RMSE_Results(6,5) = Lower_Impact;
    RMSE_Results(6,6) = Upper_Impact;
    RMSE_Results(6,7) = Upper_Impact-Lower_Impact;
    RMSE_Results(6,8) = Base_Runs_Within(1,1);

elseif i==7
    SSIM_Results(1,1) = Eq_Var_Test;
    SSIM_Results(1,2) = Base_L_Test;
    SSIM_Results(1,3) = Base_AD_Test;
    SSIM_Results(1,4) = t;
    SSIM_Results(1,5) = Lower_Base;
    SSIM_Results(1,6) = Upper_Base;
    SSIM_Results(1,7) = Upper_Base-Lower_Base;
    SSIM_Results(1,8) = Alt_Runs_Within(1,1);
    SSIM_Results(2,1) = Eq_Var_Test;
    SSIM_Results(2,2) = Impact_L_Test;
    SSIM_Results(2,3) = Impact_AD_Test;
    SSIM_Results(2,4) = t;
```

```
        SSIM_Results(2,5) = Lower_Impact;
        SSIM_Results(2,6) = Upper_Impact;
        SSIM_Results(2,7) = Upper_Impact-Lower_Impact;
        SSIM_Results(2,8) = Base_Runs_Within(1,1);

    elseif i==8
        SSIM_Results(3,1) = Eq_Var_Test;
        SSIM_Results(3,2) = Base_L_Test;
        SSIM_Results(3,3) = Base_AD_Test;
        SSIM_Results(3,4) = t;
        SSIM_Results(3,5) = Lower_Base;
        SSIM_Results(3,6) = Upper_Base;
        SSIM_Results(3,7) = Upper_Base-Lower_Base;
        SSIM_Results(3,8) = Alt_Runs_Within(1,1);
        SSIM_Results(4,1) = Eq_Var_Test;
        SSIM_Results(4,2) = Impact_L_Test;
        SSIM_Results(4,3) = Impact_AD_Test;
        SSIM_Results(4,4) = t;
        SSIM_Results(4,5) = Lower_Impact;
        SSIM_Results(4,6) = Upper_Impact;
        SSIM_Results(4,7) = Upper_Impact-Lower_Impact;
        SSIM_Results(4,8) = Base_Runs_Within(1,1);

    elseif i==9
        SSIM_Results(5,1) = Eq_Var_Test;
        SSIM_Results(5,2) = Base_L_Test;
        SSIM_Results(5,3) = Base_AD_Test;
        SSIM_Results(5,4) = t;
        SSIM_Results(5,5) = Lower_Base;
        SSIM_Results(5,6) = Upper_Base;
        SSIM_Results(5,7) = Upper_Base-Lower_Base;
        SSIM_Results(5,8) = Alt_Runs_Within(1,1);
        SSIM_Results(6,1) = Eq_Var_Test;
        SSIM_Results(6,2) = Impact_L_Test;
        SSIM_Results(6,3) = Impact_AD_Test;
        SSIM_Results(6,4) = t;
        SSIM_Results(6,5) = Lower_Impact;
        SSIM_Results(6,6) = Upper_Impact;
        SSIM_Results(6,7) = Upper_Impact-Lower_Impact;
        SSIM_Results(6,8) = Base_Runs_Within(1,1);

    end
end
```

External-to-External Demand Adjustment Script

```
%This script requires the inputs: boundary centroids
%(Bound_Centroids), external centroids (Ext_Centroids),
%regional dynamic OD (Regional_OD), Subnetwork Base OD
%(Subnet_Base_OD), external to boundary travel times
%(ExtBoundTTSource), boundary to external travel times
%(BoundExtTTSource),external to external travel times
%(ExttoExtTTSource), internal travel times in the base case
%(IntTTBase), and internal travel times in the impact scenario
%(IntTTImpact).

%NOTE - The boundary and external centroid IDs are input in their
%respective tables in columns representing the individual sections
%and that these lists are in the same order for both tables (IDs in
%section 1 input in column 1, etc.). This is done automatically if
%using an imported file grouping the boundary centroids called
%"Bound_Centroids_Grouped", which is an output from ArcGIS. This file
%is used to create "Bound_Centroids". For the external centroids, two
%options are available depending on the desired grouping strategy. The
%external centroid file, "Ext_Centroids", can either be created based
%on the list of boundary centroids or using the regionally grouped
%centroid list called "Regional_Centroids_Grouped", as an output from
%ArcGIS per the code below.

%NOTE - The user must designate the external centroid grouping strategy
%at the beginning of the code by "commenting" out the code block for
%the grouping strategy not desired. See notes below for additional
%information.

%SETUP FOR REGION'S OD TABLE MODIFICATION
%This script begins by grouping the boundary and external centroids
%based on the input files exported from ArcGIS and the desired grouping
%strategy for the external centroids. The code below performs a
%grouping strategy based on the desired code block.

%The script then uses the regional and subnetwork (base) dynamic OD
%tables, a single region's external and boundary origins, as well as
%all other regions' external and boundary centroids, and calculates
%proportions of demand bypassing versus traversing the subnetwork.
%The intermediate output is one table with existing and proposed demand
%for each boundary origin in a select "origin" section to all possible
%boundary destinations in each "destination" section (all other
sections). The final output file is titled "Joined_OD" and can be used
%in its final form as an input for the external-to-internal boundary
%demand adjustment.

tic;
%Group boundary centroids based on the exported list and Group ID
%from ArcGIS
```

```
for i=1:max(unique(Bound_Centroids_Grouped(:,4)));
    j(i,1)=(sum(Bound_Centroids_Grouped(:,4)==i))
end
Bound_Centroids=zeros(max(j(:,1)),max(unique(Bound_Centroids_Grouped(:,
4))));
for b=1:length(Bound_Centroids_Grouped(:,3))
    c=Bound_Centroids_Grouped(b,4);
    for a=1:max(unique(Bound_Centroids_Grouped(:,4)));
        if c==a
            d=length(Bound_Centroids(:,1))-
sum(Bound_Centroids(:,a)==0)+1;
            Bound_Centroids(d,a)=Bound_Centroids_Grouped(b,3);
        end
    end
end
clear i;
clear j;
clear k;
clear a;
clear b;
clear c;
clear d;

%Use the following to group external centroids by geographic region.

%IF YOU DO NOT WISH TO GROUP BY REGION, COMMENT OUT THE FOLLWOING CODE
%BLOCK

Regional_Centroids_Grouped=sortrows(Regional_Centroids_Grouped,3);
for i=1:max(unique(Regional_Centroids_Grouped(:,4)));
    j(i,1)=(sum(Regional_Centroids_Grouped(:,4)==i))
end
Ext_Centroids=zeros(max(j(:,1)),max(unique(Regional_Centroids_Grouped(:
,4))));
for b=1:length(Regional_Centroids_Grouped(:,3))
    c=Regional_Centroids_Grouped(b,4);
    for a=1:max(unique(Regional_Centroids_Grouped(:,4)));
        if c==a
            d=length(Ext_Centroids(:,1))-sum(Ext_Centroids(:,a)==0)+1;
            Ext_Centroids(d,a)=Regional_Centroids_Grouped(b,3);
        end
    end
end
clear i;
clear j;
clear k;
clear a;
clear b;
clear c;
clear d;

%Use the following to group external ORIGINS by boundary centroid list.
```

```
%IF YOU DO NOT WISH TO GROUP BY BOUNDARY CENTROID, COMMENT OUT THE
%FOLLWOING CODE BLOCK (INCLUDING THE FOLLOWING SECTION FOR
DESTINATIONS)

for j=1:length(Bound_Centroids(1,:));
    n=0;
    for i=1:length(Bound_Centroids(:,1));
        for k=1:length(ExtBoundTTSource(:,1));
            if Bound_Centroids(i,j)==ExtBoundTTSource(k,3)
                n=n+1;
                Ext_Cent(n,j)=ExtBoundTTSource(k,1);
            end
        end
    end
end
clear i;
clear j;
clear k;
clear n;
for j=1:length(Ext_Cent(1,:));
    i=unique(Ext_Cent(:,j));
    if i(1,1)==0
        i(1,:)=[];
    end
    for k=1:length(i(:,1));
        Ext_Centroids(k,j)=i(k,1);
    end
end
clear i;
clear j;
clear k;
clear Ext_Cent;

%Use the following to add DESTINATION centroids to the external
centroid
%list created based on the boundary centroids.

%IF YOU DO NOT WISH TO GROUP BY BOUNDARY CENTROID, COMMENT OUT THE
%FOLLWOING CODE BLOCK

for j=1:length(Ext_Centroids(1,:));
    k = nnz(Ext_Centroids(:,j));
    for i=1:k;
        n=Ext_Centroids(i,j)+100000;
        Ext_Centroids(i+k,j)=n;
    end
end
clear i;
clear j;
clear k;
clear n;
```

```
%DO NOT COMMENT OUT THE FOLLOWING CODE

%Dimension Internal Proportion OD table by number of "origin" sections;
%Number of "pages" (z-dimension) equals number of origin sections
(columns
%in Boundary Centroids table).

Int_Prop_OD=zeros(length(Subnet_Base_OD),4,length(Bound_Centroids(1,:))
);
z=1;
for z=1:length(Bound_Centroids(1,:));

    %Reduce the regional dynamic od to only external centroid origins'
    %OD pairs for section.
    l=1;
    for external=1:length(Ext_Centroids(:,1));
        for k=1:length(Regional_OD)
            testval=Regional_OD(k,3);
            if testval==Ext_Centroids(external,z)
                temp(l,1)=testval;
                temp(l,2)=Regional_OD(k,4);
                temp(l,3)=Regional_OD(k,6);
                temp(l,4)=Regional_OD(k,5);
                l=l+1;
            end
        end
    end

    if exist('temp')

    %Sum duplicate OD pairs
    [c,u,v]=unique(temp(:,1:3),'rows');
    d = accumarray(v,temp(:,4));
    Ext_Prop_OD=[c,d]

    %Index external destinations by section (column 5); remove
    %remaining (internal subnetwork and intra-sectional external
    %destinations).

    Ext_Prop_OD(:,5)=zeros
    for i=1:length(Ext_Prop_OD(:,1))
        for external=1:length(ExttoExtTTSource(:,1));
            if Ext_Prop_OD(i,1)==ExttoExtTTSource(external,1)
                Ext_Prop_OD(i,5)=z;
            end
        end
    end
    throw=find(Ext_Prop_OD(:,5)==0);
    Ext_Prop_OD(throw,:)=[];
```

```
    %Reduce the subnetwork dynamic od to only boundary centroid
    %origins' OD pairs for origin section "z".
    l=1;
    for boundary=1:length(Bound_Centroids(:,1));
        for k=1:length(Subnet_Base_OD)
            testval=Subnet_Base_OD(k,3);
            if testval==Bound_Centroids(boundary,z)
                Int_Prop_OD(l,1,z)=testval;
                Int_Prop_OD(l,2,z)=Subnet_Base_OD(k,4);
                Int_Prop_OD(l,3,z)=Subnet_Base_OD(k,5);
                Int_Prop_OD(l,4,z)=Subnet_Base_OD(k,6);
                l=l+1;
            end
        end
    end

    %Index boundary destinations for origin section "z" by section
    %(column 5).
    w=1;
    for w=1:length(Bound_Centroids(1,:));
        for boundary=1:length(Bound_Centroids(:,1));
            for i=1:length(Int_Prop_OD(:,1,z))
                if Int_Prop_OD(i,1,z)>0
                    if Int_Prop_OD(i,2,z)==Bound_Centroids(boundary,w)
                        Int_Prop_OD(i,5,z)=w;
                    end
                end
            end
        end
        w=w+1;
    end

    %CALULATE AVERAGE BYPASSING TRAVEL TIMES
    %Populate external matrix with average bypassing travel times by
    %OD pair (column 6) and bypass demand (column 7).
    clear i;
    for i=1:length(Ext_Prop_OD(:,1))
        for j=1:length(ExttoExtTTSource(:,1))
            if Ext_Prop_OD(i,1)==ExttoExtTTSource(j,1) &&
Ext_Prop_OD(i,2)==ExttoExtTTSource(j,3) &&
Ext_Prop_OD(i,3)==ExttoExtTTSource(j,2)
                Ext_Prop_OD(i,6)=ExttoExtTTSource(j,4);
                Ext_Prop_OD(i,7)=ExttoExtTTSource(j,5);
            end
        end
    end

    %Average the bypassing travel times for each
    %section weighted by demand (column 9); begin with sum product
    %(column 8) of average bypassing travel time (column 6) and
    %bypassing demand (column 7).
    clear i;
```

```
    clear j;
    clear k;
    for i=1:length(Ext_Prop_OD(:,1));
        Ext_Prop_OD(i,8)=Ext_Prop_OD(i,6)*Ext_Prop_OD(i,7);
    end

    for q=1:length(Ext_Centroids(1,:));
        for l=1:length(Ext_Centroids(:,q));
            for i=1:length(Ext_Prop_OD(:,1));
                if Ext_Prop_OD(i,2)==Ext_Centroids(l,q)
                    Ext_Prop_OD(i,5)=q;
                end
            end
        end

        i=q;
        for j=0:max(unique(Ext_Prop_OD(:,3)));
            tempprod(i,j+1)=sum(Ext_Prop_OD(Ext_Prop_OD(:,5)==i &
Ext_Prop_OD(:,3)==j,8))/sum(Ext_Prop_OD(Ext_Prop_OD(:,5)==i &
Ext_Prop_OD(:,3)==j,7));
            demandsum(i,j+1)=sum(Ext_Prop_OD(Ext_Prop_OD(:,5)==i &
Ext_Prop_OD(:,3)==j,4));
        end
        Ext_Prop_OD(:,5)=0;
        q=q+1;
    end

    i=max(unique(Ext_Prop_OD(:,3)));
    j=max(unique(Int_Prop_OD(:,4,z)));
    k=max([i j]);
    l=length(Ext_Centroids(1,:));
    store=zeros(k+1,2,l);
    clear i;
    clear j;
    clear k;
    clear l;

    n=0;
    for i=1:length(store(:,1,1));
        for k=1:length(store(1,1,:));
            store(i,1,k)=n;
        end
        n=n+1;
    end

    clear i;
    clear k;
    clear n;
    for i=1:max(unique(Ext_Prop_OD(:,3)));
        for k=1:length(store(1,1,:));
            store(i,2,k)=tempprod(k,i);
        end
```

```
    end

%CALULATE AVERAGE TRAVERSING TRAVEL TIMES
%Begin with weighted external to subnet travel time for origin section.
%Create table with columns: external origin centroid, boundary
%destination centroid, and time period.
    clear i;
    clear j;
    clear k;
    clear l;
    clear n;
    clear q;
    l=1;
    for i=1:length(Ext_Centroids(:,z))
        for j=1:length(Bound_Centroids(:,z))
            for k=1:max(ExtBoundTTSource(:,2))+1
                if Ext_Centroids(i,z)>0 & Ext_Centroids(i,z)<200000 &
Bound_Centroids(j,z)>0 & Bound_Centroids(j,z)<200000
                    ExtBoundTT(l,1)=Ext_Centroids(i,z);
                    ExtBoundTT(l,2)=Bound_Centroids(j,z);
                    ExtBoundTT(l,3)=k-1;
                    l=l+1;
                end
            end
        end
    end

    if exist('ExtBoundTT')

    %Populate matrix with source travel times and volumes to average
    %external travel times.
    clear i;
    clear j;
    for i=1:length(ExtBoundTT(:,1))
        for j=1:length(ExtBoundTTSource(:,1))
            if ExtBoundTT(i,1)==ExtBoundTTSource(j,1) &&
ExtBoundTT(i,2)==ExtBoundTTSource(j,3) &&
ExtBoundTT(i,3)==ExtBoundTTSource(j,2)
                ExtBoundTT(i,4)=ExtBoundTTSource(j,4);
                ExtBoundTT(i,5)=ExtBoundTTSource(j,5);
            end
        end
    end

    %Average the entering external travel times for origin section for
    %each time period weighted by demand and add to external proportion
    %table.
    clear i;
    clear j;
    clear k;
    for i=1:length(ExtBoundTT(:,1));
        ExtBoundTT(i,6)=ExtBoundTT(i,4)*ExtBoundTT(i,5);
```

```
    end

    for j=0:max(unique(ExtBoundTT(:,3)));

tempdiv(1,j+1)=sum(ExtBoundTT(ExtBoundTT(:,3)==j,6))/sum(ExtBoundTT(Ext
BoundTT(:,3)==j,5));
    end

    for i=1:length(store(:,1,1));
        for j=1:length(store(1,1,:));
            for k=1:length(tempdiv(1,:));
                if store(i,1,j)==k-1
                    store(i,3,j)=tempdiv(1,k);
                end
            end
        end
    end

    %Next, determine weighted internal travel times for origin section
     %to each destination section by time period.
    %Update internal proportion table with columns for internal travel
     %time for the base and impact scenarios.
    clear i;
    clear j;
    for i=1:length(Int_Prop_OD(:,1,z))
        for j=1:length(IntTTBase)
            if Int_Prop_OD(i,5,z)~=0
                if Int_Prop_OD(i,1,z)==IntTTBase(j,1) &&
Int_Prop_OD(i,2,z)==IntTTBase(j,2) &&
Int_Prop_OD(i,4,z)==IntTTBase(j,3)
                    Int_Prop_OD(i,6,z)=IntTTBase(j,4);
                end
            end
        end
    end
    clear i;
    clear j;
    for i=1:length(Int_Prop_OD)
        for j=1:length(IntTTImpact)
            if Int_Prop_OD(i,5,z)~=0
                if Int_Prop_OD(i,1,z)==IntTTImpact(j,1) &&
Int_Prop_OD(i,2,z)==IntTTImpact(j,2) &&
Int_Prop_OD(i,4,z)==IntTTImpact(j,3)
                    Int_Prop_OD(i,7,z)=IntTTImpact(j,4);
                end
            end
        end
    end

    %Average the internal travel times for each scenario from boundary
    %origin section to each destination section for each time period
```

```
    %weighted by demand and add to external proportion table; base
    %scenario
    clear i;
    for i=1:length(Int_Prop_OD(:,1,z));
        Int_Prop_OD(i,8,z)=Int_Prop_OD(i,3,z)*Int_Prop_OD(i,6,z);
    end

    for i=1:length(Int_Prop_OD(:,1,z));
        Int_Prop_OD(i,9,z)=Int_Prop_OD(i,3,z)*Int_Prop_OD(i,7,z);
    end
    clear i;
    clear j;
    for i=1:max(unique(Int_Prop_OD(:,5,z)));
        for j=0:max(unique(Int_Prop_OD(:,4,z)));
            tempsum(i,j+1)=sum(Int_Prop_OD(Int_Prop_OD(:,5,z)==i &
Int_Prop_OD(:,4,z)==j,8,z))/sum(Int_Prop_OD(Int_Prop_OD(:,5,z)==i &
Int_Prop_OD(:,4,z)==j,3,z));
        end
        i=i+1;
    end
    clear i;
    clear j;
    clear k;
    if exist('tempsum')
    for i=1:length(store(:,1,1));
        for j=1:length(tempsum(:,1));
            for k=1:length(tempsum(1,:));
                if store(i,1,j)==k-1
                    store(i,4,j)=tempsum(j,k);
                end
            end
        end
    end

    %and impact scenario.
    clear i;
    clear j;
    clear k;
    clear tempsum;
    for i=1:max(unique(Int_Prop_OD(:,5,z)));
        for j=0:max(unique(Int_Prop_OD(:,4,z)));
            tempsum(i,j+1)=sum(Int_Prop_OD(Int_Prop_OD(:,5,z)==i &
Int_Prop_OD(:,4,z)==j,9,z))/sum(Int_Prop_OD(Int_Prop_OD(:,5,z)==i &
Int_Prop_OD(:,4,z)==j,3,z));
        end
        i=i+1;
    end
    clear i;
    clear j;
    clear k;
    for i=1:length(store(:,1,1));
        for j=1:length(tempsum(:,1));
```

```
        for k=1:length(tempsum(1,:));
            if store(i,1,j)==k-1
                store(i,5,j)=tempsum(j,k);
            end
        end
    end
end

%Reduce the boundary to external travel time set to only external
%destinations applicable to origin section (remove origin section
%from set).
BoundExtTT=zeros(length(BoundExtTTSource),6);
clear i;
clear j;
clear k;
clear l;
clear w;
clear boundary;
l=1;
for k=1:length(BoundExtTTSource);
    BoundExtTT(l,1)=BoundExtTTSource(k,1);
    BoundExtTT(l,2)=BoundExtTTSource(k,3);
    BoundExtTT(l,3)=BoundExtTTSource(k,2);
    BoundExtTT(l,5)=BoundExtTTSource(k,4);
    BoundExtTT(l,6)=BoundExtTTSource(k,5);
    l=l+1;
end
w=1;
for w=1:length(Bound_Centroids(1,:));
    for boundary=1:length(Bound_Centroids(:,1));
        for i=1:length(BoundExtTT)
            if BoundExtTT(i,1)==Bound_Centroids(boundary,w)
                BoundExtTT(i,4)=w;
            end
        end
    end
    w=w+1;
end
throw=find(BoundExtTT(:,4)==0);
BoundExtTT(throw,:)=[];

%Average the exiting external travel times for each destination
%section for each time period weighted by demand and add to external
%proportion table (column 13).
clear i;
for i=1:length(BoundExtTT(:,1));
    BoundExtTT(i,7)=BoundExtTT(i,5)*BoundExtTT(i,6);
end

clear i;
clear j;
clear tempprod;
```

```
    for i=1:max(unique(BoundExtTT(:,4)));
        for j=0:max(unique(BoundExtTT(:,3)));
            tempprod(i,j+1)=sum(BoundExtTT(BoundExtTT(:,4)==i &
BoundExtTT(:,3)==j,7))/sum(BoundExtTT(BoundExtTT(:,4)==i &
BoundExtTT(:,3)==j,6));
        end
        i=i+1;
    end

    clear i;
    clear j;
    clear k;
    for i=1:length(store(:,1,1));
        for j=1:length(tempprod(:,1));
            for k=1:length(tempprod(1,:));
                if store(i,1,j)==k-1
                    store(i,6,j)=tempprod(j,k);
                end
            end
        end
    end

    %Sum the entering, internal, and exiting travel times for each
    %origin to destination section for each time period for the base
    %and impact scenarios in the external proportion table.
    clear i;
    clear j;
    for i=1:length(store(:,1,1));
        for j=1:length(store(1,1,:));
            if store(i,4,j)>0
                store(i,7,j)=store(i,3,j)+store(i,4,j)+store(i,6,j);
            else store(i,7,j)=0;
            end
        end
    end
    clear i;
    clear j;
    for i=1:length(store(:,1,1));
        for j=1:length(store(1,1,:));
            if store(i,5,j)>0
                store(i,8,j)=store(i,3,j)+store(i,5,j)+store(i,6,j);
            else store(i,8,j)=0;
            end
        end
    end

    %FINALIZE THE NEW ADJUSTED DYNAMIC OD TABLE
    clear i;
    clear j;
    clear k;
    for i=1:max(unique(Ext_Prop_OD(:,3)));
        for k=1:length(store(1,1,:));
```

```
            store(i,9,k)=demandsum(k,i);
        end
    end




    %SET UP INTERNAL DEMAND TABLE FOR UPDATING DEMAND
    %Find cumulative internal (traversing) demand to each destination
    %section for each time period and find proportion represented by OD
    %pairing.
    clear i;
    clear j;
    for i=1:max(unique(Int_Prop_OD(:,5,z)));
        for j=0:max(unique(Int_Prop_OD(:,4,z)));
            b(i,j+1)=sum(Int_Prop_OD(Int_Prop_OD(:,5,z)==i &
Int_Prop_OD(:,4,z)==j,3,z));
        end
        i=i+1;
    end
    clear i;
    clear j;
    clear k;
    for i=1:length(Int_Prop_OD(:,1,z));
        for j=1:length(b(:,1));
            for k=1:length(b(1,:));
                if Int_Prop_OD(i,4,z)==k-1 & Int_Prop_OD(i,5,z)==j
                    Int_Prop_OD(i,10,z)=b(j,k);
                end
            end
        end
    end
    clear i;
    for i=1:length(Int_Prop_OD(:,1,z));
        if Int_Prop_OD(i,5,z)~=0
            Int_Prop_OD(i,11,z)=Int_Prop_OD(i,3,z)/Int_Prop_OD(i,10,z);
        end
    end

    %Update test with internal demand and proportion for each
    %destination section and time period.
    clear i;
    clear j;
    clear k;
    for i=1:length(store(:,1,1));
        for j=1:length(b(:,1));
            for k=1:length(b(1,:));
                if store(i,1,j)==k-1
                    store(i,10,j)=b(j,k);
                end
            end
```

```
        end
    end

    clear i;
    clear j;
    for i=1:length(store(:,1,1));
        for j=1:length(store(1,1,:));
            store(i,11,j)=min(store(i,10,j)/store(i,9,j),0.999999999);
        end
    end

    %Solve for the theta parameter.
    syms theta
    for i = 1:length(store(:,1,1));
        for j=1:length(store(1,1,:));
            if store(i,2,j)>0 & store(i,7,j)>0 & store(i,8,j)>0 &
round((store(i,7,j)-store(i,2,j))*1000000)/1000000~=0
                store(i,12,j)=double(solve(store(i,11,j)==exp(-
theta*store(i,7,j))/(exp(-theta*store(i,7,j))+exp(-
theta*store(i,2,j)))));
            else store(i,12,j)=0;
            end
        end
    end

    clear j;
    for j=1:length(store(1,1,:));
        if j==z
            store(:,12,j)=0;
        end
    end

    %Calculate new "traversing" proportions for each destination and
     %time period.
    clear i;
    clear j;
    for i=1:length(store(:,1,1));
        for j=1:length(store(1,1,:));
            if store(i,12,j)>0
                store(i,13,j)=exp(-store(i,12,j)*store(i,8,j))/(exp(-
store(i,12,j)*store(i,8,j))+exp(-store(i,12,j)*store(i,2,j)));
            else store(i,13,j)=store(i,11,j)
            end
        end
    end

    clear i;
    clear j;
    for i=1:length(store(:,1,1));
        for j=1:length(store(1,1,:));
            if isnan(store(i,13,j))
                store(i,13,j)=store(i,11,j);
```

```
         end
    end
end

%Calculate the new cumulative "traversing" demand for each
%destination section and time period.
clear i;
clear j;
for i = 1:length(store(:,1,1));
    for j=1:length(store(1,1,:));
        if store(i,12,j)>0
            store(i,14,j)=store(i,9,j)*store(i,13,j);
        else store(i,14,j)=store(i,10,j);
        end
    end
end

%Add the new cumulative "traversing" demand to the internal demand
%matrix organized by destination section and time period.
clear i;
clear j;
clear b;
for i=1:length(store(1,1,:));
    for j=1:length(store(:,1,1));
        b(i,j)=store(j,14,i);
    end
end

clear i;
clear j;
clear k;
for i=1:length(Int_Prop_OD(:,1,z));
    for j=1:length(b(:,1));
        for k=1:length(b(1,:));
            if Int_Prop_OD(i,4,z)==k-1 & Int_Prop_OD(i,5,z)==j
                Int_Prop_OD(i,12,z)=b(j,k);
            end
        end
    end
end

%Calculate the new "traversing" demand based on the proportion
%of the original cumulative demand (by destination section and time
%period) represented by each OD pair by destination section and time
%period.
clear i;
for i=1:length(Int_Prop_OD(:,1,z));
    Int_Prop_OD(i,13,z)=Int_Prop_OD(i,11,z)*Int_Prop_OD(i,12,z);
end

clear BoundExtTT;
clear ExtBoundTT;
```

```
    clear a;
    clear b;
    clear c;
    clear d;
    clear i;
    clear j;
    clear k;
    clear l;
    clear q;
    clear u;
    clear v;
    clear w;
    clear demandsum;
    clear store;
    clear temp;
    clear tempdiv;
    clear tempprod;
    clear tempsum;
    clear test;
    clear testval;
    clear theta;
    clear throw;
    clear Ext_Prop_OD;

    end

    end

    end
    z=z+1;
end

clear boundary;
clear external;

n=1;
o=sort(unique(Subnet_Base_OD(:,3)));
for i=1:length(o)
    index=find(Subnet_Base_OD(:,3)==o(i));
    [index2,index3]=find(Int_Prop_OD(:,1,:)==o(i));
    for j=1:length(index)
        for k=1:length(index2)
            for l=1:length(unique(index3))
                if
Subnet_Base_OD(index(j),4)==Int_Prop_OD(index2(k),2,index3(l)) &
Subnet_Base_OD(index(j),6)==Int_Prop_OD(index2(k),4,index3(l))
                    Subnet_Base_OD_index(n,1)=index(j);
                    Int_Prop_OD_index(n,1)=index2(k);
                    Int_Prop_OD_index(n,2)=index3(l);
                    n=n+1;
                end
            end
```

```
        end
    end
end

for m=1:length(Int_Prop_OD_index(:,2))

Int_Prop_OD_Match(m,1)=Int_Prop_OD(Int_Prop_OD_index(m,1),13,Int_Prop_O
D_index(m,2));
end
Joined_OD=horzcat(Subnet_Base_OD(Subnet_Base_OD_index,:),Int_Prop_OD_Ma
tch);

Subnet_Base_OD_NoMatch=Subnet_Base_OD;
Subnet_Base_OD_NoMatch(Subnet_Base_OD_index,:)=[];
Subnet_Base_OD_NoMatch=horzcat(Subnet_Base_OD_NoMatch,Subnet_Base_OD_No
Match(:,5));

%Join matches with ODTs that don't match
Joined_OD=vertcat(Joined_OD,Subnet_Base_OD_NoMatch);
clear i;
for i=1:length(Joined_OD)
    if  Joined_OD(i,4)<250000 & Joined_OD(i,7)==0
        Joined_OD(i,7)=Joined_OD(i,5);
    end
end

clear i;
clear j;
clear k;
clear l;
clear m;
clear n;
clear o;
clear index;
clear index2;
clear index3;
clear Subnet_Base_OD_index;
clear Int_Prop_OD_index;
clear Int_Prop_OD_Match;
clear Subnet_Base_OD_NoMatch;

Time=toc;
```

External-to-External Demand Adjustment Script

```
%This code initiates a function file that performs the External-to-
Internal
%adjustment

for i=1:length(Ext_Centroids(:,1));
    for j=1:length(Ext_Centroids(1,:));
        if Ext_Centroids(i,j)>200000
            Ext_Centroids(i,j)=0;
        end
    end
end

for i=1:length(Bound_Centroids(:,1));
    for j=1:length(Bound_Centroids(1,:));
        if Bound_Centroids(i,j)>200000
            Bound_Centroids(i,j)=0;
        end
    end
end

OD=Subnet_Base_OD;
OD(:,5)=OD(:,7);
OD(:,7)=[];
Int_Prop_OD=zeros(length(OD(:,1)),14,length(Bound_Centroids(1,:)));

%The following initiates the associated function
for i = 1:length(Bound_Centroids(1,:))
[ Int_Prop_OD(:,:,i) ] = Ext_to_Int_Dest_Choice( Bound_Centroids(:,i),
Ext_Centroids(:,i), ExtBoundTTSource, IntTTBase, IntTTImpact, OD );
end

%The following is the function initiated by the above code block

function [ Int_Prop_OD ] = Ext_to_Int_Dest_Choice( Bound_Centroids,
Ext_Centroids, ExtBoundTTSource, IntTTBase, IntTTImpact, OD )

%This script requires the inputs: each region's boundary centroids
%(Bound_Centroids), each region's external centroids (Ext_Centroids),
%the subnetwork dynamic OD (OD), external to boundary travel times
%(ExtBoundTTSource), internal travel times in the base case
%(IntTTBase), and internal travel times in the impact scenario
%(IntTTImpact).

%SETUP FOR REGION'S OD TABLE MODIFICATION
%This script starts with a subnetwork dynamic OD table and all
%regions's boundary centroids and calculates proportions of demand at
%each boundary centroid for destinations that use at least 2 boundary
%centroids. The output is a table with columns: (1) Origin, (2)
```

```
%Destination, (3) Demand, (4) Time Period, (5) Proportion of
%Destination using Boundary Centroid.

%Remove extra zeros from centroid column imported

Bound_Centroids=Bound_Centroids(find(Bound_Centroids(:,1)>0),:);
Ext_Centroids=Ext_Centroids(find(Ext_Centroids(:,1)>0),:);

if length(Bound_Centroids)>1

if length(Ext_Centroids)>1

%Reduce the dynamic od to only boundary centroid origins OD pairs.
l=1;
for k=1:length(OD)
    for m=1:length(Bound_Centroids)
        if OD(k,3)==Bound_Centroids(m)
            Int_Prop_OD(l,1)=OD(k,3);
            Int_Prop_OD(l,2)=OD(k,4);
            Int_Prop_OD(l,3)=OD(k,5);
            Int_Prop_OD(l,4)=OD(k,6);
            l=l+1;
        end
    end
end

%Reduce to destinations that use 2 or more boundary centroid origins to
%enter the network.
index=zeros(length(Int_Prop_OD),1);
for i=1:length(Int_Prop_OD)
    for j=1:length(Int_Prop_OD)
        if
Int_Prop_OD(i,1)~=Int_Prop_OD(j,1)&&Int_Prop_OD(i,2)==Int_Prop_OD(j,2)&
&Int_Prop_OD(i,4)==Int_Prop_OD(j,4)
            index(i,1)=1;
        end
    end
end

%Calculates the proportions of each destination's demand that uses one
%of the boundary centroids.
if sum(sum(Int_Prop_OD))~=0
    Int_Prop_OD(:,5)=Int_Prop_OD(:,3);
    for i=1:length(Int_Prop_OD)
        for j=1:length(Int_Prop_OD)
            if
Int_Prop_OD(i,1)~=Int_Prop_OD(j,1)&&Int_Prop_OD(i,2)==Int_Prop_OD(j,2)&
&Int_Prop_OD(i,4)==Int_Prop_OD(j,4)
                Int_Prop_OD(i,5)=Int_Prop_OD(i,5)+Int_Prop_OD(j,3);
            end
        end
```

```
    end
    Int_Prop_OD(:,5)=Int_Prop_OD(:,3)./Int_Prop_OD(:,5);

%CALULATE AVERAGE EXTERNAL TRAVEL TIMES
%Create table with columns: external centroids origin, boundary
%centroid destination, and time period.
l=1;
for i=1:length(Ext_Centroids)
    for j=1:length(Bound_Centroids)
        for k=1:max(ExtBoundTTSource(:,2))+1
            ExtBoundTT(l,1)=Ext_Centroids(i,1);
            ExtBoundTT(l,2)=Bound_Centroids(j,1);
            ExtBoundTT(l,3)=k-1;
            l=l+1;
        end
    end
end

%Populate matrix with source travel times (column 4) and volumes
%(column 5) to average external travel times.
for i=1:length(ExtBoundTT(:,1))
    for j=1:length(ExtBoundTTSource(:,1))
        if ExtBoundTT(i,1)==ExtBoundTTSource(j,1) &&
ExtBoundTT(i,2)==ExtBoundTTSource(j,3) &&
ExtBoundTT(i,3)==ExtBoundTTSource(j,2)
            ExtBoundTT(i,4)=ExtBoundTTSource(j,4);
            ExtBoundTT(i,5)=ExtBoundTTSource(j,5);
        end
    end
end

%Average the travel times that are not equal to zero to each boundary
%origin weighted by demand, grouped by fake mega centroid.
l=1;
for i=1:length(Bound_Centroids)
    for k=1:max(ExtBoundTTSource(:,2))+1
        ExtBoundTTReg(l,1)=1;
        ExtBoundTTReg(l,2)=Bound_Centroids(i,1);
        ExtBoundTTReg(l,3)=k-1;
        ExtBoundTTReg(l,4)=0;
        l=l+1;
    end
end

Weights_1=zeros(length(ExtBoundTTReg),1);
Weights_2=zeros(length(ExtBoundTTReg),1);
for i=1:length(ExtBoundTTReg)
    for j=1:length(ExtBoundTT)
        if ExtBoundTTReg(i,2)==ExtBoundTT(j,2) &&
ExtBoundTTReg(i,3)==ExtBoundTT(j,3)&&ExtBoundTT(j,4)~=0

ExtBoundTTReg(i,4)=ExtBoundTTReg(i,4)+ExtBoundTT(j,5)*ExtBoundTT(j,4);
```

```
            Weights_1(i,1)=Weights_1(i,1)+ExtBoundTT(j,5);
            Weights_2(i,1)=Weights_2(i,1)+1;
        end
    end
end
Weights=Weights_1.*Weights_2;
ExtBoundTTReg(:,4)=ExtBoundTTReg(:,4)./Weights(:,1);
ExtBoundTTReg=ExtBoundTTReg(~isnan(ExtBoundTTReg(:,4)),:);

clear j;

%COMBINE EXTERNAL AND INTERNAL TRAVEL TIMES
%Appends the external and internal travel times to Int_Prop_OD to
%create the columns: (1) Origin, (2) Destination, (3) Demand, (4) Time
%Period, (5) Destination Demand Proportion using Boundary Centroid, (6)
%Ext Travel Time, (7) Int Travel Time Base, and (8) Int Travel Time
%Impact Scenario.

for i=1:length(Int_Prop_OD)
    for j=1:length(ExtBoundTTReg(:,1))
        if Int_Prop_OD(i,1)==ExtBoundTTReg(j,2) &&
Int_Prop_OD(i,4)==ExtBoundTTReg(j,3)
            Int_Prop_OD(i,6)=ExtBoundTTReg(j,4);
        end
    end
end

for i=1:length(Int_Prop_OD)
    for j=1:length(IntTTBase)
        if Int_Prop_OD(i,1)==IntTTBase(j,1) &&
Int_Prop_OD(i,2)==IntTTBase(j,2) && Int_Prop_OD(i,4)==IntTTBase(j,3)
            Int_Prop_OD(i,7)=IntTTBase(j,4);
        end
    end
end

for i=1:length(Int_Prop_OD)
    for j=1:length(IntTTImpact)
        if Int_Prop_OD(i,1)==IntTTImpact(j,1) &&
Int_Prop_OD(i,2)==IntTTImpact(j,2) &&
Int_Prop_OD(i,4)==IntTTImpact(j,3)
            Int_Prop_OD(i,8)=IntTTImpact(j,4);
        end
    end
end

%FINALIZE THE NEW ADJUSTED DYNAMIC OD TABLE
%Int_Prop_OD Columns: (1)Origin, (2)Destination, (3)Demand, (4)Time
%Period, (5)Desintation Proportion using Boundary Centroid, (6)
%External Travel Time, (7) Internal Travel Time Base, (8) Internal
%Travel Times Impact, (9) Total Travel Time Base, (10) Total Travel
```

```
%Time Impact Scenario, (11) Used Proportions (12) Theta Parameter, (13)
%New Proportion Using Boundary Origin, (14) Adjusted Demand.
%Calculate (9) Total Travel Time Base, (10) Total Travel Time Impact
%Scenario, Initializes (11)-(14)
if sum(sum(Int_Prop_OD))~=0
Int_Prop_OD(:,9)=Int_Prop_OD(:,6)+Int_Prop_OD(:,7);
Int_Prop_OD(:,10)=Int_Prop_OD(:,6)+Int_Prop_OD(:,8);
Int_Prop_OD(:,11)=zeros(length(Int_Prop_OD(:,1)),1);
Int_Prop_OD(:,12)=zeros(length(Int_Prop_OD(:,1)),1);
Int_Prop_OD(:,13)=zeros(length(Int_Prop_OD(:,1)),1);
Int_Prop_OD(:,14)=Int_Prop_OD(:,3);

%Extract destination and time period to perform discrete choice
%analysis.
a=sort(unique(Int_Prop_OD(:,2)));
b=max((Int_Prop_OD(:,4)));
for l=1:length(a)
    for k =1:b+1
        dest=a(l);
        test=Int_Prop_OD(Int_Prop_OD(:,2)==dest,:);
        test=test(test(:,4)==k-1,:);
        if length(test(:,1)>0)
            %Create variable to store corresponding row for greatest
            %theta value
            thetaval3=zeros(length(test(:,1)),1);
            syms theta
            for i = 1:length(test(:,1))
                %Create variable for theta values calculated for each
                %origin within test
                thetaval=zeros(length(test(:,1)),1);
                %Create variable for pairwise proportions
                thetaval2=zeros(length(test(:,1)),1);

                for j = 1:length(test(:,1))
                    %Two "IF" statements: only evaluate for different
                    %ODT and if demand and travel times are correlated
                    if i~=j
                        if
(test(i,3)>test(j,3)&&test(i,9)<test(j,9))||(test(i,3)<test(j,3)&&test(
i,9)>test(j,9))

thetaval2(j,1)=test(i,3)./(test(i,3)+test(j,3));

thetaval(j,1)=double(solve(thetaval2(j,1)==exp(-theta*test(i,9))/(exp(-
theta*test(i,9))+exp(-theta*test(j,9))),theta));
                        end
                    end
                end

                %Use the max theta value for time period,
                %destination, and origin
                throw=find(thetaval==max(thetaval));
```

```
                test(i,12)=thetaval(throw(1,1));
                %Use the corresponding pairwise proportion and index
                %for max theta value
                test(i,11)=thetaval2(throw(1,1),1);
                thetaval3(i,1)=throw(1,1);
            end

            %Find the max theta value for time period and destination
            throw2=find((test(:,12)==max(test(:,12))));
            adj_dem_1=throw2(1,1);
            adj_dem_2=thetaval3(adj_dem_1,1);
            %Store same theta value for pairwise comparisons
            test(adj_dem_2,12)=test(adj_dem_1,12);
            %Populate appropriate pairwise proportions
            test(adj_dem_2,11)=1-test(adj_dem_1,11);
            %Calculate new proportions
            if exp(-test(adj_dem_1,12).*test(adj_dem_1,10))+exp(-
test(adj_dem_1,12).*test(adj_dem_2,10))~=0
                test(adj_dem_1,13) = exp(-
test(adj_dem_1,12).*test(adj_dem_1,10))/(exp(-
test(adj_dem_1,12).*test(adj_dem_1,10))+exp(-
test(adj_dem_1,12).*test(adj_dem_2,10)));
                test(adj_dem_2,13) = exp(-
test(adj_dem_1,12).*test(adj_dem_2,10))/(exp(-
test(adj_dem_1,12).*test(adj_dem_1,10))+exp(-
test(adj_dem_1,12).*test(adj_dem_2,10)));
            else  test(adj_dem_1,13) = test(adj_dem_1,11);
                test(adj_dem_2,13) = test(adj_dem_2,11);
            end
            %Calculate new demand values

test(adj_dem_1,14)=test(adj_dem_1,13).*(test(adj_dem_1,3)+test(adj_dem_
2,3));

test(adj_dem_2,14)=test(adj_dem_2,13).*(test(adj_dem_1,3)+test(adj_dem_
2,3));
            %Copy theta and new demand
            for i=1:length(Int_Prop_OD(:,1))
                for j=1:length(test(:,1))
                    if
Int_Prop_OD(i,1)==test(j,1)&&Int_Prop_OD(i,2)==test(j,2)&&Int_Prop_OD(i
,4)==test(j,4)&&test(j,13)~=0
                        Int_Prop_OD(i,11)=test(j,11);
                        Int_Prop_OD(i,12)=test(j,12);
                        Int_Prop_OD(i,13)=test(j,13);
                        Int_Prop_OD(i,14)=test(j,14);
                    end
                end
            end
        end
    end
end
```

```
Int_Prop_OD=sortrows(Int_Prop_OD, [2 4 1]);
clear a
clear b
clear i
clear j
clear k
clear l
clear m
clear adj_dem_1
clear adj_dem_2
clear dest
clear index
clear test
clear theta
clear thetaval
clear thetaval2
clear thetaval3
clear throw
clear throw2
clear Weights
clear Weights_1
clear Weights_2

n=length(OD(:,1))-length(Int_Prop_OD(:,1));
Int_Prop_OD=vertcat(Int_Prop_OD,zeros(n,14));

else Int_Prop_OD=0;
end
else Int_Prop_OD=0;
end
else Int_Prop_OD=0;
end
else Int_Prop_OD=0;
end
end

%The following continues to compile the output file from the function

for j=1:length(Int_Prop_OD(1,1,:))
    for k=1:length(Int_Prop_OD(:,1,j))
        if Int_Prop_OD(k,14,j)~=0
            for l=1:length(OD(:,1))
                if
OD(l,3)==Int_Prop_OD(k,1,j)&&OD(l,4)==Int_Prop_OD(k,2,j)&&OD(l,6)==Int_
Prop_OD(k,4,j)
                    OD(l,5)=Int_Prop_OD(k,14,j);
                end
            end
        end
    end
end
```

Compare Boundary Demand Script

```
%This code joins three ODT matrices by matching their unique ID, which
%is the concatenated origin, destination, and time period IDs, then
%compares boundary demand values and calculates an RMSE value using the
%impact condition ODT table (Subnet_Impact_OD) as the baseline, and the
%base condition ODT (Subnet_Base_OD) and adjusted base condition ODT
%tables as the comparison values.

for z = 1:3

    if z==1
        test=OD;
    elseif z==2
        test=Subnet_Base_OD;
    elseif z==3
        test=Subnet_Impact_OD;
    end
    for i=1:length(test)
        test(i,7)=str2num(sprintf('%-
1d',[test(i,3),test(i,4),test(i,6)]));
    end

    test(:,[1 2])=[];

    if z==1
        base1=test;
    elseif z==2
        base2=test;
    elseif z==3
        base3=test;
    end
end

for z = 1:2
    if z==1
        Base1=base1;
        Base2=base2;
    elseif z==2
        Base1=Joined_OD3;
        Base2=base3;
    end

%Initialize index for matching unique IDs
n=1;
%Compare matrix unique IDs based on origins to reduce computation time
o=sort(unique(Base1(:,1)));
for i=1:length(o)
    index=find(Base1(:,1)==o(i));
    index2=find(Base2(:,1)==o(i));
    for j=1:length(index)
```

```
        for k=1:length(index2)
            if Base1(index(j),5)==Base2(index2(k),5)
                %Indices of each matrix match stored to combine later
                Base1_index(n,1)=index(j);
                Base2_index(n,1)=index2(k);
                n=n+1;
            end
        end
    end
end

%Append matrices where unique IDs match
Joined_OD3=horzcat(Base1(Base1_index,:),Base2(Base2_index,3));
%Prepare the matrices to be appended to matching IDs, values of other
%matrix demand are set to zero
Base1_NoMatch=Base1;
Base1_NoMatch(Base1_index,:)=[];
Base1_NoMatch=horzcat(Base1_NoMatch,zeros(length(Base1_NoMatch),1));
Base2_NoMatch=Base2;
Base2_NoMatch(Base2_index,:)=[];
Base2_NoMatch=horzcat(Base2_NoMatch,zeros(length(Base2_NoMatch),z));
Base2_NoMatch=Base2_NoMatch(:,[1 2 5+z 4:4+z 3]);
%Join matches with ODTs that don't match
Joined_OD3=vertcat(Joined_OD3,Base1_NoMatch,Base2_NoMatch);
clear Base1
clear Base1_NoMatch
clear Base1_index
clear Base2
clear Base2_NoMatch
clear Base2_index
clear index
clear index2
clear i
clear j
clear k
clear n
clear o
clear z
end

for i=1:length(Joined_OD3(:,1))
    Joined_OD3(i,8)=Joined_OD3(i,7)-Joined_OD3(i,3);
    Joined_OD3(i,9)=Joined_OD3(i,7)-Joined_OD3(i,6);
    Joined_OD3(i,10)=Joined_OD3(i,8).*Joined_OD3(i,8);
    Joined_OD3(i,11)=Joined_OD3(i,9).*Joined_OD3(i,9);
end
clear i;
Joined_OD3=sortrows(Joined_OD3);
%Calculate RMSE for the adjusted ODT table
RMSEADJ=sqrt((sum(Joined_OD3(:,10)))./size(Joined_OD3,1))
%Calculate RMSE for the base ODT table
RMSEBASE=sqrt((sum(Joined_OD3(:,11)))./size(Joined_OD3,1))
```

APPENDIX C

Preliminary Hypothesis Test Results: MCAPE and SSIM Index

Table C.1 Preliminary Test Results for 1-Hour Analysis Period Using MCAPE

Scenario	Location	Subnetwork Size (Order)	Impact Size	Capacity Reduction	Hypothesis Testing				Prediction Interval			
					Equal Variance*	Normality Test		Equal Mean***	Lower Bound	Upper Bound	Range	Alternate Runs Within
						Lilliefor**	A-D**					
Base	Guadalupe St	5	1	25		Y	Y		44.48	47.28	2.80	3
Impact	Guadalupe St	5	1	25	N	Y	Y	N	44.65	50.83	6.18	9
Base	Guadalupe St	7	1	25		Y	Y		45.77	49.59	3.83	4
Impact	Guadalupe St	7	1	25	Y	Y	Y	N	46.44	53.39	6.95	9
Base	Guadalupe St	9	1	25		Y	Y		37.00	39.21	2.21	1
Impact	Guadalupe St	9	1	25	N	Y	N	N	37.32	42.83	5.51	9
Base	15th St	5	2	50		Y	Y		38.92	42.75	3.83	4
Impact	15th St	5	2	50	Y	Y	Y	N	40.31	45.74	5.44	7
Base	15th St	7	2	50		Y	Y		46.82	50.78	3.96	2
Impact	15th St	7	2	50	Y	Y	Y	N	50.11	52.30	2.19	0
Base	15th St	9	2	50		Y	Y		42.16	45.23	3.07	4
Impact	15th St	9	2	50	Y	Y	Y	N	44.28	46.88	2.60	2
Base	7th St	5	2	50		Y	Y		37.87	41.16	3.29	2
Impact	7th St	5	2	50	Y	Y	Y	N	39.51	43.76	4.25	5
Base	7th St	7	2	50		Y	Y		30.30	33.94	3.64	7
Impact	7th St	7	2	50	Y	Y	Y	N	32.58	34.92	2.34	3
Base	7th St	9	2	50		N	N		27.26	28.73	1.47	0
Impact	7th St	9	2	50	Y	Y	Y	N	28.55	30.15	1.60	0
Base	Guadalupe St	5	2	50		Y	Y		43.85	47.75	3.90	7
Impact	Guadalupe St	5	2	50	Y	Y	Y	N	44.30	50.47	6.17	10
Base	Guadalupe St	7	2	50		Y	Y		43.30	46.78	3.48	4
Impact	Guadalupe St	7	2	50	Y	N	N	N	44.09	49.60	5.50	9
Base	Guadalupe St	9	2	50		Y	Y		32.84	34.75	1.91	3
Impact	Guadalupe St	9	2	50	Y	Y	Y	N	33.45	36.93	3.48	8
Base	7th St	5	3	100		Y	Y		36.24	39.60	3.36	0
Impact	7th St	5	3	100	N	N	N	N	43.41	51.64	8.23	0
Base	7th St	7	3	100		Y	Y		31.08	34.38	3.29	0
Impact	7th St	7	3	100	Y	N	N	N	33.84	40.00	6.16	0
Base	7th St	9	3	100		Y	Y		27.86	29.32	1.46	0
Impact	7th St	9	3	100	N	Y	Y	N	28.46	33.98	5.52	7
Base	Guadalupe St	5	3	100		Y	Y		45.90	49.55	3.64	0
Impact	Guadalupe St	5	3	100	Y	Y	Y	N	53.52	58.70	5.18	0
Base	Guadalupe St	7	3	100		Y	Y		42.20	45.19	2.99	0
Impact	Guadalupe St	7	3	100	Y	Y	Y	N	48.04	52.06	4.01	0
Base	Guadalupe St	9	3	100		N	Y		32.43	35.14	2.70	0
Impact	Guadalupe St	9	3	100	Y	Y	Y	N	36.67	39.29	2.62	0

* Y = Accept H_o: $\sigma_1^2 = \sigma_2^2$; N = Reject H_o, conclude H_a: $\sigma_1^2 \neq \sigma_2^2$ (at the 95-percent confidence level)
** Y = Accept H_o: Distribution is normal; N = Reject H_o, conclude H_a: Distribution is not normal (at the 95-percent confidence level)
*** Y = Accept H_o: $\mu_1 = \mu_2$; N = Reject H_o conclude H_a: $\mu_1 \neq \mu_2$ (at the 95-percent confidence level)

Table C.2 Preliminary Test Results for 1-Hour Analysis Period Using SSIM Index

Scenario	Location	Subnetwork Size (Order)	Impact Size	Capacity Reduction	Hypothesis Testing				Prediction Interval			
					Equal Variance*	Normality Test		Equal Mean***	Lower Bound	Upper Bound	Range	Alternate Runs Within
						Lilliefor**	A-D**					
Base	Guadalupe St	5	1	25		Y	Y		0.978	0.988	0.010	8
Impact	Guadalupe St	5	1	25	N	N	N	N	0.968	0.989	0.021	10
Base	Guadalupe St	7	1	25		N	Y		0.978	0.989	0.010	8
Impact	Guadalupe St	7	1	25	Y	Y	Y	N	0.973	0.986	0.014	8
Base	Guadalupe St	9	1	25		Y	Y		0.983	0.992	0.008	6
Impact	Guadalupe St	9	1	25	Y	Y	Y	N	0.979	0.990	0.011	10
Base	15th St	5	2	50		Y	Y		0.979	0.989	0.010	7
Impact	15th St	5	2	50	Y	Y	Y	N	0.975	0.988	0.013	10
Base	15th St	7	2	50		Y	Y		0.981	0.992	0.010	9
Impact	15th St	7	2	50	Y	Y	Y	N	0.978	0.988	0.010	9
Base	15th St	9	2	50		Y	Y		0.988	0.992	0.004	4
Impact	15th St	9	2	50	Y	Y	Y	N	0.985	0.991	0.005	7
Base	7th St	5	2	50		Y	Y		0.996	0.999	0.003	7
Impact	7th St	5	2	50	Y	Y	Y	N	0.994	0.999	0.005	10
Base	7th St	7	2	50		Y	Y		0.997	0.999	0.002	4
Impact	7th St	7	2	50	Y	Y	Y	N	0.995	0.998	0.003	9
Base	7th St	9	2	50		Y	Y		0.995	0.997	0.002	5
Impact	7th St	9	2	50	Y	Y	Y	N	0.993	0.997	0.003	9
Base	Guadalupe St	5	2	50		Y	Y		0.977	0.986	0.009	6
Impact	Guadalupe St	5	2	50	N	Y	Y	N	0.966	0.987	0.020	10
Base	Guadalupe St	7	2	50		Y	Y		0.983	0.992	0.009	6
Impact	Guadalupe St	7	2	50	Y	Y	Y	N	0.978	0.991	0.012	10
Base	Guadalupe St	9	2	50		Y	Y		0.992	0.997	0.005	10
Impact	Guadalupe St	9	2	50	Y	Y	Y	N	0.991	0.997	0.006	10
Base	7th St	5	3	100		Y	Y		0.996	0.998	0.002	0
Impact	7th St	5	3	100	N	Y	Y	N	0.982	0.989	0.007	0
Base	7th St	7	3	100		Y	N		0.997	0.999	0.002	0
Impact	7th St	7	3	100	N	N	N	N	0.992	0.999	0.007	10
Base	7th St	9	3	100		Y	Y		0.995	0.997	0.002	0
Impact	7th St	9	3	100	N	Y	Y	N	0.991	0.995	0.005	2
Base	Guadalupe St	5	3	100		Y	Y		0.971	0.986	0.015	0
Impact	Guadalupe St	5	3	100	Y	Y	Y	N	0.938	0.956	0.017	0
Base	Guadalupe St	7	3	100		Y	Y		0.990	0.995	0.005	0
Impact	Guadalupe St	7	3	100	Y	Y	Y	N	0.981	0.987	0.007	0
Base	Guadalupe St	9	3	100		Y	Y		0.993	0.998	0.005	0
Impact	Guadalupe St	9	3	100	Y	Y	Y	N	0.989	0.994	0.005	1

* Y = Accept H_o: $\sigma_1^2 = \sigma_2^2$; N = Reject H_o, conclude H_a: $\sigma_1^2 \neq \sigma_2^2$ (at the 95-percent confidence level)
** Y = Accept H_o: Distribution is normal; N = Reject H_o, conclude H_a: Distribution is not normal (at the 95-percent confidence level)
*** Y = Accept H_o: $\mu_1 = \mu_2$; N = Reject H_o conclude H_a: $\mu_1 \neq \mu_2$ (at the 95-percent confidence level)

Table C.3 Preliminary Test Results for 2-Hour Analysis Period Using MCAPE

Scenario	Location	Subnetwork Size (Order)	Impact Size	Capacity Reduction	Hypothesis Testing				Prediction Interval			
					Equal Variance*	Normality Test		Equal Mean***	Lower Bound	Upper Bound	Range	Alternate Runs Within
						Lilliefor**	A-D**					
Base	Guadalupe St	5	1	25		Y	Y		46.46	49.13	2.67	2
Impact	Guadalupe St	5	1	25	Y	Y	Y	N	47.55	52.25	4.70	7
Base	Guadalupe St	7	1	25		Y	Y		47.32	49.61	2.28	3
Impact	Guadalupe St	7	1	25	N	Y	Y	N	47.27	53.82	6.55	10
Base	Guadalupe St	9	1	25		Y	Y		37.32	38.59	1.27	0
Impact	Guadalupe St	9	1	25	N	N	N	N	37.01	42.37	5.36	10
Base	15th St	5	2	50		Y	Y		39.88	43.97	4.09	1
Impact	15th St	5	2	50	Y	Y	Y	N	42.75	47.36	4.60	2
Base	15th St	7	2	50		Y	Y		49.25	52.35	3.10	0
Impact	15th St	7	2	50	Y	Y	Y	N	52.14	54.52	2.37	0
Base	15th St	9	2	50		Y	Y		44.30	47.03	2.73	0
Impact	15th St	9	2	50	Y	Y	Y	N	46.85	48.67	1.82	0
Base	7th St	5	2	50		Y	Y		39.26	40.92	1.66	0
Impact	7th St	5	2	50	Y	Y	Y	N	40.85	44.03	3.18	0
Base	7th St	7	2	50		Y	Y		30.93	33.16	2.24	1
Impact	7th St	7	2	50	Y	Y	Y	N	32.94	34.71	1.77	0
Base	7th St	9	2	50		Y	Y		27.73	29.26	1.53	0
Impact	7th St	9	2	50	Y	Y	Y	N	29.35	30.68	1.33	0
Base	Guadalupe St	5	2	50		Y	Y		46.84	49.39	2.55	4
Impact	Guadalupe St	5	2	50	Y	Y	Y	N	47.83	51.53	3.70	7
Base	Guadalupe St	7	2	50		Y	Y		44.10	46.09	1.99	1
Impact	Guadalupe St	7	2	50	N	N	N	N	44.90	48.98	4.08	7
Base	Guadalupe St	9	2	50		Y	Y		33.70	35.30	1.60	2
Impact	Guadalupe St	9	2	50	N	Y	Y	N	34.29	37.56	3.27	7
Base	7th St	5	3	100		Y	Y		37.39	39.62	2.23	0
Impact	7th St	5	3	100	N	N	N	N	44.58	52.69	8.10	0
Base	7th St	7	3	100		Y	Y		31.50	33.63	2.13	0
Impact	7th St	7	3	100	N	N	N	N	33.14	40.80	7.66	0
Base	7th St	9	3	100		Y	Y		28.16	29.61	1.46	0
Impact	7th St	9	3	100	N	N	N	N	29.00	34.34	5.34	4
Base	Guadalupe St	5	3	100		Y	Y		47.46	49.69	2.23	0
Impact	Guadalupe St	5	3	100	Y	Y	Y	N	54.83	57.99	3.16	0
Base	Guadalupe St	7	3	100		Y	N		42.64	44.51	1.87	0
Impact	Guadalupe St	7	3	100	Y	Y	Y	N	47.69	50.60	2.90	0
Base	Guadalupe St	9	3	100		Y	Y		33.93	35.33	1.40	0
Impact	Guadalupe St	9	3	100	Y	Y	Y	N	36.99	39.49	2.51	0

* Y = Accept H_o: $\sigma_1^2 = \sigma_2^2$; N = Reject H_o, conclude H_a: $\sigma_1^2 \neq \sigma_2^2$ (at the 95-percent confidence level)
** Y = Accept H_o: Distribution is normal; N = Reject H_o, conclude H_a: Distribution is not normal (at the 95-percent confidence level)
*** Y = Accept H_o: $\mu_1 = \mu_2$; N = Reject H_o conclude H_a: $\mu_1 \neq \mu_2$ (at the 95-percent confidence level)

Table C.4 Preliminary Test Results for 2-Hour Analysis Period Using SSIM Index

Scenario	Location	Subnetwork Size (Order)	Impact Size	Capacity Reduction	Hypothesis Testing				Prediction Interval			
					Equal Variance*	Normality Test		Equal Mean***	Lower Bound	Upper Bound	Range	Alternate Runs Within
						Lilliefor**	A-D**					
Base	Guadalupe St	5	1	25		Y	Y		0.956	0.970	0.014	8
Impact	Guadalupe St	5	1	25	Y	N	N	N	0.947	0.965	0.018	6
Base	Guadalupe St	7	1	25		Y	Y		0.969	0.980	0.011	6
Impact	Guadalupe St	7	1	25	Y	Y	Y	N	0.958	0.979	0.020	10
Base	Guadalupe St	9	1	25		Y	Y		0.980	0.988	0.007	8
Impact	Guadalupe St	9	1	25	Y	N	N	N	0.976	0.987	0.011	10
Base	15th St	5	2	50		Y	Y		0.983	0.988	0.005	4
Impact	15th St	5	2	50	N	Y	Y	N	0.976	0.987	0.011	10
Base	15th St	7	2	50		Y	N		0.975	0.988	0.012	7
Impact	15th St	7	2	50	Y	Y	Y	N	0.972	0.980	0.008	1
Base	15th St	9	2	50		Y	Y		0.989	0.993	0.004	3
Impact	15th St	9	2	50	Y	N	Y	N	0.987	0.991	0.004	5
Base	7th St	5	2	50		Y	Y		0.996	0.997	0.001	1
Impact	7th St	5	2	50	N	Y	Y	N	0.993	0.997	0.003	7
Base	7th St	7	2	50		Y	Y		0.996	0.997	0.001	4
Impact	7th St	7	2	50	N	Y	Y	N	0.994	0.997	0.003	9
Base	7th St	9	2	50		Y	Y		0.992	0.995	0.003	6
Impact	7th St	9	2	50	Y	Y	Y	N	0.991	0.994	0.003	7
Base	Guadalupe St	5	2	50		Y	Y		0.953	0.973	0.021	8
Impact	Guadalupe St	5	2	50	Y	Y	Y	N	0.947	0.966	0.019	7
Base	Guadalupe St	7	2	50		Y	Y		0.976	0.986	0.009	3
Impact	Guadalupe St	7	2	50	Y	Y	Y	N	0.968	0.983	0.014	8
Base	Guadalupe St	9	2	50		Y	Y		0.989	0.994	0.005	10
Impact	Guadalupe St	9	2	50	Y	Y	Y	Y	0.989	0.993	0.004	9
Base	7th St	5	3	100		Y	Y		0.996	0.997	0.001	0
Impact	7th St	5	3	100	N	Y	Y	N	0.976	0.981	0.005	0
Base	7th St	7	3	100		Y	Y		0.995	0.997	0.002	0
Impact	7th St	7	3	100	N	N	N	N	0.989	0.996	0.007	8
Base	7th St	9	3	100		Y	Y		0.992	0.995	0.003	0
Impact	7th St	9	3	100	Y	N	N	N	0.987	0.993	0.006	2
Base	Guadalupe St	5	3	100		Y	Y		0.951	0.965	0.014	0
Impact	Guadalupe St	5	3	100	Y	Y	Y	N	0.910	0.927	0.017	0
Base	Guadalupe St	7	3	100		Y	Y		0.983	0.991	0.008	0
Impact	Guadalupe St	7	3	100	Y	Y	Y	N	0.971	0.981	0.009	0
Base	Guadalupe St	9	3	100		Y	Y		0.992	0.996	0.004	0
Impact	Guadalupe St	9	3	100	Y	Y	Y	N	0.990	0.993	0.003	0

* Y = Accept H_o: $\sigma_1^2 = \sigma_2^2$; N = Reject H_o, conclude H_a: $\sigma_1^2 \neq \sigma_2^2$ (at the 95-percent confidence level)
** Y = Accept H_o: Distribution is normal; N = Reject H_o, conclude H_a: Distribution is not normal (at the 95-percent confidence level)
*** Y = Accept H_o: $\mu_1 = \mu_2$; N = Reject H_o conclude H_a: $\mu_1 \neq \mu_2$ (at the 95-percent confidence level)

APPENDIX D

Detailed Results of the Subnetwork Size Evaluation

Table D.1 Subnetwork Size Evaluation Results for 1-Hour Analysis: Guadalupe Street, 1-Link Scenarios

Scenario	Location	Size (Order)	% Cap. Red.	Hypothesis Testing				Prediction Interval			Alternate Runs Within PI	Notes
				Equal Variance*	Normality Test		Equal Mean***	Lower Bound	Upper Bound	Range		
					Lilliefor**	A-D**						
1-Link Impact Scenarios												
Base	Guadalupe St	5	25	Y	Y	Y	Y	1.73	4.81	3.08	10	
Impact	Guadalupe St	5	25		Y	Y		2.42	4.27	1.85	9	
Base	Guadalupe St	7	25	Y	Y	Y	Y	1.57	4.37	2.80	10	
Impact	Guadalupe St	7	25		Y	Y		2.33	3.90	1.57	9	
Base	Guadalupe St	9	25	Y	Y	Y	Y	1.64	3.40	1.76	10	
Impact	Guadalupe St	9	25		Y	Y		1.84	3.33	1.49	10	
Base	Guadalupe St	5	50	Y	Y	Y	Y	1.73	4.81	3.08	2	
Impact	Guadalupe St	5	50		-	-		-10.15	17.70	27.85	10	
Base	Guadalupe St	7	50	N	Y	Y	Y	1.57	4.37	2.80	2	
Impact	Guadalupe St	7	50		-	-		0.94	5.59	4.65	10	
Base	Guadalupe St	9	50	Y	Y	Y	Y	1.64	3.40	1.76	2	
Impact	Guadalupe St	9	50		-	-		0.19	4.29	4.11	10	
Base	Guadalupe St	5	100	Y	Y	Y	N	1.73	4.81	3.08	0	
Impact	Guadalupe St	5	100		-	-		0.03	12.34	12.30	10	
Base	Guadalupe St	7	100	Y	Y	Y	N	1.57	4.37	2.80	1	
Impact	Guadalupe St	7	100		-	-		-3.03	11.88	14.92	10	
Base	Guadalupe St	9	100	Y	Y	Y	Y	1.64	3.40	1.76	2	
Impact	Guadalupe St	9	100		-	-		-1.60	6.98	8.58	10	

* Y = Accept H_o: $\sigma_1^2 = \sigma_2^2$; N = Reject H_o, conclude H_a: $\sigma_1^2 \neq \sigma_2^2$ (at the 95-percent confidence level)
** Y = Accept H_o: Distribution is normal; N = Reject H_o, conclude H_a: Distribution is not normal (at the 95-percent confidence level)
*** Y = Accept H_o: $\mu_1 = \mu_2$; N = Reject H_o conclude H_a: $\mu_1 \neq \mu_2$ (at the 95-percent confidence level)

Table D.2 Subnetwork Size Evaluation Results for 1-Hour Analysis: 7th Street, 1-Link Scenarios

Scenario	Location	Size (Order)	% Cap. Red.	Hypothesis Testing				Prediction Interval			Alternate Runs Within PI	Notes
				Equal Variance*	Normality Test		Equal Mean***	Lower Bound	Upper Bound	Range		
					Lilliefor**	A-D**						
1-Link Impact Scenarios												
Base	7th St	5	25	N	Y	Y	Y	1.94	3.10	1.16	2	
Impact	7th St	5	25		-	-		1.92	3.89	1.97	10	
Base	7th St	7	25	N	Y	Y	Y	1.63	2.53	0.90	2	
Impact	7th St	7	25		-	-		1.83	2.68	0.85	9	
Base	7th St	9	25	N	Y	Y	Y	0.91	2.42	1.51	2	
Impact	7th St	9	25		-	-		1.10	2.06	0.96	9	
Base	7th St	5	50	Y	Y	Y	Y	1.94	3.10	1.16	2	
Impact	7th St	5	50		-	-		-3.13	8.61	11.75	10	
Base	7th St	7	50	Y	Y	Y	Y	1.63	2.53	0.90	2	
Impact	7th St	7	50		-	-		-0.78	5.38	6.16	10	
Base	7th St	9	50	Y	Y	Y	Y	0.91	2.42	1.51	2	
Impact	7th St	9	50		-	-		-0.57	3.93	4.50	10	
Base	7th St	5	100	Y	Y	Y	N	1.94	3.10	1.16	0	
Impact	7th St	5	100		-	-		2.27	16.22	13.95	8	
Base	7th St	7	100	Y	Y	Y	N	1.63	2.53	0.90	0	
Impact	7th St	7	100		-	-		-2.20	8.54	10.74	10	
Base	7th St	9	100	N	Y	Y	Y	0.91	2.42	1.51	2	
Impact	7th St	9	100		-	-		0.38	3.07	2.69	10	

* Y = Accept H_o: $\sigma_1^2 = \sigma_2^2$; N = Reject H_o, conclude H_a: $\sigma_1^2 \neq \sigma_2^2$ (at the 95-percent confidence level)
** Y = Accept H_o: Distribution is normal; N = Reject H_o, conclude H_a: Distribution is not normal (at the 95-percent confidence level)
*** Y = Accept H_o: $\mu_1 = \mu_2$; N = Reject H_o conclude H_a: $\mu_1 \neq \mu_2$ (at the 95-percent confidence level)

Table D.3 Subnetwork Size Evaluation Results for 1-Hour Analysis: 15th Street, 1-Link Scenarios

Scenario	Location	Size (Order)	% Cap. Red.	Hypothesis Testing				Prediction Interval			Alternate Runs Within PI	Notes
				Equal Variance*	Normality Test		Equal Mean***	Lower Bound	Upper Bound	Range		
					Lilliefor**	A-D**						
1-Link Impact Scenarios												
Base	15th St	5	25	Y	Y	Y	Y	2.01	3.68	1.66	2	
Impact	15th St	5	25		-	-		-1.63	7.25	8.88	10	
Base	15th St	7	25	N	N	N	Y	0.31	5.88	5.57	2	
Impact	15th St	7	25		-	-		0.65	5.05	4.40	9	
Base	15th St	9	25	N	Y	N	Y	1.31	3.36	2.04	2	
Impact	15th St	9	25		-	-		1.49	3.04	1.55	9	
Base	15th St	5	50	Y	Y	Y	Y	2.01	3.68	1.66	2	
Impact	15th St	5	50		-	-		-8.03	13.81	21.84	10	
Base	15th St	7	50	N	N	N	Y	0.31	5.88	5.57	2	
Impact	15th St	7	50		-	-		-1.70	9.24	10.94	10	
Base	15th St	9	50	N	Y	N	Y	1.31	3.36	2.04	2	
Impact	15th St	9	50		-	-		2.07	2.92	0.84	5	
Base	15th St	5	100	Y	Y	Y	N	2.01	3.68	1.66	0	
Impact	15th St	5	100		-	-		0.89	9.83	8.94	10	
Base	15th St	7	100	N	N	N	Y	0.31	5.88	5.57	2	
Impact	15th St	7	100		-	-		-2.11	9.26	11.37	10	
Base	15th St	9	100	Y	Y	N	Y	1.31	3.36	2.04	2	
Impact	15th St	9	100		-	-		-1.25	6.80	8.05	10	

* Y = Accept H_o: $\sigma_1^2 = \sigma_2^2$; N = Reject H_o, conclude H_a: $\sigma_1^2 \neq \sigma_2^2$ (at the 95-percent confidence level)
** Y = Accept H_o: Distribution is normal; N = Reject H_o, conclude H_a: Distribution is not normal (at the 95-percent confidence level)
*** Y = Accept H_o: $\mu_1 = \mu_2$; N = Reject H_o conclude H_a: $\mu_1 \neq \mu_2$ (at the 95-percent confidence level)

Table D.4 Subnetwork Size Evaluation Results for 1-Hour Analysis: Guadalupe Street, 2-Link Scenarios

Scenario	Location	Size (Order)	% Cap. Red.	Hypothesis Testing				Prediction Interval			Alternate Runs Within PI	Notes
				Equal Variance*	Normality Test		Equal Mean***	Lower Bound	Upper Bound	Range		
					Lilliefor**	A-D**						
2-Link Impact Scenarios												
Base	Guadalupe St	5	25	Y	Y	N	Y	1.53	4.69	3.16	2	
Impact	Guadalupe St	5	25		-	-		-7.58	14.53	22.11	10	
Base	Guadalupe St	7	25	Y	Y	Y	Y	1.53	4.51	2.98	2	
Impact	Guadalupe St	7	25		-	-		-5.92	12.57	18.49	10	
Base	Guadalupe St	9	25	Y	N	Y	Y	1.57	3.90	2.34	2	
Impact	Guadalupe St	9	25		-	-		-7.13	13.05	20.17	10	
Base	Guadalupe St	5	50	N	Y	N	Y	1.53	4.69	3.16	10	
Impact	Guadalupe St	5	50		Y	Y		2.40	3.90	1.50	8	
Base	Guadalupe St	7	50	Y	Y	Y	Y	1.53	4.51	2.98	10	
Impact	Guadalupe St	7	50		Y	Y		2.23	4.16	1.94	9	
Base	Guadalupe St	9	50	N	N	Y	Y	1.57	3.90	2.34	10	
Impact	Guadalupe St	9	50		Y	Y		2.20	3.25	1.05	6	
Base	Guadalupe St	5	100	Y	Y	N	N	1.53	4.69	3.16	0	
Impact	Guadalupe St	5	100		-	-		4.09	12.32	8.23	2	
Base	Guadalupe St	7	100	N	Y	Y	N	1.53	4.51	2.98	0	
Impact	Guadalupe St	7	100		-	-		3.47	5.75	2.28	2	
Base	Guadalupe St	9	100	N	N	Y	Y	1.57	3.90	2.34	2	
Impact	Guadalupe St	9	100		-	-		2.18	4.56	2.38	9	Borderline
Base	Guadalupe St	11	100	Y	Y	Y	N	1.23	2.53	1.30	1	
Impact	Guadalupe St	11	100		-	-		-8.78	13.86	22.64	10	Borderline

* Y = Accept H_o: $\sigma_1^2 = \sigma_2^2$; N = Reject H_o, conclude H_a: $\sigma_1^2 \neq \sigma_2^2$ (at the 95-percent confidence level)
** Y = Accept H_o: Distribution is normal; N = Reject H_o, conclude H_a: Distribution is not normal (at the 95-percent confidence level)
*** Y = Accept H_o: $\mu_1 = \mu_2$; N = Reject H_o conclude H_a: $\mu_1 \neq \mu_2$ (at the 95-percent confidence level)

Table D.5 Subnetwork Size Evaluation Results for 1-Hour Analysis: 7th Street, 2-Link Scenarios

Scenario	Location	Size (Order)	% Cap. Red.	Hypothesis Testing				Prediction Interval			Alternate Runs Within PI	Notes
				Equal Variance*	Normality Test		Equal Mean***	Lower Bound	Upper Bound	Range		
					Lilliefor**	A-D**						
2-Link Impact Scenarios												
Base	7th St	5	25	Y	Y	N	Y	1.93	2.97	1.04	2	
Impact	7th St	5	25		-	-		0.00	4.85	4.85	10	
Base	7th St	7	25	Y	Y	Y	Y	1.36	2.32	0.96	2	
Impact	7th St	7	25		-	-		-0.06	3.66	3.72	10	
Base	7th St	9	25	Y	Y	Y	Y	0.85	2.16	1.31	2	
Impact	7th St	9	25		-	-		-0.96	4.03	4.99	10	
Base	7th St	5	50	Y	Y	N	N	1.93	2.97	1.04	5	
Impact	7th St	5	50		Y	Y		2.31	3.52	1.21	8	
Base	7th St	7	50	Y	Y	Y	N	1.36	2.32	0.96	6	
Impact	7th St	7	50		Y	Y		1.58	2.74	1.16	9	
Base	7th St	9	50	N	Y	Y	Y	0.85	2.16	1.31	10	
Impact	7th St	9	50		Y	Y		1.15	1.77	0.62	6	
Base	7th St	5	100	Y	Y	N	N	1.93	2.97	1.04	0	
Impact	7th St	5	100		-	-		5.82	14.14	8.32	0	
Base	7th St	7	100	N	Y	Y	N	1.36	2.32	0.96	0	
Impact	7th St	7	100		-	-		2.68	2.92	0.24	0	
Base	7th St	9	100	Y	Y	Y	Y	0.85	2.16	1.31	2	
Impact	7th St	9	100		-	-		-1.98	5.50	7.48	10	
Base	7th St	11	100	N	N	N	Y	0.88	2.50	1.62	2	
Impact	7th St	11	100		-	-		0.92	2.61	1.69	10	

* Y = Accept H_o: $\sigma_1^2 = \sigma_2^2$; N = Reject H_o, conclude H_a: $\sigma_1^2 \neq \sigma_2^2$ (at the 95-percent confidence level)
** Y = Accept H_o: Distribution is normal; N = Reject H_o, conclude H_a: Distribution is not normal (at the 95-percent confidence level)
*** Y = Accept H_o: $\mu_1 = \mu_2$; N = Reject H_o conclude H_a: $\mu_1 \neq \mu_2$ (at the 95-percent confidence level)

Table D.6 Subnetwork Size Evaluation Results for 1-Hour Analysis: 15th Street, 2-Link Scenarios

Scenario	Location	Size (Order)	% Cap. Red.	Hypothesis Testing				Prediction Interval			Alternate Runs Within PI	Notes
				Equal Variance*	Normality Test		Equal Mean***	Lower Bound	Upper Bound	Range		
					Lilliefor**	A-D**						
2-Link Impact Scenarios												
Base	15th St	5	25	Y	Y	Y	Y	1.89	3.60	1.72	1	
Impact	15th St	5	25		Y	Y		-8.22	14.49	22.71	10	
Base	15th St	7	25	N	N	N	Y	0.33	5.30	4.97	2	
Impact	15th St	7	25		Y	Y		1.89	4.10	2.21	8	
Base	15th St	9	25	N	Y	Y	Y	1.24	3.15	1.91	2	
Impact	15th St	9	25		Y	Y		0.59	3.92	3.33	10	
Base	15th St	5	50	Y	Y	Y	N	1.89	3.60	1.72	10	
Impact	15th St	5	50		Y	Y		2.19	4.05	1.86	10	
Base	15th St	7	50	N	N	N	Y	0.33	5.30	4.97	10	
Impact	15th St	7	50		Y	Y		2.45	3.75	1.30	5	
Base	15th St	9	50	Y	Y	Y	Y	1.24	3.15	1.91	9	
Impact	15th St	9	50		Y	Y		1.71	3.27	1.56	10	
Base	15th St	5	100	Y	Y	Y	N	1.89	3.60	1.72	0	
Impact	15th St	5	100		Y	Y		1.42	8.13	6.70	10	
Base	15th St	7	100	N	N	N	Y	0.33	5.30	4.97	2	
Impact	15th St	7	100		Y	Y		1.50	5.54	4.04	10	
Base	15th St	9	100	N	Y	Y	Y	1.24	3.15	1.91	2	
Impact	15th St	9	100		Y	Y		1.85	3.74	1.89	8	
Base	15th St	11	100	Y	Y	Y	Y	1.26	2.72	1.46	2	
Impact	15th St	11	100		Y	Y		-4.61	9.20	13.80	10	

* Y = Accept H_o: $\sigma_1^2 = \sigma_2^2$; N = Reject H_o, conclude H_a: $\sigma_1^2 \neq \sigma_2^2$ (at the 95-percent confidence level)
** Y = Accept H_o: Distribution is normal; N = Reject H_o, conclude H_a: Distribution is not normal (at the 95-percent confidence level)
*** Y = Accept H_o: $\mu_1 = \mu_2$; N = Reject H_o conclude H_a: $\mu_1 \neq \mu_2$ (at the 95-percent confidence level)

Table D.7 Subnetwork Size Evaluation Results for 1-Hour Analysis: Guadalupe Street, 3-Link Scenarios

Scenario	Location	Size (Order)	% Cap. Red.	Hypothesis Testing				Prediction Interval			Alternate Runs Within PI	Notes
				Equal Variance*	Normality Test		Equal Mean***	Lower Bound	Upper Bound	Range		
					Lilliefor**	A-D**						
3-Link Impact Scenarios												
Base	Guadalupe St	5	25	Y	Y	Y	Y	1.55	4.50	2.95	2	
Impact	Guadalupe St	5	25		-	-		-2.67	8.74	11.41	10	
Base	Guadalupe St	7	25	Y	Y	Y	Y	2.23	4.78	2.56	2	
Impact	Guadalupe St	7	25		-	-		-6.05	13.99	20.04	10	
Base	Guadalupe St	9	25	Y	Y	Y	Y	1.25	4.00	2.75	2	
Impact	Guadalupe St	9	25		-	-		-6.84	13.01	19.86	10	
Base	Guadalupe St	5	50	Y	Y	Y	Y	1.55	4.50	2.95	2	
Impact	Guadalupe St	5	50		-	-		-1.84	7.92	9.76	10	
Base	Guadalupe St	7	50	Y	Y	Y	Y	2.23	4.78	2.56	2	
Impact	Guadalupe St	7	50		-	-		-5.74	12.55	18.29	10	
Base	Guadalupe St	9	50	Y	Y	Y	Y	1.25	4.00	2.75	2	
Impact	Guadalupe St	9	50		-	-		-6.53	12.05	18.58	10	
Base	Guadalupe St	5	100	Y	Y	Y	N	1.55	4.50	2.95	0	
Impact	Guadalupe St	5	100		Y	Y		6.01	7.56	1.56	0	
Base	Guadalupe St	7	100	Y	Y	Y	N	2.23	4.78	2.56	7	
Impact	Guadalupe St	7	100		Y	Y		3.43	5.64	2.21	5	
Base	Guadalupe St	9	100	Y	Y	Y	Y	1.25	4.00	2.75	10	
Impact	Guadalupe St	9	100		Y	Y		2.16	3.70	1.54	7	Borderline
Base	Guadalupe St	11	100	Y	Y	Y	N	1.01	1.82	0.80	1	
Impact	Guadalupe St	11	100		Y	Y		1.68	2.31	0.63	1	Borderline

* Y = Accept H_o: $\sigma_1^2 = \sigma_2^2$; N = Reject H_o, conclude H_a: $\sigma_1^2 \neq \sigma_2^2$ (at the 95-percent confidence level)
** Y = Accept H_o: Distribution is normal; N = Reject H_o, conclude H_a: Distribution is not normal (at the 95-percent confidence level)
*** Y = Accept H_o: $\mu_1 = \mu_2$; N = Reject H_o conclude H_a: $\mu_1 \neq \mu_2$ (at the 95-percent confidence level)

Table D.8 Subnetwork Size Evaluation Results for 1-Hour Analysis: 7th Street, 3-Link Scenarios

Scenario	Location	Size (Order)	% Cap. Red.	Hypothesis Testing				Prediction Interval			Alternate Runs Within PI	Notes
				Equal Variance*	Normality Test		Equal Mean***	Lower Bound	Upper Bound	Range		
					Lilliefor**	A-D**						
3-Link Impact Scenarios												
Base	7th St	5	25	Y	N	N	Y	1.92	2.93	1.01	2	
Impact	7th St	5	25		-	-		-1.06	6.44	7.50	10	
Base	7th St	7	25	N	N	Y	Y	1.23	2.81	1.58	2	
Impact	7th St	7	25		-	-		0.58	3.76	3.17	10	
Base	7th St	9	25	Y	Y	Y	Y	0.84	2.18	1.34	2	
Impact	7th St	9	25		-	-		-1.12	3.82	4.94	10	
Base	7th St	5	50	Y	N	N	N	1.92	2.93	1.01	1	
Impact	7th St	5	50		-	-		0.45	5.28	4.84	10	
Base	7th St	7	50	Y	N	Y	Y	1.23	2.81	1.58	2	
Impact	7th St	7	50		-	-		-4.30	9.02	13.32	10	
Base	7th St	9	50	Y	Y	Y	Y	0.84	2.18	1.34	2	
Impact	7th St	9	50		-	-		-1.15	4.10	5.25	10	
Base	7th St	5	100	Y	N	N	N	1.92	2.93	1.01	0	
Impact	7th St	5	100		Y	Y		8.98	10.68	1.70	0	
Base	7th St	7	100	Y	N	Y	N	1.23	2.81	1.58	6	
Impact	7th St	7	100		Y	Y		2.12	3.36	1.24	4	
Base	7th St	9	100	Y	Y	Y	N	0.84	2.18	1.34	10	
Impact	7th St	9	100		Y	Y		1.36	2.17	0.81	6	
Base	7th St	11	100	Y	N	N	Y	0.83	2.53	1.70	10	
Impact	7th St	11	100		Y	Y		1.36	2.15	0.78	7	

* Y = Accept H_o: $\sigma_1^2 = \sigma_2^2$; N = Reject H_o, conclude H_a: $\sigma_1^2 \neq \sigma_2^2$ (at the 95-percent confidence level)
** Y = Accept H_o: Distribution is normal; N = Reject H_o, conclude H_a: Distribution is not normal (at the 95-percent confidence level)
*** Y = Accept H_o: $\mu_1 = \mu_2$; N = Reject H_o conclude H_a: $\mu_1 \neq \mu_2$ (at the 95-percent confidence level)

Table D.9 Subnetwork Size Evaluation Results for 1-Hour Analysis: 15th Street, 3-Link Scenarios

Scenario	Location	Size (Order)	% Cap. Red.	Hypothesis Testing				Prediction Interval			Alternate Runs Within PI	Notes
				Equal Variance*	Normality Test		Equal Mean***	Lower Bound	Upper Bound	Range		
					Lilliefor**	A-D**						
3-Link Impact Scenarios												
Base	15th St	5	25	N	Y	Y	Y	1.68	3.78	2.10	2	
Impact	15th St	5	25		-	-		2.53	3.23	0.69	5	
Base	15th St	7	25	Y	N	N	Y	0.55	5.60	5.04	2	
Impact	15th St	7	25		-	-		-9.39	15.35	24.74	10	
Base	15th St	9	25	Y	Y	Y	Y	1.24	3.18	1.94	2	
Impact	15th St	9	25		-	-		-1.00	6.33	7.33	10	
Base	15th St	5	50	N	Y	Y	Y	1.68	3.78	2.10	2	
Impact	15th St	5	50		-	-		1.68	4.15	2.47	10	
Base	15th St	7	50	N	N	N	Y	0.55	5.60	5.04	2	
Impact	15th St	7	50		-	-		2.56	5.03	2.47	6	
Base	15th St	9	50	Y	Y	Y	Y	1.24	3.18	1.94	2	
Impact	15th St	9	50		-	-		-3.19	8.23	11.42	10	
Base	15th St	5	100	Y	Y	Y	N	1.68	3.78	2.10	0	
Impact	15th St	5	100		-	-		-2.69	13.83	16.52	10	
Base	15th St	7	100	Y	N	N	Y	0.55	5.60	5.04	2	
Impact	15th St	7	100		-	-		-5.66	13.82	19.47	10	
Base	15th St	9	100	Y	Y	Y	Y	1.24	3.18	1.94	2	
Impact	15th St	9	100		-	-		-0.01	5.64	5.64	10	
Base	15th St	11	100	Y	Y	Y	Y	1.23	2.72	1.49	2	
Impact	15th St	11	100		-	-		0.40	4.51	4.10	10	

* Y = Accept H_o: $\sigma_1^2 = \sigma_2^2$; N = Reject H_o, conclude H_a: $\sigma_1^2 \neq \sigma_2^2$ (at the 95-percent confidence level)
** Y = Accept H_o: Distribution is normal; N = Reject H_o, conclude H_a: Distribution is not normal (at the 95-percent confidence level)
*** Y = Accept H_o: $\mu_1 = \mu_2$; N = Reject H_o conclude H_a: $\mu_1 \neq \mu_2$ (at the 95-percent confidence level)

Table D.10 Subnetwork Size Evaluation Results for 2-Hour Analysis: Guadalupe Street, 1-Link Scenarios

Scenario	Location	Size (Order)	% Cap. Red.	Hypothesis Testing				Prediction Interval			Alternate Runs Within PI	Notes
				Equal Variance*	Normality Test		Equal Mean***	Lower Bound	Upper Bound	Range		
					Lilliefor**	A-D**						
1-Link Impact Scenarios												
Base	Guadalupe St	5	25		Y	Y		1.58	4.41	2.83	10	
Impact	Guadalupe St	5	25	N	Y	Y	Y	2.41	3.74	1.33	9	
Base	Guadalupe St	7	25		Y	Y		1.80	4.01	2.21	10	
Impact	Guadalupe St	7	25	N	Y	Y	Y	2.53	3.57	1.04	6	
Base	Guadalupe St	9	25		Y	Y		1.75	3.16	1.41	10	
Impact	Guadalupe St	9	25	Y	Y	Y	Y	1.84	3.24	1.40	10	
Base	Guadalupe St	5	50		Y	Y		1.58	4.41	2.83	2	
Impact	Guadalupe St	5	50	Y	-	-	Y	-6.61	13.63	20.24	10	
Base	Guadalupe St	7	50		Y	Y		1.80	4.01	2.21	2	
Impact	Guadalupe St	7	50	N	-	-	Y	1.35	5.31	3.97	10	
Base	Guadalupe St	9	50		Y	Y		1.75	3.16	1.41	2	
Impact	Guadalupe St	9	50	Y	-	-	Y	-0.10	4.57	4.67	10	
Base	Guadalupe St	5	100		Y	Y		1.58	4.41	2.83	0	
Impact	Guadalupe St	5	100	Y	-	-	N	-2.47	12.83	15.31	10	
Base	Guadalupe St	7	100		Y	Y		1.80	4.01	2.21	1	
Impact	Guadalupe St	7	100	Y	-	-	N	-3.97	11.93	15.90	10	
Base	Guadalupe St	9	100		Y	Y		1.75	3.16	1.41	2	
Impact	Guadalupe St	9	100	Y	-	-	Y	-2.56	7.79	10.34	10	

* Y = Accept H_o: $\sigma_1^2 = \sigma_2^2$; N = Reject H_o, conclude H_a: $\sigma_1^2 \neq \sigma_2^2$ (at the 95-percent confidence level)
** Y = Accept H_o: Distribution is normal; N = Reject H_o, conclude H_a: Distribution is not normal (at the 95-percent confidence level)
*** Y = Accept H_o: $\mu_1 = \mu_2$; N = Reject H_o conclude H_a: $\mu_1 \neq \mu_2$ (at the 95-percent confidence level)

Table D.11 Subnetwork Size Evaluation Results for 2-Hour Analysis: 7th Street, 1-Link Scenarios

Scenario	Location	Size (Order)	% Cap. Red.	Hypothesis Testing				Prediction Interval			Alternate Runs Within PI	Notes
				Equal Variance*	Normality Test		Equal Mean***	Lower Bound	Upper Bound	Range		
					Lilliefor**	A-D**						
1-Link Impact Scenarios												
Base	7th St	5	25		Y	Y		1.76	2.56	0.80	2	Appears correct
Impact	7th St	5	25	N	-	-	N	1.58	3.32	1.74	10	
Base	7th St	7	25		N	N		1.53	2.24	0.71	1	Borderline
Impact	7th St	7	25	Y	-	-	N	1.27	3.19	1.92	10	
Base	7th St	9	25		Y	Y		1.06	2.20	1.14	2	
Impact	7th St	9	25	Y	-	-	Y	-0.24	3.53	3.78	10	
Base	7th St	5	50		Y	Y		1.76	2.56	0.80	2	
Impact	7th St	5	50	Y	-	-	Y	-1.76	6.48	8.23	10	Borderline
Base	7th St	7	50		N	N		1.53	2.24	0.71	2	
Impact	7th St	7	50	Y	-	-	Y	-0.38	4.39	4.77	10	Borderline
Base	7th St	9	50		Y	Y		1.06	2.20	1.14	2	
Impact	7th St	9	50	N	-	-	Y	0.36	2.98	2.62	10	
Base	7th St	5	100		Y	Y		1.76	2.56	0.80	0	
Impact	7th St	5	100	Y	-	-	N	1.61	13.77	12.16	10	
Base	7th St	7	100		N	N		1.53	2.24	0.71	0	
Impact	7th St	7	100	Y	-	-	N	-1.34	6.69	8.03	10	
Base	7th St	9	100		Y	Y		1.06	2.20	1.14	2	
Impact	7th St	9	100	Y	-	-	Y	-0.65	4.12	4.77	10	

* Y = Accept H_o: $\sigma_1^2 = \sigma_2^2$; N = Reject H_o, conclude H_a: $\sigma_1^2 \neq \sigma_2^2$ (at the 95-percent confidence level)
** Y = Accept H_o: Distribution is normal; N = Reject H_o, conclude H_a: Distribution is not normal (at the 95-percent confidence level)
*** Y = Accept H_o: $\mu_1 = \mu_2$; N = Reject H_o conclude H_a: $\mu_1 \neq \mu_2$ (at the 95-percent confidence level)

Table D.12 Subnetwork Size Evaluation Results for 2-Hour Analysis: 15th Street, 1-Link Scenarios

Scenario	Location	Size (Order)	% Cap. Red.	Hypothesis Testing				Prediction Interval			Alternate Runs Within PI	Notes
				Equal Variance*	Normality Test		Equal Mean***	Lower Bound	Upper Bound	Range		
					Lilliefor**	A-D**						
1-Link Impact Scenarios												
Base	15th St	5	25		Y	Y		2.18	3.49	1.31	2	
Impact	15th St	5	25	N	-	-	Y	1.68	4.21	2.53	10	
Base	15th St	7	25		N	N		0.45	5.94	5.49	2	
Impact	15th St	7	25	N	-	-	Y	-0.45	6.92	7.37	10	
Base	15th St	9	25		Y	Y		1.28	3.37	2.09	2	
Impact	15th St	9	25	N	-	-	Y	-0.11	4.66	4.77	10	
Base	15th St	5	50		Y	Y		2.18	3.49	1.31	1	
Impact	15th St	5	50	Y	-	-	N	-7.11	13.98	21.09	10	
Base	15th St	7	50		N	N		0.45	5.94	5.49	2	
Impact	15th St	7	50	N	-	-	Y	1.31	6.39	5.08	10	
Base	15th St	9	50		Y	Y		1.28	3.37	2.09	2	
Impact	15th St	9	50	N	-	-	Y	0.68	4.35	3.67	10	
Base	15th St	5	100		Y	Y		2.18	3.49	1.31	0	
Impact	15th St	5	100	N	-	-	N	-5.71	19.49	25.19	10	
Base	15th St	7	100		N	N		0.45	5.94	5.49	2	
Impact	15th St	7	100	N	-	-	Y	1.65	6.13	4.48	9	
Base	15th St	9	100		Y	Y		1.28	3.37	2.09	2	
Impact	15th St	9	100	N	-	-	Y	1.94	3.92	1.98	8	

* Y = Accept H_o: $\sigma_1^2 = \sigma_2^2$; N = Reject H_o, conclude H_a: $\sigma_1^2 \neq \sigma_2^2$ (at the 95-percent confidence level)
** Y = Accept H_o: Distribution is normal; N = Reject H_o, conclude H_a: Distribution is not normal (at the 95-percent confidence level)
*** Y = Accept H_o: $\mu_1 = \mu_2$; N = Reject H_o conclude H_a: $\mu_1 \neq \mu_2$ (at the 95-percent confidence level)

Table D.13 Subnetwork Size Evaluation Results for 2-Hour Analysis: Guadalupe Street, 2-Link Scenarios

Scenario	Location	Size (Order)	% Cap. Red.	Hypothesis Testing				Prediction Interval			Alternate Runs Within PI	Notes
				Equal Variance*	Normality Test		Equal Mean***	Lower Bound	Upper Bound	Range		
					Lilliefor**	A-D**						
2-Link Impact Scenarios												
Base	Guadalupe St	5	25		Y	Y		1.45	4.33	2.88	2	
Impact	Guadalupe St	5	25	Y	-	-	Y	-10.90	17.32	28.22	10	
Base	Guadalupe St	7	25		N	N		-2.92	11.39	14.31	10	
Impact	Guadalupe St	7	25	N	-	-	Y	-3.12	10.75	13.87	9	
Base	Guadalupe St	9	25		Y	Y		1.77	3.54	1.76	2	
Impact	Guadalupe St	9	25	Y	-	-	Y	-7.23	13.09	20.32	10	
Base	Guadalupe St	5	50		Y	Y		1.45	4.33	2.88	10	
Impact	Guadalupe St	5	50	N	Y	Y	Y	2.34	3.45	1.11	8	
Base	Guadalupe St	7	50		Y	Y		1.76	4.14	2.38	10	
Impact	Guadalupe St	7	50	Y	Y	Y	Y	2.26	4.04	1.78	10	
Base	Guadalupe St	9	50		Y	Y		1.77	3.54	1.76	10	
Impact	Guadalupe St	9	50	Y	Y	Y	Y	2.20	3.15	0.95	8	
Base	Guadalupe St	5	100		Y	Y		1.45	4.33	2.88	0	
Impact	Guadalupe St	5	100	N	-	-	N	5.41	7.85	2.44	0	
Base	Guadalupe St	7	100		Y	Y		1.76	4.14	2.38	1	
Impact	Guadalupe St	7	100	N	-	-	N	1.27	7.02	5.75	10	
Base	Guadalupe St	9	100		Y	Y		1.77	3.54	1.76	2	
Impact	Guadalupe St	9	100	Y	-	-	N	1.08	5.46	4.37	10	
Base	Guadalupe St	11	100		Y	Y		1.36	2.52	1.16	1	
Impact	Guadalupe St	11	100	Y	-	-	N	-3.32	8.33	11.65	10	

* Y = Accept H_o: $\sigma_1^2 = \sigma_2^2$; N = Reject H_o, conclude H_a: $\sigma_1^2 \neq \sigma_2^2$ (at the 95-percent confidence level)
** Y = Accept H_o: Distribution is normal; N = Reject H_o, conclude H_a: Distribution is not normal (at the 95-percent confidence level)
*** Y = Accept H_o: $\mu_1 = \mu_2$; N = Reject H_o conclude H_a: $\mu_1 \neq \mu_2$ (at the 95-percent confidence level)

Table D.14 Subnetwork Size Evaluation Results for 2-Hour Analysis: 7th Street, 2-Link Scenarios

Scenario	Location	Size (Order)	% Cap. Red.	Hypothesis Testing				Prediction Interval			Alternate Runs Within PI	Notes
				Equal Variance*	Normality Test		Equal Mean***	Lower Bound	Upper Bound	Range		
					Lilliefor**	A-D**						
2-Link Impact Scenarios												
Base	7th St	5	25		Y	Y		1.71	2.47	0.76	2	
Impact	7th St	5	25	Y	-	-	Y	0.71	3.54	2.83	10	
Base	7th St	7	25		Y	Y		1.26	2.07	0.81	2	
Impact	7th St	7	25	N	-	-	Y	1.67	1.74	0.08	2	
Base	7th St	9	25		Y	Y		1.00	2.05	1.05	2	
Impact	7th St	9	25	Y	-	-	Y	-0.54	3.73	4.27	10	
Base	7th St	5	50		Y	Y		1.71	2.47	0.76	4	
Impact	7th St	5	50	Y	Y	Y	N	2.00	2.98	0.97	8	
Base	7th St	7	50		Y	Y		1.26	2.07	0.81	6	
Impact	7th St	7	50	Y	Y	Y	N	1.67	2.34	0.67	4	
Base	7th St	9	50		Y	Y		1.00	2.05	1.05	10	
Impact	7th St	9	50	Y	Y	Y	Y	1.14	1.85	0.70	9	
Base	7th St	5	100		Y	Y		1.71	2.47	0.76	0	
Impact	7th St	5	100	Y	-	-	N	3.40	15.18	11.78	0	
Base	7th St	7	100		Y	Y		1.26	2.07	0.81	0	
Impact	7th St	7	100	Y	-	-	N	0.32	5.95	5.63	10	
Base	7th St	9	100		Y	Y		1.00	2.05	1.05	1	
Impact	7th St	9	100	Y	-	-	N	-2.90	6.84	9.74	10	
Base	7th St	11	100		Y	Y		0.94	2.53	1.59	2	
Impact	7th St	11	100	Y	-	-	Y	-0.54	4.54	5.08	10	

* Y = Accept H_o: $\sigma_1^2 = \sigma_2^2$; N = Reject H_o, conclude H_a: $\sigma_1^2 \neq \sigma_2^2$ (at the 95-percent confidence level)
** Y = Accept H_o: Distribution is normal; N = Reject H_o, conclude H_a: Distribution is not normal (at the 95-percent confidence level)
*** Y = Accept H_o: $\mu_1 = \mu_2$; N = Reject H_o conclude H_a: $\mu_1 \neq \mu_2$ (at the 95-percent confidence level)

Table D.15 Subnetwork Size Evaluation Results for 2-Hour Analysis: 15th Street, 2-Link Scenarios

Scenario	Location	Size (Order)	% Cap. Red.	Hypothesis Testing				Prediction Interval			Alternate Runs Within PI	Notes
				Equal Variance*	Normality Test		Equal Mean***	Lower Bound	Upper Bound	Range		
					Lilliefor**	A-D**						
2-Link Impact Scenarios												
Base	15th St	5	25		Y	Y		2.11	3.36	1.26	1	
Impact	15th St	5	25	Y	-	-	N	-6.52	13.49	20.01	10	
Base	15th St	7	25		N	N		0.46	5.38	4.92	1	
Impact	15th St	7	25	N	-	-	N	-121.27	140.73	262.00	10	
Base	15th St	9	25		N	N		1.28	3.17	1.89	2	
Impact	15th St	9	25	N	-	-	Y	1.94	2.57	0.63	6	
Base	15th St	5	50		Y	Y		2.11	3.36	1.26	1	
Impact	15th St	5	50	Y	Y	Y	N	-6.52	13.49	20.01	10	
Base	15th St	7	50		N	N		0.46	5.38	4.92	2	
Impact	15th St	7	50	Y	Y	Y	Y	-7.98	14.52	22.50	10	
Base	15th St	9	50		N	N		1.28	3.17	1.89	2	
Impact	15th St	9	50	N	Y	Y	Y	1.94	2.57	0.63	6	
Base	15th St	5	100		Y	Y		2.11	3.36	1.26	0	
Impact	15th St	5	100	N	-	-	N	-9.18	22.31	31.50	10	
Base	15th St	7	100		N	N		0.46	5.38	4.92	2	Outlier issue
Impact	15th St	7	100	N	-	-	Y	2.31	5.39	3.09	7	
Base	15th St	7	100		Y	Y		1.52	3.72	2.20	0	Outlier removed
Impact	15th St	7	100	N	-	-	N	2.31	5.39	3.09	7	
Base	15th St	9	100		N	N		1.28	3.17	1.89	1	
Impact	15th St	9	100	Y	-	-	N	0.74	5.52	4.78	10	
Base	15th St	11	100		Y	Y		1.35	2.71	1.36	1	
Impact	15th St	11	100	Y	-	-	N	-0.79	6.02	6.81	10	

* Y = Accept H_o: $\sigma_1^2 = \sigma_2^2$; N = Reject H_o, conclude H_a: $\sigma_1^2 \neq \sigma_2^2$ (at the 95-percent confidence level)
** Y = Accept H_o: Distribution is normal; N = Reject H_o, conclude H_a: Distribution is not normal (at the 95-percent confidence level)
*** Y = Accept H_o: $\mu_1 = \mu_2$; N = Reject H_o conclude H_a: $\mu_1 \neq \mu_2$ (at the 95-percent confidence level)

Table D.16 Subnetwork Size Evaluation Results for 2-Hour Analysis: Guadalupe Street, 3-Link Scenarios

Scenario	Location	Size (Order)	% Cap. Red.	Hypothesis Testing				Prediction Interval			Alternate Runs Within PI	Notes
				Equal Variance*	Normality Test		Equal Mean***	Lower Bound	Upper Bound	Range		
					Lilliefor**	A-D**						
3-Link Impact Scenarios												
Base	Guadalupe St	5	25		Y	Y		1.56	4.12	2.57	2	
Impact	Guadalupe St	5	25	Y	-	-	Y	-2.59	8.08	10.67	10	
Base	Guadalupe St	7	25		Y	Y		2.42	4.47	2.06	2	
Impact	Guadalupe St	7	25	N	-	-	Y	2.16	5.56	3.40	10	
Base	Guadalupe St	9	25		Y	Y		1.64	3.51	1.86	2	
Impact	Guadalupe St	9	25	Y	-	-	Y	-5.04	11.00	16.04	10	
Base	Guadalupe St	5	50		Y	Y		1.56	4.12	2.57	2	
Impact	Guadalupe St	5	50	N	-	-	Y	0.83	4.68	3.84	10	
Base	Guadalupe St	7	50		Y	Y		2.42	4.47	2.06	2	
Impact	Guadalupe St	7	50	Y	-	-	Y	-1.87	8.29	10.16	10	
Base	Guadalupe St	9	50		Y	Y		1.64	3.51	1.86	2	
Impact	Guadalupe St	9	50	Y	-	-	Y	-3.10	8.35	11.45	10	
Base	Guadalupe St	5	100		Y	Y		1.56	4.12	2.57	0	
Impact	Guadalupe St	5	100	Y	Y	Y	N	4.95	6.43	1.48	0	
Base	Guadalupe St	7	100		Y	Y		2.42	4.47	2.06	6	
Impact	Guadalupe St	7	100	Y	Y	Y	N	3.37	5.37	1.99	6	
Base	Guadalupe St	9	100		Y	Y		1.64	3.51	1.86	10	
Impact	Guadalupe St	9	100	Y	Y	Y	N	2.23	3.67	1.44	8	
Base	Guadalupe St	11	100		Y	Y		0.99	1.71	0.72	2	
Impact	Guadalupe St	11	100	Y	Y	Y	N	1.50	2.01	0.51	2	

* Y = Accept H_o: $\sigma_1^2 = \sigma_2^2$; N = Reject H_o, conclude H_a: $\sigma_1^2 \neq \sigma_2^2$ (at the 95-percent confidence level)
** Y = Accept H_o: Distribution is normal; N = Reject H_o, conclude H_a: Distribution is not normal (at the 95-percent confidence level)
*** Y = Accept H_o: $\mu_1 = \mu_2$; N = Reject H_o conclude H_a: $\mu_1 \neq \mu_2$ (at the 95-percent confidence level)

Table D.17 Subnetwork Size Evaluation Results for 2-Hour Analysis: 7th Street, 3-Link Scenarios

Scenario	Location	Size (Order)	% Cap. Red.	Hypothesis Testing				Prediction Interval			Alternate Runs Within PI	Notes
				Equal Variance*	Normality Test		Equal Mean***	Lower Bound	Upper Bound	Range		
					Lilliefor**	A-D**						
3-Link Impact Scenarios												
Base	7th St	5	25		Y	Y		1.71	2.37	0.67	2	
Impact	7th St	5	25	Y	-	-	Y	0.42	4.12	3.70	10	Borderline
Base	7th St	7	25		N	N		1.19	2.57	1.38	2	
Impact	7th St	7	25	Y	-	-	N	-0.16	4.95	5.10	10	Borderline
Base	7th St	9	25		Y	Y		1.00	2.05	1.04	2	
Impact	7th St	9	25	Y	-	-	Y	0.34	3.22	2.88	10	
Base	7th St	5	50		Y	Y		1.71	2.37	0.67	1	
Impact	7th St	5	50	Y	-	-	N	0.06	4.78	4.73	10	
Base	7th St	7	50		N	N		1.19	2.57	1.38	2	
Impact	7th St	7	50	Y	-	-	Y	-2.65	7.08	9.73	10	Borderline
Base	7th St	9	50		Y	Y		1.00	2.05	1.04	2	
Impact	7th St	9	50	N	-	-	Y	1.50	1.54	0.05	1	
Base	7th St	5	100		Y	Y		1.71	2.37	0.67	0	
Impact	7th St	5	100	Y	Y	Y	N	8.69	9.93	1.24	0	
Base	7th St	7	100		N	N		1.19	2.57	1.38	0	
Impact	7th St	7	100	Y	Y	Y	N	2.54	3.52	0.97	0	
Base	7th St	9	100		Y	Y		1.00	2.05	1.04	9	
Impact	7th St	9	100	Y	Y	Y	N	1.44	2.20	0.75	6	
Base	7th St	11	100		Y	Y		0.91	2.54	1.64	10	
Impact	7th St	11	100	Y	Y	Y	Y	1.46	2.34	0.88	8	

* Y = Accept H_o: $\sigma_1^2 = \sigma_2^2$; N = Reject H_o, conclude H_a: $\sigma_1^2 \neq \sigma_2^2$ (at the 95-percent confidence level)
** Y = Accept H_o: Distribution is normal; N = Reject H_o, conclude H_a: Distribution is not normal (at the 95-percent confidence level)
*** Y = Accept H_o: $\mu_1 = \mu_2$; N = Reject H_o conclude H_a: $\mu_1 \neq \mu_2$ (at the 95-percent confidence level)

Table D.18 Subnetwork Size Evaluation Results for 2-Hour Analysis: 15th Street, 3-Link Scenarios

Scenario	Location	Size (Order)	% Cap. Red.	Hypothesis Testing				Prediction Interval			Alternate Runs Within PI	Notes
				Equal Variance*	Normality Test		Equal Mean***	Lower Bound	Upper Bound	Range		
					Lilliefor**	A-D**						
3-Link Impact Scenarios												
Base	15th St	5	25		Y	Y		2.01	3.38	1.38	1	
Impact	15th St	5	25	Y	-	-	N	-2.68	9.51	12.19	10	
Base	15th St	7	25		N	N		0.77	5.61	4.84	2	
Impact	15th St	7	25	Y	-	-	Y	-4.21	10.92	15.13	10	
Base	15th St	9	25		N	N		1.28	3.18	1.90	2	
Impact	15th St	9	25	N	-	-	Y	1.12	3.95	2.82	10	
Base	15th St	5	50		Y	Y		2.01	3.38	1.38	2	
Impact	15th St	5	50	Y	-	-	Y	-0.25	5.73	5.98	10	
Base	15th St	7	50		N	N		0.77	5.61	4.84	2	
Impact	15th St	7	50	N	-	-	Y	-1.08	8.50	9.59	10	
Base	15th St	9	50		N	N		1.28	3.18	1.90	2	
Impact	15th St	9	50	N	-	-	Y	0.74	4.08	3.34	10	
Base	15th St	5	100		Y	Y		2.01	3.38	1.38	0	
Impact	15th St	5	100	N	-	-	N	-9.42	22.85	32.27	10	
Base	15th St	7	100		N	N		0.77	5.61	4.84	1	
Impact	15th St	7	100	Y	-	-	N	-6.60	17.66	24.26	10	
Base	15th St	9	100		N	N		1.28	3.18	1.90	2	
Impact	15th St	9	100	N	-	-	Y	1.23	4.30	3.07	10	Borderline
Base	15th St	11	100		Y	Y		1.34	2.70	1.36	2	
Impact	15th St	11	100	N	-	-	Y	1.07	3.65	2.59	10	

* Y = Accept H_o: $\sigma_1^2 = \sigma_2^2$; N = Reject H_o, conclude H_a: $\sigma_1^2 \neq \sigma_2^2$ (at the 95-percent confidence level)
** Y = Accept H_o: Distribution is normal; N = Reject H_o, conclude H_a: Distribution is not normal (at the 95-percent confidence level)
*** Y = Accept H_o: $\mu_1 = \mu_2$; N = Reject H_o conclude H_a: $\mu_1 \neq \mu_2$ (at the 95-percent confidence level)

APPENDIX E

Detailed Results of the Logit Formula Evaluation

Table E.1 Assessment of Grouping Strategies for Guadalupe Street Scenarios

Scenario	Boundary Centroid Grouping	External Centroid Grouping	Total Demand	Total Demand Diff.	Total Demand Error	RMSE for Subnetwork	
						Full Demand Matrix	Boundary Origins Only
Subnetwork Size 5; 3-Link 100-Percent Capacity Reduction							
Impact	-	-	22,536	-	-	-	-
Base	-	-	23,213	677	3.0%	12.61	13.05
Adjusted	Demand Prop	Boundary	22,757	221	1.0%	12.06	12.04
Adjusted	Max Demand	Boundary	22,713	177	0.8%	12.04	12.01
Adjusted	Max Demand	Region	23,034	498	2.2%	12.46	12.78
Adjusted	Region	Region	22,994	458	2.0%	12.10	12.12
Subnetwork Size 5; 3-Link 50-Percent Capacity Reduction							
Impact	-	-	23,337	-	-	-	-
Base	-	-	23,213	-124	0.5%	3.69	3.49
Adjusted	Demand Prop	Boundary	23,193	-144	0.6%	4.60	5.25
Adjusted	Max Demand	Boundary	23,246	-91	0.4%	4.85	5.69
Adjusted	Max Demand	Region	23,300	-37	0.2%	4.51	5.09
Adjusted	Region	Region	23,178	-159	0.7%	4.63	5.31
Subnetwork Size 7; 3-Link 100-Percent Capacity Reduction							
Impact	-	-	37,060	-	-	-	-
Base	-	-	37,302	242	0.7%	10.75	13.59
Adjusted	Demand Prop	Boundary	37,034	-26	0.1%	10.61	13.35
Adjusted	Max Demand	Boundary	36,978	-82	0.2%	10.63	13.39
Adjusted	Max Demand	Region	37,206	146	0.4%	10.70	13.51
Adjusted	Region	Region	37,178	118	0.3%	10.67	13.46
Subnetwork Size 7; 3-Link 50-Percent Capacity Reduction							
Impact	-	-	37,194	-	-	-	-
Base	-	-	37,302	108	0.3%	3.35	3.94
Adjusted	Demand Prop	Boundary	37,327	133	0.4%	3.48	4.21
Adjusted	Max Demand	Boundary	37,285	91	0.2%	3.78	4.79
Adjusted	Max Demand	Region	37,293	99	0.3%	3.63	4.51
Adjusted	Region	Region	37,345	151	0.4%	3.55	4.35

Subnetwork Size 9; 3-Link 100-Percent Capacity Reduction							
Impact	-	-	50,763	-	-	-	-
Base	-	-	51,162	399	0.8%	8.99	12.70
Adjusted	Demand Prop	Boundary	51,166	403	0.8%	9.00	12.72
Adjusted	Max Demand	Boundary	51,050	287	0.6%	8.99	12.70
Adjusted	Max Demand	Region	50,950	187	0.4%	9.07	12.83
Adjusted	Region	Region	51,087	324	0.6%	8.99	12.70
Subnetwork Size 9; 3-Link 50-Percent Capacity Reduction							
Impact	-	-	51,133	-	-	-	-
Base	-	-	51,162	29	0.1%	2.26	2.87
Adjusted	Demand Prop	Boundary	51,214	81	0.2%	2.67	3.67
Adjusted	Max Demand	Boundary	51,199	66	0.1%	2.55	3.43
Adjusted	Max Demand	Region	51,087	-46	0.1%	2.88	4.06
Adjusted	Region	Region	51,199	66	0.1%	2.62	3.56
Subnetwork Size 5; 2-Link 100-Percent Capacity Reduction							
Impact	-	-	20,547	-	-	-	-
Base	-	-	20,566	19	0.1%	8.17	7.71
Adjusted	Demand Prop	Boundary	19,971	-576	2.8%	7.87	7.10
Adjusted	Max Demand	Boundary	20,292	-255	1.2%	8.73	8.81
Adjusted	Max Demand	Region	20,467	-80	0.4%	7.99	7.33
Adjusted	Region	Region	20,388	-159	0.8%	7.97	7.30
Subnetwork Size 5; 2-Link 50-Percent Capacity Reduction							
Impact	-	-	20,841	-	-	-	-
Base	-	-	20,566	-275	1.3%	11.50	11.53
Adjusted	Demand Prop	Boundary	20,531	-310	1.5%	11.46	11.46
Adjusted	Max Demand	Boundary	20,586	-255	1.2%	11.51	11.53
Adjusted	Max Demand	Region	20,576	-265	1.3%	11.50	11.53
Adjusted	Region	Region	20,357	-484	2.3%	11.06	10.72
Subnetwork Size 7; 2-Link 100-Percent Capacity Reduction							
Impact	-	-	32,828	-	-	-	-
Base	-	-	32,890	62	0.2%	3.77	4.20
Adjusted	Demand Prop	Boundary	32,520	-308	0.9%	4.75	6.12
Adjusted	Max Demand	Boundary	32,489	-339	1.0%	4.35	5.37
Adjusted	Max Demand	Region	32,770	-58	0.2%	4.14	4.95
Adjusted	Region	Region	32,738	-90	0.3%	3.69	4.03

Subnetwork Size 7; 2-Link 50-Percent Capacity Reduction							
Impact	-	-	31,996	-	-	-	-
Base	-	-	32,890	894	2.8%	9.77	11.79
Adjusted	Demand Prop	Boundary	32,922	926	2.9%	9.79	11.83
Adjusted	Max Demand	Boundary	32,893	897	2.8%	9.87	11.97
Adjusted	Max Demand	Region	32,894	898	2.8%	9.80	11.84
Adjusted	Region	Region	32,916	920	2.9%	9.77	11.80
Subnetwork Size 9; 2-Link 100-Percent Capacity Reduction							
Impact	-	-	48,746	-	-	-	-
Base	-	-	48,787	41	0.1%	2.37	2.56
Adjusted	Demand Prop	Boundary	48,598	-148	0.3%	3.33	4.40
Adjusted	Max Demand	Boundary	48,667	-79	0.2%	3.31	4.36
Adjusted	Max Demand	Region	48,528	-218	0.4%	3.37	4.46
Adjusted	Region	Region	48,670	-76	0.2%	3.17	4.11
Subnetwork Size 9; 2-Link 50-Percent Capacity Reduction							
Impact	-	-	48,069	-	-	-	-
Base	-	-	48,787	718	1.5%	9.88	13.32
Adjusted	Demand Prop	Boundary	48,787	718	1.5%	9.92	13.38
Adjusted	Max Demand	Boundary	48,735	666	1.4%	9.90	13.34
Adjusted	Max Demand	Region	48,666	597	1.2%	9.97	13.46
Adjusted	Region	Region	48,780	711	1.5%	9.90	13.34
Subnetwork Size 5; 1-Link 100-Percent Capacity Reduction							
Impact	-	-	18,534	-	-	-	-
Base	-	-	18,582	48	0.3%	7.73	6.23
Adjusted	Demand Prop	Boundary	17,995	-539	2.9%	8.03	6.86
Adjusted	Max Demand	Boundary	18,023	-511	2.8%	7.58	5.90
Adjusted	Max Demand	Region	18,460	-74	0.4%	8.06	6.92
Adjusted	Region	Region	18,114	-420	2.3%	7.56	5.87
Subnetwork Size 5; 1-Link 50-Percent Capacity Reduction							
Impact	-	-	18,643	-	-	-	-
Base	-	-	18,582	-61	0.3%	3.81	3.20
Adjusted	Demand Prop	Boundary	18,532	-111	0.6%	3.84	3.26
Adjusted	Max Demand	Boundary	18,543	-100	0.5%	3.81	3.19
Adjusted	Max Demand	Region	18,561	-82	0.4%	3.82	3.22
Adjusted	Region	Region	18,197	-446	2.4%	5.37	5.97

Subnetwork Size 7; 1-Link 100-Percent Capacity Reduction							
Impact	-	-	29,154	-	-	-	-
Base	-	-	29,294	140	0.5%	6.23	4.84
Adjusted	Demand Prop	Boundary	29,188	34	0.1%	6.98	6.66
Adjusted	Max Demand	Boundary	28,972	-182	0.6%	6.55	5.66
Adjusted	Max Demand	Region	29,170	16	0.1%	6.73	6.09
Adjusted	Region	Region	29,256	102	0.3%	6.43	5.37
Subnetwork Size 7; 1-Link 50-Percent Capacity Reduction							
Impact	-	-	29,181	-	-	-	-
Base	-	-	29,294	113	0.4%	3.44	3.47
Adjusted	Demand Prop	Boundary	29,528	347	1.2%	5.15	6.56
Adjusted	Max Demand	Boundary	29,327	146	0.5%	3.80	4.18
Adjusted	Max Demand	Region	29,282	101	0.3%	3.71	4.00
Adjusted	Region	Region	29,379	198	0.7%	4.03	4.61
Subnetwork Size 9; 1-Link 100-Percent Capacity Reduction							
Impact	-	-	43,353	-	-	-	-
Base	-	-	43,401	48	0.1%	3.08	3.45
Adjusted	Demand Prop	Boundary	43,207	-146	0.3%	3.26	3.81
Adjusted	Max Demand	Boundary	43,196	-157	0.4%	3.27	3.83
Adjusted	Max Demand	Region	43,367	14	0.0%	3.27	3.83
Adjusted	Region	Region	43,285	-68	0.2%	3.29	3.88
Subnetwork Size 9; 1-Link 50-Percent Capacity Reduction							
Impact	-	-	43,368	-	-	-	-
Base	-	-	43,401	33	0.1%	2.47	2.78
Adjusted	Demand Prop	Boundary	43,439	71	0.2%	2.72	3.28
Adjusted	Max Demand	Boundary	43,501	133	0.3%	2.85	3.52
Adjusted	Max Demand	Region	43,468	100	0.2%	2.65	3.14
Adjusted	Region	Region	43,450	82	0.2%	2.63	3.11

Table E.2 Assessment of Grouping Strategies for 7th Street Scenarios

Scenario	Boundary Centroid Grouping	External Centroid Grouping	Total Demand	Total Demand Diff.	Total Demand Error	RMSE for Subnetwork	
						Full Demand Matrix	Boundary Origins Only
Subnetwork Size 5; 3-Link 100-Percent Capacity Reduction							
Impact	-	-	30,823	-	-	-	-
Base	-	-	31,108	285	0.9%	5.31	3.39
Adjusted	Demand Prop	Boundary	30,424	-399	1.3%	16.47	21.63
Adjusted	Max Demand	Boundary	29,566	-1257	4.1%	9.85	11.86
Adjusted	Max Demand	Region	30,638	-185	0.6%	6.41	5.98
Adjusted	Region	Region	31,070	247	0.8%	5.36	3.52
Subnetwork Size 5; 3-Link 50-Percent Capacity Reduction							
Impact	-	-	31,002	-	-	-	-
Base	-	-	31,108	106	0.3%	3.36	2.89
Adjusted	Demand Prop	Boundary	30,139	-863	2.8%	8.72	11.34
Adjusted	Max Demand	Boundary	29,985	-1,017	3.3%	9.19	12.00
Adjusted	Max Demand	Region	30,759	-243	0.8%	4.85	5.56
Adjusted	Region	Region	31,117	115	0.4%	3.72	3.60
Subnetwork Size 7; 3-Link 100-Percent Capacity Reduction							
Impact	-	-	44,718	-	-	-	-
Base	-	-	44,701	-17	0.0%	3.18	2.43
Adjusted	Demand Proportions	Boundary	44,651	-67	0.1%	3.41	2.97
Adjusted	Max Demand	Boundary	44,826	108	0.2%	3.96	4.05
Adjusted	Max Demand	Region	44,615	-103	0.2%	3.42	2.98
Adjusted	Region	Region	44,560	-158	0.4%	3.84	3.82
Subnetwork Size 7; 3-Link 50-Percent Capacity Reduction							
Impact	-	-	44,768	-	-	-	-
Base	-	-	44,701	-67	0.1%	2.99	2.20
Adjusted	Demand Prop	Boundary	44,820	52	0.1%	4.65	5.33
Adjusted	Max Demand	Boundary	44,811	43	0.1%	3.91	4.09
Adjusted	Max Demand	Region	44,697	-71	0.2%	4.85	5.66
Adjusted	Region	Region	44,663	-105	0.2%	6.17	7.69

Subnetwork Size 9; 3-Link 100-Percent Capacity Reduction							
Impact	-	-	52,308	-	-	-	-
Base	-	-	52,277	-31	0.1%	2.82	2.25
Adjusted	Demand Prop	Boundary	52,184	-124	0.2%	3.90	4.43
Adjusted	Max Demand	Boundary	52,142	-166	0.3%	3.92	4.47
Adjusted	Max Demand	Region	52,167	-141	0.3%	4.50	5.44
Adjusted	Region	Region	52,221	-87	0.2%	4.36	5.21
Subnetwork Size 9; 3-Link 50-Percent Capacity Reduction							
Impact	-	-	52,360	-	-	-	-
Base	-	-	52,277	-83	0.2%	2.39	1.92
Adjusted	Demand Prop	Boundary	52,287	-73	0.1%	4.73	6.07
Adjusted	Max Demand	Boundary	52,345	-15	0.0%	4.79	6.16
Adjusted	Max Demand	Region	52,294	-66	0.1%	5.00	6.48
Adjusted	Region	Region	52,508	148	0.3%	4.85	6.26
Subnetwork Size 5; 2-Link 100-Percent Capacity Reduction							
Impact	-	-	30,564	-	-	-	-
Base	-	-	30,764	200	0.7%	5.70	4.01
Adjusted	Demand Prop	Boundary	29,601	-963	3.2%	10.18	12.19
Adjusted	Max Demand	Boundary	30,196	-368	1.2%	15.61	20.23
Adjusted	Max Demand	Region	30,377	-187	0.6%	7.32	7.45
Adjusted	Region	Region	30,794	230	0.8%	6.72	6.31
Subnetwork Size 5; 2-Link 50-Percent Capacity Reduction							
Impact	-	-	30,747	-	-	-	-
Base	-	-	30,764	17	0.1%	3.25	2.83
Adjusted	Demand Prop	Boundary	30,307	-440	1.4%	16.00	21.44
Adjusted	Max Demand	Boundary	29,612	-1,135	3.7%	8.81	11.47
Adjusted	Max Demand	Region	30,412	-335	1.1%	4.79	5.56
Adjusted	Region	Region	30,816	69	0.2%	3.38	3.10
Subnetwork Size 7; 2-Link 100-Percent Capacity Reduction							
Impact	-	-	42,481	-	-	-	-
Base	-	-	42,479	-2	0.0%	3.33	2.37
Adjusted	Demand Prop	Boundary	42,408	-73	0.2%	5.60	6.60
Adjusted	Max Demand	Boundary	42,414	-67	0.2%	4.14	4.12
Adjusted	Max Demand	Region	42,466	-15	0.0%	5.03	5.68
Adjusted	Region	Region	42,526	45	0.1%	5.91	7.09

Subnetwork Size 7; 2-Link 50-Percent Capacity Reduction							
Impact	-	-	42,604	-	-	-	-
Base	-	-	42,479	-125	0.3%	2.79	2.18
Adjusted	Demand Prop	Boundary	42,420	-184	0.4%	5.02	6.15
Adjusted	Max Demand	Boundary	42,432	-172	0.4%	3.29	3.25
Adjusted	Max Demand	Region	42,470	-134	0.3%	3.38	3.41
Adjusted	Region	Region	42,328	-276	0.6%	3.90	4.34
Subnetwork Size 9; 2-Link 100-Percent Capacity Reduction							
Impact	-	-	51,962	-	-	-	-
Base	-	-	51,812	-150	0.3%	2.28	1.98
Adjusted	Demand Prop	Boundary	51,928	-34	0.1%	5.50	7.36
Adjusted	Max Demand	Boundary	52,094	132	0.3%	5.69	7.65
Adjusted	Max Demand	Region	51,762	-200	0.4%	5.81	7.83
Adjusted	Region	Region	51,908	-54	0.1%	5.81	7.82
Subnetwork Size 9; 2-Link 50-Percent Capacity Reduction							
Impact	-	-	51,912	-	-	-	-
Base	-	-	51,812	-100	0.2%	2.56	2.07
Adjusted	Demand Prop	Boundary	51,821	-91	0.2%	3.93	4.72
Adjusted	Max Demand	Boundary	51,841	-71	0.1%	3.94	4.74
Adjusted	Max Demand	Region	51,838	-74	0.1%	4.32	5.37
Adjusted	Region	Region	51,838	-74	0.1%	4.33	5.37
Subnetwork Size 5; 1-Link 100-Percent Capacity Reduction							
Impact	-	-	21,000	-	-	-	-
Base	-	-	21,226	226	1.1%	7.34	4.25
Adjusted	Demand Prop	Boundary	21,100	100	0.5%	7.58	4.97
Adjusted	Max Demand	Boundary	20,979	-21	0.1%	7.50	4.74
Adjusted	Max Demand	Region	21,106	106	0.5%	7.44	4.56
Adjusted	Region	Region	21,170	170	0.8%	7.37	4.33
Subnetwork Size 5; 1-Link 50-Percent Capacity Reduction							
Impact	-	-	21,201	-	-	-	-
Base	-	-	21,226	25	0.1%	3.10	2.25
Adjusted	Demand Prop	Boundary	21,220	19	0.1%	3.23	2.57
Adjusted	Max Demand	Boundary	21,192	-9	0.0%	3.23	2.56
Adjusted	Max Demand	Region	21,208	7	0.0%	3.21	2.52
Adjusted	Region	Region	21,224	23	0.1%	3.10	2.25

Subnetwork Size 7; 1-Link 100-Percent Capacity Reduction							
Impact	-	-	40,979	-	-	-	-
Base	-	-	40,876	-103	0.3%	3.56	2.55
Adjusted	Demand Prop	Boundary	40,481	-498	1.2%	6.68	8.38
Adjusted	Max Demand	Boundary	39,813	-1,166	2.8%	7.51	9.68
Adjusted	Max Demand	Region	40,730	-249	0.6%	3.94	3.49
Adjusted	Region	Region	40,714	-265	0.6%	3.89	3.37
Subnetwork Size 7; 1-Link 50-Percent Capacity Reduction							
Impact	-	-	40,940	-	-	-	-
Base	-	-	40,876	-64	0.2%	3.11	2.30
Adjusted	Demand Prop	Boundary	40,507	-433	1.1%	6.36	8.18
Adjusted	Max Demand	Boundary	39,835	-1,105	2.7%	7.25	9.55
Adjusted	Max Demand	Region	40,824	-116	0.3%	3.57	3.37
Adjusted	Region	Region	40,727	-213	0.5%	3.69	3.63
Subnetwork Size 9; 1-Link 100-Percent Capacity Reduction							
Impact	-	-	51,839	-	-	-	-
Base	-	-	51,735	-104	0.2%	2.58	2.00
Adjusted	Demand Prop	Boundary	51,720	-119	0.2%	3.72	4.30
Adjusted	Max Demand	Boundary	51,691	-148	0.3%	3.73	4.31
Adjusted	Max Demand	Region	51,676	-163	0.3%	3.90	4.62
Adjusted	Region	Region	51,671	-168	0.3%	3.93	4.66
Subnetwork Size 9; 1-Link 50-Percent Capacity Reduction							
Impact	-	-	51,819	-	-	-	-
Base	-	-	51,735	-84	0.2%	2.49	1.95
Adjusted	Demand Prop	Boundary	51,737	-82	0.2%	3.75	4.44
Adjusted	Max Demand	Boundary	51,732	-87	0.2%	3.75	4.44
Adjusted	Max Demand	Region	51,760	-59	0.1%	3.74	4.44
Adjusted	Region	Region	51,793	-26	0.1%	3.74	4.43

Table E.3 Assessment of Grouping Strategies for 15th Street Scenarios

Scenario	Boundary Centroid Grouping	External Centroid Grouping	Total Demand	Total Demand Diff.	Total Demand Error	RMSE for Subnetwork	
						Full Demand Matrix	Boundary Origins Only
Subnetwork Size 5; 3-Link 100-Percent Capacity Reduction							
Impact	-	-	19,706	-	-	-	-
Base	-	-	19,799	93	0.5%	4.70	5.43
Adjusted	Demand Prop	Boundary	19,281	-425	2.2%	5.38	6.44
Adjusted	Max Demand	Boundary	19,155	-551	2.8%	5.90	7.19
Adjusted	Max Demand	Region	18,726	-980	5.0%	10.05	12.98
Adjusted	Region	Region	18,526	-1180	6.0%	8.23	10.48
Subnetwork Size 5; 3-Link 50-Percent Capacity Reduction							
Impact	-	-	19,736	-	-	-	-
Base	-	-	19,799	63	0.3%	3.81	3.88
Adjusted	Demand Prop	Boundary	19,351	-385	2.0%	5.16	6.05
Adjusted	Max Demand	Boundary	19,289	-447	2.3%	7.69	9.71
Adjusted	Max Demand	Region	18,892	-844	4.3%	10.58	13.72
Adjusted	Region	Region	18,711	-1,025	5.2%	9.05	11.61
Subnetwork Size 7; 3-Link 100-Percent Capacity Reduction							
Impact	-	-	24,920	-	-	-	-
Base	-	-	24,977	57	0.2%	3.66	4.14
Adjusted	Demand Prop	Boundary	24,508	-412	1.7%	8.69	11.61
Adjusted	Max Demand	Boundary	24,564	-356	1.4%	8.72	11.64
Adjusted	Max Demand	Region	24,003	-917	3.7%	8.60	11.47
Adjusted	Region	Region	24,188	-732	2.9%	5.78	7.41
Subnetwork Size 7; 3-Link 50-Percent Capacity Reduction							
Impact	-	-	24,890	-	-	-	-
Base	-	-	24,977	87	0.3%	2.99	2.97
Adjusted	Demand Prop	Boundary	24,601	-289	1.2%	8.38	11.20
Adjusted	Max Demand	Boundary	24,656	-234	0.9%	8.42	11.25
Adjusted	Max Demand	Region	24,224	-666	2.7%	8.38	11.19
Adjusted	Region	Region	24,308	-582	2.3%	5.54	7.08

Subnetwork Size 9; 3-Link 100-Percent Capacity Reduction							
Impact	-	-	38,455	-	-	-	-
Base	-	-	38,488	33	0.1%	3.04	2.92
Adjusted	Demand Prop	Boundary	38,379	-76	0.2%	6.10	8.36
Adjusted	Max Demand	Boundary	38,380	-75	0.2%	6.10	8.37
Adjusted	Max Demand	Region	38,276	-179	0.5%	6.28	8.65
Adjusted	Region	Region	38,433	-22	0.1%	6.12	8.39
Subnetwork Size 9; 3-Link 50-Percent Capacity Reduction							
Impact	-	-	38,486	-	-	-	-
Base	-	-	38,488	2	0.0%	2.79	2.25
Adjusted	Demand Prop	Boundary	38,481	-5	0.0%	4.40	5.54
Adjusted	Max Demand	Boundary	38,481	-5	0.0%	4.41	5.54
Adjusted	Max Demand	Region	38,376	-110	0.3%	4.60	5.88
Adjusted	Region	Region	38,508	22	0.1%	4.38	5.49
Subnetwork Size 5; 2-Link 100-Percent Capacity Reduction							
Impact	-	-	17,842	-	-	-	-
Base	-	-	18,053	211	1.2%	4.08	4.31
Adjusted	Demand Prop	Boundary	19,553	1,711	9.6%	8.63	11.06
Adjusted	Max Demand	Boundary	18,633	791	4.4%	8.22	10.48
Adjusted	Max Demand	Region	19,222	1,380	7.7%	11.41	14.89
Adjusted	Region	Region	19,220	1,378	7.7%	8.55	10.94
Subnetwork Size 5; 2-Link 50-Percent Capacity Reduction							
Impact	-	-	17,920	-	-	-	-
Base	-	-	18,053	133	0.7%	3.35	3.11
Adjusted	Demand Prop	Boundary	18,083	163	0.9%	5.61	6.82
Adjusted	Max Demand	Boundary	17,807	-113	0.6%	8.65	11.21
Adjusted	Max Demand	Region	18,184	264	1.5%	7.67	9.82
Adjusted	Region	Region	17,996	76	0.4%	5.28	6.32
Subnetwork Size 7; 2-Link 100-Percent Capacity Reduction							
Impact	-	-	24,628	-	-	-	-
Base	-	-	24,680	52	0.2%	3.45	3.95
Adjusted	Demand Prop	Boundary	25,031	403	1.6%	5.05	6.45
Adjusted	Max Demand	Boundary	24,987	359	1.5%	5.08	6.48
Adjusted	Max Demand	Region	25,133	505	2.1%	5.51	7.12
Adjusted	Region	Region	24,653	25	0.1%	5.00	6.37

Subnetwork Size 7; 2-Link 50-Percent Capacity Reduction							
Impact	-	-	24,626	-	-	-	-
Base	-	-	24,680	54	0.2%	2.98	3.03
Adjusted	Demand Prop	Boundary	24,670	44	0.2%	4.39	5.40
Adjusted	Max Demand	Boundary	24,670	44	0.2%	4.39	5.40
Adjusted	Max Demand	Region	24,552	-74	0.3%	4.70	5.88
Adjusted	Region	Region	24,537	-89	0.4%	3.92	4.66
Subnetwork Size 9; 2-Link 100-Percent Capacity Reduction							
Impact	-	-	36,219	-	-	-	-
Base	-	-	36,266	47	0.1%	3.00	2.92
Adjusted	Demand Prop	Boundary	36,298	79	0.2%	4.24	5.33
Adjusted	Max Demand	Boundary	36,298	79	0.2%	4.25	5.34
Adjusted	Max Demand	Region	36,341	122	0.3%	4.42	5.65
Adjusted	Region	Region	36,248	29	0.1%	5.96	8.22
Subnetwork Size 9; 2-Link 50-Percent Capacity Reduction							
Impact	-	-	36,206	-	-	-	-
Base	-	-	36,266	60	0.2%	2.69	2.46
Adjusted	Demand Prop	Boundary	36,251	45	0.1%	3.86	4.81
Adjusted	Max Demand	Boundary	36,254	48	0.1%	3.86	4.80
Adjusted	Max Demand	Region	36,237	31	0.1%	3.85	4.80
Adjusted	Region	Region	36,308	102	0.3%	3.57	4.28
Subnetwork Size 5; 1-Link 100-Percent Capacity Reduction							
Impact	-	-	15,449	-	-	-	-
Base	-	-	15,681	232	1.5%	4.35	4.94
Adjusted	Demand Prop	Boundary	14,318	-1,131	7.3%	6.65	8.20
Adjusted	Max Demand	Boundary	14,308	-1,141	7.4%	6.57	8.09
Adjusted	Max Demand	Region	15,553	104	0.7%	15.66	20.16
Adjusted	Region	Region	14,832	-617	4.0%	5.91	7.18
Subnetwork Size 5; 1-Link 50-Percent Capacity Reduction							
Impact	-	-	15,590	-	-	-	-
Base	-	-	15,681	91	0.6%	3.76	3.99
Adjusted	Demand Prop	Boundary	14,494	-1,096	7.0%	6.34	7.79
Adjusted	Max Demand	Boundary	14,504	-1,086	7.0%	6.10	7.45
Adjusted	Max Demand	Region	15,742	152	1.0%	15.65	20.31
Adjusted	Region	Region	15,004	-586	3.8%	5.31	6.34

Subnetwork Size 7; 1-Link 100-Percent Capacity Reduction							
Impact	-	-	22,338	-	-	-	-
Base	-	-	22,448	110	0.5%	3.21	3.23
Adjusted	Demand Prop	Boundary	22,098	-240	1.1%	4.77	5.75
Adjusted	Max Demand	Boundary	21,979	-359	1.6%	5.06	6.19
Adjusted	Max Demand	Region	21,619	-719	3.2%	6.27	7.95
Adjusted	Region	Region	21,496	-842	3.8%	4.27	4.98
Subnetwork Size 7; 1-Link 50-Percent Capacity Reduction							
Impact	-	-	22,438	-	-	-	-
Base	-	-	22,448	10	0.0%	3.00	2.81
Adjusted	Demand Prop	Boundary	22,134	-304	1.4%	6.02	7.62
Adjusted	Max Demand	Boundary	22,103	-335	1.5%	6.46	8.26
Adjusted	Max Demand	Region	21,845	-593	2.6%	7.97	10.41
Adjusted	Region	Region	21,748	-690	3.1%	4.05	4.63
Subnetwork Size 9; 1-Link 100-Percent Capacity Reduction							
Impact	-	-	32,631	-	-	-	-
Base	-	-	32,593	-38	0.1%	2.50	2.71
Adjusted	Demand Prop	Boundary	33,097	466	1.4%	11.59	16.22
Adjusted	Max Demand	Boundary	33,365	734	2.2%	11.36	15.89
Adjusted	Max Demand	Region	32,400	-231	0.7%	11.06	15.46
Adjusted	Region	Region	32,387	-244	0.7%	11.06	15.45
Subnetwork Size 9; 1-Link 50-Percent Capacity Reduction							
Impact	-	-	32,602	-	-	-	-
Base	-	-	32,593	-9	0.0%	2.29	2.05
Adjusted	Demand Prop	Boundary	33,319	717	2.2%	11.47	16.04
Adjusted	Max Demand	Boundary	33,507	905	2.8%	11.22	15.68
Adjusted	Max Demand	Region	32,566	-36	0.1%	10.73	14.97
Adjusted	Region	Region	32,566	-36	0.1%	10.14	14.13

Table E.4 Assessment of Grouping Strategies Relative to Subnetwork Size Evaluation

Location	Size	# Links	% Cap. Red.	Grouping Strategy		Improvement		Stat. Diff.
				Boundary	External	Demand Estimation	RMSE	
Guadalupe Street	5	3	100	Demand Prop	Boundary	Y	Y	Y
				Max Demand	Boundary	Y*	Y*	
				Max Demand	Region	Y	Y	
				Region	Region	Y	Y	
Guadalupe Street	5	3	50	Demand Prop	Boundary	N	N	N
				Max Demand	Boundary	Y	N	
				Max Demand	Region	Y*	N*	
				Region	Region	N	N	
Guadalupe Street	7	3	100	Demand Prop	Boundary	Y*	Y*	Y
				Max Demand	Boundary	Y	Y	
				Max Demand	Region	Y	Y	
				Region	Region	Y	Y	
Guadalupe Street	7	3	50	Demand Prop	Boundary	N	N*	N
				Max Demand	Boundary	Y*	N	
				Max Demand	Region	Y	N	
				Region	Region	N	N	
Guadalupe Street	9	3	100	Demand Prop	Boundary	N	N	Y
				Max Demand	Boundary	Y	N	
				Max Demand	Region	Y*	N	
				Region	Region	Y	Y*	
Guadalupe Street	9	3	50	Demand Prop	Boundary	N	N	N
				Max Demand	Boundary	N	N*	
				Max Demand	Region	N*	N	
				Region	Region	N	N	
Guadalupe Street	5	2	100	Demand Prop	Boundary	N	Y	Y
				Max Demand	Boundary	N	N	
				Max Demand	Region	N*	Y*	
				Region	Region	N	Y	
Guadalupe Street	5	2	50	Demand Prop	Boundary	N	Y	N
				Max Demand	Boundary	Y*	N	
				Max Demand	Region	Y	Y	
				Region	Region	N	Y*	
Guadalupe Street	7	2	100	Demand Prop	Boundary	N	N	Y
				Max Demand	Boundary	N	N	
				Max Demand	Region	Y*	N	
				Region	Region	N	Y*	
Guadalupe Street	7	2	50	Demand Prop	Boundary	N	N	N
				Max Demand	Boundary	N*	N	
				Max Demand	Region	N	N	
				Region	Region	N	N*	

Guadalupe Street	9	2	100	Demand Prop Max Demand Max Demand Region	Boundary Boundary Region Region	N N N N*	N N N N*	Y
Guadalupe Street	9	2	50	Demand Prop Max Demand Max Demand Region	Boundary Boundary Region Region	N N N* N	N Y N Y*	N
Guadalupe Street	5	1	100	Demand Prop Max Demand Max Demand Region	Boundary Boundary Region Region	N N N* N	N Y N Y*	Y
Guadalupe Street	5	1	50	Demand Prop Max Demand Max Demand Region	Boundary Boundary Region Region	N N N* N	N Y* N N	N
Guadalupe Street	7	1	100	Demand Prop Max Demand Max Demand Region	Boundary Boundary Region Region	Y N Y* Y	N N N N*	Y
Guadalupe Street	7	1	50	Demand Prop Max Demand Max Demand Region	Boundary Boundary Region Region	N N Y* N	N N N* N	N
Guadalupe Street	9	1	100	Demand Prop Max Demand Max Demand Region	Boundary Boundary Region Region	N N Y* N	N* N N N	N
Guadalupe Street	9	1	50	Demand Prop Max Demand Max Demand Region	Boundary Boundary Region Region	N* N N N	N N N N*	N
7th Street	5	3	100	Demand Prop Max Demand Max Demand Region	Boundary Boundary Region Region	N N Y* Y	N N N N*	Y
7th Street	5	3	50	Demand Prop Max Demand Max Demand Region	Boundary Boundary Region Region	N N N N*	N N N N*	Y
7th Street	7	3	100	Demand Prop Max Demand Max Demand Region	Boundary Boundary Region Region	N* N N N	N* N N N	Y
7th Street	7	3	50	Demand Prop Max Demand Max Demand Region	Boundary Boundary Region Region	Y Y* N N	N N* N N	N

7th Street	9	3	100	Demand Prop Max Demand Max Demand Region	Boundary Boundary Region Region	N N N N*	N* N N N	Y
7th Street	9	3	50	Demand Prop Max Demand Max Demand Region	Boundary Boundary Region Region	Y Y* Y N	N* N N N	N
7th Street	5	2	100	Demand Prop Max Demand Max Demand Region	Boundary Boundary Region Region	N N Y* N	N N N N*	Y
7th Street	5	2	50	Demand Prop Max Demand Max Demand Region	Boundary Boundary Region Region	N N N N*	N N N N*	Y
7th Street	7	2	100	Demand Prop Max Demand Max Demand Region	Boundary Boundary Region Region	N N N* N	N N* N N	Y
7th Street	7	2	50	Demand Prop Max Demand Max Demand Region	Boundary Boundary Region Region	N N N* N	N N* N N	Y
7th Street	9	2	100	Demand Prop Max Demand Max Demand Region	Boundary Boundary Region Region	Y* Y N Y	N* N N N	Y
7th Street	9	2	50	Demand Prop Max Demand Max Demand Region	Boundary Boundary Region Region	Y Y* Y Y	N* N N N	N
7th Street	5	1	100	Demand Prop Max Demand Max Demand Region	Boundary Boundary Region Region	Y Y* Y Y	N N N N*	Y
7th Street	5	1	50	Demand Prop Max Demand Max Demand Region	Boundary Boundary Region Region	Y Y Y* Y	N N N N*	N
7th Street	7	1	100	Demand Prop Max Demand Max Demand Region	Boundary Boundary Region Region	N N N* N	N N N N*	Y
7th Street	7	1	50	Demand Prop Max Demand Max Demand Region	Boundary Boundary Region Region	N N N* N	N N N* N	N

7th Street	9	1	100	Demand Prop Max Demand Max Demand Region	Boundary Boundary Region Region	N* N N N	N* N N N	N
7th Street	9	1	50	Demand Prop Max Demand Max Demand Region	Boundary Boundary Region Region	Y N Y Y*	N N N N*	N
15th Street	5	3	100	Demand Prop Max Demand Max Demand Region	Boundary Boundary Region Region	N* N N N	N* N N N	Y
15th Street	5	3	50	Demand Prop Max Demand Max Demand Region	Boundary Boundary Region Region	N* N N N	N* N N N	N
15th Street	7	3	100	Demand Prop Max Demand Max Demand Region	Boundary Boundary Region Region	N N* N N	N N N N*	Y
15th Street	7	3	50	Demand Prop Max Demand Max Demand Region	Boundary Boundary Region Region	N N* N N	N N N N*	N
15th Street	9	3	100	Demand Prop Max Demand Max Demand Region	Boundary Boundary Region Region	N N N Y*	N* N N N	N
15th Street	9	3	50	Demand Prop Max Demand Max Demand Region	Boundary Boundary Region Region	N* N* N N	N N N N*	N
15th Street	5	2	100	Demand Prop Max Demand Max Demand Region	Boundary Boundary Region Region	N N* N N	N N* N N	Y
15th Street	5	2	50	Demand Prop Max Demand Max Demand Region	Boundary Boundary Region Region	N Y N Y*	N N N N*	Y
15th Street	7	2	100	Demand Prop Max Demand Max Demand Region	Boundary Boundary Region Region	N N N Y*	N N N N*	N
15th Street	7	2	50	Demand Prop Max Demand Max Demand Region	Boundary Boundary Region Region	Y* Y* N N	N N N N*	N

15th Street	9	2	100	Demand Prop Max Demand Max Demand Region	Boundary Boundary Region Region	N N N Y*	N* N N N	Y
15th Street	9	2	50	Demand Prop Max Demand Max Demand Region	Boundary Boundary Region Region	Y Y Y* N	N N N N*	N
15th Street	5	1	100	Demand Prop Max Demand Max Demand Region	Boundary Boundary Region Region	N N Y* N	N N N N*	Y
15th Street	5	1	50	Demand Prop Max Demand Max Demand Region	Boundary Boundary Region Region	N N N* N	N N N N*	Y
15th Street	7	1	100	Demand Prop Max Demand Max Demand Region	Boundary Boundary Region Region	N* N N N	N N N N*	N
15th Street	7	1	50	Demand Prop Max Demand Max Demand Region	Boundary Boundary Region Region	N* N N N	N N N N*	N
15th Street	9	1	100	Demand Prop Max Demand Max Demand Region	Boundary Boundary Region Region	N N N* N	N N N N*	N
15th Street	9	1	50	Demand Prop Max Demand Max Demand Region	Boundary Boundary Region Region	N N N* N*	N N N N*	N

* Best performing grouping strategy

REFERENCES

Astarita, V., K. Er-Rafia, M. Florian, M. Mahut, and S. Velan. "Comparison of Three Models for Dynamic Network Loading." *Transportation Research Record No. 1771*, Transportation Research Board of the National Academies, Washington, D.C., 2001, pp. 179-190.

Bar-Gera, Hillel. "Continuous and Discrete Trajectory Models for Dynamic Traffic Assignment." Networks and Spatial Economics 5, Springer Science + Business Media, Inc., The Netherlands, 2005, pp. 41-70.

Ben-Akiva, Moshe, Michel Bierlaire, Jon Bottom, Haris Koutsopoulos, and Rabi Mishalani. "Development of a Route Guidance Generation System for Real-Time Application." *Proceedings of the 8th IFAC/IFIP/IFORS Symposium on Transportation Systems*, Chania, Greece, 1997.

Ben-Akiva, Moshe, Haris Koutsopoulos, Rabi Mishalani, and Qi Yang. "Simulation Laboratory for Evaluating Dynamic Traffic Management Systems." *Journal of Transportation Engineering*, July/August 1997, pp. 283-289.

Boyles, Stephen D. "Bush-based Sensitivity Analysis for Approximating Subnetwork Diversion." *Transportation Research Part B 46*, Elsevier Ltd., 2012, pp. 139-155.

Boyles, Stephen D. "Improved Bush-Based Sensitivity Analysis in Network Equilibrium." *Submitted for presentation only to the 92nd Annual Meeting of the Transportation Research Board*, Washington, D.C., 2012.

Boyles, Stephen, Satish V. Ukkusuri, S. Travis Waller, and Kara M. Kockelman. "A Comparison of Static and Dynamic Traffic Assignment Under Tolls in the Dallas-Fort Worth Region." *Innovations in Travel Demand Modeling, Volume 2: Papers*, Conference Proceedings 42, Transportation Research Board, Washington, D.C., 2008, pp. 114-117.

Boyles, Stephen and S. Travis Waller. "Traffic Network Design and Analysis." Wiley Encyclopedia of Operations Research and Management Science, John Wiley & Sons, Inc., 2011.

Bringardner, Jack W., Mason D. Gemar, Stephen D. Boyles, and Randy B. Machemehl. "Establishing the Variation of Dynamic Traffic Assignment Results Using Subnetwork Origin-Destination Matrices." *Submitted for Presentation and Publication at the 93rd Annual Meeting of the Transportation Research Board*, Washington, D.C., July 2013.

Carey, Malachy and Eswaran Subrahmanian. “An Approach to Modelling Time-Varying Flows on Congested Networks.” *Transportation Research Part B*, Elsevier Ltd., 2000, pp. 157-183.

Chabini, Ismail and Brian Dean. “Technical Report 2 - Shortest Path Problems in Discrete-Time Dynamic Networks: Complexity, Algorithms and Implecations.” *Algorithms and High Performance Computing for Dynamic Shortest Paths and Analytical Dynamic Traffic Assignment Models, Technical Report, New England (Region One) UTC Report DTRS95-G-001.*, Massachusetts Institute of Technology, Cambridge, MA, 2000.

Chen, Anthony, Chao Yang, Sirisak Kongsomsaksakul, and Ming Lee. “Network-based Accessibility Measures for Vulnerability Analysis of Degradable Transportation Networks.” *Networks and Spatial Economics*, Springer Science + Business Media, LLC, December 2010, pp. 241-256.

Chen, Bi Yu, William H.K. Lam, Agachai Sumalee, Qingquan Li, and Zhi-Chun Li. “Vulnerability analysis for large-scale and congested road networks with demand uncertainty.” *Transportation Research Part A*, Elsevier Ltd., 2011, pp. 501-516.

Chien, Steven I., Kyriacos C. Mouskos, and Athanasios K. Ziliaskopoulos, “Development of a Simulation/Assignment Model for the NJDOT I-80 ITS Priority Corridor.” Report No. FHWA-NJ-2005-011, New Jersey Institute of Technology, Newark, NJ, 2005.

Chiu, Yi-Chang, Jon Bottom, Michael Mahut, Alex Paz, Ramachandran Balakrishna, Travis Waller, and Jim Hicks. “Dynamic Traffic Assignment: A Primer.” *Transportation Research Circular E-C153*, Transportation Research Board, Washington, D.C., 2011.

Cools, Mario, Elke Moons, and Geert Wets. “Assessing the Quality of Origin-Destination Matrices Derived from Activity Travel Surveys.” *Transportation Research Record 2183*, Washington, D.C., 2010, pp. 49-59.

Daganzo, Carlos F. “The Cell Transmission Model: A Dynamic Representation of Highway Traffic Consistent with the Hydrodynamic Theory.” *Transportation Research Part B*, Elsevier Ltd., 1994, pp. 269-287.

Daganzo, Carlos F. “The Cell Transmission Model, Part II: Network Traffic.” *Transportation Research Part B*, Elsevier Ltd., 1995, pp. 79-93.

Danczyk, Adam and Henry X. Liu. “Unexpected Cause, Unexpected Effect: Empirical Observations of Twin Cities Traffic Behavior after the I-35W Bridge Collapse and Reopening.” *Proceedings of Transportation Research Board [CD ROM]*, Washington, D.C., July 2009.

Djukic, Tamara, S.P. Hoogendoorn, and J.W.C van Lint. "Reliability Assessment of Dynamic OD Estimation Methods Based on Structural Similarity Index." *Submitted for Presentation and Publication at the 92nd Annual Meeting of the Transportation Research Board*, Washington, D.C., January 2013.

ESRI ArcGIS 10.1 Website. "How Grouping Analysis Works." ESRI, 2013, http:// http://resources.arcgis.com/en/help/main/10.1/index.html#//005p0000004w000000. Accessed July 21, 2013.

Florian, Michael, Michael Mahut, and Nicolas Tremblay. "Application of a Simulation-based Dynamic Traffic Assignment Model." *European Journal of Operational Research 189*, Elsevier Ltd., 2008, pp. 1381-1392.

Handy, S.L. and D.A. Niemeier. "Measuring Accessibility: An Exploration of Issues and Alternatives." *Environment and Planning*, Volume 29, 1997, p. 1175-1194.

Hanson, Susan and Genevieve Giuliano. The Geography of Urban Transportation. *3rd Edition*, The Guilford Press, New York, NY, 2004.

Highway Capacity Manual 2010. Transportation Research Board, Washington, D.C., 2010.

Jayakrishnan, R., Jun-Seok Oh, Abd-El Kader Sahraoui. "Calibration and Path Dynamics Issues in Microscopic Simulation for Advanced Traffic Management and Information Systems." *Paper No. 01-3437*, Prepared for 80th Annual Meeting of the Transportation Research Board, Washington, DC, 2001.

Jenelius, Erik, Tom Petersen, and Lars-Goran Mattsson. "Importance and Exposure in Road Network Vulnerability Analysis." *Transportation Research Part A*, Elsevier Ltd., 2006, pp. 537-560.

Kamga, Camille N., Kyriacos C. Mouskos, and Robert E. Paaswell. "A Methodology to Estimate Travel Time Using Dynamic Traffic Assignment (DTA) Under Incident Conditions." *Transportation Research Part C 19*, Elsevier Ltd., 2011, pp. 1215-1224.

Kim, C, E.B. Lee, and C.L. Monismith. "Construction and Traffic Analysis of Interstate 15 (Devore II) Concrete Pavement Reconstruction Project." *Report No. UCPRC-RR-2008-05*, University of California Pavement Research Center, Davis/Berkeley, CA, March 2008.

Knoop, V.L., M. Snelder, and H.J. van Zuylen. “Comparison of Link-level Robustness Indicators.” *Proceedings of the Third International Symposium on Transportation Network Reliability*, Hague, Netherlands, 2007.

Koppelman, Frank S. and Chandra Bhat. “A Self Instructing Course in Mode Choice Modeling: Multinomial and Nested Logit Models”. USDOT Federal Transit Administration. January 31, 2006.

Lam, Terence C. and Kenneth A. Small. “The Value of Time and Reliability: Measurement from a Value Pricing Experiment.” *Transportation Research Part E*, Elsevier Science Ltd., 2001, pp. 231-251.

Lighthill, M. J. and G. B. Whitham. “On Kinematic Waves II: A Theory of Traffic Flow on Long Crowded Roads.” *Proceedings of the Royal Society of London Series A 229*, 1955, pp. 317-345.

Lo, Hong K., X.W. Luo, and Barbara W.Y. Siu. “Degradable Transport Network: Travel Time Budget of Travelers with Heterogeneous Risk Aversion.” *Transportation Research Part B*, Elsevier Science Ltd., 2006, pp. 792-806.

Mahmassani, Hani S. and Srinivas Peeta. “Network Performance Under System Optimal and User Equilibrium Dynamic Assignments: Implications for Advanced Traveler Information Systems.” *Transportation Research Record No. 1408*, Transportation Research Board of the National Academies, Washington, D.C., 1993, pp. 83-93.

Mahut, Michael, Michael Florian, Nicolas Tremblay, Mark Campbell, David Patman, and Zorana Krnic McDaniel. “Calibration and Application of a Simulation-Based Dynamic Traffic Assignment Model.” *Transportation Research Record No. 1876*, Transportation Research Board of the National Academies, Washington, D.C., 2004, pp. 101-111.

McCray, Talia M., Martin E.H. Lee-Gosselin, and Mei-Po Kwan. “Netting Action and Activity Space/Time: Are Our Methods Keeping Pace with Evolving Behaviour Patterns?” *10th International Conference on Travel Behaviour Research*, 2003.

Merchant, Deepak K. and George L. Nemhauser. “A Model and an Algorithm for the Dynamic Traffic Assignment Problems.” *Transportation Science, Vol. 12, No. 3*, Operations Research Society of America, August 1978, pp. 183-199.

Newell, G. F. “A Simplified Theory of Kinematic Waves in Highway Traffic, Part I: General Theory.” *Transportation Research Part B 27*, Pergamon Press Ltd., Great Britain, 1993, pp. 281-287.

Newell, G. F. “A Simplified Theory of Kinematic Waves in Highway

Traffic, Part II: Queuing at Freeway Bottlenecks." *Transportation Research Part B 27*, Pergamon Press Ltd., Great Britain, 1993, pp. 289-303.

Newell, G. F. "A Simplified Theory of Kinematic Waves in Highway Traffic, Part III: Multi-destination Flows." *Transportation Research Part B 27*, Pergamon Press Ltd., Great Britain, 1993, pp. 305-313.

Peeta, Srinivas and Athanasios Ziliaskopoulos. "Foundations of Dynamic Traffic Assignment: The Past, the Present and the Future." *Networks and Spatial Economics, 1*, Kluwer Academic Publishers, 2001, pp. 233-265.

Pesti, Geza, Chi-Leung Chu, Kevin Balke, Xiaosi Zeng, Jeff Shelton, and Nadeem Chaudhary. "Regional Impact of Roadway Construction on Traffic and Border Crossing Operations in the El Paso Region."*CIITR Project 186050-0001: Regional Impact of Roadway Construction on Traffic and Border Crossing Operations in the El Paso Region,* Center for International Intelligent Transportation Research, Texas Transportation Institute, College Station, TX, October 2010.

Pool, C. Matt, Jennifer Duthie, and Natalia Ruiz Juri. "Task #8: Standardize DTA Data and Modeling Requirements for Bottleneck Analysis as a Means." *Technical Memorandum, TxDOT Research Project #0-6657: Investigating Regional Dynamic Traffic Assignment Modeling for Improved Bottleneck Analysis*, Center for Transportation Research, Austin, TX, 2012.

Pool, C. Matt, Michael Levin, Travis Owens, Natalia Ruiz Juri, and S. Travis Waller. "DTA 2012: Improving the Convergence of Simulation-Based Dynamic Traffic Assignment Methodologies." *CTR Technical Report*, Center for Transportation Research, Austin, TX, 2012.

Shao, Hu, William H.K. Lam, Qiang Meng, and Mei Lam Tam. "Demand-Driven Traffic Assignment Problem Based on Travel Time Reliability." *Transportation Research Record No. 1985*, Transportation Research Board of the National Academies, Washington, D.C., 2006, pp. 220-230.

Sheffi, Yosef. Urban Transportation Networks: Equilibrium Analysis with Mathematical Programming Methods. Prentice-Hall, Inc, Englewood Cliffs, NJ, 1985.

Sisiopiku, Virginia P., Xuping Li, Kyriacos C. Mouskos, Camille Kamga, Curtis Barrett, and Abdul M. Abro. "Dynamic Traffic Assignment Modeling for Incident Management." *Transportation Research Record No. 1994*, Transportation Research Board of the National Academies, Washington, D.C., 2007, pp. 110-116.

Sisiopiku, Virginia P. and Ozge Cavusoglu. “Incident and Emergency Medical Services Management from a Regional Perspective.” *International Journal of Environmental Research and Public Health 9*, June 2012, pp. 2266-2282.

Siu, Barbara W.Y. and Hong K. Lo. “Doubly Uncertain Transportation Network: Degradable Capacity and Stochastic Demand.” *European Journal of Operational Research 191*, Elsevier, 2008, pp. 166-181.

Smith, M.J. “The Existence, Uniqueness and Stability of Traffic Equilibria.” *Transportation Research Part B 13*, Pergamon Press Ltd., Great Britain, 1979, pp. 295-304.

Smith, M.J. “The Existence and Calculation of Traffic Equilibria.” *Transportation Research Part B 17*, Pergamon Press Ltd., Great Britain, 1983, pp. 291-303.

Smith, M.J. “A New Dynamic Traffic Model and the Existence and Calculation of Dynamic User Equilibria on Congested Capacity-Constrained Road Networks.” *Transportation Research Part B 27*, Pergamon Press Ltd., Great Britain, 1993, pp. 49-63.

Taylor, Michael A.P. and Glen M. D’Este. “Chapter 2, Transport Network Vulnerability: a Method for Diagnosis of Critical Locations in Transport Infrastructure Systems.” *Critical Infrastructure Reliability and Vulnerability*, Springer Science + Business Media, LLC, 2007, pp. 9-30.

Taylor, Michael A.P., Somenahalli V.C. Sekhar, and Glen M. D’Este. “Application of Accessibility Based Methods for Vulnerability Analysis of Strategic Road Networks.” *Networks and Spatial Economics*, Springer Science + Business Media, LLC, 2006, pp. 267-291.

Ullman, Gerald L., Richard J. Porter, and Ganesh Karkee. “Implementation Guide for Monitoring Work Zone Safety and Mobility Impacts.” *FHWA/TX-10/0-5771-P1*, Texas Transportation Institute, College Station, TX, September 2009.

Wang, Zhou, Alan C. Bovik, Hamid R. Sheikh, and Eero P. Simoncelli. “Image Quality Assessment: From Error Visibility to Structural Similarity.” *IEEE Transactions on Image Processing*, Vol. 13, No. 4, April 2004, pp. 600-612.

Xie, Chi, Kara M. Kockelman, and S. Travis Waller. “A Maximum Entropy Method for Subnetwork Origin-Destination Trip Matrix Estimation.” *Transportation Research Record 2196*. TZransportation Research Board, Washington, D.C., January 2010.

Yperman, Isaak. The Link Transmission Model for Dynamic Network Loading. *PhD Dissertation*, Katholieke Universiteit Leuven, Leuven, Belgium, June 2007.

Zhou, Xuesong, Sevgi Erdogan, and Hani S. Mahmassani. “Dynamic Origin-Destination Trip Demand Estimation for Subarea Analysis.” *Submitted for presentation at 85th Annual Meeting of the Transportation Research Board*, Washington, D.C., January 2006.

Ziliaskopoulos, Athanasios and Hani S. Mahmassani. “Time-Dependent, Shortest-Path Algorithm for Real-Time Intelligent Vehicle Highway System Applications.” *Transportation Research Record No. 1408*, Transportation Research Board of the National Academies, Washington, D.C., 1993, pp. 94-100.

Ziliaskopoulos, Athanasios and S. Travis Waller. “An Internet Based Geographic Information System that Integrates Data, Models and Users for Transportation Applications.” *Transportation Research Part C 8*, Elsevier Ltd., 2000, pp. 427-444.